



**Preclinical development of an immunotherapy against
antibiotic-resistant *Staphylococcus aureus***

**Präklinische Entwicklung einer Immuntherapie zur
Behandlung Antibiotika-resistenter
*Staphylococcus aureus***

Doctoral thesis for a doctoral degree
at the Graduate School of Life Sciences,
Julius-Maximilians-Universität Würzburg,
Section Infection and Immunity

submitted by

Babett Oesterreich

from Greifswald

Würzburg 2015

Submitted on:

Members of the *Promotionskomitee*:

Chairperson: Prof. Dr. Caroline Kisker

Primary Supervisor: PD. Dr. Knut Ohlsen

Supervisor (Second): Prof. Dr. Roland Kontermann

Supervisor (Third): Prof. Dr. Manfred Lutz

Date of Public Defence:

Date of Receipt of Certificates:

Affidavit

I hereby confirm that my thesis entitled "Preclinical development of an immunotherapy against *Staphylococcus aureus*" is the result of my own work. I did not receive any help or support from commercial consultants. All sources and / or materials applied are listed and specified in the thesis.

Furthermore, I confirm that this thesis has not yet been submitted as part of another examination process neither in identical nor in similar form.

Würzburg,

Eidesstattliche Erklärung

Hiermit erkläre ich an Eides statt, die Dissertation „Präklinische Entwicklung einer Immuntherapie zur Behandlung Antibiotika-resistenter *Staphylococcus aureus*“ eigenständig, d.h. insbesondere selbständig und ohne Hilfe eines kommerziellen Promotionsberaters angefertigt und keine anderen als die von mir angegebenen Quellen und Hilfsmittel verwendet zu haben.

Ich erkläre außerdem, dass die Dissertation weder in gleicher noch in ähnlicher Form bereits in einem anderen Prüfungsverfahren vorgelegen hat.

Würzburg,

“Success needs Preparation”

-unknown-

für Hildegard & Hans

Acknowledgement

I want to place on record my thanks to everyone who helped me draft this thesis, especially I like to thank:

- PD Dr. Knut Ohlsen for his competent guidance and support during this work
- The principal of the Faculty Prof. Dr. Jörg Vogel for the opportunity to work on his institute and for providing me with all the necessary facilities for the research
- Prof. Dr. Roland Kontermann for the scientific discussions and the preparation of the Second Opinion
- Prof. Dr. Manfred Lutz for the intensive scientific exchanges and the preparation of the Third Opinion

All cooperation partners at the Julius-Maximilians University Würzburg and University of Stuttgart.

I am grateful to all colleagues of the Ohlsen and Zierbuhr group for sharing expertise, sincere and valuable guidance and encouragement extended to me.

I also thank my family and friends for the unceasing encouragement, support and attention.

I also place on record, my sense of gratitude to one and all, who directly or indirectly, have lent their hand in this venture.

Table of Contents

1. Summary	11
2. Zusammenfassung	12
3. Introduction	13
3.1. The pathogen <i>Staphylococcus aureus</i>	13
3.2. Antibody based therapy.....	16
3.3. Antibody - Function derives from architecture	18
3.4. Phagocytosis.....	20
3.5. Antibody engineering.....	22
3.6. Humanization of murine antibodies for human therapy.....	23
3.7. Immunodominant antigen A (IsaA) - A putative transglycosylase	24
3.8. Transglycosylases.....	26
3.9. Alpha-toxin - A freely secreted toxin	28
3.10. Aim of the thesis.....	29
4. Material	30
4.1. Equipment.....	30
4.2. Consumables	31
4.3. Chemicals	31
4.4. Buffer and Solutions	32
4.5. Enzymes, Kits and Reagents	33
4.6. Media and Supplements.....	34
4.7. Antibodies	34
4.8. Plasmids	35
4.9. Bacterial strains.....	35
5. Methods	38
5.1. Molecular biological Methods	38
5.1.1. Culturing of bacteria	38
5.1.2. Preparation of bacteria stocks for <i>in vivo</i> experiments.....	38
5.1.3. Preparation of bacteria for <i>in vivo</i> experiments.....	38
5.1.4. Cryoconservation of bacterial cultures.....	39
5.1.5. Transformation of competent <i>E. coli</i> cells	39
5.1.6. Preparation of Plasmid DNA.....	39
5.1.7. Quantification of DNA	39
5.1.8. Polymerase chain reaction	39
5.1.9. DNA restriction digestion	40
5.1.10. Agarose gel electrophoresis with DNA	40
5.1.11. DNA purification from agarose gels	41
5.1.12. DNA Ligation	41
5.1.13. DNA sequencing	41
5.1.14. Cloning of scFv fragments.....	41

5.1.15. Cloning of scFv-Fc fragments	41
5.1.16. Cloning of complete UK-66 IgG antibodies	42
5.1.17. Humanization of mouse UK-66 antibody.....	43
5.2. Cell culture Methods.....	43
5.2.1. Cultivation of mammalian cells	43
5.2.2. Stable transfection of plasmids.....	43
5.2.3. Selection of high producer clones.....	44
5.2.4. Determination of cell specific antibody production	45
5.2.5. Cryopreservation of mammalian cell lines	45
5.3. Biochemical Methods	47
5.3.1. Expression of recombinant proteins.....	47
5.3.2. Lysis of bacteria	47
5.3.3. Protein Purification	47
5.3.4. Immobilized metal affinity chromatography	48
5.4. Antibody Purification.....	48
5.4.1. SDS-PAGE.....	49
5.4.2. Western Blot.....	49
5.4.3. Dot Blot	50
5.4.4. Thermal stability	50
5.5. Functional characterization.....	50
5.5.1. Biosensor measurements of antibody affinity.....	50
5.5.2. ELISA studies.....	51
5.5.3. Analysis of antibody binding on bacteria and human PMNs via flow cytometry studies.....	51
5.5.4. Immunofluorescence studies	52
5.5.5. Purification of human neutrophils.....	52
5.5.6. Phagocytosis assay.....	52
5.6. Killing assay	53
5.7. <i>In vivo</i> experiments	53
5.7.1. Ethics statement.....	53
5.7.2. Experimental set up.....	53
5.7.3. Survival analysis.....	54
6. Results.....	55
6.1. Humanization of mouse UK-66 antigen binding domain	55
6.2. Expression and purification of mouse and humanized scFv fragments by <i>E. coli</i> TG1	56
6.3. Expression and purification of recombinant IsaA by <i>E. coli</i> M15Rep4 and BL21	57
6.4. Comparative binding studies of mouse and humanized UK-66 antigen binding domain	58
6.4.1. Western Blot studies to analyse the binding of rIsaA by mouse and humanized UK-66 antigen binding domain	58

6.4.2.	Binding affinity analysis of mouse and humanized UK-66 antigen binding domains by ELISA studies.....	59
6.4.3.	Immunofluorescence studies and flow cytometry analysis to detect the binding of native IsaA by scFv mUK-66 and hUK-66	60
6.5.	Comparative binding studies of mouse and humanized UK-66 full antibody.....	62
6.5.1.	Comparative binding studies of full mouse and humanized UK-66 antibody	63
6.5.2.	Determination of mouse and humanized UK-66 binding affinity by Surface Plasmon Resonance (SPR).....	64
6.5.3.	Humanized UK-66 IgG1 binds native expressed IsaA of clinically relevant <i>S. aureus</i> strains.....	65
6.6.	Generation of stable cell lines producing scFv-Fc and full humanized UK-66 IgGs	67
6.6.1.	Development of cell lines for UK-66 production	67
6.6.2.	Cloning of the vector constructs	67
6.6.3.	Characterization of clones	68
6.7.	Characterization of hUK-66 using <i>in vitro</i> studies	71
6.7.1.	<i>In vitro</i> characterization of hUK-66 IgGs biological function	72
6.7.2.	<i>In vitro</i> analysis of biological activity of hUK-66 IgG1 in blood samples of high risk patients	73
6.7.3.	Investigation of hUK-66 IgG1- dependent opsono-phagocytosis of <i>S. aureus</i> by human neutrophils in whole blood.....	75
6.7.4.	Investigation of hUK-66 IgG1 dependent respiratory burst induction in human neutrophils.....	78
6.7.5.	Investigation of hUK-66 IgG1 dependent killing of <i>S. aureus</i> Newman by human whole blood	80
6.7.6.	<i>In vitro</i> analysis of biological activity of hUK-66 IgG1 in purified human PMNs	82
6.7.7.	<i>In vitro</i> analysis of combined hUK-66 IgG1 and hUK-tox antibody in human whole blood samples.....	84
6.8.	<i>In vitro</i> mouse blood killing assays to investigate the therapeutic efficacy of murine and humanized UK-66 combined with hUK-tox IgG1	86
6.8.1.	Fc part of hUK-66 IgG1 and hUK-tox IgG1 is bound by FcγR1a of HEK293 cells.....	87
6.9.	Characterization of UK-66 IgG1's therapeutic potency using a mouse pneumonia model.....	90
6.10.	Prophylactic treatment of <i>S.aureus</i> induced pneumonia with mUK-66 IgG1	91
6.11.	Therapy of pneumonia by prophylactic treatment with mUK-66 IgG1	92
6.12.	Treatment of <i>S. aureus</i> pneumonia with mUK-66 IgG1 in a therapeutic infection model.....	93
6.13.	Prophylactic therapy of pneumonia with humanized antibody hUK-66 IgG1	94
6.14.	Prophylactic therapy of pneumonia with hUK-tox IgG1.....	95
6.15.	Treatment of <i>S. aureus</i> -induced pneumonia with hUK-tox IgG1	96
6.16.	Therapeutic efficacy of combination of hUK-66 and hUK-tox IgG1 in a mouse pneumonia model.....	97
6.17.	Treatment of <i>S. aureus</i> -induced pneumonia with combination of hUK-66 and hUK-tox IgG1 in a mouse pneumonia model.....	98

7. Discussion.....	100
7.1. Humanization and reshaping of murine UK-66 antibody	101
7.2. IsaA – The right target for an antibody based therapy	103
7.3. Generation of hUK-66 producing cell lines	104
7.4. Therapeutic efficacy of hUK-66 <i>in vitro</i>	106
7.4.1. <i>In vitro</i> characterization of hUK-66 and hUK-66 related subclasses.....	106
7.4.2. <i>In vitro</i> analysis of biological activity of hUK-66 IgG1 in blood samples of high risk patients	109
7.5. Therapeutic efficacy of hUK-66 <i>in vivo</i>	116
8. Outlook.....	120
9. References	122
10. List of figures.....	140
11. List of tables.....	140
12. List of abbreviations.....	143
13. Appendix	145
13.1. IsaA.....	145
13.1.1. IsaA-Nucleotide sequence.....	145
13.1.2. IsaA-Vector maps.....	145
13.2. Antigen binding domains	145
13.2.1. Antigen binding domain scFv mUK-66.....	145
13.2.2. Antigen binding domain scFv hUK-66(1)	146
13.2.3. Antigen binding domain scFv hUK-66(2)	146
13.2.4. Vectors used for cloning antigenbinding domains scFv	147
14. Curriculum vitae.....	148
14.1. Professional Experience and Education	148
14.2. Qualification	149
14.3. Publication.....	149
14.4. Conference Contribution.....	149

1. Summary

The Gram-positive bacterium *Staphylococcus aureus* is the leading cause of nosocomial infections. In particular, diseases caused by methicillin-resistant *S. aureus* (MRSA) are associated with higher morbidity, mortality and medical costs due to showing resistance to several classes of established antibiotics and their ability to develop resistance mechanisms against new antibiotics rapidly. Therefore, strategies based on immunotherapy approaches have the potential to close the gap for an efficient treatment of MRSA.

In this thesis, a humanized antibody specific for the immunodominant staphylococcal antigen A (IsaA) was generated and thoroughly characterized as potential candidate for an antibody based therapy. A murine monoclonal antibody was selected for humanization based on its binding characteristics and the ability of efficient staphylococcal killing in mouse infection models. The murine antibody was humanized by CDR grafting and mouse and humanized scFv as well as scFv-Fc fragments were constructed for comparative binding studies to analyse the successful humanization. After these studies, the full antibody with the complete Fc region was constructed as isotype IgG1, IgG2 and IgG4, respectively to assess effector functions, including antibody-dependent killing of *S. aureus*. The biological activity of the humanized antibody designated hUK-66 was analysed *in vitro* with purified human PMNs and whole blood samples taken from healthy donors and patients at high risk of *S. aureus* infections, such as those with diabetes, end-stage renal disease, or artery occlusive disease (AOD).

Results of the *in vitro* studies show, that hUK-66 was effective in antibody-dependent killing of *S. aureus* in blood from both healthy controls and patients vulnerable to *S. aureus* infections. Moreover, the biological activity of hUK-66 and hUK-66 combined with a humanized anti-alpha-toxin antibody (hUK-tox) was investigated *in vivo* using a mouse pneumonia model. The *in vivo* results revealed the therapeutic efficacy of hUK-66 and the antibody combination of hUK-66 and hUK-tox to prevent staphylococcal induced pneumonia in a prophylactic set up.

Based on the experimental data, hUK-66 represents a promising candidate for an antibody-based therapy against antibiotic resistant MRSA.

2. Zusammenfassung

Staphylococcus aureus ist ein bedeutender nosokomialer Erreger, der eine Vielzahl von Infektionen im Menschen verursacht. Besonders Krankheiten, die durch Methicillin resistente *S. aureus* (MRSA) verursacht werden, sind mit einer erhöhten Morbidität, einer höheren Sterblichkeitsrate und hohen medizinischen Kosten verbunden. Seine besondere medizinische Bedeutung erlangte *S. aureus* durch die Ausbildung von Resistenzen gegen eine Vielzahl von Antibiotika und seiner Fähigkeit auch gegen neu entwickelte Antibiotika schnell Resistenzmechanismen auszubilden. Aus diesem Grund, ist die Entwicklung von neuen Therapieansätzen von besonderer Bedeutung, um die entstandene Lücke für eine effektive MRSA-Therapie zu schließen.

In dieser Arbeit wurde ein humanisierter monoklonaler Antikörper entwickelt und charakterisiert, der spezifisch an das „immunodominant staphylococcal antigen A“ (IsaA) bindet. Dieser Antikörper wurde auf Grund seiner Eigenschaft, in einem Mausmodell effektiv *S. aureus* abzutöten, als vielversprechender Kandidat für eine Antikörper-Therapie ausgewählt. Der murine Vorläuferantikörper wurde mittels „CDR grafting“ humanisiert und durch die Generierung von humanisierten und murinen scFv und scFv-Fc Fragmenten, die in vergleichenden Bindungsstudien getestet wurden, konnte der Erfolg der Humanisierung beurteilt werden. Im Anschluss wurde der vollständige Antikörper mit vollständig funktionaler Fc-Region in den Isotypen IgG1, IgG2 und IgG4 hergestellt. Die Funktionalität des humanisierten Antikörpers wurde *in vitro* mittels aufgereinigter PMNs und Blutproben von gesunden Spendern und Patienten bestimmt, die ein hohes Risiko für *S. aureus* Infektionen besitzen wie Diabetiker, Dialyse-Patienten und Patienten mit arterieller Verschlusskrankheit.

Die Ergebnisse der *in vitro*-Studien zeigen, dass der anti-IsaA-Antikörper hUK-66 nicht nur *S. aureus* effektiv in Blutproben von gesunden Spendern abtötet, sondern auch in Blutproben von Patienten mit erhöhter Anfälligkeit für *S. aureus* Infektionen. Darüber hinaus wurde die biologische Aktivität des humanisierten Antikörpers gegen IsaA als Monotherapie und in Kombination mit einem humanisierten anti-alpha-Toxin-Antikörper (hUK-tox) *in vivo* in einem Maus Pneumonie Modell untersucht. Hierbei konnte gezeigt werden, dass die prophylaktische Verabreichung von hUK-66 sowie die Kombination von hUK-66 und hUK-tox, die Bildung einer Staphylokokken-induzierten Pneumonie mit Todesfolge signifikant senkt.

3. Introduction

3.1. The pathogen *Staphylococcus aureus*

Staphylococcus aureus (*S. aureus*) is a commensal gram positive coccus bacterium and can be distinguished from other staphylococcal species on the basis of the gold pigmentation of colonies (Fig. 1). *S. aureus* is positive for catalase, mannitol-fermentation and nitrate reduction [1] and was first identified in 1880 by the surgeon Sir Alexander Ogston [2]. Humans are a natural reservoir of *S. aureus*. Thirty to 50 percent of healthy individuals are colonized and 10 to 20 percent are persistently colonized by *S. aureus*, which can be found as part of the normal skin flora and in anterior nares of the nasal passages [3], [4], [5], [6]. Colonized persons are at high risk for subsequent infections [7], [8], [9]. Especially, among patients with type 1 diabetes, intravenous drug users, patients undergoing hemodialysis, surgical patients and patients with qualitative or quantitative defects in leukocyte function are at increased risk for staphylococcal disease [5], [10], [11], [12], [13], [14], [15], [16], [17], [18]. Furthermore, *S. aureus* is responsible for the majority of skin and soft tissue infections in humans, including impetigo, folliculitis, cellulitis and infected ulcers and wounds [19], [20]. In addition, *S. aureus* can cause invasive and life threatening infections, such as bacteremia, abscesses, pneumonia, osteomyelitis, meningitis, endocarditis and sepsis [21]. This pathogen is also a predominant cause of a variety of nosocomial infections, including ventilator-associated pneumonia, intravenous catheter-associated infections, postsurgical wound infections, as well as invasive infections in neutropenic patients and in patients undergoing solid organ and hematopoietic stem cell transplants [22]. The treatment of these infections has been complicated by the emergence of methicillin-resistant *S. aureus* (MRSA) strains, which are becoming increasingly resistant to multiple antibiotics [23], [24].(Fig. 2)

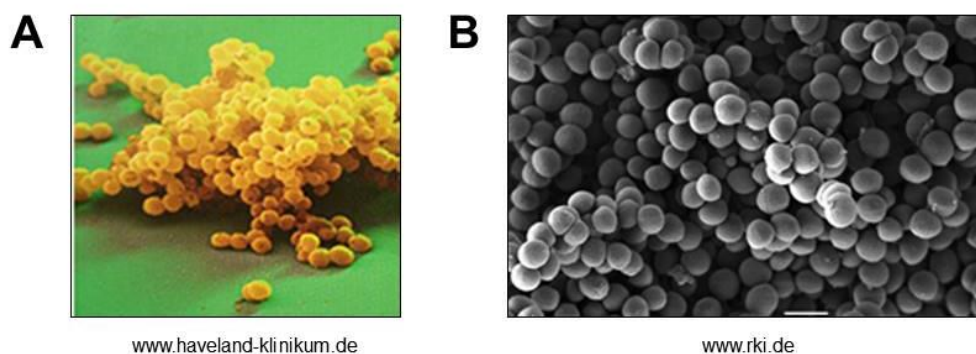
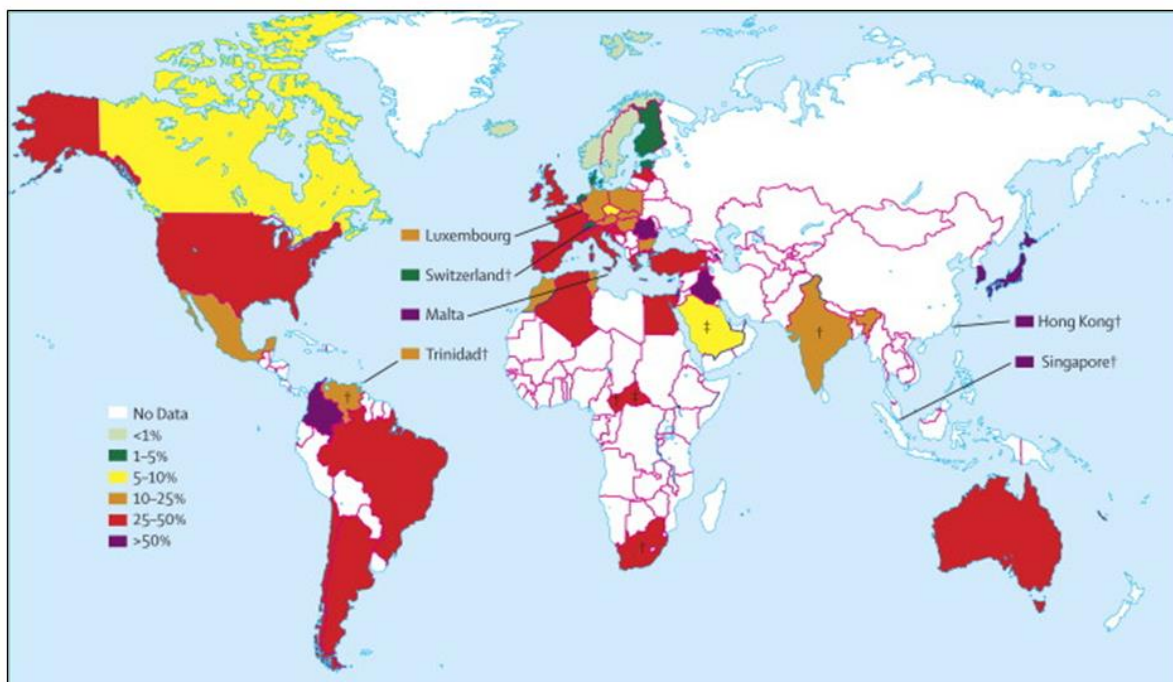


Fig. 1 Coloured and non-coloured electron microscope image of *S. aureus*.

A) *S. aureus* is a gram positive coccus which can be distinguished from other *Staphylococcus* species by its gold pigmentation. B) Furthermore, *S. aureus* grow in grape like structures.

The pathogen *S. aureus* has an extensive repertoire of virulence factors that contribute to the pathogenesis of infections like capsule, surface proteins, toxins, enzymes and other bacterial

components [21]. Although, *S. aureus* is a commensal, a breach of the skin or mucosal barrier allows staphylococci access to adjoining tissues or the bloodstream. The expression of a large number of cell surface proteins by *S. aureus* like proteins of the MSCRAMM [25] and SERAM class [26], fibronectin-binding proteins, extracellular adherence proteins [27] and different invasins, mediates the adherence and invasion to host structures. These molecules promote host colonization, alter leukocyte recruitment or function, inhibit complement and antimicrobial peptides, and cause destruction of leukocytes [28], [29], [30] (Fig. 3).



Grundmann et al., 2006

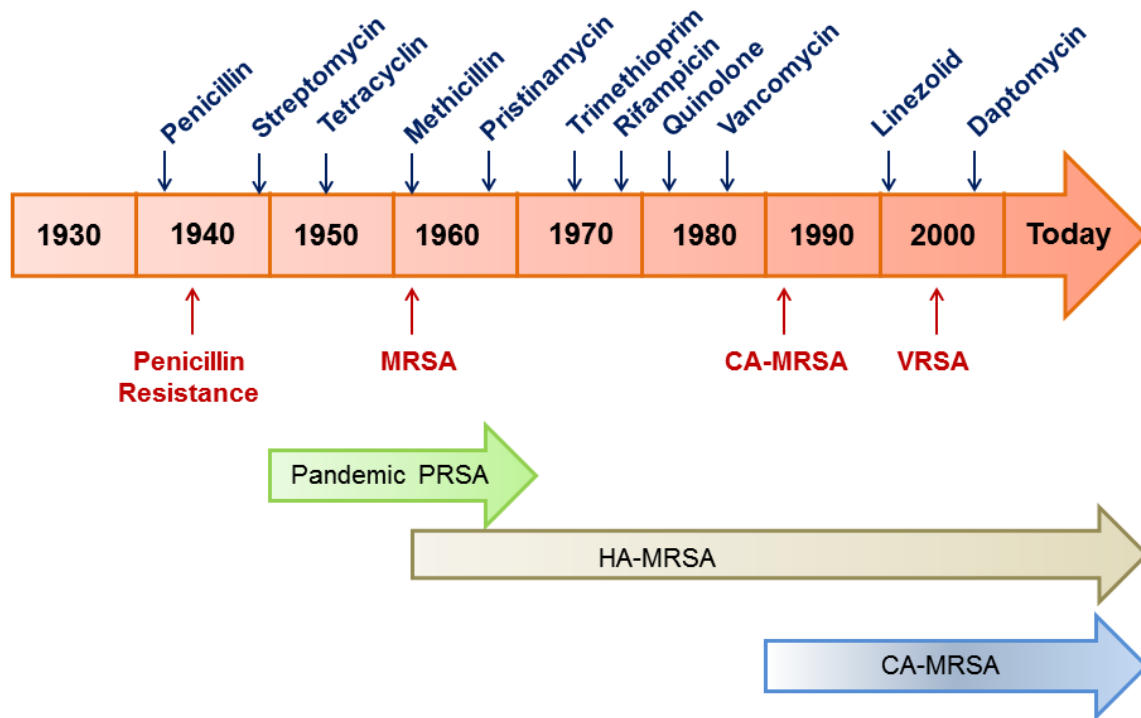
Fig. 2 Percentage of MRSA isolates worldwide.

MRSA is associated with higher mortality and medical cost due to the fact that most of the MRSA strains are resistant to several classes of established antibiotics. Grundmann et al., analysed the distribution of MRSA worldwide and the presence of MRSA is presented as percentage from 100 isolates identified as *S. aureus*.

History has shown that the introduction of a new antibiotic is frequently followed by the development of bacterial antibiotic resistance. This process demonstrates the remarkable capacity of *S. aureus* for adapting to new types of antimicrobial agents. As a consequence, there is a growing population of *S. aureus* that is resistant to traditional antibiotics and their derivatives [31]. Moreover, the resistance is moving from the hospital to the community [32]. Community-associated MRSA (CA-MRSA) infection was first reported in the early 1990s [33]. CA-MRSA disseminated rapidly, is epidemic and the most abundant cause of bacterial infections in the community [34]. In contrast to healthcare-associated MRSA (HA-MRSA) infections, CA-MRSA infections occur in healthy individuals with no exposure to the healthcare setting. These observations imply that CA-MRSA strains have enhanced virulence compared to HA-MRSA strains [35]. A further threatening trend is the emergence of

isolates with resistance to vancomycin, the antibiotic of choice against MRSA strains, and also newly introduced drugs, such daptomycin and linezolid [36] (Fig. 3).

The therapeutic options for these pathogens are extremely limited and the need of new treatment options in the presence of growing numbers of elderly patients and patients undergoing surgery or transplantation and a dramatic increases in population in neonatal intensive care units will produce an even greater number of immunocompromised individuals at risk of these infections [37], [38]. Therefore, there is an urgent need for the development of new anti-infectious agents, since the widespread of antimicrobial drug resistance and the increase of immunocompromised patients in whom antimicrobial therapy is not as effective as in patients with intact immunity [39]. In addition, novel classes of antibiotics are needed for MRSA, because current drug classes exhibit toxicities and emerging resistance [40], [41], [42]. New therapeutic approaches to treat or preventing infection diseases, including phage therapy [43]; quorum sensing inhibitors [44] and bacteria-lytic enzymes [45] are in an early stage of preclinical development. The development of immunological approaches, such vaccines and monoclonal antibodies (mAbs), are promising candidates for alternative treatments. Since antibodies have already a broad range of applications in fields of oncology, rheumatology, autoimmunity and neurodegeneration [46], [47], [48]. In the field of infectious disease, mAbs starting to become more and more attractive, since a) widespread of antimicrobial drug resistance, b) an increase of immunocompromised hosts in whom antibiotic therapy is not as effective as in hosts with intact immunity, c) the appearance of new pathogenic microbes for which no therapy exists and d) the re-emergence of pathogens in drug-resistant forms [39].



Modified from DeLeo et al., 2009

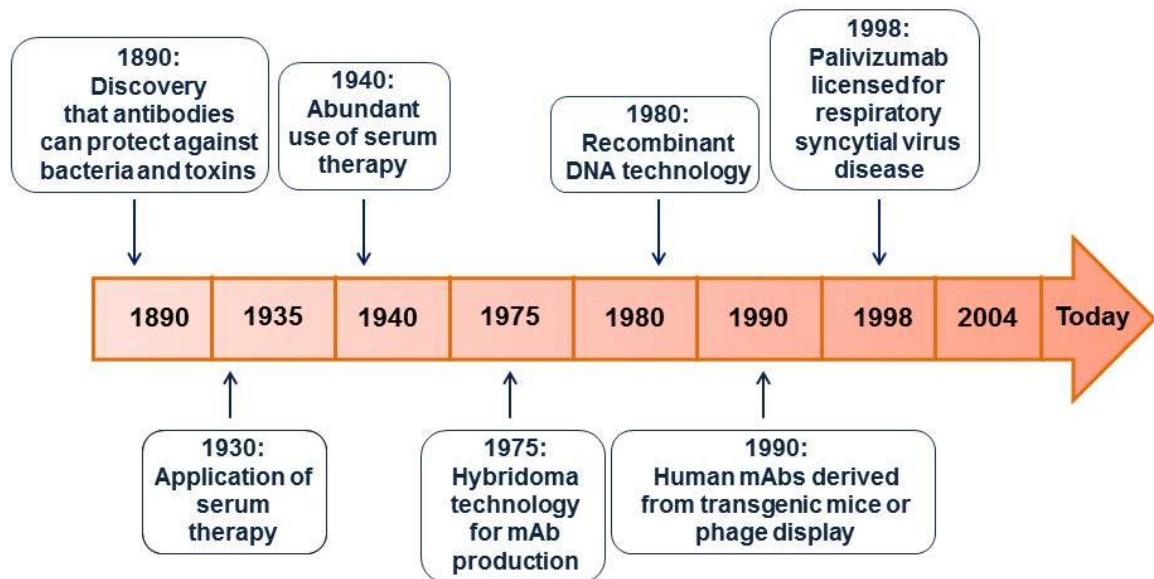
Fig. 3 Emergence of antibiotic-resistant *S. aureus*.

Penicillin was highly effective against staphylococcal infections in the beginning of the 1940s. However, first penicillinase-producing *S. aureus* emerged in the mid-1940s. Several “epidemic waves” of antibiotic-resistant *S. aureus* have occurred since then. Introduction of new antibiotics in clinical use results in selection of antibiotic-resistant *S. aureus* shortly.

3.2. Antibody based therapy

Monoclonal antibodies (mAbs) are the fastest-growing category of therapeutics entering clinical studies [49], [50]. The ability of specific antibodies to protect against bacterial toxins was discovered by Behring and Kitasato in the early 1890s [51]. Based on this observation, serum therapy was used against different infectious diseases by the 1930s including pneumococcal pneumonia, meningococcal meningitis and anthrax [52], [53]. Only five years after the introduction of serum therapy, the use of serum therapy was declined rapidly due to the discovery of sulphonamides [54] (Fig. 4). Since then, the field of infectious diseases has missed the mAb therapeutic revolution of the past decades. In contrast, mAbs have provided new effective therapies in the field of oncology and rheumatology [39], while only one mAb has been licensed for the treatment of infectious diseases [55]. The antibody therapeutics were revolutionized 1975 by the discovery of the hybridoma technology. This method was used to produce mAbs by immortalizing b-cells [56]. This innovation allowed the generation of homogenous antibodies in high quantities. Together with the development of new methods for cloning, and recombinant DNA technology, the hybridoma technology was supplemented to modify antibody molecules, including the synthesis of chimeric and humanized antibodies [57], [58], [59], [60]. In the last decades of the twentieth century, new techniques were

developed including, the immortalization of human peripheral b-cells, direct cloning of variable genes into phage expression libraries and the creation of transgenic mice producing full human antibodies [61], [62].



Modified from Casadevall et al., 2004

Fig. 4 Development of an antibody based therapy: historical overview.

In the 1890s the therapeutic potential of immune serum was discovered and until the 1930s, serum from animals was used to treat different infection diseases. However, the discovery of antibiotics 1940 replaced serum therapy. The revolution of antibody based therapies rise with the development of mAbs by hybridoma technology 1975 and since then mAbs provide new options for treatment in the field of infectious diseases.

Today, mAbs are the most developed category of biological pharmaceuticals and a very attractive approach as an antimicrobial strategy, since their prophylactic and therapeutic potential and their advantages over antibiotics e.g. high specificity [63], [64], [57], [39]. Antibodies reveal less cross-reactivity with host tissue, they only target a specific microbe, so that their systemic administration affect no beneficial microbes. Furthermore, application of mAbs will not result in selection for resistance of microbes [65], [66]. Specific antibodies have the potential to be synergistic with conventional antimicrobial therapy. Hence, combination therapy with current antimicrobial agents can be more effective than the application relative to either alone. Studies from Pacht et al., demonstrated that the combination of Mycograb together with the lipid-associated amphotericin B produced a significant clinical and culture-confirmed improvement in outcome for patients with invasive candidiasis [67]. Furthermore, results from Akiyama et al., using a mouse thigh infection model, revealed that the therapeutic effect of ceftazidime was enhanced by a combined therapy with an anti-lipopolysaccharide antibody [68]. Moreover, antibody cocktails even provide a greater biological activity by targeting multiple epitopes and providing different effector functions through various isotypes. In addition, combination therapy with mAb cocktails prevents

escape and emergence of resistant mutants. For example, Prabakaran et al., combined a pooled of chimeric antibodies to protect mice from lethal H5N1 infections [69], [70]. Antibodies have also the potential to replace lost immunity [71], [72]. Known mechanisms of action of marketed mAbs are: antagonist action by blocking a cell receptor interaction with its ligand, Fc domain mediated recruitment of immune cells to target tissue, antibody-dependent cellular cytotoxicity (ADCC) or complement-dependent cytotoxicity (CDC), as well as receptor-mediated apoptosis, receptor down regulation and the delivery of radioisotopes or chemotherapeutic drugs via mAb bio conjugates [73].

3.3. Antibody - Function derives from architecture

The multifunctional nature of antibodies derives from their structural design. Antibodies belong to the family of immunoglobulins, which can be distinguished by their C regions into five different classes: IgM, IgD, IgG, IgA and IgE. They function as adaptor molecules containing binding sites for antigens and for effector molecules. IgG antibodies composed of two different polypeptide chains, which are termed as heavy and light chain. Each IgG molecule consists of two heavy chains and two light chains and they form a Y-shape protein. Each arm of this Y-shape structure forms an antigen binding domain by the association of the variable domain of the light chain and the variable domain of the heavy chain. The constant domain is formed by the pairing of the two heavy chains. The two heavy chains are linked to each other by disulfide bonds and each heavy chain is linked to a light chain by a disulfide bond. There are two types of light chain, termed lambda and kappa and each IgG molecule either has κ chains or λ chains. There are no functional differences between the both light chains. The antigen binding site is located at the top of the Y-shaped antibody and is corresponding to the variable region of both heavy and light chain. The variable region of the antigen binding site includes regions, which are complementary to the shape of the specific antigen, called complementary determining region (CDR). Three CDRs are located on the heavy chain and three on the light chain [74]. The flexible stretch link of antigen binding domain and Fc part is termed hinge region and allows the independent movement of the two Fab arms. The antigen binding domain is named Fab fragment and consists of the complete light chains paired with the V_H and C_{H1} domains of the heavy chain. The Fc fragment contains no antigen binding domain and corresponds to the paired C_{H2} and C_{H3} domains (Fig. 5). This part of the antibody molecule interacts with the specific receptors on different cell types and the functional differences between the isotypes are mainly determined in the Fc fragment [75].

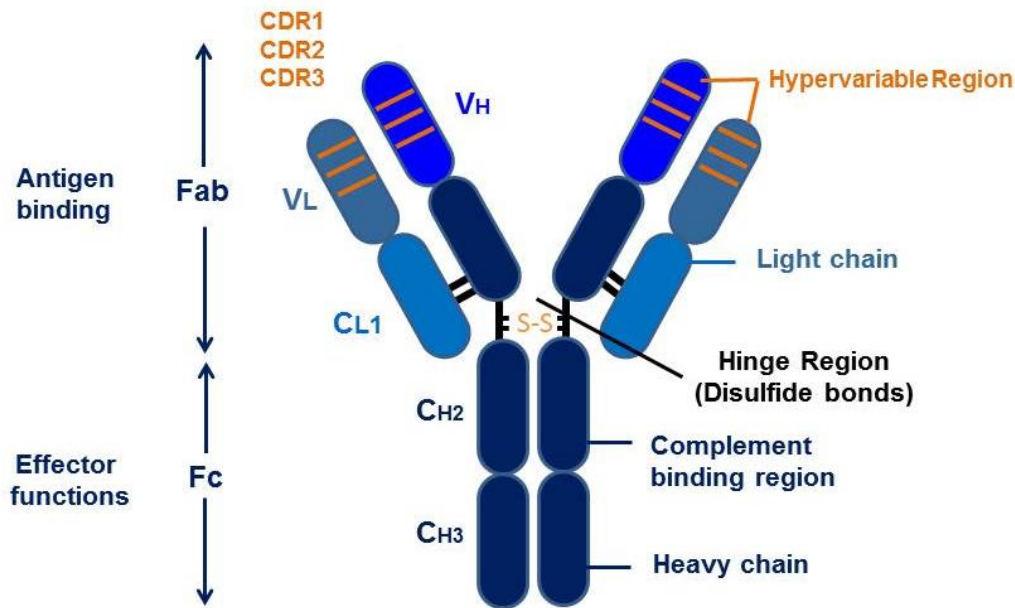


Fig. 5 Schematic structure of an IgG antibody molecule.

An antibody is composed of two identical heavy chains (dark blue) and two identical light chains (blue). Each chain has a constant part (C) and a variable part (V). The antigen binding site is located in the top of the arms of the Fab fragment and is formed by the light and heavy chain (V_H+V_L). This region contains the complementary determining regions (CDRs). The heavy chains form the Fc part and mediate effector functions and include also the complement binding region. The Fab fragment and the Fc part are linked by the hinge region, which is responsible for the flexibility and movement of the antibody's arms.

The class of IgG antibodies is the most abundant class in the bloodstream and also present in tissue fluids. IgG promotes neutralization of viruses and toxins, agglutination of bacteria and binding of antigens to opsonize bacteria for phagocytosis and it is also the only class of antibodies that can cross the placenta. Antibodies can participate in host defence in different ways: I) Antibodies can directly bind to pathogens and their products and thereby blocking their access to cells. This process is known as neutralization and protects the host from tissue damage and invasion by microorganisms. II) The antigen binding domain of an antibody binds structures of the bacterial surface and the Fc-part provides a platform to activate the complement cascade and to mediate antibody-dependent cell cytotoxicity [76]. III) In addition, antibodies enable phagocytes to ingest and destroy the pathogen by binding the pathogenic antigen with their antigen binding domain and the antibody's Fc part is bound by receptors of phagocytes. The coating of pathogens and foreign particles in this way is termed opsonization (Fig. 6).

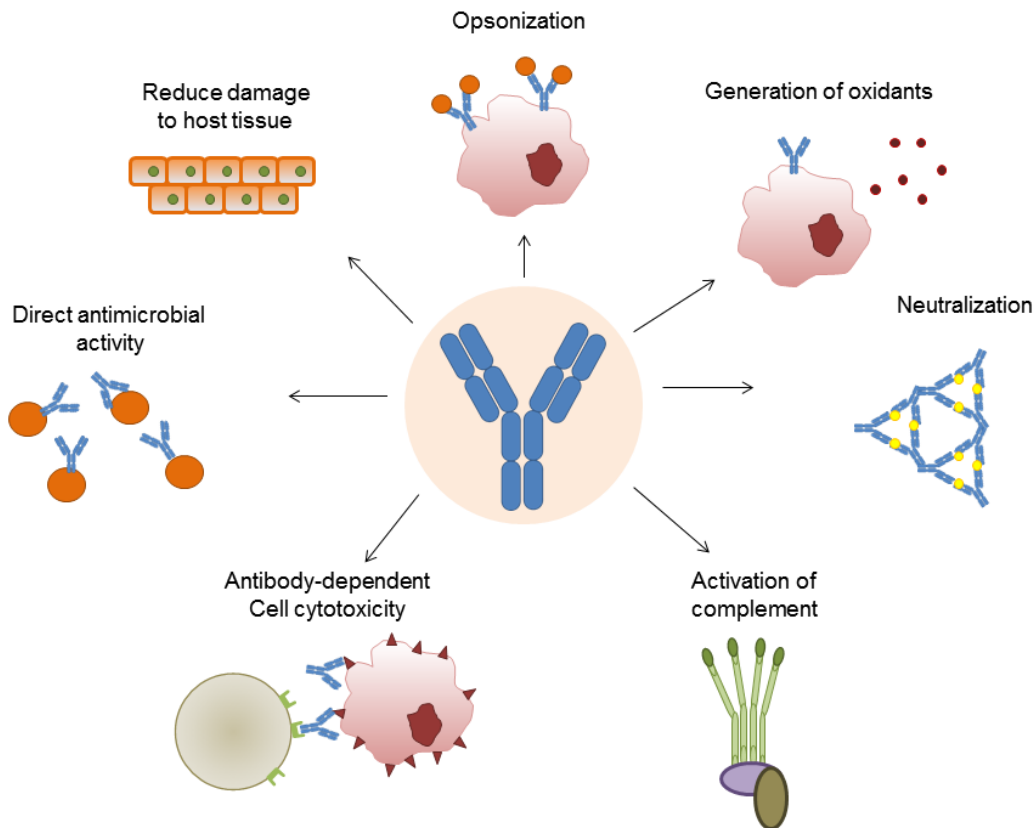


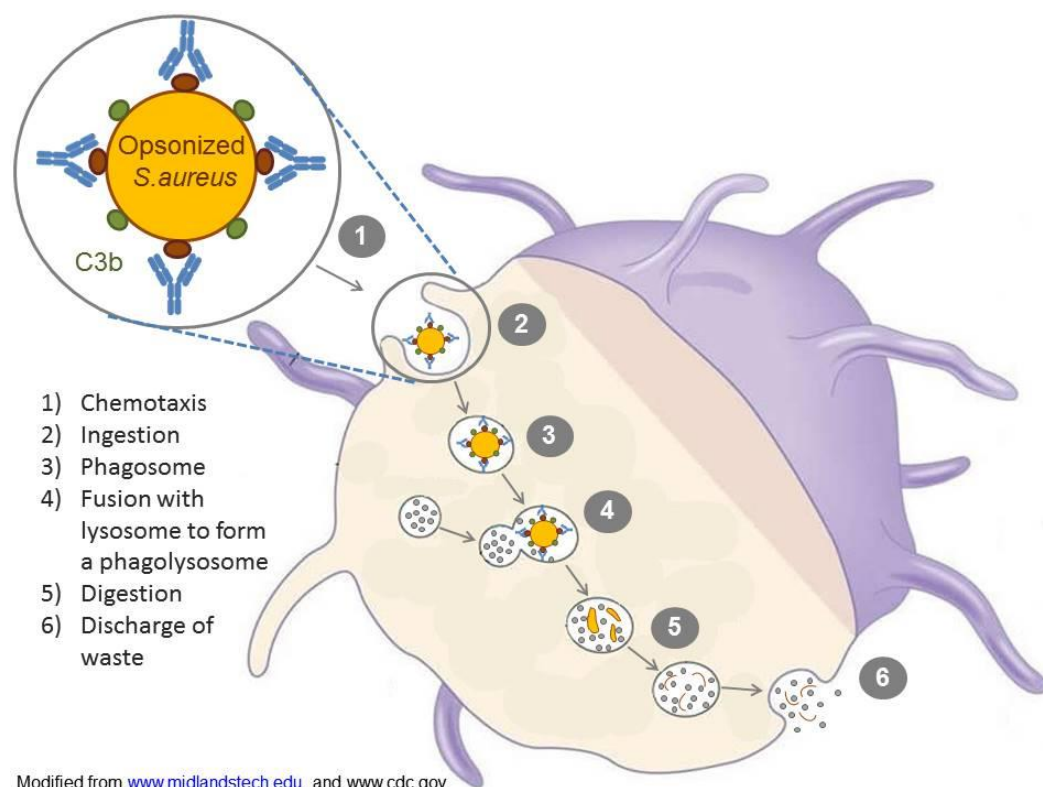
Fig. 6 Antibodies mediate a large panel of direct and indirect functions.

The IgG antibody mediates different biological effects. Direct functions like toxin and virus neutralization, complement activation and further antimicrobial functions such as the generation of oxidants are independent from host immune system. Indirect functions, like antibody-dependent cellular cytotoxicity, opsono-phagocytosis or immunomodulation, depend on other host cells and mediators.

3.4. Phagocytosis

Antibody mediated opsono-phagocytosis is the most efficient defence of the innate immune system against pathogenic microbes. In the 1880s, Elie Metchnikoff observed specialized phagocytic cells ingesting bacteria [77]. The cells of the first line of defence are professional phagocytes, such as neutrophils, macrophages and monocytes, which ingest and eliminate bacteria [29]. Neutrophils are the most prominent cellular component of the innate immune system and provide the primary defence against pathogens such as *S. aureus* [78]. These lymphocytes are rapidly recruited to sites of infection by bacterial-derived N-formyl peptides and these peptides enhance important capabilities of neutrophils like the activation of NADPH oxidase, production of granule proteins and the assembling of actin for mobilization [79], [80]. Most frequently, *S. aureus* is coated with antibody or complement, which is recognized by receptors of the phagocyte to facilitate engulfment. The cross-linking of these Fcγ receptors (FcγRs) on the cell surface of neutrophils activates the respiratory burst and activates the phagocytic pathway [81]. Neutrophils express FcγRI, a high affinity receptor for IgG1 and IgG3, and FcγRII, a receptor with medium affinity for IgG1 [82]. After

internalization, the microbe is located in the phagosome. Neutrophils containing granules, named lysosomes, in their cytoplasm, which are filled with digestive and antibacterial compounds like defensins, proteinases, elastases, myeloperoxidases, metalloproteases and reactive oxygen species [83], [84], [85], [86]. [87]. The development of oxygen species is caused by the NADPH oxidase complex that assembles at the phagosomal membrane. Electrons are transferred from the cytoplasmic NADPH to oxygen on the phagosomal side of the membrane, generating first superoxide and a range of other reactive oxygen species [88], [89], [90]. This oxidative burst is essential for killing of microorganisms. Importantly, patients with defective NADPH oxidase have frequent infections with *S. aureus* [91]. Like oxygen species, reactive nitrogen intermediates contribute to pathogen eradication and are an important element of the antimicrobial agents [92]. The phagosome matures by a series of fusion events with granules filled lysosomes and culminating in the formation of the mature phagolysosome, where the ingested microbe is killed by oxidative and non-oxidative mechanism (Fig. 7). Designing antibodies, which enhance the mechanisms of phagocytosis, is one of the most attractive approaches for an antibody based therapy against antibiotic resistant microbes.



Modified from www.midlandstech.edu and www.cdc.gov

Fig. 7 The mechanism of Phagocytosis.

Phagocytosis is actin-dependent ingestion and killing of microorganisms. The process, by which phagocytes are attracted to pathogens, is called chemotaxis. The phagocytes adhere to microbes via receptors. Pseudopods of the phagocytes engulf the bacteria and enclose them into the phagosome. The fusion with granules filled lysosomes results in a phagolysosome where the microbes are killed by lysosomal enzymes and oxidizing agents.

3.5. Antibody engineering

The development of hybridoma technology in 1975 by Köhler and Milstein, relying on the fusion of a myeloma cell line with b-cells from an immunized animal, opens the gate for the generation of recombinant rodent antibodies [56]. The immortalization of b-cells, producing specific antibodies, allows the manipulation and adaptation of antibodies. Molecular cloning and sequencing of the antigen binding domain form the basis of antibody modelling [93]. Moreover, after the variable region genes have been cloned, the antibody domains can be further engineered to produce antibodies with lower immunogenicity, higher affinity, altered specificity or with enhanced stability [94], [95], [96], [97]. After two decades, the first therapeutic antibody for a cancer indication was approved by the FDA for marketing in 1997. Antibody engineering has become an important discipline, encompassing protein production and stability, as well as the improvement of affinity, specificity and biological effector functions [98]. Efficient bacterial expression systems allow the rapid production of functional recombinant antibody fragments for analysis [99]. The smallest functional antibody-derived unit is the antigen binding domain, consisting of the variable region of the heavy (V_H) and light chain (V_L). The antigen binding domain (Fv) can be expressed as polypeptide by the introduction of a linker sequence between V_H and V_L . The resulting fragment is named single chain Fv fragment (scFv). scFvs have a molecular weight of 25-28 kDa and the most common linker is a flexible $(Gly_4Ser)_3$ decapentapeptide [100]. In addition to scFvs, another commonly used recombinant antibody fragment is Fab. Fab fragments consist of two polypeptide chains, containing the light and heavy chain variable and one constant domain (C_H1 domain). The two chains are linked together by a disulfide bond. The antigen binding domain with a complete Fc part is named scFv-Fc fragment. Based on the antibody structure, antibodies with two specificities can be designed, so called bispecific antibodies. These antibodies bind multiple epitopes [101] (Fig. 8). Furthermore, the high specificity of antibodies for their targets makes it possible to design antibodies, which deliver harmful cargos to their targets [102]. In addition, introduction of point mutations in the sequence of the antigen binding domain or into the sequence of the constant domain allows the modification of the affinity or the enhancement of the effector function of the antibody.

Antibody engineering had revealed major success in refinement and manufacturing of basic IgG. As a consequence, mAbs are the most developed category of biological pharmaceuticals.

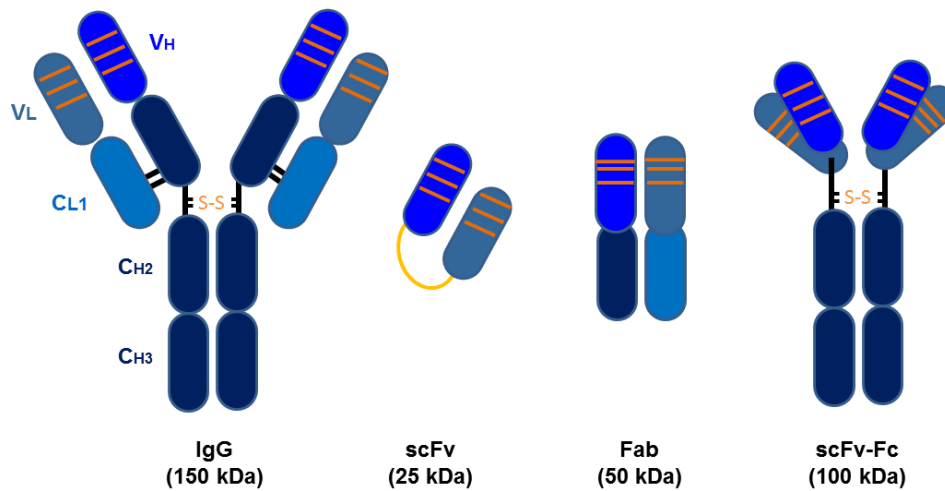


Fig. 8 Antibody engineering for designing antibodies and their functional fragments.

Overview of various antibody fragments of biotechnological and clinical interest. The antigen binding domain of the heavy and light chain can be combined via linker sequence to generate scFv fragments. Two scFv fragments combined with the constant domain CH2 and CH3 results in a scFv-Fc fragment. The combination of the antigen binding domain with CL1 and CH1 domain is named Fab fragment.

3.6. Humanization of murine antibodies for human therapy

The majority of hybridomas are of murine origin and murine antibodies have been developed for human applications [103], [104]. However, murine antibodies have a short half-life in serum, only some of the different classes can mediate effector functions and the murine mAbs can elicit an immune response in patients, characterized by human anti-mouse antibodies (HAMA) [64], [105]. To overcome side effects of murine antibodies in therapy, a variety of humanization techniques have been developed to replace murine antibody sequences with ones of human origin (Fig. 9A). The replacement of the murine constant regions with those from human antibodies results in a chimeric antibody, which demonstrates reduced immunogenicity [106], [107], [108]. Nonetheless, clinical trials have demonstrated that chimeric antibodies are still capable to trigger a HAMA response specific for the murine variable regions [109]. To further reduce immunogenicity, the murine CDR regions are transplanting to a homologous framework [110], [111]. This humanization strategy is termed CDR grafting and reduces, but does not eliminate, the risk of HAMA. The transfer of CDR regions results in humanized antibodies, which contain the murine CDR regions in a complete human framework (Fig. 9B). The humanized antibody preserved binding properties of the original mouse antibody, since the CDRs are responsible for antigen contact and binding [110], [111]. However, the substitution of key residues in the human framework by the ones from the murine antibody can modulate the binding affinity. Therefore, the most challenging issue in the CDR grafting is the identification of the essential murine framework residues for affinity [112]. New technologies have been discovered to prevent HAMA response of engineered antibodies. For this purpose, transgenic mice were developed, in which the native immunoglobulin repertoire has been replaced with human V-genes to

generate human antibodies. Further approaches are the phage display and the generation of mAbs from single human b-cells [113], [114], [115].

Immunological strategies based on therapeutic antibodies have the potential to close the gap for an efficient treatment of antibiotic resistant MRSA. However, before a promising antibody candidate can be selected, a target for future immunotherapy has to be identified and characterized by following properties: cell surface exposure, *in vivo* expression by the majority of clinical relevant strains, triggering an immune response and the antigen should be highly conserved between different strains.

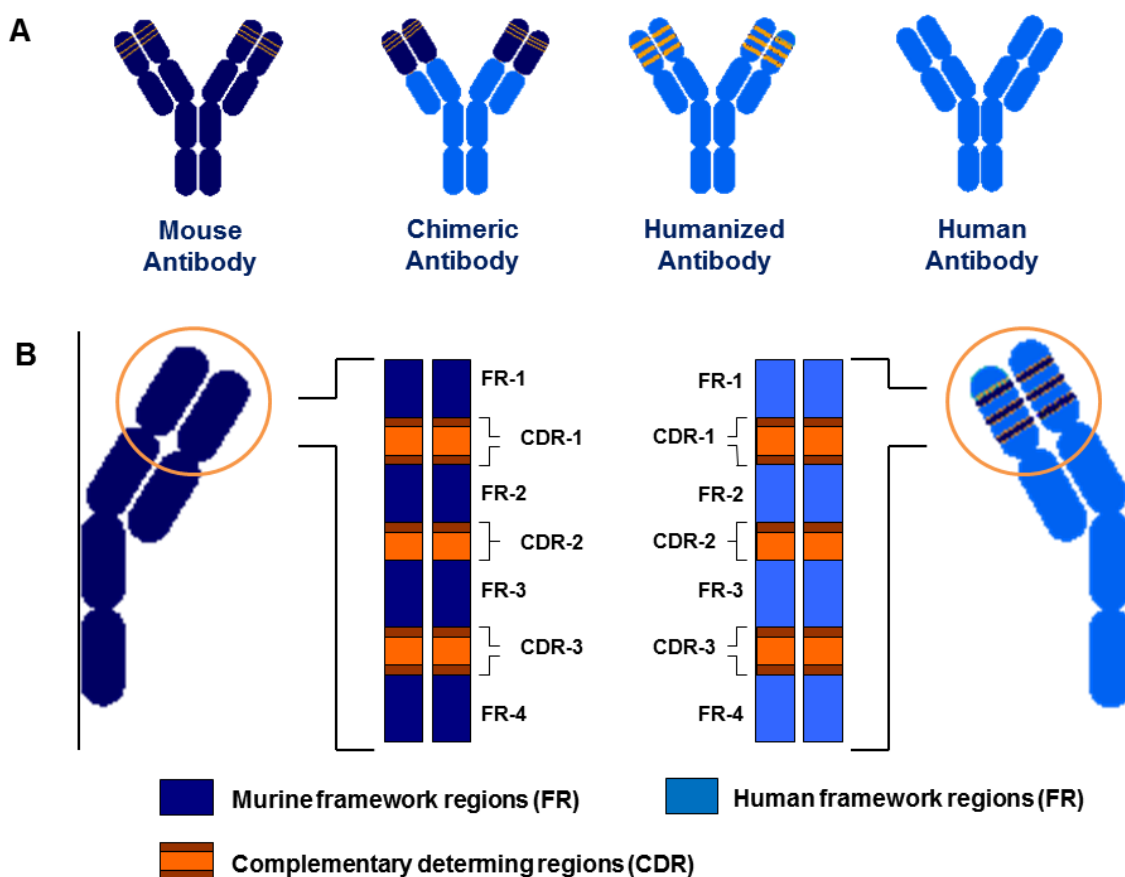


Fig. 9 Humanization of murine antibody by CDR grafting.

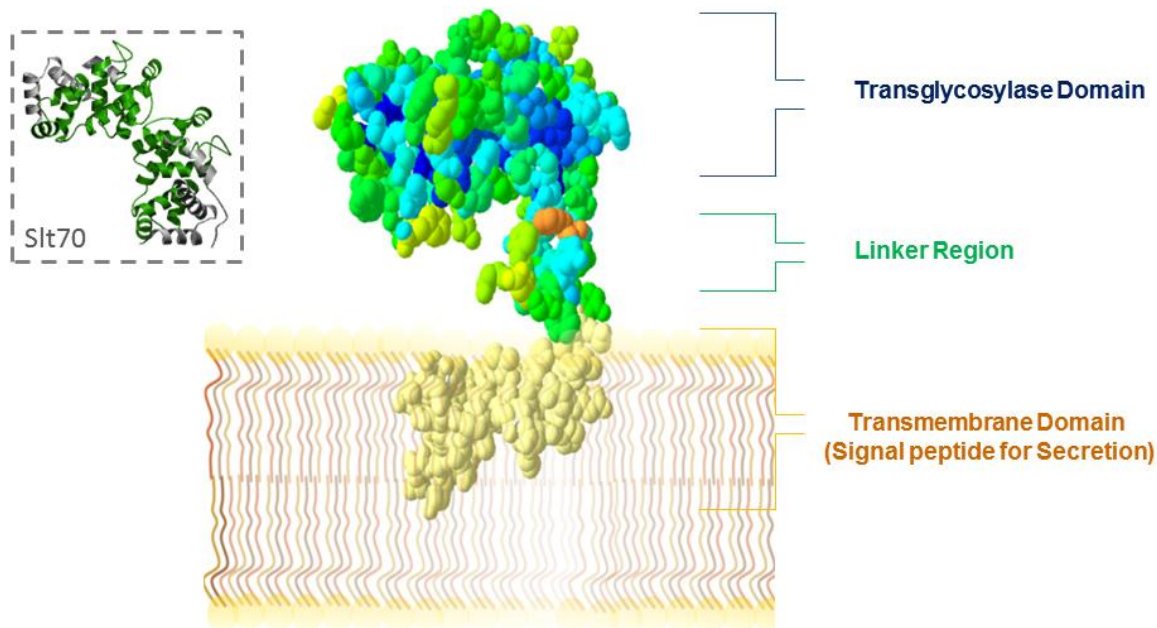
A) The purpose of humanization is to preserve binding affinity of the original murine antibody, but to reduce its immunogenicity. Therefore, the constant domains of mouse are replaced by a human framework to generate a chimeric antibody. Antibodies, which are complete human besides the murine CDR regions termed as humanized antibodies. B) The CDR regions are identified from the antigen binding domain and transferred to a human homologue framework.

3.7. Immunodominant antigen A (IsaA) - A putative transglycosylase

The immunodominant antigen A (IsaA) was identified as immunodominant structure, which is expressed *in vivo* during sepsis cause by MRSA. In this study, the antibody response in human sera from healthy donors was compared with those from patients 1 and 14 days after

the detection of MRSA in blood culture. Results from this study revealed a significant higher titer of anti-staphylococcal antibodies in patients with diagnosed sepsis compared to healthy individuals. Notable, none of the patients with high anti-staphylococcal antibody titers died of a septic shock [116]. Especially, antibodies against the 29 kDa IsaA protein were developed in patients with diagnosed sepsis.

The amino acid sequence indicated that IsaA possesses no Gram-positive bacterial cell wall sorting signal [117] and is a secretory protein consisting of 233 aa, including a N-terminal signal peptide of 29 aa. In its C-terminal region, IsaA possesses a sequence similar to the lytic transglycosylase (SLT) domain. Among bacterial proteins, the IsaA SLT motif shows high similarity to *E. coli* soluble transglycosylase Slt70 (Fig. 10) [118]. The SLT domain consists of three motifs that form the lytic transglycosylase catalytic region [119]. A spacer region between motif II and III was lacking in IsaA and homology in motif III was low, but all these motifs were found in the staphylococcal protein. Moreover, a glutamate, which had been shown to be involved in Slt70 catalytic activity, and adjacent conserved serine residue in motif I were also maintained in IsaA [120]. Bioinformatic analysis of IsaA revealed that this protein is an exclusive paralogues in *S. aureus* and *S. lugdunensis* [121]. IsaA is a 29kDa, highly immunogenic, non-covalently cell wall bound lytic transglycosylase [118]. Based on its hydrolytic activity, IsaA assists in cell wall expansion, turnover, growth and cell separation [121]. Recently, it was shown that extracellular IsaA levels effect biofilm formation in *S. aureus* [122]. Therefore, IsaA is localized in the cell wall fraction for active bacterial growth and exists in the culture supernatant, where it acts as signal molecule [123]. Strains of *S. aureus* lacking IsaA are affected in normal growth and cell wall metabolism and demonstrate a clumping phenotype. However, the paralogue SceD, a second lytic transglycosylase, is able to compensate the loss of IsaA [121]. Furthermore, *isaA* gene expression is stimulated during the exponential growth phase and repressed in the stationary phase [123]. Therefore, IsaA protein is already detectable in the early growth phase and sustained during the exponential growth phase [123]. IsaA is a complex regulated protein. Aerated and microaerobic cultures indicated that IsaA expression is differentially regulated according to oxygen availability by SarA, SrrAB and YycFG [121]. Under anaerobic conditions, IsaA is down regulated [124]. The essential two-component system YycG and YycF are expressed during exponential growth and regulates IsaA via YycF binding to the promoter region of the IsaA gene [125].



Modified from J. Nelke (Bachelor 2013), calculated with I-TASSER

Fig. 10 Hypothetical structure of IsaA.

IsaA reveals high sequence similarities to the *E. coli* transglycosylases Slt70 and consists of a transglycosylase domain, a linker region and a transmembrane domain.

It is likely that IsaA production is stimulated by YycF at the beginning of the growth phase and then attenuated by *agr* system from the late exponential phase [126]. IsaA is also important for successful host pathogen interactions of *S. aureus*. In a mouse sepsis arthritis model the bacterial load in kidney 13 days after infection, revealed attenuated pathogenicity of *isa* mutant compared to the wild type. This finding reinforces the link between cell wall metabolism and bacterial fitness in this organism [121].

3.8. Transglycosylases

The cell wall is essential for survival of bacteria. The bacterial cell wall differs from the cell envelope of all other organisms by the presence of peptidoglycan (PG). Peptidoglycan (PG) is a heteropolymer comprising the rigid layer within bacterial cell walls. The repeating subunit of PG is composed of β -1,4-linked N-acetyl-D-glucosaminyl (GlcNAc) and N-acetyl-D-muramyl (MurNAc) residues. The glycan chains are cross linked together through peptides which stem from the 3-O-D-lactyl moiety of the muramyl residues to from a three-dimensional array covering the entire surface of the bacterial cytoplasmatic membrane [127]. However, the bacterial cell wall is a dynamic structure, which is continually expanded and turned over. This metabolism involves the creation of sites for the insertion of flagella, the creation of pores for secretion systems and during cell growth for insertion of peptidoglycan precursor (PG). A key class of enzymes responsible for cleaving PG to accommodate these requirements is the lytic transglycosylase (LT) [128]. Lytic transglycosylases (LTs) are

ubiquitous amongst the eubacteria except for the mycoplasmas. The variety of LT is classified into four distinct families based on sequence similarities and identified consensus motifs. Family-1 LTs, including IsaA, share a conserved E-S motif, with the glutamyl residue being essential for catalysis [129]. Despite lacking sequence similarities, most of the LTs are α -helical and their catalytic domains possess a “lysozyme” fold [128]. These lysozyme-like enzymes catalyze the cleavage of the β -1,4-glycoside bond between MurNAc and GlcNAc, which results in 1,6-anhydro-N-acetylmuramyl residue (Fig. 11) [130], [127]. By virtue of their ability to cleave the polysaccharide backbone of the PG layer, LTs play an important role in synthesis, degradation and recycling of PG. Together with amidases, LTs function is to split the septum and thereby permit the separation of dividing cells [131], [132]. They have also been implicated with insertion of protein complexes such as secretion systems, flagella and pili [133].

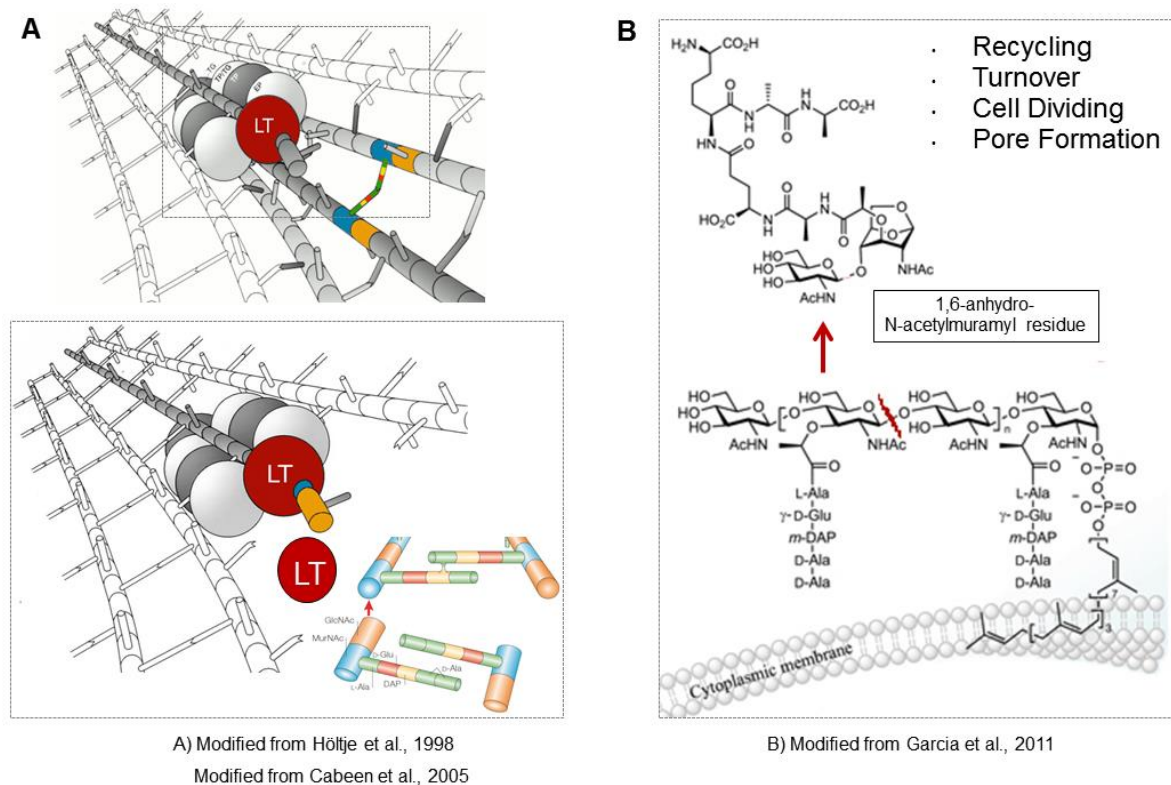


Fig. 11 Function of lytic transglycosylase (LT).

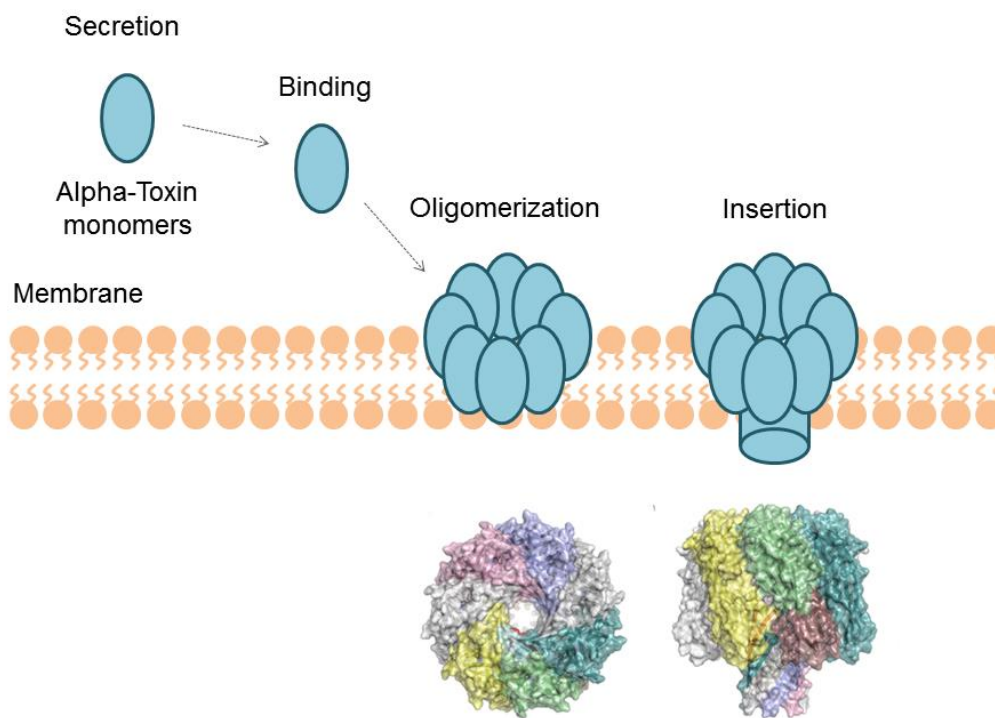
A) The LT is associated with the bacterial cell wall in a multi-enzyme complex and cleaves the polysaccharide backbone. B) After cleavage, the 1,6-anhydro-N-acetylmuramyl residues were transported for recycling. This mechanism of cell wall cleavage is essential for cell dividing, pore formation and cell wall turn over.

The role of LTs in pathogenesis is not fully understood, a number of LTs have been shown to be up-regulated during host infections. Furthermore, LT reaction products have been demonstrated to play a role in infectious disease [134]. This enzyme class possesses a great potential as target for an antibacterial therapy, based on their important cellular functions and that they act on structures unique for bacteria.

Further promising targets for an antibody based therapy are essential virulence factors such toxins which can be neutralized by antibody binding.

3.9. Alpha-toxin - A freely secreted toxin

S. aureus produces a large number of toxins that are grouped on the basis of their mechanism of actions [21]. One of the most investigated, since their discovery in the early 1960s [135], is the 33 kDa alpha-toxin (AT). This cytolytic pore-forming toxin is secreted as a water-soluble monomer by the majority of clinical relevant *S. aureus* strains and has been demonstrated to play a key role in different mouse and rabbit models of *S. aureus* disease like dermonecrosis, pneumonia and sepsis [136], [137]. The binding of AT monomers on the host membrane results in a formation of a barrel-shaped oligomeric pore that penetrates the membrane [138] (Fig. 12). In recent studies, it was shown that AT directly upregulates ADAM10 metalloprotease activity, which results in cleavage of host E-cadherin and the disruption of the epithelial barrier [139].



Modified from Huyet et al., Plos one, 2013

Fig. 12 Pore formation by alpha-toxin (AT).

Native AT is secreted as hydrophilic molecule. After binding to the host membrane, toxin molecules oligomerize to form stable protein complexes. This process is associated with an exposure of lipid-binding domains, resulting from conformational changes, that enables the spontaneously insertion into the membrane.

Alpha-toxin injures the lung and other tissues by its ability to form pores and thereby causes diseases ranging from minor skin infections to life-threatening deep tissue infections and toxinoses. In various animal models, immunization with antibodies directed against the

staphylococcal alpha-toxin protects against *S. aureus* colonization or infection and results in a significant increase of survival in the treated animals compared to untreated animals [140], [141], [142], [143].

Currently, promising clinical trials with anti-alpha-toxin antibodies are ongoing based on the promising animal data. For this study, a humanized anti-alpha-toxin IgG1 antibody (hUK-tox) was chosen to be tested in a combinatorial therapy with hUK-66 IgG1.

3.10. Aim of the thesis

Antibodies are routinely used in the fields of biochemistry, molecular biology and medical research but the greatest achievement has been their use as therapeutic agent. Antibodies are powerful tools in the treatment of diseases such breast cancer, leukemia, asthma, arthritis, Crohn's disease and transplant rejection. However, only one mAb has been licensed for the treatment of respiratory-syncytial-virus infection and at this time there is no antibacterial antibody in clinical used.

The aim of this work is the development of a humanized antibody as a candidate for an antibody-based therapy against antibiotic resistant MRSA. Therefore, the mouse monoclonal antibody (mUK-66), specific for the immunodominant staphylococcal antigen A (IsaA), was selected by its anti-staphylococcal activity in mouse infection models for humanization by CDR grafting. In this study, the humanized anti-IsaA antibody (hUK-66) is analysed by its binding affinity and characterized in terms of *in vitro* and *in vivo* functionality. In the course of this work, the biological activity of hUK-66 was analysed *in vitro* with whole blood samples from healthy donors and patients at high risk of *S. aureus* infections. *In vivo*, a mouse pneumonia model is established to analyse the antibody's potency. Furthermore, the work presented in this thesis includes first results for a combined antibody therapy consisting of hUK-66 IgG1 and the humanized anti-alpha-toxin antibody (UK-tox).

4. Material

All used consumables were purchased from BioRad (Munich, Germany), Greiner Bio One (Frickenhausen, Germany), Peqlab (Erlangen, Germany), Macherey-Nagel (Dueren, Germany), Millipore (Darmstadt, Germany), MP Biomedicals (Eschwege, Germany), Sarstedt (Germany), SIGMA Alderich (Taufkirchen, Germany), Roth (Karlsruhe, Germany), Applichem (Darmstadt, Germany) and MERCK (Darmstadt, Germany).

All used antibiotics, chemicals, enzymes and solutions were purchase from Applichem (Darmstadt, Germany), BioRad (Munich, Germany), GE Healthcare (Munich, Germany), Invitrogen (Darmstadt, Germany), MBI-Fermentas (Schwerte, Germany), MERCK (Darmstadt, Germany), New England Biolabs (Ipswich, Great Britanien), Peqlab (Erlangen, Germany), Promega (Madison (WI) USA), Qiagen (Hilden, Germany), Roche (Penzberg, Germany), Roth (Karlsruhe, Germnay) and Sigma-Aldrich (Taufkirchen, Germany).

4.1. Equipment

Table 4.1 Equipment

Equipment	Manufacturer
Blot system semi dry	Invitrogen, Eugene (O), USA
Centrifuge Pico 17, Biofug 13R,	Heraeus, Hanau, Germany
Cryogenic Vials	Thermo Scientific, Rochester (NY), USA
Flow Cytometer	FACS Calibur, BD
Freezer, -80°C	Thermo Fisher Scientific, Schwerte, Germany
Gel documentation system	Intas, Göttingen, Germany
Gel electrophoresis system DNA Sub Cell	Bio-Rad, Champaign, USA
Glas bottles	Brand, Wertheim, Germany
Heat Block Thermostat 5320	Eppendorf, Hamburg, Germany
Heat Block Labtherm [®]	Liebisch, Bielefeld, Germany
Homogenisator Dispomix [®]	BioLab Products, Gödenstorf, Germany
Incubator for rotation Mini 10	Hybaid, Heidelberg, Germany
Incubator for shaking SM-30, Innova 4300	Edmund Bühler, Hechingen, Germany New Brunswick Scientific, Hamburg, Germany
Microplate reader Tecan infinite M200, Multiskan	Thermo Electron, Dreieich, Germany
Microscope	Zeiss, Oberkochen, Germany
Light microscope Telaval 31, Fluorescence microscope Axiolab, Confocal microscope LSM 510	
pH meter pH720	inoLab, Weilheim, Germany
Photometer Ultrospec 3100 pro	Amersham, Freiburg, Germany
Pipettes	Eppendorf
Pipettor accu-jet [®] pro	Brand
Protein Page system	BioRad,
Sonicator	Sonica, Newton (CT), USA
Spectrophotometer Nano-drop ND-1000	Peqlab, Erlangen, Germany
Temperature/ CO ₂ controlled incubator	Triad, Manasquan (NY), USA
Thermocycler T3	Biometra, Göttingen, Germany

4.2. Consumables

Table 4.2 Consumables

Consumables	Manufacturer
Bioreactor, Cell line adhere	Integra, Zizers, Switzerland
Blotting Membrane Nitrocellulose	GE Healthcare, Munich, Germany
Blotting Whatman paper	GE Healthcare, Munich, Germany
Centrifugal Filter Units	Millipore, Darmstadt, Germany Satorius Stedim, Hartenstein, Germany
Columns	Greiner, Frickenhausen, Germany
Cuvettes	Brand, Wertheim, Germany
Cryotubes	Nunc G,bH, Wiesbaden-Biebrich, Germany
Culture flasks	Greiner, Frickenhausen, Germany
Culture plates, 24-well, 12-well, 6-well,	Greiner, Frickenhausen, Germany
Dialysis tube ZelluTrans	Roth, Karlsruhe, Germany
Falcon Tubes, 15 ml, 50 ml	Sarstedt, Nürnberg, Germany
Filter Units	Laborhaus Scheller, Euerbach, Germany
Hyodermic needle G20, G30	Braun, Hartenstein, Germany
Micro 96-well plate	Nunc Thermo Scientific, Roskilde, Denmark
Microscope slides	Hartenstein, Würzburg, Germany
Microscope slide covers	Hartenstein, Würzburg, Germany
Microtubes, 2ml, 1.5ml	Sarstedt, Nürnberg, Germany
Monovettes, Heparin	Sarstedt, Nürnberg, Germany
Multify-Set Safety	Sarstedt, Nürnberg, Germany
Parafilm	Pechiney Plastic Packaging,
Petri Dishes	Greiner, Frickenhausen, Germany
PCR reaction tubes	Sarstedt, Nürnberg, Germany
pH indicator strips, pH 0-14	Macherey Nagel, Düren, Germany
Syringes	Hartenstein, Würzburg, Germany
Tips 1000 µl, 200 µl, 10 µl	Sarstedt, Nürnberg, Germany

4.3. Chemicals

Table 4.3 Chemicals

Chemicals	Manufacturer
Acetic Acid	Roth, Karlsruhe, Germany
Agar	Roth, Karlsruhe, Germany
Agarose	PeqLab, Erlangen, Germany
Ammoniumperoxodisulfat (APS)	Roth, Karlsruhe, Germany
Ampicillin	Roth, Karlsruhe, Germany
Bovine Serum Albumin Fr.	Roth, Karlsruhe, Germany
6-Carboxylfluoresceindiacetate, succinimidyl ester (CFSE)	Invitrogen, Eugene (O), USA
DMSO	Invitrogen, Eugene (O), USA
1,4 Dithiothreitol (DTT)	Roth, Karlsruhe, Germany
EDTA	Roth, Karlsruhe, Germany
Erythromycin	Roth, Karlsruhe, Germany

Ethanol abs.	Roth, Karlsruhe, Germany
Ethanol, denatured	Roth, Karlsruhe, Germany
Ethidiumbromid-Solution	Roth, Karlsruhe, Germany
Glucose D(+)	Roth, Karlsruhe, Germany
Glycine	Roth, Karlsruhe, Germany
Hydrochloric acid 37%	Roth, Karlsruhe, Germany
Hydrogen peroxide 30%	Roth, Karlsruhe, Germany
Imidazol	Roth, Karlsruhe, Germany
Kanamycin	Roth, Karlsruhe, Germany
Luria Broth (LB) Medium	Roth, Karlsruhe, Germany
Magnesium chloride	Roth, Karlsruhe, Germany
Methanol	Roth, Karlsruhe, Germany
Milkpowder	Roth, Karlsruhe, Germany
MSX	Sigma-Aldrich, Steinheim, Germany
2-Propanol	Roth, Karlsruhe, Germany
Polyacrylamide	Roth, Karlsruhe, Germany
Potassium chloride	Roth, Karlsruhe, Germany
Sodium bicarbonate	Roth, Karlsruhe, Germany
Sodium carbonate	Roth, Karlsruhe, Germany
Sodium chloride	Roth, Karlsruhe, Germany
Sodium dodecyl sulphate pellets (SDS)	Roth, Karlsruhe, Germany
Sodium hydroxide pellets	Roth, Karlsruhe, Germany
Spectinomycin	Roth, Karlsruhe, Germany
Sulfuric acid, 96%	Roth, Karlsruhe, Germany
TEMED	Roth, Karlsruhe, Germany
Tris	Roth, Karlsruhe, Germany
Triton-X100	Roth, Karlsruhe, Germany
Tween20	Roth, Karlsruhe, Germany
Zeocin	Invitrogen, Eugene (O) USA

4.4. Buffer and Solutions

Table 4.4 Buffer and Solutions

Buffer/ Solution	Components
Anode buffer I, 10x	40 g Tris-Base, 0.1 l MetOH, pH 10.4
Anode buffer II, 10x	3 g Tris-Base, 0.1 l MetOH, pH 10.4
CaCl ₂ , 100 mM	219 g CaCl ₂ , adjust volume to 1 l
Coomassie destaining solution	0.33 l EtOH, 0.1 l acetic acid (add H ₂ O to 1 l)
Coomassie staining solution	0.6 g G250, 0.6 g R250, 0.45 l EtOH, 0.09 l acetic acid (add H ₂ O to 1 l)
DNA Loading Dye, 6x	6 ml Glycerol, 0.6 ml 1 M Tris-HCl (pH 8), 0.12 ml 0.5 M EDTA (pH 8), 3.3 ml H ₂ O, 6 mg Bromphenolblue
Erythrocytes lysis buffer, 10x	9 g NH ₄ Cl, 1g KHCO ₃ , 37 mg EDTA, adjust to 100 ml H ₂ O
HBSS	Invitrogen, Eugene (O) USA
Kathode buffer, 10x	5 g ε-aminocaprene acid, 0.1 l MetOH, pH 10.4
Periplasmatic preparation buffer	30 mM Tris-HCl (pH 8), 1 mM EDTA, 20% Succrose (add H ₂ O to 1l)

Phosphate buffered saline (PBS, 10x)	80 g NaCl, 2 g KCl, 27 g Na ₂ HPO ₄ , 2.5 g KH ₂ PO ₄ dissolve in 1 l H ₂ O, adjust to pH 7.4
Buffer I	50 mM Tris-HCl, pH 7.5, 10 mM EDTA, pH 8, 0.1 mg/ml RNase A (100 ml buffer)
Buffer II	0.2 N NaOH, 1% SDS
Buffer III	3 M sodium acetate, pH 4.8
IMAC binding buffer	50 mM NaPO ₄ , 0.5 mM NaCl, pH 7.4
IMAC elution buffer	50 mM NaH ₂ PO ₄ , 500 mM NaCl, 100 mM Imidazole
IMAC wash buffer	50 mM NaH ₂ PO ₄ , 500 mM NaCl, 20-200 mM Imidazole
IPTG, 1M	0.125 g IPTG, adjust to 1 ml
MgCl ₂ , 1M	20.3 g MgCl ₂ , adjust to 0.1 l
NaCl, 5M	293 g NaCl, adjust volume to 1 l
Na ₂ EDTA	186 g Na ₂ EDTA, pH 8 adjust to 1 l
Protein A binding buffer	Macherey Nagel, Düren, Germany
Protein A elution buffer	50 mM Glycine-HCl, pH 2.7 and pH1.9
Protein A neutralization buffer	1 M Tris-HCl, pH 8, 1.5 M NaCl, 1mM EDTA (add to 0.1 l H ₂ O)
SDS, 10%	1 g SDS pellets, adjust to 10 ml
SDS running buffer, 10x	30 g Tris-Base, 144 g Glycine, 10 g SDS (add H ₂ O to 1l)
SDS sample buffer, 4x	20 ml Glycerol, 5 g SDS, 13 ml 1 M Tris-HCl (pH 6.8), 0.2 g Bromphenoleblue (add H ₂ O to 50 ml)
TAE buffer, 50x	242 g Tris, 100 ml 0.5 M Na ₂ EDTA (pH8), 57 ml acetic acid, adjust to 1 l H ₂ O
TBS, 10x	0.5 M Tris-HCl, pH 7.4, 1.5 M NaCl (add to 1 l H ₂ O)
TCA, 100%	500 g TCA, 230 ml H ₂ O
Tris, 1M	122 g Tris, adjust to 1 l
Tryptophan Blue solution	Invitrogen, Eugene (O), USA
X-gal	200 mg X-gal dissolve in 10 ml dimethylformamide

4.5. Enzymes, Kits and Reagents

Enzyme reactions were performed in buffers and solutions provided by the manufacturer.

Table 4.5 Enzymes, Kits and Reagents

Kits	Manufacturer
Anartic Phosphatase	New England BioLabs,
Antibody capture kit	GE Healthcare, Munich, Germany
DnaseI	Roche, Mannheim, Germany
ECL™ Advance Detection Kit	GE Healthcare, Freiburg, Germany
Ficoll	GE Healthcare, Freiburg, Germany
Gene Clean® Kit III	MP Biomedicals, Ohio, USA
GeneRuler™ 1 kb DNA Ladder	Fermentas, Darmstadt, Germany
Lipofectamine	Invitrogen, Eugene (O), USA
Lysozym	Sigma-Aldrich, Taufkirchen, Germany
Nucleotidetriphosphate (100 mM)	Qiagen, Hilden, Germany
PCR-Purification Kit	Qiagen, Hilden, Germany
pGEMT®-T Vector system	Promega, Mannheim, Germany

Phusion™ High-Fidelity DNA Polymerase	NEB, Frankfurt, Germany
Protease Inhibitor Mix	Roche, Penzberg, Germany
Protino® Protein Purification System	Machery-Nagel, Düren, Germany
Quick T4 Ligation Kit	New England BioLabs, Ipswich, England
Restriction enzymes: ApaLI, NcoI, NotI, SfiI, XhoI	New England BioLabs, Ipswich, England
T4 Ligation Kits	New England BioLabs, Ipswich, England
TMB Solution	Invitrogen, Eugene(O), USA
Trypsin-EDTA, 10x	Invitrogen, Eugene (O), USA

4.6. Media and Supplements

Table 4.6 Media and Supplements

Media/Supplement	Components/ Manufacturer
FCS	Invitrogen, Eugene (O), USA
Insulin, human recombinant	PAN Biotech, Aidenbach, Germany
Luria Bertani (LB)	10 g Peptone, 10 g NaCl, 5 g Yeast extract (add to 1 l H ₂ O)
OptiMEM	Invitrogen, Eugene (O), USA
RPMI 1640	Invitrogen, Eugene (O), USA
RPMI 1640 without (L)-glutamine	Invitrogen, Eugene (O), USA
Trypsin, EDTA, 100x	Invitrogen, Eugene (O), USA
Trypton-Yeast	8 g Peptone, 5 g Yeast extract, 2.5 g NaCl, adjust to 1 l H ₂ O

4.7. Antibodies

Table 4.7 Antibodies

Antibody	Conjugated	Species	Company	Storage
Anti-His	HRP	Rabbit	MicroMol, #414	-20°C
Anti-human CD32	PE	Mouse	Biozol, 303206	4°C
Anti-human CD64	PE	Mouse	Biozol, 305008	4°C
Anti-human IgG	PE	Goat	Antibodies-online, ABIN117687	4°C
Anti-human IgG		Goat	Biozol, 2062-01	4°C
Anti-human IgG	HRP	Goat	Antibodies-online, ABIN117685	-20°C
Anti-human IgG F(ab') ₂	FITC	Goat	Biozol, BZL08564	4°C
Anti-human IgG1	HRP	Mouse	Antibodies-online, ABIN289146	-20°C
Anti-human IgG2	HRP	Mouse	Biozol, 9060-05	4°C
Anti-human IgG3	HRP	Mouse	Biozol, 9210-05	4°C
Anti-human IgG4	HRP	Mouse	Biozol, 9200-05	4°C
Anti-mouse IgG+IgM	HRP	Rabbit	Jackson, 315-035-048	-20°C
Anti-mouse IgG	HRP	Rabbit	Jackson, 315-035-008	-20°C
Anti-mouse IgG1	HRP	Rabbit	LifeSpan, C70235/20993	LS- -20°C
Anti-Myc		Rabbit	Biozol, bs-0842R	-20°C
Anti-Myc	HRP	Rabbit	Antibodies-online, ABIN398408	4°C
Anti-rabbit	HRP	Goat	SAB, L3012	4°C

4.8. Plasmids

Table 4.8 Plasmids

Plasmids	Description
pAB	Amp ^r , His-Tag, Myc-Tag
pEE6.4	MSX ^r , Lonza [®]
pEE12.4	MSX ^r , Lonza [®]
pEMT11	Kan ^r
pGMT	Amp ^r
pHEN2	Amp ^r
pQE30	Amp ^r ,
pSEC TagA	Zeo ^r

4.9. Bacterial strains

Table 4.9 Bacterial strains

Strain	Genotype and/or Description	Reference	
<i>S. aureus</i>			
SA001	CAMRSA	MW2 (USA400)	RKI, Wernigerode
SA002	EMRSA	EMRSA-15	RKI, Wernigerode
SA003	MRSA 05-01702	Cip-R, MFL-R, ST 5	RKI, Wernigerode
SA004	MRSA 07-00929	Cip-R, MFL-S, ST 8	RKI, Wernigerode
SA005	MRSA 07-01643	Cip-R, MFL-S, ST 22	RKI, Wernigerode
SA006	MRSA 07-03310	Cip-R, MFL-S, ST 45	RKI, Wernigerode
SA007	MRSA 05-01977	Cip-R, MFL-R, ST 228	RKI, Wernigerode
SA008	MRSA 08 00465-1	Cip-R, MFL-R, ST 239	RKI, Wernigerode
SA009	<i>S. aureus</i> ANS46	SSC <i>mec</i> III	
SA010	<i>S. aureus</i> BK2464	SSC <i>mec</i> II	
SA011	<i>S. aureus</i> Col	Δ <i>isaA</i>	
SA012	<i>S. aureus</i> Cowan	DU 5889	
SA013	<i>S. aureus</i> FUS239		
SA014	<i>S. aureus</i> HDE288	SSC <i>mec</i> IV	
SA015	<i>S. aureus</i> LAC	USA300	
SA016	<i>S. aureus</i> MA12	Wild type	Rachelt et al., 2001
SA017	<i>S. aureus</i> MA12 <i>spa</i> ⁻	Insertion mutant <i>spa</i> ⁻	U. Wallner, IMIB Würzburg
SA018	<i>S. aureus</i> MA12 <i>spa</i> ⁻ <i>/isaA</i> ⁻	Insertion mutant <i>spa</i> ⁻ / <i>isaA</i> ⁻	U. Wallner, IMIB Würzburg
SA019	<i>S. aureus</i> Newman	Wild type	IMIB, Würzburg
SA020	<i>S. aureus</i> Newman GFP	Wild type, pJL74 GFP, pCN54 exchanged of P <i>cad</i> promotor with constitutive SarAP1 promotor, Erm ^r	J. Liese, University Tübingen
SA021	<i>S. aureus</i> Newman CFP	Wild type, pJL76 CFP, pCN54 exchanged of P <i>cad</i> promotor with constitutive SarAP1 promotor, Erm ^r	J. Liese, University Tübingen
SA022	<i>S. aureus</i> Newman YFP	Wild type, pJL77 YFP, pCN54 exchanged of P <i>cad</i> promotor with constitutive SarAP1 promotor, Erm ^r	J. Liese, University Tübingen
SA023	<i>S. aureus</i> RN4220	NCTC 8325-4r, restriction mutant with 11 bp depletion in <i>rsbU</i>	Kreiswirth, 1983
SA024	<i>S. aureus</i> SH1000		
SA025	<i>S. aureus</i> Wood46	Wild type	

SA026	<i>S. aureus</i> Xen29	Luminescent strain	U. Wallner, IMIB, Würzburg
SA027	<i>S. aureus</i> Xen29 <i>isaA</i> ⁻	Luminescent strain, Insertion mutant <i>isaA</i>	U. Wallner, IMIB, Würzburg
SA028	<i>S. aureus</i> 8325	Wild type	U. Wallner, IMIB, Würzburg
SA029	<i>S. aureus</i> 8325 <i>spa</i> ⁻	Insertion mutant <i>spa</i> ⁻	U. Wallner, IMIB, Würzburg
SA030	<i>S. aureus</i> 8325 <i>spa</i> ⁻ / <i>isaA</i> ⁻	Insertion mutant <i>spa</i> ⁻ / <i>isaA</i> ⁻	U. Wallner, IMIB, Würzburg
<i>E. coli</i>			
EC001	<i>E. coli</i> BL21	F ⁻ , <i>ompT hsdS_B(r_B⁻, m_B⁻)</i> , <i>dcm gal λ</i> (DE3)	Merck Bioscience
EC002	<i>E. coli</i> DH5α	F ⁻ , <i>endA1, hsdR17 (r_K⁻, m_K⁻)</i> , <i>supE44, thi-1, recA1, GyrA96, relA1, λ⁻, Δ(argF-lac)U169, Φ80d/lacZ ΔM15</i>	MBI-Fermentas
EC003	<i>E. coli</i> KRX	K-12 <i>supE thi-1 Δ(lac-proAB) Δ(mcrB-hsdSM)5, (r_K⁻m_K⁻)</i> , F' [<i>traD36 proAB⁺ lac^f lacZΔM15</i>] <i>ΔompT, endA1, recA1, gyrA96 (Nal^r), thi-1, hsdR17 (rK⁻, mK⁺), e14(McrA), relA1, supE44, Δ(lacproAB), Δ(rhaBAD)</i>	Promega
EC004	<i>E. coli</i> M15	pRep4, F ⁻ <i>lacZD M15 lacIq traD36 proA⁺ proB⁺, Kan^r</i>	Qiagen
EC005	<i>E. coli</i> TG1	K-12 <i>supE thi-1 Δ(lac-proAB) Δ(mcrB-hsdSM)5, (r_K⁻m_K⁻)</i> , F' [<i>traD36 proAB⁺ lac^f lacZΔM15</i>]	R. Kontermann, University Stuttgart
EC006	<i>E. coli</i> TG1 pAB scFv Gal12	pAB, Amp ^r , Insert: scFv Gal12	R. Kontermann, University Stuttgart
BO001	<i>E. coli</i> TG1 pHEN2	pHEN2, Amp ^r	B. Oesterreich, this study
BO002	<i>E. coli</i> TG1 pAB	pAB, Amp ^r	B. Oesterreich, this study
BO003	<i>E. coli</i> TG1 pEE6.4	pEE6.4, MSX ^r	B. Oesterreich, this study
BO004	<i>E. coli</i> TG1 pEE12.4	pEE12.4, MSX ^r	B. Oesterreich, this study
BO005	<i>E. coli</i> TG1 pMA mUK-66	pMA, Amp ^r , Insert: scFv mUK-66	B. Oesterreich, this study
BO006	<i>E. coli</i> TG1 pMA hUK-66(1)	pMA, Amp ^r , Insert: scFv hUK-66(1)	B. Oesterreich, this study
BO007	<i>E. coli</i> TG1 pMA hUK-66(2)	pMA, Amp ^r , Insert: scFv hUK-66(2)	B. Oesterreich, this study
BO008	<i>E. coli</i> TG1 pMA human IgG1	pMA, Amp ^r , Insert: UK-66 human IgG1	B. Oesterreich, this study
BO009	<i>E. coli</i> TG1 pMA human IgG2	pMA, Amp ^r , Insert: UK-66 human IgG2	B. Oesterreich, this study
BO010	<i>E. coli</i> TG1 pMA human IgG4	pMA, Amp ^r , Insert: UK-66 human IgG4	B. Oesterreich, this study
BO011	<i>E. coli</i> TG1 pSEC TagA Fc human IgG1	pSEC TagA, Zeo ^r , Insert: Fc human IgG1	B. Oesterreich, this study
BO012	<i>E. coli</i> TG1 pHEN2 scFv mUK-66 (hc)	pHEN2, Amp ^r , Insert: scFv mUK-66 (heavy chain)	B. Oesterreich, this study
BO013	<i>E. coli</i> TG1 pHEN2 scFv mUK-66 (lc)	pHEN2, Amp ^r , Insert: scFv mUK-66 (light chain)	B. Oesterreich, this study

BO014	<i>E. coli</i> TG1 pAB scFv mUK-66	pAB, Amp ^r , Insert: scFv mUK-66	B. Oesterreich, this study
BO015	<i>E. coli</i> TG1 pAB scFv hUK-66(1)	pAB, Amp ^r , Insert: scFv hUK-66(1)	B. Oesterreich, this study
BO016	<i>E. coli</i> TG1 pAB scFv hUK-66(2)	pAB, Amp ^r , Insert: scFv hUK-66(2)	B. Oesterreich, this study
BO017	<i>E. coli</i> TG1 pSEC TagA scFv-Fc mUK-66	pSEC TagA,Zeo ^r , Insert: scFv-Fc mUK-66	B. Oesterreich, this study
BO018	<i>E. coli</i> TG1 pSEC TagA scFv-Fc hUK-66(1)	pSEC TagA,Zeo ^r , Insert: scFv-Fc hUK-66(1)	B. Oesterreich, this study
BO019	<i>E. coli</i> TG1 pSEC TagA scFv-Fc hUK-66(2)	pSEC TagA,Zeo ^r , Insert: scFv-Fc hUK-66(2)	B. Oesterreich, this study
BO020	<i>E. coli</i> TG1 pEE6.4 hUK-66 IgG1 (hc)	pEE6.4, MSX ^r , Insert: hUK-66 IgG1 (heavy chain)	B. Oesterreich, this study
BO021	<i>E. coli</i> TG1 pEE6.4 hUK-66 IgG2 (hc)	pEE6.4, MSX ^r , Insert: hUK-66 IgG2 (heavy chain)	B. Oesterreich, this study
BO022	<i>E. coli</i> TG1 pEE6.4 hUK-66 IgG4 (hc)	pEE6.4, MSX ^r , Insert: hUK-66 IgG4 (heavy chain)	B. Oesterreich, this study
BO023	<i>E. coli</i> TG1 pEE12.4 hUK-66 IgG1	pEE12.4, MSX ^r , Insert: hUK-66 IgG1	B. Oesterreich, this study
BO024	<i>E. coli</i> TG1 pEE12.4 hUK-66 IgG2	pEE12.4, MSX ^r , Insert: hUK-66 IgG2	B. Oesterreich, this study
BO025	<i>E. coli</i> TG1 pEE12.4 hUK-66 IgG4	pEE12.4, MSX ^r , Insert: hUK-66 IgG4	B. Oesterreich, this study
BO026	<i>E. coli</i> TG1 pEE12.4 mUK-66 IgG1	pEE12.4, MSX ^r , Insert: mUK-66 IgG1	B. Oesterreich, this study
BO027	<i>E. coli</i> BL21 pEM11 IsaA	pETM11, Kan ^r , Insert: IsaA, C-term. His Tag	B. Oesterreich, this study
BO028	<i>E. coli</i> KRX pEM11 IsaA	pETM11, Kan ^r , Insert: IsaA, C-term. His Tag	B. Oesterreich, this study
BO029	<i>E. coli</i> M15 pRep4, pQE30_IsaA	pE30, Kan ^r , Amp ^r , Insert: IsaA, N-term. His Tag	P.Bouret, IMIB, Würzburg

5. Methods

5.1. Molecular biological Methods

5.1.1. Culturing of bacteria

All strains were propagated in lysogenic broth (LB) at 37°C with shaking at 175 rpm. When required, antibiotics were added to media at the following concentration: kanamycin 50 µg/ml; spectinomycin 100 µg/ml, erythromycin 5 µg/ml, and ampicillin 100 µg/ml. *E. coli* strains, used for expression of antibody fragments, were propagated in Trypton-Yeast broth (TY). The generation of *S. aureus* MA12 $\Delta isaA$ and Δspa mutants was achieved by allelic replacement and confirmed by PCR and Western blotting. All *S. aureus* mutant strains applied in this thesis were constructed by Ursula Wallner. The *E. coli* strain M15Rep4 which was used for expression of recombinant IsaA was constructed by Partrick Bourdet. For *in vivo* experiments, glycerin stocks of *S. aureus* Newman was harvested at mid-log phase and stored at -80°C (performed by TA Ursula Wallner). The optical densities of the cultures were measured at 600 nm with a photometer (Eppendorf).

5.1.2. Preparation of bacteria stocks for *in vivo* experiments

Stocks of bacteria for *in vivo* experiments were prepared to reduce variability of bacteria between two experiments and to minimize variance of overnight cultures. All stocks of one batch are grown at the same conditions and the lethal dose for each new batch was determined *in vivo*. For every new batch, the strain was plated on B agar from its cryo stock. Colonies from plate were inoculated in 3 ml BHI broth and incubated overnight at 37°C with shaking. After this, 50 ml BHI broth was inoculated with the prepared overnight culture and incubated for 3.5 h at 37°C. The complete culture was spin down for 10 min at 4000 rpm at 4°C. After resuspending the pellet in 20 ml BHI broth, 4 ml glycerol was added and the bacteria suspension was aliquot in 2 ml. Aliquots were storage at -80°C.

5.1.3. Preparation of bacteria for *in vivo* experiments

For infection studies, *S. aureus* Newman stock samples were thawed for 15 min at room temperature. After washing in 50 ml of sterile PBS (centrifugation at 4000 rpm at 4°C for 20 min), the pellet was diluted to a concentration of 2×10^8 cfu/mouse. The infectious dose for the used stock was determined before in dose titration experiments. Infection was performed using a total volume of 20 µl. The infectious dose was controlled by measuring optical

density at 600 nm ($1 \text{ OD}_{600} = 5.7 \times 10^9 \text{ ml}^{-1}$) and by plating appropriate dilutions in duplicate on LB agar and cfu were counted after 24 hours of incubation.

5.1.4. Cryoconservation of bacterial cultures

For long-term storage at -80°C , glycerol stocks of bacterial cultures were provided with 15% final glycerol concentration.

5.1.5. Transformation of competent *E. coli* cells

Chemical-competent BL21, DH5 α and TG1 cells were thawed on ice and incubated with DNA solution for 45 min on ice. Bacteria were then transformed by heat shock at 42°C for 2 min. After heat shock, 1 ml LB media was added immediately and cells were incubated at 37°C , shaking at 200 rpm for 1 h. The whole bacteria suspension was applied on an agar plate containing the appropriate antibiotic and incubated at 37°C overnight.

5.1.6. Preparation of Plasmid DNA

Bacteria were cultured overnight in 5 ml LB medium containing appropriate antibiotics at 37°C . The culture was centrifuged and the supernatant discarded. The bacterial pellet was resuspended in 150 μl buffer 1, followed by adding 150 μl of buffer 2. The bacterial suspension was inverted several times and incubated for 5 min at RT. After adding 150 μl of buffer 3, the bacterial suspension was incubated for 5 min on ice and then centrifuged for 15 min at 13,000 rpm. The supernatant was transferred to a fresh tube and centrifugation procedure was repeated. The supernatant was collected and DNA was precipitated with 70% isopropanol. After centrifugation for 15 min at 13,000 rpm at RT, supernatant was discarded and plasmid DNA was washed with 70% Ethanol. The DNA was harvest, air-dried and diluted in 30 μl sterile ddH $_2\text{O}$. Plasmid DNA samples were stored at -20°C .

5.1.7. Quantification of DNA

The concentration and purity of DNA was determined by measuring the optical density with the spectrophotometer Nanodrop[®] according to instructions of manufacturer.

5.1.8. Polymerase chain reaction

Polymerase chain reaction (PCR) was used to amplify DNA fragments and to introduce restriction sites via primers for a subsequent cloning step. The amplification reaction includes the sample of template DNA, two oligonucleotide primers, deoxynucleotide triphosphates (dNTPs), reaction buffer and the thermostable DNA Phusion polymerase. PCR results in the

exponential synthesis of a distinct DNA sequence by repeated denaturation, hybridization and extension cycles with 25-35 cycles usually.

Table 5.1 Preparation scheme for PCR

Component	Volume	Final Concentration
Template DNA: cDNA (Dilution 1:50)	1 µl	50-100 ng
Forward primer (c= 10 pmol/µl)	1 µl	0.2 µM
Reverse primer (c= 10 pmol/µl)	1 µl	0.2 µM
Phusion buffer, 5x	10 µl	1x
dNTP Mix (c= 20 mM/nucleotide)	1 µl	0.4 mM/ nucleotide
Phusion Polymerase	0.1 µl	0.008 Units/µl
ddH ₂ O	Adjust to 20 µl	

Table 5.2 PCR Program for amplification of UK-66 heavy and light chain

Step	Temperature	Time	Cycles
Initial denaturing	95°C	2 min	1
Denaturing	95°C	45 s	
Annealing	60°C	45 s	34
Extension	70°C	3 min	
Final extension	72°C	3 min	1

Table 5.3 PCR program for amplification of antigen binding domain scFv UK-66

Step	Temperature	Time	Cycles
Initial denaturing	94°C	5 min	1
Denaturing	94°C	1 min	
Annealing	50°C	1 min	35
Extension	72°C	1 min	
Final extension	70°C	5 min	1

5.1.9. DNA restriction digestion

For restriction digestion of DNA fragments or plasmid DNA endonucleases from New England Biolabs were used and restriction digestion was performed following the manufacturer's protocol.

5.1.10. Agarose gel electrophoresis with DNA

Agarose gel electrophoresis enables the user to control the PCR products or restriction digestions, but also to fractionate DNA molecules by size in order to purify them from the gel. Agarose gel electrophoresis was performed in 0.5x Tris-Acetate-EDTA-buffer (TAE-buffer) with agarose concentrations of 1%. DNA was detected by ethidium bromide (EtBr) (final concentration: 0.025 µg/ml). As size standard, the Fermentas 1 kb DNA ladder was used.

After electrophoresis, the gel was placed on an UV light box and the ethidium bromide-stained DNA was visualized using the imaging system LSM.

5.1.11. DNA purification from agarose gels

DNA fragments visualized on an UV light box were removed from the gel by the use of scalpels. Once excised, the DNA was eluted from the jellified agarose following the instructions of the Gene Clean Kit (MP Biomedicals). Elution volume was 15 μ l.

5.1.12. DNA Ligation

Purified and restriction enzyme-treated DNA fragments were ligated into the desired plasmid vectors, which have been treated with the respective restriction enzymes. The concentration of vector and insert DNA has been determined via agarose gel electrophoresis. A molar ratio of 1:3 of vector and insert was used for the ligation reaction. All ligations were performed with T4 DNA ligase and the provided buffer (New England Biolabs) either for 5 min at RT or overnight at 16°C. Following the reaction, the ligated DNA was transformed into an appropriate strain.

5.1.13. DNA sequencing

Sequence confirmation of the final expression vectors was performed by MWG (Ebersberg, Germany) and SeqLab (Göttingen, Germany). Results were analysed using the program CLC sequence viewer (Qiagen, Aarhus, Denmark), Vector NTii (Life technologies, Darmstadt, Germany) and Bioedit (Ibis Bioscience, Carlsbad CA, USA).

5.1.14. Cloning of scFv fragments

The shuttle vector pHEN2 and the expression vectors pAB were cloned at the Institute of Cell Biology and Immunology, University of Stuttgart (AG Kontermann). The sequences of heavy and light chain of the antibody UK-66 were cloned via XhoI and SfiI, respectively ApaI and NotI, into pHEN2, a shuttle vector with a linker region to combine heavy and light chain. The sequence of the scFv fragment was then cloned into the expression vector pAB, which contained a His- and a Myc-Tag for purification. *E. coli* TG1 was used as expression strain (Fig. 13).

5.1.15. Cloning of scFv-Fc fragments

The vector pSEC for expression of scFv-Fv fragments in mammalian cells were cloned at the Institute of Cell Biology and Immunology, University Stuttgart (AG Kontermann) and contains

a human IgG1 Fc part. The sequence of scFv UK-66 was cloned via XhoI and NotI into pSEC. For expression, HEK293 cells were transiently transfected and scFv-Fc UK-66 were purified from supernatant via the His-Tag.

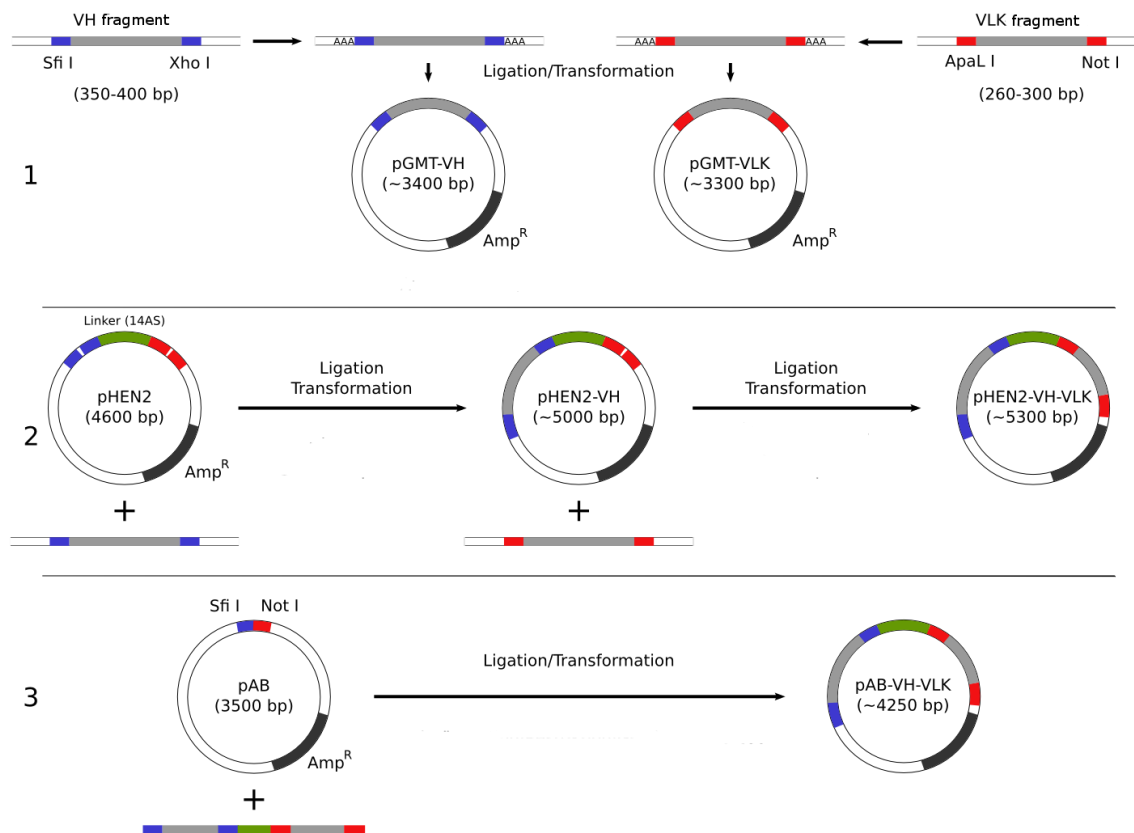


Fig. 13 Cloning strategy for UK-66 scFv fragments.

1) RNA of the hybridoma clone UK-66 was isolated and reverse translated into cDNA. The PCR products of heavy and light chain were amplified via degenerated primer pairs to determine the sequence of the antigen binding domain of UK-66. 2) For generation of a scFv fragment, the sequence of light and heavy chain was connected via a linker region using the plasmid pHEN2. 3) Afterwards, the sequence of the scFv fragment was cloned into the expression vector pAB, containing a pelB leader sequence for the periplasmic transport and a His- and Myc-tag for purification.

5.1.16. Cloning of complete UK-66 IgG antibodies

Sequences of the complete mouse and humanized UK-66 (hUK-66) were synthesized by GeneArt. The sequences of the heavy and light antigen binding domain of UK-66 were combined with the sequence of the Fc part. For the hUK-66, the isotypes IgG1, IgG2 and IgG4 were constructed. The murine UK-66 was constructed as IgG1 isotype. Antibodies were expressed with the Lonza[®] Biologic GS gene expression system. The genes of heavy and light chain were cloned via NotI and BamHI into pEE12.4. Each gene is under the control of a separate hCMV-MIE promoter. Antibodies were expressed by stably transfected CHO.K1 cells.

5.1.17. Humanization of mouse UK-66 antibody

The aim of antibody humanization is to engineer a monoclonal antibody that shows no or neglectable immunogenic reactions in humans although produced by a nonhuman species. Humanization of the UK-66 antibody was performed by Prof. Dr. R. Kontermann by using the complementarity-determining region (CDR) grafting method. In this context, intact murine variable domains were included onto a human framework region (FR), obtained from the closest human germline V segments to preserve the antigen-binding affinity. Therefore, the FR residues of potential importance for antigen binding were identified by computer-assisted homology modeling.

Two humanized versions of mouse UK-66, denoted hUK66-1 and hUK66-2, were generated by transferring the key murine FR residues onto a human antibody framework (selection were based on their homology to the mouse antibody framework) together with the mouse CDR residues. The light and heavy chain variable regions were then directly grafted into the human antibody light and heavy chains.

5.2. Cell culture Methods

5.2.1. Cultivation of mammalian cells

All cell culture procedures were performed in a sterile bench applying sterile working techniques. Subconfluent grown cells were passaged every 2-3 days if indicated with trypsin/EDTA. HEK293 and CHO.K1 cells were cultivated in RPMI 1640 supplemented with 10% fetal calf serum. MonoMac-6 cells were cultivated with RPMI supplemented with 10% fetal calf serum, 1% Penicillin/Streptomycin, 1% non-essential amino acid, 1% sodium pyruvate and 0.1% human insulin.

5.2.2. Stable transfection of plasmids

Transfections were performed with the help of polycationic lipids lipo- and nanofectamine (Invitrogen, Darmstadt, Germany). Cells were cultivated at least two passages before transfection and were used when growing in the exponential phase. Cells (1×10^5 /ml) were seeded 24 h before transfection in a 6-well plate and incubated overnight at 37°C in a humidified CO₂ incubator. Transfection solution 1 was prepared by adding 3 µg purified Plasmid DNA in 100 µl OptiMEM medium. Solution 2 contained 10 µl nanofectamine in 100 µl OptiMEM medium. Solutions were gently mixed by pipetting and incubated for 20 min at RT. During this time, cell medium was exchanged with 2 ml OptiMEM medium. After incubation, transfection complex was added drop wise to the cells and incubated overnight at

37°C in a humidified CO₂ incubator. The next day, OptiMEM medium was exchanged with selection medium.

5.2.3. Selection of high producer clones

The selection of positively transfected cells started 24 h after transfection by exchanging the medium with a culture medium containing the adequate selection marker as selection pressure. Medium was exchanged every third day during selection process. In course of the selection, non-transfected cells died and while transfected cells were able to replicate. After two weeks, an outgrowth of positively transfected cells was obtained.

Selection of high producer clones was performed by single cell dilution and increase of selection pressure. Single cell dilution was performed after expansion of positively transfected cells. Therefore, 100 µl medium was added to all wells of a 96 well plate, except well A1. 200 µl of the cell suspension (1×10^5 cells /ml) were added to well A1. 100 µl from the first well was transferred to the well B1. The 1:2 dilutions were repeated down the entire column, discarding 100 µl from H1. Additionally, 100 µl of medium was added to all wells of column 1. With an 8-channel pipettor, a 1:2 dilution across the entire plate were performed, discarding 100 µl from each well of column 12. The final volume of all wells was adjusted to 200 µl by adding 100 µl medium. The plate was then incubated at 37°C in a humidified CO₂ incubator. Supernatants of all wells were analysed for antibody production after 10 days of growth. Wells, containing producer of antibodies in the highest dilution factor compared to well A1, was cultivated as A1 in a new plate (Fig. 14).

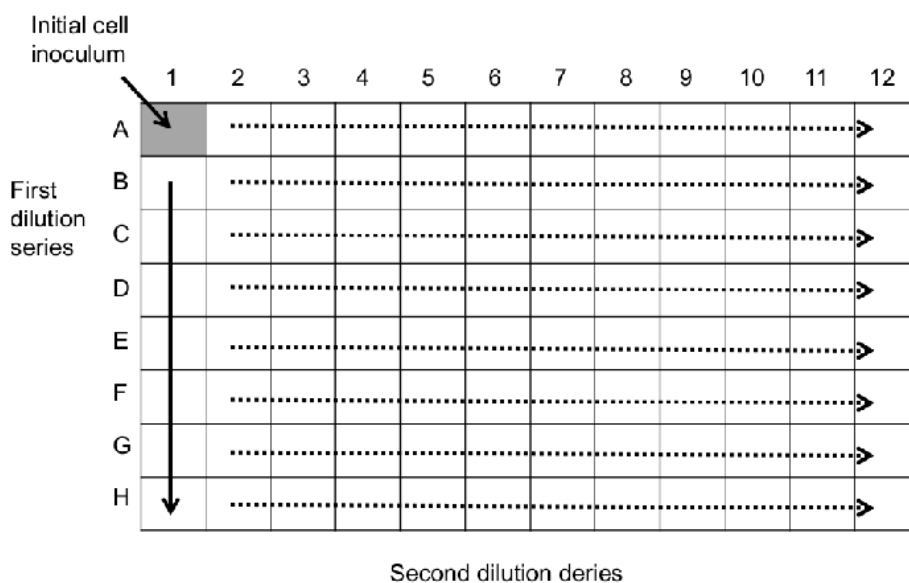


Fig. 14 Pipette scheme to perform a single cell dilution.

Positively transfected cells were inoculated in well A1 and diluted 1:2 from A1 to B1 until H1. From the first line (A1-H1), a further 1:2 dilution was performed from line 1 to line 12.

After the selection of three highest producing cell lines, further selection was performed in the presence of increasing MSX concentrations. Each cell line was cultivated in a 6-well plate (1×10^5 cells/ml per well) in selective medium containing a range from 50 μ M to 500 μ M MSX. Medium was exchanged every 5 days and plates were incubated in a humidified CO₂ incubator. Cell populations growing in different MSX concentrations were tested for their productivity. Selected cell lines were expanded and secured as a cryopreserved stock.

Afterwards, the producer cell line was cultivated in a two compartment bioreactor system (Integra Bioscience) for long term production.

5.2.4. Determination of cell specific antibody production

Production of specific antibodies were analysed by binding ELISA. Therefore, supernatants of producer clones were collected and stored at 4°C.

The UK-66 IgG concentration of the supernatant was determined by a calibration curve. Therefore, growth medium was spiked with defined concentrations of UK-66 IgG. Supernatants were diluted 1:5 and incubated for 1 h at 37°C. After three washing steps, bound proteins were detected with secondary antibodies conjugated to horse radish peroxidase (HRP). Concentration of UK-66 IgG in the supernatant was calculated by Graph Pad Prism 5.

5.2.5. Cryopreservation of mammalian cell lines

Cells were cryopreserved in freezing medium containing 90% FCS and 10% DMSO. Table 5.4 displays used cell lines and description. Table 5.5 demonstrates cell lines generated in this work.

Table 5.4 Cell lines description

Cell lines	Description
CHO	Chinese hamster ovary cells, IMIB stock
CHO-K1	Chinese hamster ovary cells, Lonza®
HEK293	Human embryonal kidney cells, R. Kontermann, University Stuttgart
MonoMac-6	Human acute monocytic leukemia established from the peripheral blood of a 64-year-old man with relapsed acute monocytic leukemia (AML FAB M5) in 1985 following myeloid metaplasia, ATCC

Table 5.5 cell lines and stable transfected cell lines

Nr.	Cell line	Insert+Plasmid	Resistance	Medium
1	CHO			RPMI1640+gln+10% FCS+1% Pen/Strep
2	CHO-K1			RPMI1640+gln+10% FCS+1% Pen/Strep
3	HEK293			RPMI1640+gln+10% FCS+1% Pen/Strep
4	MonoMac-6			RPMI1640+gln+10% FCS+1% Pen/Strep+1% non-essential aa+ 1% sodium pyruvate+0.1% human Insuline
5	NSO			RPMI1640+gln+10% FCS+1% Pen/Strep
6	HEK293	scFv-Fc mUK-66, pSEC	Zeo ^R	RPMI1640+gln+10% FCS+1% Pen/Strep+50 mg/ml Zeocin
7	HEK293	scFv-Fc hUK-66(2), pSEC	Zeo ^R	RPMI1640+gln+10% FCS+1% Pen/Strep+50 mg/ml Zeocin
8	CHO-K1	hUK-66 IgG1, pEE12.4	MSX ^R	RPMI1640-gln+10% dFCS+1% Pen/Strep+25 µM MSX
9	CHO-K1	hUK-66 IgG2, pEE12.4	MSX ^R	RPMI1640-gln+10% dFCS+1% Pen/Strep+25 µM MSX
10	CHO-K1	hUK-66 IgG4, pEE12.4	MSX ^R	RPMI1640-gln+10% dFCS+1% Pen/Strep+25 µM MSX
11	CHO-K1	hUK-66 IgG1, pEE12.4	MSX ^K	RPMI1640-gln+10% dFCS+1% Pen/Strep+50 µM MSX
12	CHO-K1	hUK-66 IgG1, pEE12.4	MSX ^K	RPMI1640-gln+10% dFCS+1% Pen/Strep+100 µM MSX
13	CHO-K1	hUK-66 IgG1, pEE12.4	MSX ^R	RPMI1640-gln+10% dFCS+1% Pen/Strep+150 µM MSX
14	CHO-K1	hUK-66 IgG1, pEE12.4	MSX ^R	RPMI1640-gln+10% dFCS+1% Pen/Strep+200 µM MSX
15	CHO-K1	hUK-66 IgG1, pEE12.4	MSX ^R	RPMI1640-gln+10% dFCS+1% Pen/Strep+300 µM MSX
16	CHO-K1	hUK-66 IgG1, pEE12.4	MSX ^R	CHO CD1+10% dFCS+1% Pen/Strep+100 µM MSX
17	CHO-K1	hUK-66 IgG1, pEE12.4	MSX ^K	CHO CD1+10% dFCS+1% Pen/Strep+150 µM MSX
18	CHO-K1	hUK-66 IgG1, pEE12.4	MSX ^K	Power CHO GS+10% dFCS+1% Pen/Strep+25 µM MSX
19	CHO-K1	hUK-66 IgG1, pEE12.4	MSX ^R	Power CHO GS+10% dFCS+1% Pen/Strep+50 µM MSX
20	CHO-K1	hUK-66 IgG1, pEE12.4	MSX ^R	Power CHO GS+10% dFCS+1% Pen/Strep+100 µM MSX
21	CHO-K1	hUK-66 IgG1, pEE12.4	MSX ^R	RPMI1640 (-gln)+1% Pen/Strep+ 25µM MSX (serum-free)
22	CHO-K1	hUK-66 IgG1, pEE12.4	MSX ^R	RPMI1640 (-gln)+0.5% dFCS+1% Pen/Strep+ 25µM MSX
23	CHO-K1	hUK-66 IgG1, pEE12.4	MSX ^K	RPMI1640 (-gln)+2.5% dFCS+1% Pen/Strep+ 25µM MSX
24	CHO-K1	hUK-66 IgG1, pEE12.4	MSX ^K	CHO CD1+1% Pen/Strep+ 25µM MSX (serum-free)
25	CHO-K1	hUK-66 IgG1 N297A, pEE12.4	MSX ^R	RPMI1640-gln+10% dFCS+1% Pen/Strep+25 µM MSX
26	CHO-K1	mUK-66 IgG1 N297A, pEE12.4	MSX ^R	RPMI1640-gln+10% dFCS+1% Pen/Strep+25 µM MSX

27	CHO-K1	Chimeric UK-69 (18-6-2) IgG1, pEE12.4	MSX ^R	RPMI1640-gln+10% Pen/Strep+25 µM MSX	dFCS+1%
28	CHO-K1	Chimeric UK-69 (35-7-2) IgG1, pEE12.4	MSX ^R	RPMI1640-gln+10% Pen/Strep+25 µM MSX	dFCS+1%
29	CHO-K1	Human FcyRIa (extrac. domain), pSEC	Zeo ^R	RPMI1640+gln+10% Pen/Strep+50 mg/ml Zeocin	FCS+1%
30	CHO-K1	Human FcyRIIa LR (extrac. domain), pSEC	Zeo ^R	RPMI1640+gln+10% Pen/Strep+50 mg/ml Zeocin	FCS+1%
31	CHO-K1	Human FcyRIIa HR (extrac. domain), pSEC	Zeo ^R	RPMI1640+gln+10% Pen/Strep+50 mg/ml Zeocin	FCS+1%

5.3. Biochemical Methods

5.3.1. Expression of recombinant proteins

In this work, the recombinant protein IsaA and the murine and humanized antigen binding domains of UK-66 were expressed using *E. coli*.

The staphylococcal protein IsaA was expressed in *E. coli* BL21 and M15Rep4. Expression of antigen binding domains mUK-66 and hUK-66 was performed in *E. coli* TG1. All proteins were expressed under the control of the *lac*-promotor. The *lac*-operon is induced by lactose when metabolized by the bacteria. A constant activity of the *lac*-operon is achieved by the structural analog Isopropyl-β-D-1-thiogalactopyranoside (IPTG). IPTG binds, similar to lactose, to the *lacI* repressor and prevents its binding to the *lac*-operator. Bacteria cannot metabolize IPTG resulting in a constant induction of the *lac*-promotor.

Full antibodies hUK-66 IgG1, IgG2, IgG4 and the Fc mutant hUK-66 IgG1 N297A were expressed by CHO.K1 cells (Lonza®) via stable transfection. The scFv-Fc fragments were expressed by transiently transfected HEK293.

5.3.2. Lysis of bacteria

For IsaA purification *E. coli* TG1 bacteria were lysed in binding buffer and protease inhibitor 0.5 M (Roche) was added as well as DnaseI (Roche). Cells were lysed with subsequent sonification (20 sec maximum amplitude, 10 sec break, repeated for 3 min). *E. coli* BL21 cells were lysed with lysozyme (0.2 mg) and French press. Insoluble components and non-lysed cells were separated by centrifugation (15 min, 10,000 rpm, 4°C).

5.3.3. Protein Purification

The recombinant IsaA protein was previously cloned into the expression vector pQE30 (by P. Bourdet), creating a N-terminal His₆ fusion tag. The *E. coli* strain M15 pREP4 was chosen as expression strain. An overnight culture was prepared by inoculating expression strain into 25

ml of LB_{Amp/Kan} at 37°C. The resulting inoculum was grown into 1 liter of LB_{Amp/Kan} at 37°C. The expression was induced during mid-exponential growth phase (OD_{600nm} ≈ 0.6) by addition of 0.5 mM IPTG and incubation was pursued overnight at 18°C.

For epitope characterization, IsaA was also cloned into the expression vector pETM-11, creating a C-terminal His₆ fusion tag to improve expression and stability properties of IsaA. The *E. coli* strain BL21 was chosen as expression strain.

Bacterial strain *E. coli* TG1 was transformed with the expression vector pAB containing the sequence of the scFv mUK-66, hUK-66(1) and hUK-66(2). From a 20 ml (2xTY, 100 µg/ml ampicillin, 1% glucose) overnight culture, 1l culture was inoculated and grown at 37°C and 200 rpm until OD₆₀₀ of 0.6 was reached. Protein expression was induced by IPTG and the culture was incubated overnight at RT. Bacteria were harvest by centrifugation and resuspended in 50 ml periplasmatic preparation buffer. After addition of lysozyme (50 µg/ml), the suspension was incubated for 15 min on ice. Before the suspension was centrifuged, 1 mM MgSO₄ was added to stabilize the spheroblasts. The supernatant was dialyzed against PBS overnight and subjected to immobilized metal affinity chromatography (IMAC). The concentration of the purified protein was determined photometrically.

5.3.4. Immobilized metal affinity chromatography

Recombinant IsaA and antibody fragments scFv were purified manually by covalent binding of its C-terminal His-Tag to positively charged nickel ions. Protein from periplasmatic production was applied to 1 ml Ni-NTA resin and equilibrated with 10 ml IMAC binding buffer. Non-bound protein was washed from the resin with IMAC wash buffer (50 mM NaH₂PO₄ [pH 7], 300 mM NaCl, 20 mM imidazole). Bound protein was eluted by increasing concentrations of imidazole (20 mM – 200 mM) in wash and elution buffer in which less tightly bound host cell proteins were removed in a washing step before the final elution. The elution was finalized by the application of elution buffer (50 mM NaH₂PO₄ [pH 7], 300 mM NaCl, 500 mM imidazole). Protein containing fractions were pooled and dialyzed against 1xPBS buffer to remove imidazole. For rIsaA, protein fractions were dialyzed against 1xPBS with 350 mM NaCl to remove imidazole. The protein concentration was measured by Nano Drop.

5.4. Antibody Purification

Antibodies were purified from cell culture supernatant by affinity chromatography on immobilized Protein G. Antibodies were produced either in house or externally at Biotem or Evitria. Samples of cell culture supernatants were incubated with the protein G resin overnight at 4°C with rotation and then loaded onto columns equilibrated with binding buffer (TBS, pH 5.0). The columns were washed with 10 volumes of binding buffer and IgG was

eluted in elution buffer (100 mM glycine HCl, pH 2.7). The collected fractions were immediately pH-neutralized with 1 M Tris-HCl, pH 9.0. After elution, antibody containing fractions were collected and dialyzed in PBS, pH 7.4 overnight at 4°C. The antibody concentration was measured at an OD of 280 nm and antibody quality was examined by SDS-PAGE and ELISA studies.

5.4.1. SDS-PAGE

Proteins were separated by 12% SDS-PAGE according to table 5.6. SDS page were Coomassie stained or analysed by Western Blot techniques.

Table 5.6 Preparation of SDS-PAGE (separation gels)

Separation Gel	
1.6 ml	H ₂ O
2 ml	Acrylamide/Bis-Acrylamide (30%/0.4%)
1.3 ml	1.5 M Tris-HCl buffer, pH 8.8
0.05 ml	10% SDS
0.05 ml	10% Ammoniumpersulfate
0.002 ml	TEMED

Table 5.7 Preparation of SDS-PAGE (sample gels)

Sample Gel	
2 ml	H ₂ O
0.5 ml	Acrylamide/Bis-Acrylamide (30%/0.4%)
0.38 ml	1 M Tris-HCl buffer, pH 6.8
0.03 ml	10% SDS
0.03 ml	10% Ammoniumpersulfate
0.003 ml	TEMED

5.4.2. Western Blot

Proteins were transferred from SDS page to nitrocellulose membranes (Bio-Rad) by semi-dry blotting. Transfer was carried out at 240 mA. The membrane was incubated for 1h in 5% BSA in Tris buffered saline with 0,075% Tween-20 (TBST) at RT and, subsequently incubated with the primary antibody diluted in 2.5% BSA at 4°C overnight. The membrane was washed 3 times in TBST for 10 min to remove unbound antibodies. Binding of the secondary antibody was performed in 2.5% BSA-TBST for 1h at RT. The membrane was washed 3 times with TBST for 10 min. The binding of HRP-conjugated secondary antibody was detected by treating the membrane with ECL-solution.

For Western Blot studies to analyse IsaA in different *S. aureus* strains by hUK-66 IgG1, overnight culture of *S. aureus* strains were prepared, 2 ml of samples were harvested after

OD 600 nm adjustment at 0.6 and resuspended in sample buffer for separation by SDS page and transferred to a nitrocellulose membrane using a semi-dry transfer system.

5.4.3. Dot Blot

Dot blot analysis was performed to determine binding of an antigen by generated specific antibodies. The binding signal was visualized by an ECL detection system on film. All used peptides and proteins were solved in 1xPBS. A volume of 5 μ l was dropped on a nitrocellulose membrane and incubated for 20 min at RT. The Dot blot was developed under the same conditions described for Western blot membrane.

5.4.4. Thermal stability

Thermal stability of rIsaA, scFv mUK-66, scFv hUK-66(1) and scFv hUK-66(2) were determined by dynamic light scattering and performed by Nadine Fuss (AG Kontermann, Uni Stuttgart). Therefore, 100 μ g of the respective protein was diluted in PBS to a final volume of 1 ml, sterile filtered and transferred to a quartz cuvette. At a rising temperature gradient from 30 to 90°C (1°C steps with 2 min equilibration time), dynamic laser light scattering intensity (kcps) was measured. From these measurements, the protein specific melting point was determined as the temperature of an explicit increase in the measured light scattering intensity.

5.5. Functional characterization

5.5.1. Biosensor measurements of antibody affinity

Affinity of antibody derivatives of UK-66 was determined by Surface Plasmon Resonance (SPR) using a Biacore 200 system (Biaffin, Germany). Antibodies were reversibly immobilized by an anti Fab antibody and covalently coupled at high density to a CM5 sensor chip according to the manufacturer's instructions (antibody capture kit, GE Healthcare, Germany). The concentration of UK-66 on the anti-Fab surface was between 0.4 nM and 400 nM. Chips coated with the capture antibody alone served as controls for monitoring non-specific binding. Affinity measurements were performed in buffer containing 10 mM HEPES (pH 7.4, 150 mM NaCl, 3.4 mM EDTA, 0.005% Tween20). Sensorgrams were recorded at a flow rate of 30 μ l/min at 25°C and the capture surface was regenerated after each cycle using 10 mM glycine (pH 1.7). The dissociation constants (K_D) were calculated using BIAevaluation software 4.0.1 after fitting the sensorgrams to a 1:1 Langmuir binding model.

5.5.2. ELISA studies

ELISA studies were performed to measure the affinity of murine and hUK-66 and their corresponding antigen binding domain fragments for *S. aureus* antigen IsaA. Therefore, 96-well plates (MaxiSorp; Nunc, Roskilde Denmark) were coated with rIsaA diluted in PBS (pH 7) to a final concentration of 10 µg/ml (50 µl/well). The plates were then incubated overnight at 4°C. After blocking non-specific sites with 5% bovine serum albumin (BSA) in PBS (200 µl/well), the mouse and hUK-66 IgG1 antibodies were added at various dilutions. The plates were incubated for 1 h at 37°C and washed with PBS 0.05% Tween 20 (PBS-T) followed by an incubation with a horseradish peroxidase-conjugated secondary antibodies (diluted 1:5,000) for 1 h at 37°C. After a final wash with PBS-T, 3,3',5,5'-tetramethylbenzidine (TMB) was added to each well (50 µl) for 10 min at 37°C and titers were measured at 450 nm on a Multiskan ELISA reader. All titers were measured in duplicate and the mean values calculated.

The binding specificities of the mouse and hUK-66 antibodies were assessed in a competitive ELISA. Therefore, a 96-well plate was coated with 10 µg/ml rIsaA (50 µl/well) and incubated overnight at 4°C. The plate was then washed with PBS-T and blocked with 5% BSA for 2 h at room temperature. In parallel tubes, the mouse and hUK-66 antibodies were pre-incubated with equal volume of rIsaA (serially diluted from a starting concentration of 100 µg/ml). The antibody/antigen mixtures were then transferred to rIsaA antigen pre-coated plates and incubated for 15 min at RT. The plates were washed six times and then incubated with HRP-conjugated secondary antibody (1 : 5,000). After incubation for 1 h at 37°C, TMB substrate (Invitrogen) was added to each well. The plates were then read in an ELISA reader at OD 450 nm.

5.5.3. Analysis of antibody binding on bacteria and human PMNs via flow cytometry studies

Flow cytometry experiments were performed to analyse the presence of IsaA on the surface of *S. aureus in vitro* using UK-66. UK-66 was incubated with *S. aureus* MA12 *spa*⁻ and its isogenic *isaA* mutant. Bacteria were washed twice with PBS and the cell density was adjusted to 1×10^6 cfu in 100 µl FACS buffer (PBS + 5% FCS) for 30 min at 37°C. Bacteria were mixed with 200 µl UK-66 (various concentrations) and incubated at 37°C on a rotating shaker for 30 min. Bacteria were washed twice with FACS buffer and incubated with FITC-conjugated anti-human IgG1 antibody for 30 min at 37°C. After washing, bacteria were resuspended in 300 µl FACS buffer.

For analysis of human leucocytes binding UK-66, whole blood samples from donors were used. Erythrocytes were lysed by incubation with 1x erythrocytes lysis buffer (14 ml 1x lysis

buffer to 1 ml blood) for 5 min at RT. Cell mixtures were centrifuged for 5 min at 1200 rpm and resuspended in 5 ml ice-cold PBS. After the third washing step, cells were mixed with 15 ml FACS buffer. Samples of 100 μ l human leucocytes were stained with Alexa488 conjugated hUK-66 antibody (dilution series from 5 to 5000 nM hUK-66) for 1h at 4°C in a shaker incubator. Samples were washed three times and resuspended in 200 μ l FACS buffer.

5.5.4. Immunofluorescence studies

Immunofluorescence analysis was performed to confirm the expression of IsaA on the surface of *S. aureus* strain MA12. The mutant strain, MA12 Δspa , was chosen to reduce the non-specific binding of IgG to *S. aureus* Protein A. Bacteria were grown overnight and harvested by centrifugation at 13,000 rpm. The bacterial pellet was washed twice with PBS and the cell density was adjusted to 5×10^8 CFU/ml. After blocking with 5% FCS in PBS for 1 h, the bacteria were incubated with hUK-66 IgG1 (diluted 1 : 5,000) for 30 min at 37°C. The bacterial pellet was washed three times with PBS/0.05% Tween 20 and then stained with fluorescein isothiocyanate (FITC)-conjugated anti-human IgG1 (diluted 1 : 10,000) for 30 min at 37°C. After washing, the fluorescently-labeled bacteria were resuspended in 100 μ l PBS, dried, and fixed on slides. Surface expression of IsaA was determined by examining the slides under a fluorescence microscope (Leica, Wetzlar, Germany) with the same exposure settings for each comparison group. Images were processed using the Gimp software Version 2.0 (GNU image manipulator).

5.5.5. Purification of human neutrophils

Heparinized human whole blood samples were diluted 1:1 with 1xPBS and carefully added to the top of 15 ml Ficoll filled falcon tubes. Tubes were centrifuged for 30 min at 1000 rpm (without active brake in centrifuge). Plasma and buffy coat was removed and PMN fraction was resuspended 1:3 in polyvinyl alcohol. After incubation for 45 min at RT, supernatant was collected and centrifuged for 3 min at 1000 rpm. Cell pellet was resuspended in 16 ml H₂O for 30 s followed by adding 4 ml 5xPBS. After centrifugation (3 min at 1200 rpm), cells were resuspended in HBSS.

5.5.6. Phagocytosis assay

Phagocytosis by neutrophils was analysed using carboxyfluorescein succinimidyl ester (CFSE)-stained *S. aureus* Newman strain. The intensity of CFSE fluorescence by human neutrophils is dependent on the number of ingested bacteria. Therefore, bacteria were stained at 37°C for 20 min with 20 μ M CFSE in 500 μ l PBS containing 5% FCS. After washing, the bacteria were added to 100 μ l blood samples and incubated for 20 min at 37°C.

Samples, incubated at 4°C, served as negative control. All samples were prepared for flow cytometry analysis using the phagotest kit (Glycotope, Heidelberg, Germany).

5.6. Killing assay

Heparinized human blood samples were incubated with *S. aureus* strain Newman to measure antibody-dependent killing bacteria as determined by colony forming unit (cfu) counting. Therefore, bacteria were washed twice with PBS and the cell density was adjusted to 5×10^7 cfu in 100 μ l PBS. Bacteria were then mixed with 100 μ l human whole blood and incubated at 37°C on a rotating shaker for 60 min. Antibody hUK-66 in concentration of 0.075 and 0.9 mg/ml was then added. The isotype-matched control antibody, Trastuzumab, and the immunoglobulin preparation for intravenous application in humans, Gammunex[®], were used as controls. Subsequently, all eukaryotic cells were lysed by exposure to 1% saponin solution for 20 min at 4°C. The samples were then serially diluted in duplicates and three samples of each dilution were then plated onto LB agar plates in duplicate and incubated overnight at 37°C. Colonies were counted and the percentage of surviving bacteria was calculated in percentage to the samples containing bacteria and blood as 100%.

5.7. *In vivo* experiments

5.7.1. Ethics statement

All animal studies were conducted according to the guidelines of the Federation of European Laboratory Animal Science Associations (FELSA). All experiments were approved by the local authority Government of Lower Franconia (Regierung von Unterfranken) in Würzburg, Germany.

5.7.2. Experimental set up

A pneumonia infection model was used to evaluate the efficacy of mouse IgG1 antibody mUK-66 and humanized IgG1 antibodies hUK-66 and hUK-tox. Animals received either an intranasal or an intravenous injection of PBS, isotype control or therapeutic antibody (mUK-66, hUK-66, hUK-tox) at different concentrations one hour prior to or after the intranasal infection with *S. aureus* Newman. Following infection, animals were monitored for 72 hours for severity of disease. *S. aureus* infectious doses were prepared according to standard protocol and stored at -80°C. For infection studies, *S. aureus* Newman stock samples were thawed for 15 min at room temperature. After washing in 50 ml of sterile PBS (centrifugation at 4000 rpm at 4°C for 20 min), the pellet was diluted to a final concentration of 2×10^8 cfu/mouse. The infectious dose for the used stock was determined earlier in dose titration

experiments. Infection was performed using a total volume of 20 μl . The infectious dose was controlled by measuring optical density at 600 nm (OD_{600} value of $1=5.7 \times 10^8 \text{ ml}^{-1}$) and by plating appropriate dilutions in duplicate on LB agar and cfu were counted after 24 hours of incubation. Before injection a mouse was warmed on a heated animal shelf (part of IVIS 100 PerkinElmer) for 5 to 10 minutes at 37°C to dilate the tail vein. Afterwards the mouse was put inside a mouse restrainer and 100 μl PBS with or without antibody was injected into the lateral tail vein. For intranasal infection, mice were anesthetized with 2.5% isoflurane. When shallow breathing was observed, mice were inoculated with 20 μl of *S. aureus* suspension. The inoculum was applied with a pipette and allowed to be inhaled by the mouse. Following inoculation, mice were checked frequently for recovery. During course of infection, body weight was documented daily and mice were monitored twice daily for behavior, fur conditions, hunched posture and signs of morbundancy. The animals were sacrificed, if the human endpoint has been reached to a disease score sheet.

5.7.3. Survival analysis

Survival curves were prepared using GraphPad Prism 5 and statistical significance was determined using Log Rank test.

6. Results

6.1. Humanization of mouse UK-66 antigen binding domain

Monoclonal antibodies (mAb) are the fastest-growing biological pharmaceuticals entering clinical studies. These adaptor molecules are derived from a single clone of cells and recognize a unique antigen [144]. The production of mAbs has been greatly refined since the introduction of the hybridoma technique by Kohler and Milstein in 1975 [56], a method to immortalize antibody-producing b-cells by fusing murine splenic-derived b-cells with immortal myeloid cell lines. The resulting hybridoma clone produces mouse antibody. Murine antibodies are easier to produce, but are limited by a short half-life in serum, only some can trigger human effector functions and the risk to elicit an immune response, named human anti-mouse antibodies (HAMA) [64]. HAMA can result in enhanced clearance of antibody from serum, blocking of its therapeutic effect and hypersensitivity reactions. Reduction of immunogenicity of the murine anti-IsaA antibody (mUK-66) was achieved by transplanting the complementarity determining regions (CDRs) onto a human framework. This method is called CDR-grafting and the humanized UK-66 is named hUK-66. CDR-grafted antibodies appear to have a better pharmacokinetics than rodent mAbs, an extended serum half-life in humans and a reduced immunogenicity. For humanization of mUK-66, the sequence of the antigen binding domain of mUK-66 had first to be determined. Therefore, total RNA was isolated from the hybridoma clone, mUK-66, and double stranded cDNA was synthesized by reverse transcriptase. Sequence analysis was performed via PCR reactions with cDNA from mUK-66 using as template. The PCR fragments encoding the VL and VH regions were then cloned into the pGEMT vector to determine the sequence of the variable region of mUK-66. Humanization of the mUK-66 antibody was performed using the complementarity-determining region (CDR) grafting method. This method based on the principle, that framework region (FR) residues of potential importance for antigen binding were identified by computer-assisted homology modelling. Two humanized versions of mUK-66, denoted hUK66-1 and hUK66-2, were generated by transferring the key murine CDR residues onto a human antibody framework (selected based on its homology to the mouse antibody framework). The variable regions of light and heavy chain were then directly grafted into the human antibody light and heavy chains (Fig. 15). The z-score of the heavy chain of both humanized versions is +1.351. The humanized version 2 is more similar to the mouse parental sequence and its light chain z-score is -1.583, while the humanized version 1 has a higher z-score of humanness -0.262.

Antigen binding domain of UK-66 (heavy chain)

	FR1	CDR1	FR2	CDR2
Mouse	DVKLVESGGGLV KLGGSLKLSCS	ASGFTFS NYYMS WVRQT	PE KRLE	LV ADINGNGGSTYYPD TVKG
Human	EVQLLESGGGLV QPGGSLRLSCA	ASGFTFS NYYMS WVRQA	PGK GLEWVSD INGNGGSTYYPD	TVKG
	FR3	CDR3	FR4	
Mouse	RFTISRDN AKNTLYLQMS SLK SE TALYYCVR RG GYALDY	WGQ	GTT	TVSS
Human	RFTISRDN SKNTLYLQMNS LR A EDTAVYYCVR RG GYALDY	WGQ	GTT	TVSS

Antigen binding domain of UK-66 (light chain)

	FR1	CDR1	FR2
Mouse	DVVM TQTP	L SLPVSLGDQAS IS CRSSQSLVH INGNTYLH	WYLQKPGQ SPK LLIY
Human-1	E IVL TQ SPG TLS LPGE	RATL SCRSSQSLVH INGNTYLH	WY Q QKPGQ APK LLIY
Human-2	DVVM TQTP	L SLSVTPGQPAS IS CRSSQSLVH INGNTYLH	WYLQKPGQ SPQ LLIY
	CDR2	FR3	CDR3
Mouse	RVS NRFS GV PDRFSGSGSGTDFTL KIS R VEA ED LG VY FC	SQ STHVPWTFGGG TKLE LKR	
Human-1	RVS NRFS GI	PDRFSGSGSGTDFTL TIS R LEP ED FA VY YC	SQ STHVPWTFGGG TKLE LKR
Human-2	RVS NRFS GV PDRFSGSGSGTDFTL KIS R VEA ED VG VY YC	SQ STHVPWTFGGG TKLE LKR	

Fig. 15 Sequence of antigen binding domain UK-66

Identification of the mouse UK-66 antigen binding domain was the basis for the humanization process. For the heavy and light chain of UK-66, two humanized variants were generated. The mouse CDRs (red) of the antigen binding domain of the heavy chain were included into frame work (FR grey) of the human germ line 3-23 based of the high z-score of humanness 1.351. The mouse CDRs of the light chain were transferred into the frame of the human germ line 2 (A18, A27) with a z-score of -0.262 and -1.583. The differences in the amino acid sequence between human and mouse are highlighted by bold letters.

6.2. Expression and purification of mouse and humanized scFv fragments by *E. coli* TG1

After humanization of the antigen binding domain, the encoding sequence was used for the overexpression of single chain fragments (scFv) mUK-66 and the two variants of hUK-66 by *E. coli* TG1 (Fig. 16). The scFv fragment consists of the antigen binding domain of heavy and light chain, connected by a linker sequence. The scFv peptide has a molecular weight of 25 kDa. For expression, the vector pAB was chosen, containing a His- and Myc-Tag for purification.

The mouse and humanized scFv UK-66 fragments were purified by IMAC affinity purification. Figure 16 displays the purified scFv fragments in SDS Page, confirmed by Western Blot analysis.

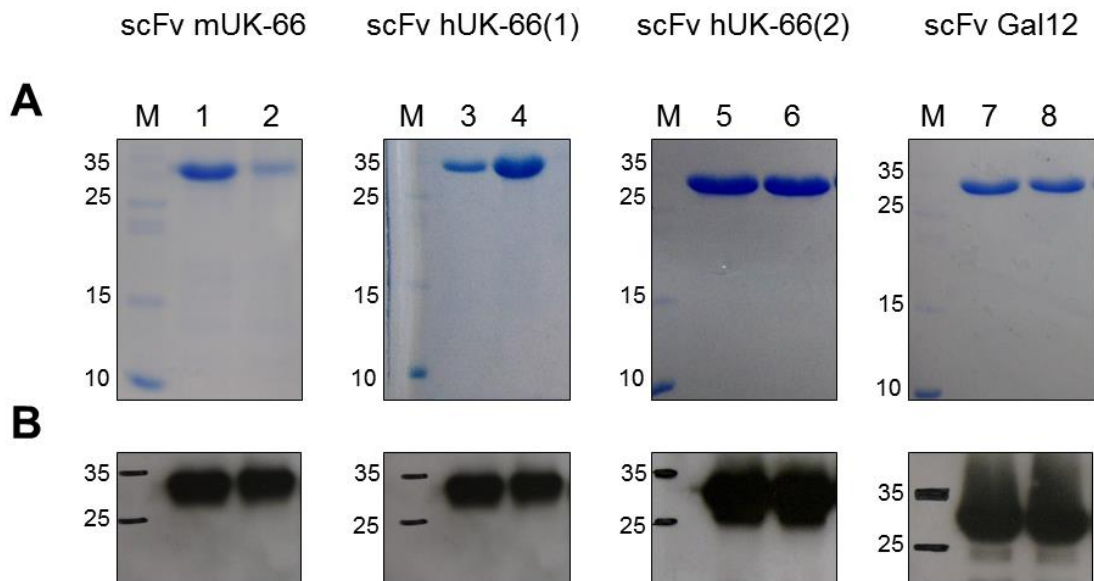


Fig. 16 Purification of mouse and humanized scFv UK-66 fragments: (A) SDS-Page and (B) Western Blot analysis.

The scFv fragments were expressed by *E. coli* TG1 and purified by IMAC affinity purification. M Marker, 1-2 Eluat scFv mUK-66, 3-4 Eluat scFv hUK-66(1), 5-6 Eluat scFv hUK-66(2), 7-8 Eluat scFv Gal12. (B) Western Blot studies were performed to confirm scFv fragments. The scFv fragments were detected via binding of a HRP-conjugated anti-Myc antibody.

6.3. Expression and purification of recombinant *IsaA* by *E. coli* M15Rep4 and BL21

The target structure of UK-66 is the antigen *IsaA*. Therefore, *rlsaA* was overexpressed and purified to perform comparative binding studies. The protein *rlsaA* was cloned into the plasmid pQE30, containing a N-terminal His-Tag, and was transferred into the expression strain *E. coli* M15Rep4. To investigate the effect of the His-Tag position on *rlsaA* structure, another construct was generated into pETM11, containing a C-terminal His-Tag. The expression of *rlsaA* in pETM11 was performed in *E. coli* BL21. Figure 17 displays a SDS-Page of *rlsaA* purification fractions expressed by *E. coli* M15Rep4. The protein *IsaA* has a molecular weight of 29 kDa, but after purification degradation products were detected in the eluat fraction.

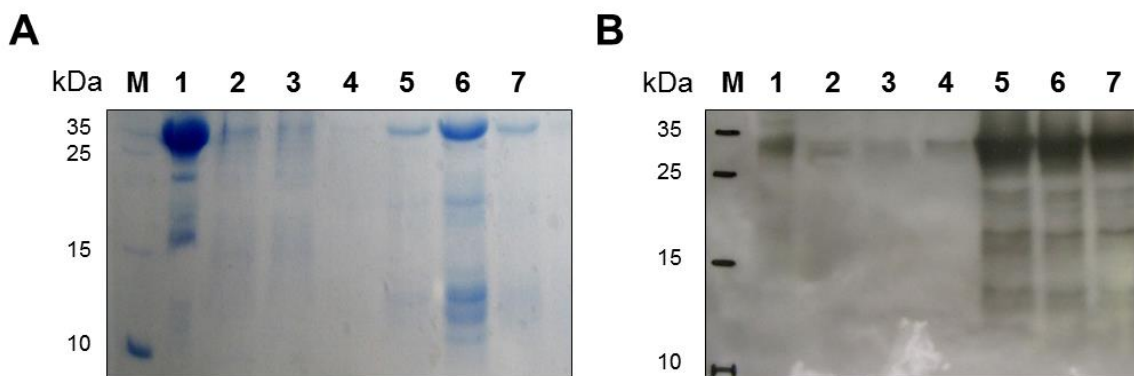


Fig. 17 Purification of rIsaA using expression strain *E. coli* M15Rep4 (A) SDS-Page and (B) Western Blot analysis.

(A) rIsaA was expressed by *E. coli* M15Rep4 and purified by IMAC affinity purification. M Marker, 1 Cell pellet, 2 Cell lysate, 3 Flow through, 4 Wash fractions, 5-7 Eluat fractions. Eluat fractions were collected and dialysed. (B) Western Blot studies were performed to confirm rIsaA eluat after purification. The rIsaA was detected via binding of mUK-66 IgG1 and a HRP-conjugated anti-mouse secondary antibody.

The purified rIsaA was confirmed by Western Blot analysis via binding by mouse UK-66 IgG1 antibody and a HRP-conjugated anti-mouse secondary antibody. Figure 17 shows that rIsaA was successfully purified and suggests that the signals under 29 kDa are degradation products of IsaA.

6.4. Comparative binding studies of mouse and humanized UK-66 antigen binding domain

CDR grafting of antigen-binding sites from mouse onto a human frame work can be critical for binding affinity of designed antibodies to their target antigens. For the successful recreation of the antigen-binding site, it is necessary to consider the interaction between the β -sheets of the frame work and the loops of the antigen binding domain to preserve the key contacts with the CDRs. Therefore, binding studies were performed to confirm that the binding affinity of both hUK-66 is preserved to their target the antigen IsaA. In these affinity studies, UK-66 binding of recombinant and native IsaA was analysed and the most promising humanized candidate was determined for further investigations.

6.4.1. Western Blot studies to analyse the binding of rIsaA by mouse and humanized UK-66 antigen binding domain

Western Blot studies were performed to analyse the successful humanization of mUK-66. Results of the Western Blot studies presented in figure 18, demonstrate that both humanized variants of UK-66 and the recombinant mouse scFv UK-66 bind rIsaA and also its

degradation products. As a control, rlsaA was detected via its His-Tag, the anti-His-HRP antibody detected only intact rlsaA and not its degradation products.

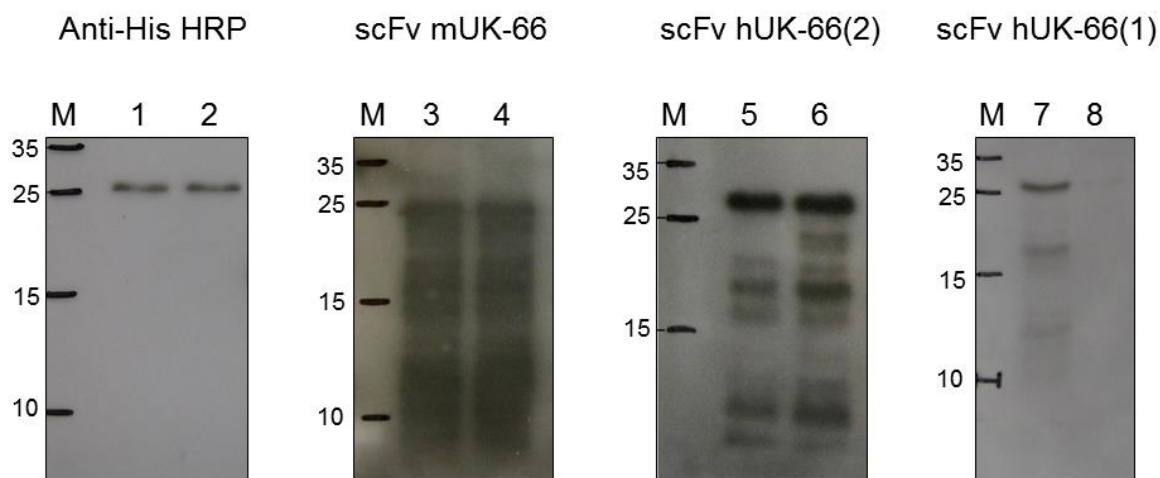


Fig. 18 Comparative Western Blot studies of mouse and humanized scFv fragments.

The protein rlsaA has a molecular weight of 29 kDa and was bound by mouse and humanized scFv UK-66 fragments using two concentrations 1:500 and 1:1000. All UK-66 fragments detect degradation products of rlsaA. As a control, rlsaA was detected by its His-Tag via HRP-conjugated anti-His antibody. Eluat of rlsaA are presented in lines 1-8, M is the Marker line.

To quantify the binding affinity of hUK-66 scFv fragments, binding ELISA studies were performed.

6.4.2. Binding affinity analysis of mouse and humanized UK-66 antigen binding domains by ELISA studies

Comparative binding ELISA studies were performed to analyse binding specificities of humanized and mouse scFv UK-66 fragments *in vitro*. Therefore, serial dilution of humanized and mouse scFv UK-66 fragments were tested and the half maximal binding to immobilized rlsaA (10 μ g/ml) was determined. For the scFv mUK-66, the half maximal binding was determined at 8 nM. For the both humanized scFv fragments, the half maximal binding was reached for hUK-66(1) at a concentration of 800 nM and for hUK-66(2) at a concentration of 80 nM (Fig. 19A). Results from the binding ELISA studies were confirmed by competitive ELISA studies. Therefore, soluble rlsaA competes for free antigen binding domains against coated rlsaA. A serial dilution of soluble rlsaA was incubated with the concentration of scFv at half maximal binding (determined in binding ELISA studies Fig. 5A). Results from the competitive ELISA studies (Fig. 19B) indicate that recombinant mouse and both humanized scFv fragments bind specifically rlsaA. Comparative binding studies were also performed with the generated scFv-Fc mUK-66 and hUK-66(2) fragment. Results, displayed in figure 19(C+D), confirm binding specificity. Overall, data from comparative binding studies revealed the successful humanization of the mouse antigen binding domain UK-66 by preservation of

the binding affinity to rlsaA. Based on the fact, that the binding affinity of the second humanized variant is closer to the parental mouse binding affinity, all following experiments were performed with hUK-66(2) and this antibody is designated hUK-66.

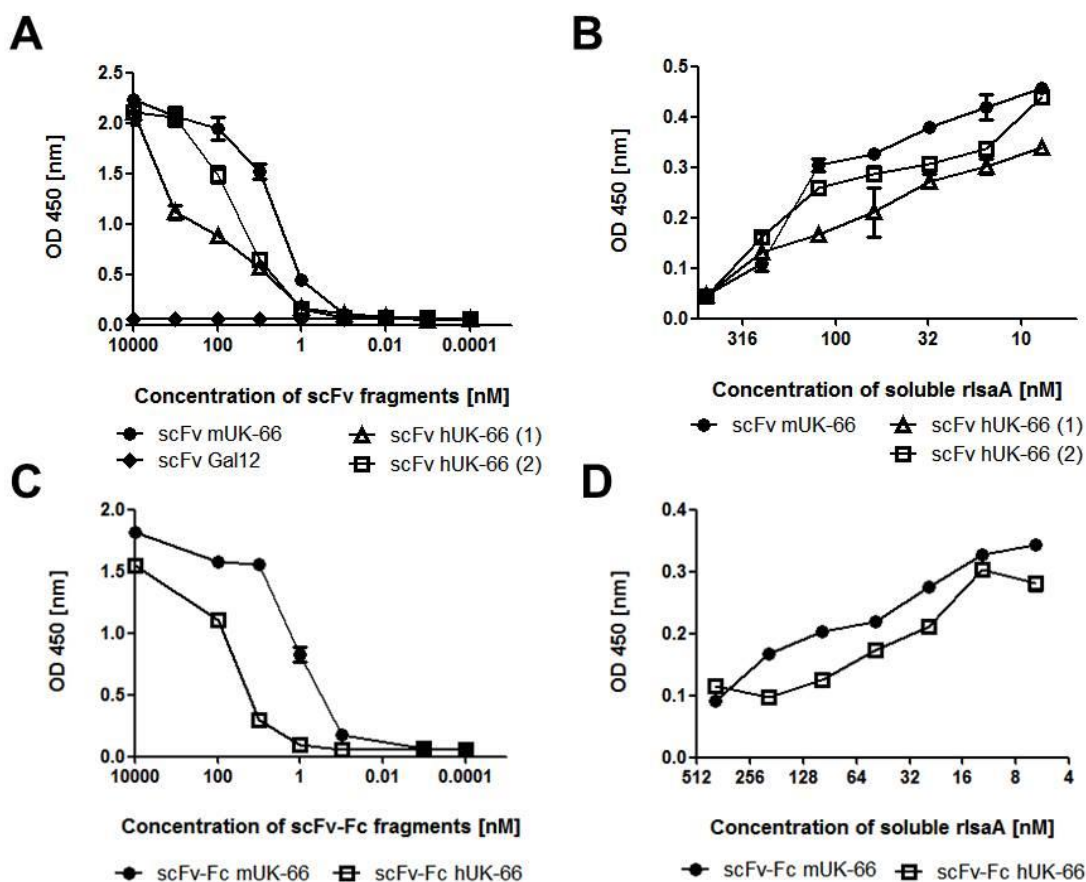


Fig. 19 Comparative binding studies of mouse and humanized scFv fragments: (A, C) binding ELISA, (B, D) competitive ELISA.

Binding affinities of scFv fragments mUK-66, hUK-66(1) and hUK-66(2) were analysed by binding ELISA studies. Microtiter plates were coated with 10 µg/ml rlsaA and incubated with serial diluted concentrations of scFv fragments. The scFv fragment Gal12 serves as negative control. (A) Binding of rlsaA by scFv fragments were analysed by HRP-conjugated anti-Myc antibody. (B) Affinity of mouse and humanized scFv fragments was analysed by competitive ELISA. Studies were performed with K_d concentration calculated from binding ELISA. Binding of scFv UK-66 fragments was inhibited by decreasing concentration of soluble rlsaA and analysed with HRP-conjugated anti-Myc antibody. The constant concentration of mUK66 was 8 nM, hUK66(1) was 800 nM and hUK-66(2) was 80 nM. (C) Binding affinity of scFv-Fc mUK-66 and hUK-66(2) was characterized by binding ELISA. Binding of rlsaA by scFv-Fc fragments were analysed by HRP-conjugated anti-human IgG1 antibody. Half maximal binding concentration (K_d) of scFv-Fc mUK-66 was determined as 8 nM and for scFv-Fc hUK-66(2) as 80 nM. Specificity of both scFv-Fc fragments were analysed by competitive ELISA (D) using K_d concentration calculated from binding ELISA. Both scFv-Fc fragments bind rlsaA specifically and concentration dependent.

6.4.3. Immunofluorescence studies and flow cytometry analysis to detect the binding of native IsaA by scFv mUK-66 and hUK-66

One of the most important properties of a therapeutic antibody is the binding to its target. The mUK-66 IgG1 can only exert its anti-staphylococcal activity following binding of the target

antigen IsaA on the bacterial cell surface. Therefore, immunofluorescence studies were performed to confirm that the humanized scFv-Fc hUK-66(2) recognizes native IsaA expressed on the bacterial cell surface. Based on the fact, that staphylococcal protein A binds antibodies via their Fc parts, the protein A mutant *S. aureus* MA12 Δ spa and its isogenic *isaA*⁻ mutant was used to avoid unspecific binding of the antibody fragments. The binding of scFv-Fc hUK-66 was analysed by FITC-conjugated anti-human IgG1. Results from immunofluorescence studies reveal that the hUK-66 scFv-Fc fragment binds specifically IsaA expressed on the bacterial cell surface (Fig. 20A). The results from immunofluorescence studies were further confirmed by binding ELISA studies with viable *S. aureus* (Fig. 20B). The successful coating of bacteria were analysed by crystal violet staining. Binding specificity of UK-66 scFv fragments was determined by using *S. aureus* MA12 Δ spa and its isogenic *isaA*⁻ mutant. Results from these studies show that the mouse and the hUK-66 scFv fragment detect IsaA specifically on the bacterial cell surface.

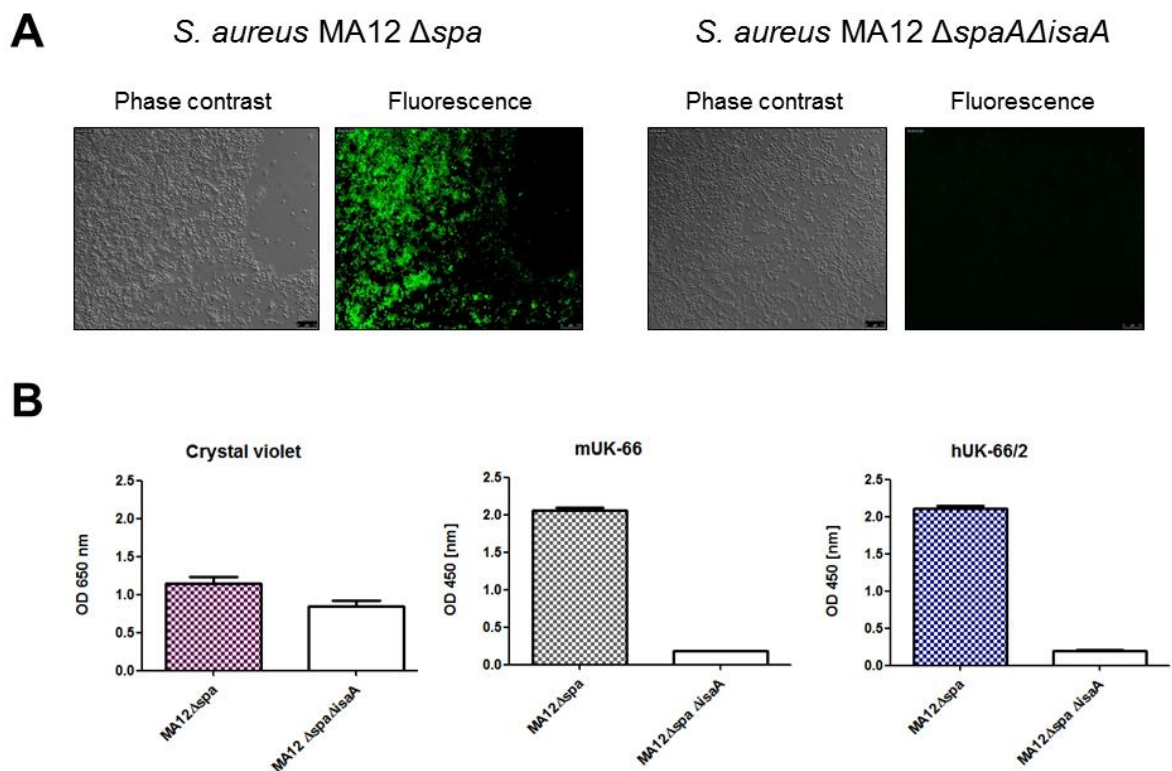


Fig. 20 Humanized UK-66 scFv-Fc fragment detects IsaA expressed on the bacterial cell surface using indirect immunofluorescence (A) and ELISA studies with viable bacteria (B).

(A) Bacteria were detected by scFv-Fc hUK-66 followed by FITC-conjugated anti-human IgG1 antibody. Only *S. aureus* MA12 Δ spa mutant showed surface expression of IsaA while no signal could be detected on the double mutant *S. aureus* MA12 Δ spa Δ isaA. (B) Microtiter plates were coated with 1×10^7 cfu/ml viable cells. Bacterial IsaA was detected via binding by scFv UK-66 fragments and a HRP-conjugated anti-Myc secondary antibody.

For an effective anti-staphylococcal immunotherapy, target specificity is critical. The binding of mouse and hUK-66 scFv-Fc fragments were analysed by flow cytometry studies to show that the UK-66 scFv-Fc fragments bind IsaA expressed by viable bacteria in solution. This study was performed with *S. aureus* MA12 Δ spa and its isogenic *isaA*⁻ mutant to avoid

unwanted cross reaction with staphylococcal protein A (spa). Figure 21 demonstrates that the mouse hUK-66 scFv-Fc fragments detect IsaA, expressed on the bacterial cell surface, specifically since the *S. aureus* MA12 $\Delta spa\Delta isaA$ mutant strain shows no fluorescence signal.

Results of the immunofluorescence study as well as flow cytometry analysis confirm that the mouse and hUK-66 antigen binding domain binds specific native IsaA, expressed on the bacterial surface.

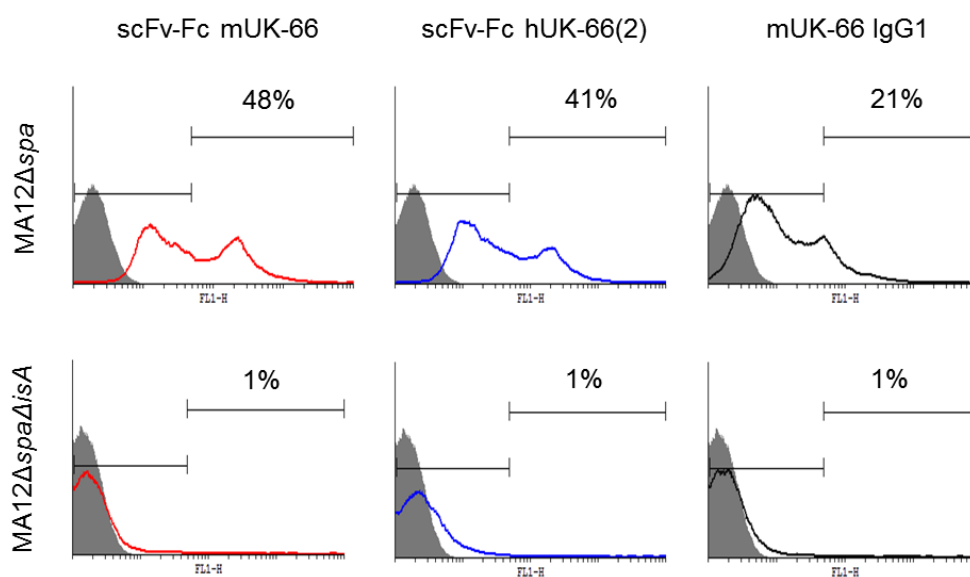


Fig. 21 Mouse and humanized UK-66 scFv-Fc fragments bind specifically IsaA on the bacterial surface determined by FACS analysis.

Samples contained 1×10^6 bacteria/100 μ l and were stained with indicated UK-66 scFv-Fc fragments and full mUK-66 IgG1, respectively. Binding of IsaA was confirmed by staining samples with FITC-conjugated anti-human IgG1 antibody. Results demonstrate the specific binding of IsaA on the bacterial cell surface by the murine and humanized UK-66 antigen binding domain. The isogenic *isaA*⁻ mutant of MA12 Δspa served as negative control.

6.5. Comparative binding studies of mouse and humanized UK-66 full antibody

After the successful humanization of the mouse UK-66 antigen binding domain, full length mouse and humanized antibodies were generated using the Lonza GS gene expression system. Therefore, the sequence of the murine light chain CDRs was determined and exchanged with the sequence of the human CDRs of germline 2-A27 to generate the sequence for the complete light chain. For the complete heavy chain of IgG1, the sequence of the murine CDRs of the murine heavy chain was exchanged with the sequence of the human CDRs of the human germline 3-23. The sequences were synthesized by GeneArt. The Lonza GS gene was used for selection in CHO cells and is part of the vectors pEE6.4 and pEE12.4. Both vectors contain a highly efficient transcription cassette under a control of

hCMV-MIE promoter. The DNA of the heavy chain was cloned into the polylinker, downstream of the hCMV-MIE promoter and upstream of the SV40 sequence of pEE6.4. Vector pEE12.4 was used for construction of a double gene vector. After introduction of the light chain DNA into the vector pEE12.4, the complete expression cassette of the heavy chain was isolated from pEE6.4 and included into pEE12.4. Both polypeptide chains are expressed simultaneously with each gene under the control of a separate hCMV-MIE promoter. The production of complete humanized antibodies is described in section 5.2.

In the previous binding experiments, the second humanized variant hUK-66(2) reveals comparable binding affinities to parental mouse UK-66. Therefore, the complete hUK-66 antibody contains the antigen binding domain hUK-66(2). To address different effector function by hUK-66, the Fc part was designed as IgG1, IgG2 and IgG4. The binding properties of full mouse and hUK-66 antibodies were analysed by comparative binding studies.

6.5.1. Comparative binding studies of full mouse and humanized UK-66 antibody

The binding affinities of full mouse and hUK-66 antibody were analysed by ELISA and quantified by SPR studies.

The half maximal binding affinity to immobilized rlsaA was analysed by binding ELISA studies. For the mouse UK-66 IgG1 antibody, the half maximal binding was determined for 40 nM. The same half maximal binding concentration was achieved for hUK-66 IgG1 and IgG4. A 10-fold decrease of binding affinity was observed for hUK-66 IgG2. Results from the binding ELISA studies were confirmed by competitive ELISA studies. A serial dilution of soluble rlsaA was incubated with the concentration of antibody at their half maximal binding (determined in binding ELISA studies). Results from the competitive ELISA studies (Fig. 22) display that recombinant mouse and hUK-66 antibodies bind specifically rlsaA.

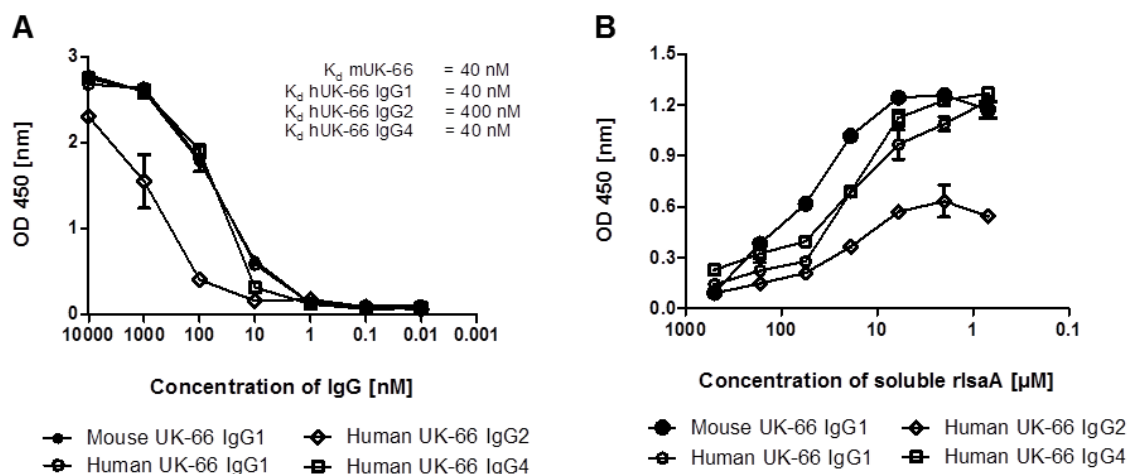


Fig. 22 Comparative binding studies of mouse and humanized scFv fragments: (A) Binding ELISA, (B) Competitive ELISA.

(A) Binding affinities of mUK-66 IgG1 and hUK-66 IgG1, IgG2 and IgG4 were analysed by binding ELISA studies. Microtiter plates were coated with 10 µg/ml rIsaA and incubated with serial diluted concentrations of antibodies. Binding of rIsaA by UK-66 antibody were analysed by HRP-conjugated anti-Isotype antibody. (B) Affinity of mouse and humanized UK-66 antibodies was analysed by competitive ELISA. Studies were performed with K_d concentration calculated from binding ELISA. Binding of UK-66 antibody was inhibited by decreasing concentration of soluble rIsaA and analysed with HRP-conjugated anti-Isotype antibody. The constant concentration of mUK66 IgG1 was 40 nM, hUK-66 IgG1 and IgG4 was 40 nM and of hUK-66 IgG2 was 400 nM.

6.5.2. Determination of mouse and humanized UK-66 binding affinity by Surface Plasmon Resonance (SPR)

The binding kinetics of rIsaA to immobilized mouse or hUK-66 IgG1 were determined by label-free surface plasmon resonance using a Biacore 2000 system. Results from SPR analysis revealed a high affinity and a slow off-rate of both antibodies to rIsaA, indicating a high specific interaction (Fig. 23). The dissociation constant K_D was determined for mUK-66 IgG1 as 1.7 nM and for the hUK-66 IgG1 antibody for 4.8 nM. Both binding affinities demonstrate a high affine and specific binding of UK-66 IgG1 to rIsaA.

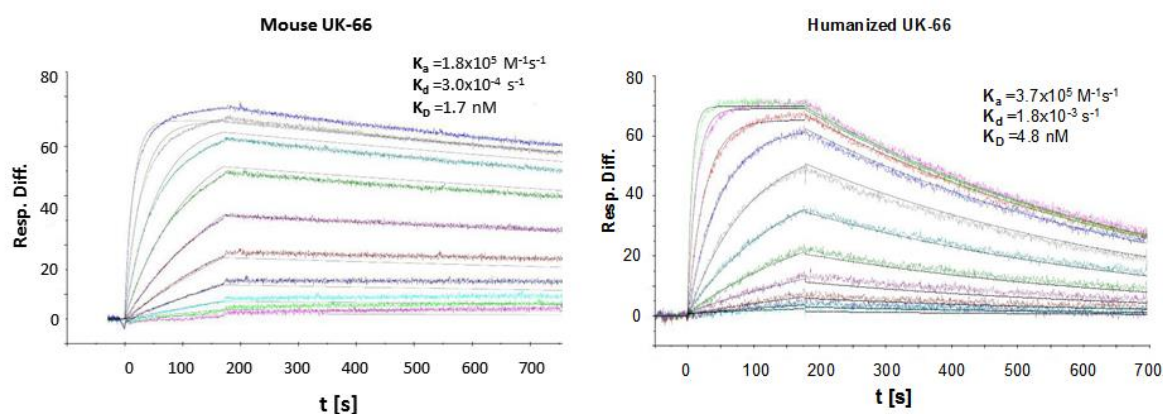


Fig. 23 Affinity of mouse and humanized UK-66 IgG1 analysed by SPR.

UK-66 IgG1 antibodies were immobilized on the sensor chip surface and interacted with soluble rIsaA of different concentrations (0.8-400 nM). Sensorgrams were adjusted at a flow rate of 30 $\mu\text{l}/\text{min}$. From these sensorgrams, a dissociation constant (K_D) was determined of 1.7 nM for the mouse UK-66 IgG1 and of 4.8 nM for the humanized UK-66 IgG1 antibody. The figure shows one representative result from two independent experiments with identical kinetic constants.

6.5.3. Humanized UK-66 IgG1 binds native expressed IsaA of clinically relevant *S. aureus* strains

Western Blot studies were performed to demonstrate that IsaA of different clinically relevant *S. aureus* strains is bound by hUK-66 IgG1. For these studies, *S. aureus* strains were used including both MRSA and MSSA. *S. aureus* strains represent different sequence types (ST) of seven house-keeping genes. Historically, MRSA-ST5 and MRSA-ST239 were responsible for causing HA-MRSA. MRSA-ST239 is distributed in Argentina, Czech Republic and Portugal. EMRSA 15 (ST5) circulates in the UK and the USA, and demonstrates genetic characteristics of HA-MRSA. Most of CA-MRSA cases in the US are caused by LAC (USA300-ST8) and MW2 (USA400-ST1). Results from Western Blot studies reveal that hUK-66 IgG1 recognizes the antigen IsaA (29 kDa) in all tested strains independently (Fig. 24).

The results from the Western Blot studies were confirmed by binding ELISA experiments with viable *S. aureus* cells. Therefore, viable bacteria of different *S. aureus* strains were coated overnight on microtiter plates. The specific binding of hUK-66 on staphylococcal IsaA was detected by using Protein A mutants and their isogenic *isaA*⁻/*spa*⁻ double mutants (strains generated and confirmed by U. Wallner).

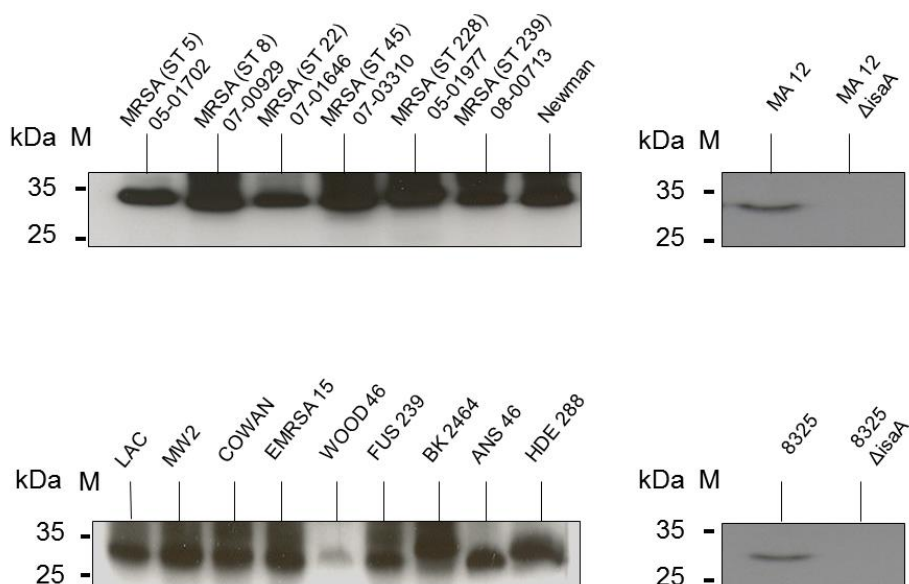


Fig. 24 Binding of hUK-66 IgG1 to IsaA expressed on different *S. aureus* strains.

Cell lysates of clinically relevant MRSA and MSSA strains were prepared from overnight cultures and incubated with hUK-66 IgG1 (1:5000) for 1h at RT. Binding of hUK-66 IgG1 was detected with the HRP-conjugated anti-human IgG1 secondary antibody. The *S. aureus* strains MA12 and 8325 and its isogenic *isaA*⁻ mutants was used to confirm the specific binding of IsaA by hUK-66 IgG1.

Results from binding ELISA studies are presented in figure 25. The antibody hUK-66 IgG1 reveal a specific binding of native IsaA expressed on the bacterial cell surface of different *S. aureus* strains and confirmed by this the results of the Western Blot analysis.

Taken together the data from ELISA, flow cytometry, immunofluorescence studies as well as the SPR data demonstrate the successful humanization of the mouse UK-66 antigen binding domain and the generation of a complete hUK-66 IgG antibody, which recognizes recombinant and native IsaA in an immobilized state and on the bacterial cell surface. Furthermore, hUK-66 IgG1 detects IsaA expressed by different clinically relevant *S. aureus* strains including MRSA and MSSA.

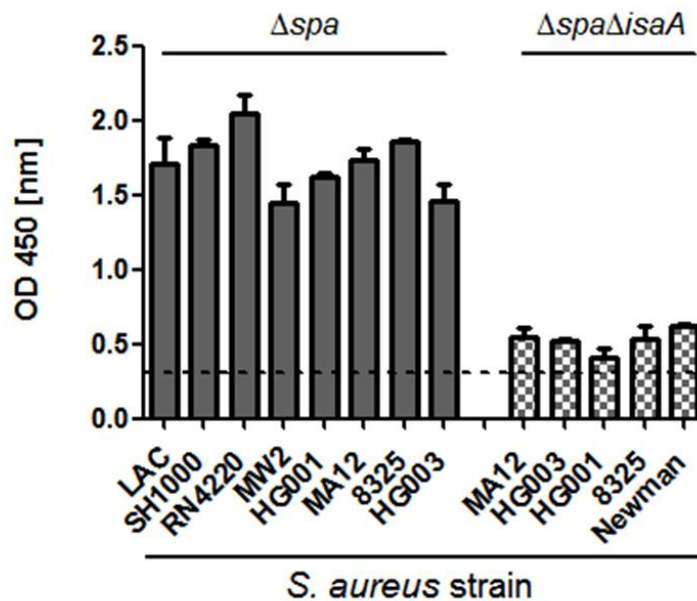


Fig. 25 hUK-66 IgG1 binds specifically native expressed *IsaA* of different *S. aureus* strains. *IsaA* was detected of various *S. aureus* strains via binding by hUK-66 IgG1. Therefore, 1×10^7 cells/100 μ l from an overnight culture were coated on a micro titer plate overnight at 4°C. The antibody hUK-66 IgG1 (1:5000) was incubated for 1h at RT. Binding of hUK-66 IgG1 was detected with the HRP-conjugated anti-human IgG1 secondary antibody. The isogenic *isaA*⁻/*spa*⁻ double mutants were used to confirm the specific binding of *IsaA* by hUK-66 IgG1.

6.6. Generation of stable cell lines producing scFv-Fc and full humanized UK-66 IgGs

For the *in vitro* characterization of hUK-66, antibodies were produced *in house* by stably transfected cell line CHO-K1. The amount of antibodies necessary for *in vivo* experiments, were produced by the companies Evitria and Catalent.

6.6.1. Development of cell lines for UK-66 production

For the characterization of UK-66 as a promising candidate for an antibody based therapy, different constructs of UK-66 specific antibodies were generated. These were murine and humanized scFv fragments, scFv-Fc fragments and full length IgGs. The scFv and scFv-Fc fragments are composed of the antigen binding domain of UK-66, the scFv-Fc fragment combines the antigen binding domain with a full human IgG1 Fc part. A major requirement for the full length IgG was to induce effector function of immune cells. Therefore an IgG1, IgG2 and an IgG4 were considered as a backbone for hUK-66.

6.6.2. Cloning of the vector constructs

To generate sufficient UK-66 antibodies for biochemical and functional characterization, cell lines were developed by the use of the Lonza® GS gene expression system. The GS gene was used for selection in CHO cells and is part of the vectors pEE6.4 and pEE12.4. Both

vectors contain a highly efficient transcription cassette under a control of hCMV-MIE promoter. The DNA of the heavy chain was cloned into the polylinker, downstream of the hCMV-MIE promoter and upstream of the SV40 sequence of pEE6.4. Vector pEE12.4 was used for construction of a double gene vector. After introduction of the light chain DNA into the vector pEE12.4, the complete expression cassette of the heavy chain was isolated from pEE6.4 and included into pEE12.4. Both polypeptide chains are expressed simultaneously with each gene under the control of a separate hCMV-MIE promoter.

6.6.3. Characterization of clones

Producer clones were selected by their growth of the selected pools. At least 5 cell clones, expressing complete IgGs, were expanded and tested for their specific productivity under comparable conditions. Cells were incubated for at least 5 days and IgG titers and scFv-Fc titers were measured by binding ELISA studies. The different production rates of the chosen clones are displayed in figure 27. In general, the correct scFv-Fc fragments as well as full antibodies were expressed in all batches therefore these pools are suitable for a small-scale production. Figure 26 demonstrates the purification of hUK-66 IgG1 and scFv-Fc hUK-66 from CHO-K1 cell culture supernatant and HEK293 supernatant, respectively.

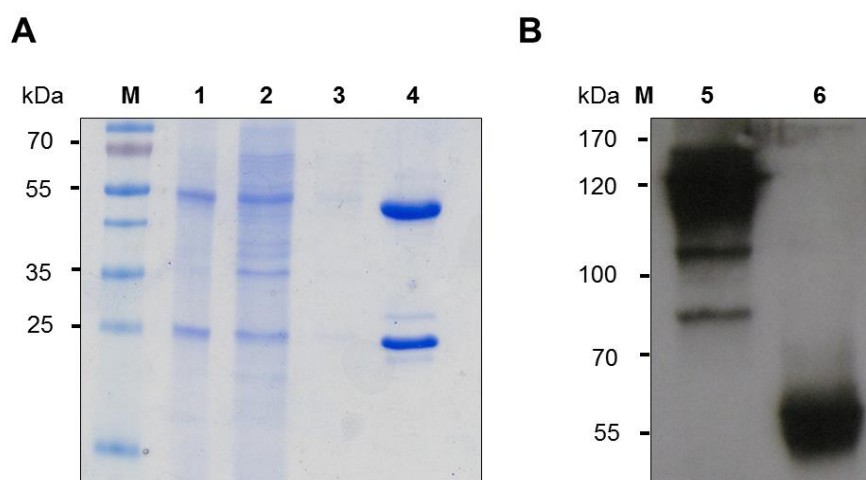


Fig. 26 Expression of hUK-66 IgG1 by CHO-K1 (A) and scFv-Fc UK-66 by HEK293 (B).

(A) SDS Page of cell culture supernatant, which was purified by Protein A affinity purification. M Marker, 1 Cell culture supernatant, 2 Flow through, 3 Wash fraction, 4 Eluat. Eluat fractions were collected and dialysed. **(B)** scFv-Fc eluat was analysed by Western Blot studies via binding of anti-human IgG1 HRP antibody under reduced and non-reduced conditions. 5 Eluat scFv-Fc under non reduced conditions, 6 Eluat scFv-Fc under reduced conditions.

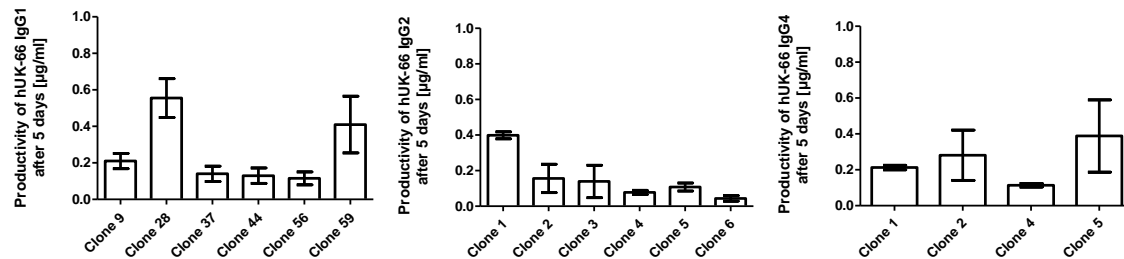


Fig. 27 Production rate of hUK-66 IgG1, IgG2 and IgG4 expression of randomly selected stable CHO-K1 clones.

Cell population were selected and expanded. After 5 days of cultivation antibody titer of the supernatants were determined by binding ELISA. Data represented mean \pm SD of productivity from 5 d cultivation.

For the IgG1 construct, the clones with the best combination of productivity and growth were chosen for further selection with MSX refinement and media optimization.

Clone hUK-66 IgG1 (28) was seeded into a 6-well plate and incubated with cultivation media RPMI or CHO media containing various concentrations of MSX (25-50-100-150-200-300 μ M). After 5 d of cultivation, specific productivity of hUK-66 IgG1 was analysed by binding ELISA (Fig. 28).

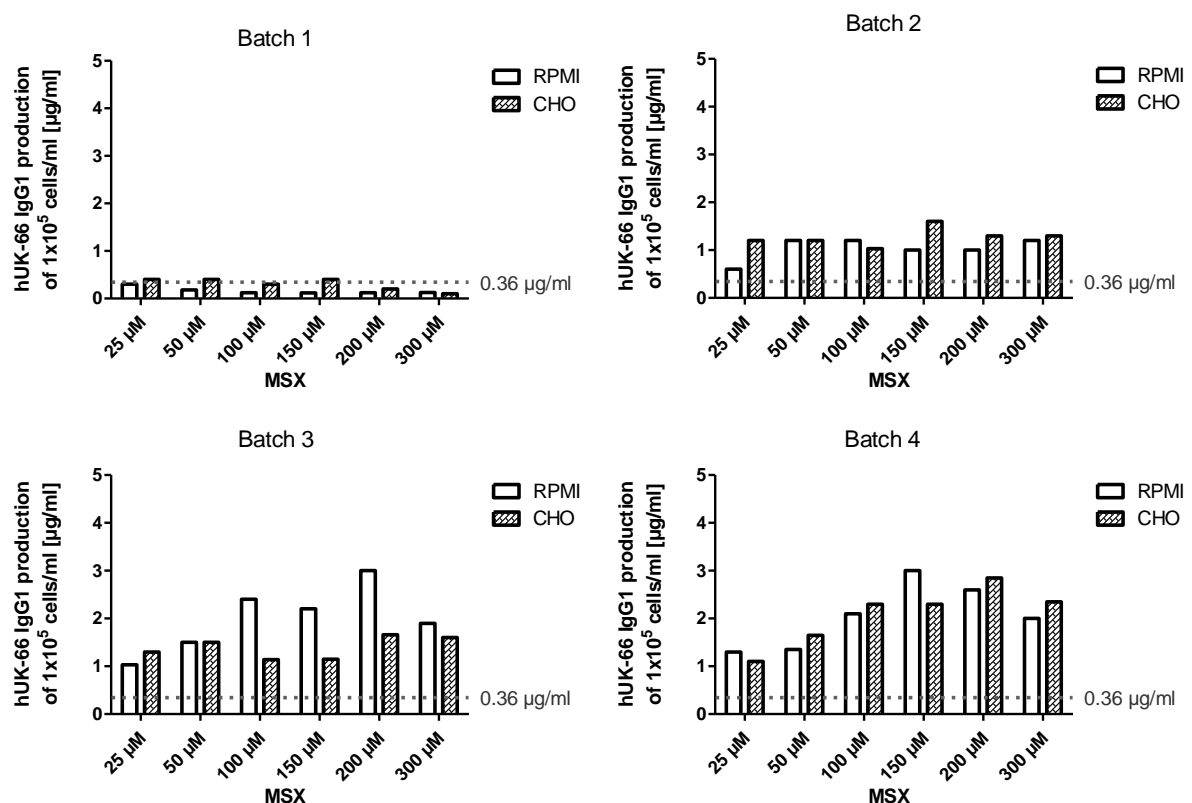


Fig. 28 Productivity of clone hUK-66 IgG1 (28) after MSX refinement.

Clone 28 was cultivated in a 6-well plate with culture media CHO or RPMI containing different concentrations of MSX (25-50-100-150-200-300 μ M). After 5 d of cultivation, hUK-66 IgG1 titer was analysed in supernatant by binding ELISA, grey line shows productivity after first selection.

The production of hUK-66 IgG1 is enhanced by increase MSX concentrations but not by cultivation of cells in CHO medium.

To further optimize the productivity of hUK-66 IgG1 producing clones, clone 28 (25 μ M MSX selection) was seeded into a 96-well plate for single cell dilution to isolate a high producer clone from cell population. After three passages, cells from four wells were expanded and their productivity was analysed by binding ELISA (Fig. 29).

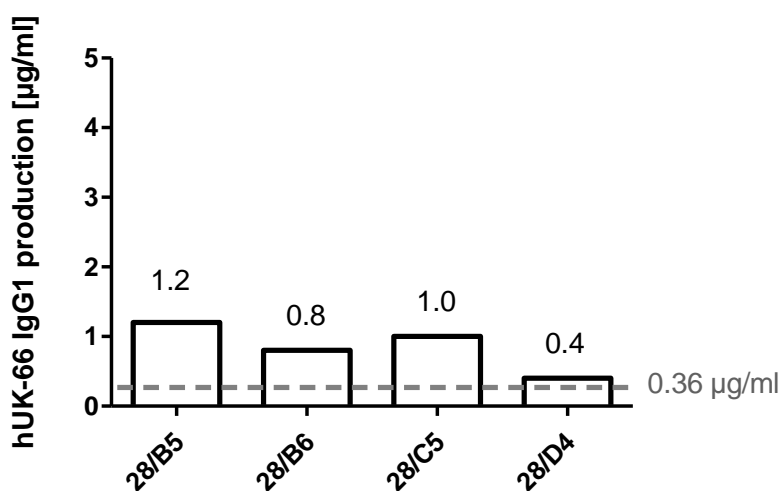


Fig. 29 Productivity of hUK-66 IgG1 after three passages of single cell dilution of clone 28.

After three passages, clones of four wells were tested for their specific productivity by binding ELISA. All clones demonstrate an increased productivity compare to the production rate after the first selection.

Comparison of the productivity of clone 28 after single cell dilution and MSX refinement demonstrates that the MSX refinement results in a more efficient selection of producer clones.

After the MSX refinement, the clone hUK-66 IgG1 (28-150 μ M MSX) was chosen for cultivation in a bioreactor. Based on the fact, that the CHO medium does not increase productivity of hUK-66 IgG1 significantly compared to the standard medium RPMI 1640. RPMI was chosen as medium for bioreactor cultivation. To reduce the cost of cultivation, the clone 28-150 μ M MSX was adapted to FCS free medium. Therefore, cells were cultivated for four weeks with reduction of FCS concentration. Productivity of hUK-66 IgG1 by CHO-K1 cells under FCS reduced conditions was analysed by binding ELISA. Results from figure 30 displays that the reduction of FCS in the culture medium has no significant effect on the antibody production.

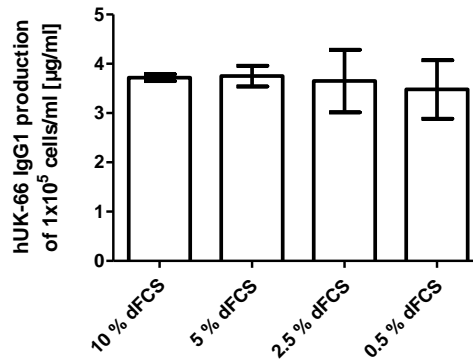


Fig. 30 Adaption of CHO-K1 hUK-66 IgG1 producer to FCS free medium.

Clones were cultivated for four weeks under reduced FCS conditions (5-2.5-0.5%). Clones selected for each FCS concentration were cultivated for one week and hUK-66 IgG1 productivity was examined by binding ELISA.

Medium of bioreactor was exchanged every 10 d and antibody containing supernatant was harvest. Concentration of hUK-66 IgG1 was determined by binding ELISA. After 10 d of incubation, an average production rate of 22 µg/ml was determined (Fig. 31). Cultivation of clone 28-150 µM MSX in a bioreactor system results in a five time increased productivity compared to productivity in a 75cm² cell culture flask.

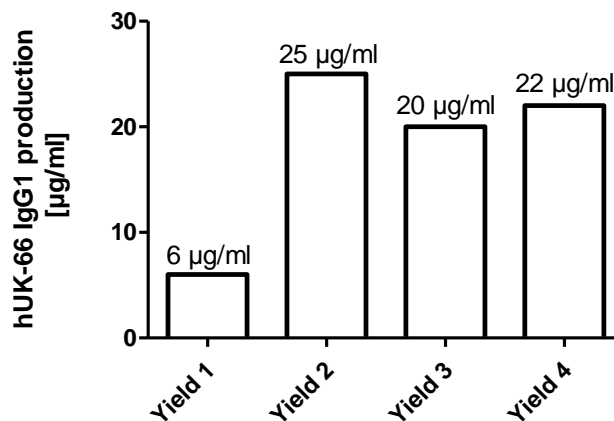


Fig. 31 Productivity of clone 28-200 µM MSX in a bioreactor system.

Clone 28-150 µM MSX was cultivated in a bioreactor system for 7 weeks. Every 10 d medium was exchanged, antibody containing supernatant was collected and antibody concentration was determined by binding ELISA.

6.7. Characterization of hUK-66 using *in vitro* studies

Recently, the functionality of mouse UK-66 IgG1 was analysed by binding and *in vivo* studies performed by Lorenz *et al.*, 2011. In this work, the therapeutic potency of mUK-66 IgG1 was demonstrated in two different mouse models using a central venous catheter-related infection and a sepsis survival model. In both models, mUK-66 IgG1 revealed protection against staphylococcal infection. Furthermore, Lorenz *et al.*, 2011 demonstrated the activation of professional phagocytes by mUK-66 IgG1 and the antibody dependent production of microbial induced reactive oxygen metabolites.

Based on these results, *in vitro* studies with human whole blood were performed to compare the biological activity between mouse and hUK-66 IgG1.

6.7.1. *In vitro* characterization of hUK-66 IgGs biological function

The biological function of hUK-66 IgG isotypes were examined by applying human like physiological conditions with a focus on the antibody-mediated killing of *S. aureus* Newman. However, different isotypes of hUK-66 was designed to cover different effector functions mediated by them. The antibody hUK-66 IgG3 was not generated since its difficult production based on its extended hinge region. Each of the modulated isotypes mediates various effector functions. IgG1 antibodies activate complement by C1q binding, while IgG2 and IgG4 activate complement by alternative pathways. IgG1 and IgG2 are bound by Fcγ receptors (FcγRs) which are most important to mediate phagocytosis e.g. CD16, CD32, CD64. However, IgG4 antibodies are very attractive by their antigen dependent long-term t-cell stimulation. To investigate the antibody-mediated activity of the full length hUK-66 IgG isotypes, human whole blood from healthy donors was incubated with *S. aureus* Newman in the presence of hUK-66 IgG1, IgG2 or IgG4 for 60 min at 37°C. To evaluate the number of viable bacteria and thereby the percentage of killed bacteria in regards to untreated control samples, cells were lysed by 1% Saponine and cfus were enumerated by plating (Fig. 32). Results from these assays revealed that hUK-66 IgG1 reduced the percentage of viable bacteria significantly compared to untreated samples, samples treated with isotype control Trastuzumab or human intravenous immunoglobulin pool (IVIg). In additions, hUK-66 isotypes IgG2 and IgG4 displayed no antibody mediated staphylococcal clearance. Therefore, hUK-66 IgG1 was chosen as lead antibody for further characterization of its biological activity.

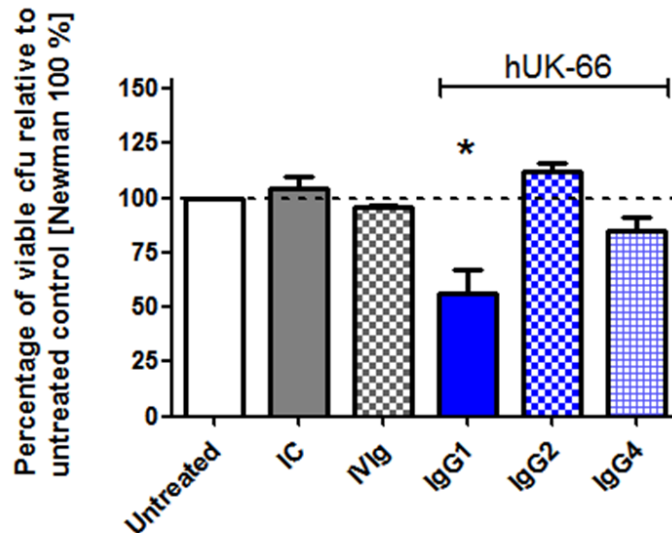


Fig. 32 Impact of hUK-66 IgG isotypes on antibody dependent killing of *S. aureus* Newman.

Heparinized blood samples from healthy donors were infected with *S. aureus* Newman and treated with either hUK-66 IgG1, IgG2, IgG4 for 60 min at 37°C. Trastuzumab served as IgG1 isotype control (IC) and the intravenous immunoglobulin mixture Gammunex® (IVIg) as a positive control. After lysis of eukaryotic cells, viable bacteria were enumerated by plate counting. The values were expressed as mean percentage with SD relative to the level of untreated blood/bacteria samples (set at 100%). Data represent three independent experiments from three different donors. The dash line in the graphs demonstrates the 100% reference value of control bacteria samples. * P<0.05, t-test.

6.7.2. *In vitro* analysis of biological activity of hUK-66 IgG1 in blood samples of high risk patients

The major goal for immunotherapeutic antibodies determined to battle staphylococcal infections must be a benefit for healthy subjects but also for immunocompromised and hospitalized patients suffering from acute infections. Therefore, a patient study was performed to investigate hUK-66 IgG1's potency to mediate staphylococcal killing in blood samples of patients with diabetes, end-stage renal disease, or artery occlusive disease (AOD). These patients groups are known for their deficiency in neutrophil mediated killing based on reduced development of oxidative burst. In this study, the impact of hUK-66 IgG1 mediated opsonophagocytosis in blood of the patients groups was investigated regarding the distinction of uptake and killing of *S. aureus* and the generation of an antibody generated respiratory burst by PMNs. The following experiments were performed with human whole blood samples and analysed by flow cytometry. Figure 33 displays the FACS analysis of human whole blood. The different cell population was identified as granulocytes, lymphocytes and monocytes by cell specific marker antibodies. Based on the fact, that neutrophils are the essential host defence against pathogenic staphylococci, the engulfment, the development of oxidative burst products and the killing of *S. aureus* by granulocytes was analysed.

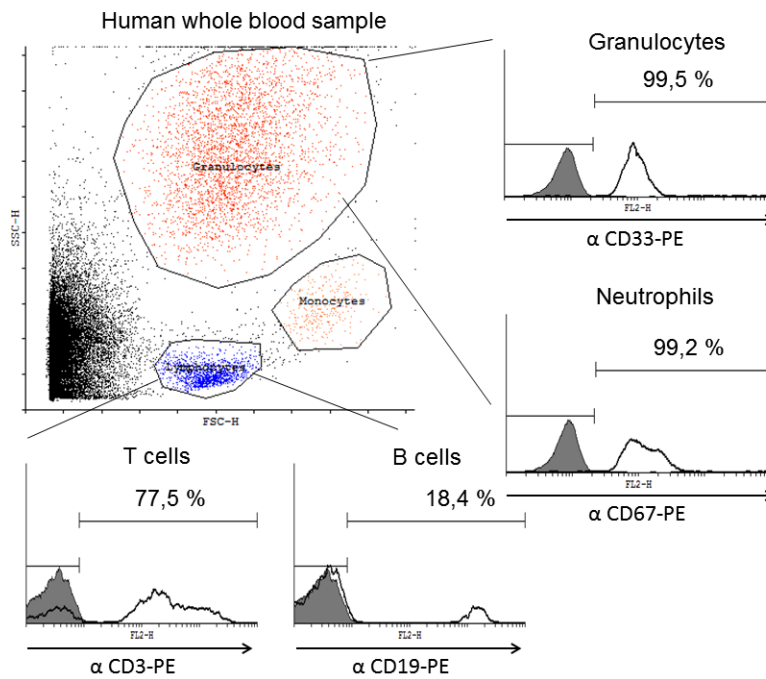


Fig. 33 Analysis of cell population in human whole blood samples by flow cytometry.

Heparinized blood samples from healthy donors were stained with PE-conjugated antibodies specific for t-cells, b-cells, granulocytes and neutrophils. Distribution of cell population in human blood was determined as 57% granulocytes, 32% lymphocytes and 6% monocytes. Lymphocytes were further distinguished as 77,5% t-cells and 18,4% b-cells. As expected, almost all identified granulocytes are neutrophils.

To investigate the engulfment of staphylococci by human granulocytes, *S. aureus* were stained with CFSE and granulocytes positive for fluorescent bacteria were analysed (Fig. 34).

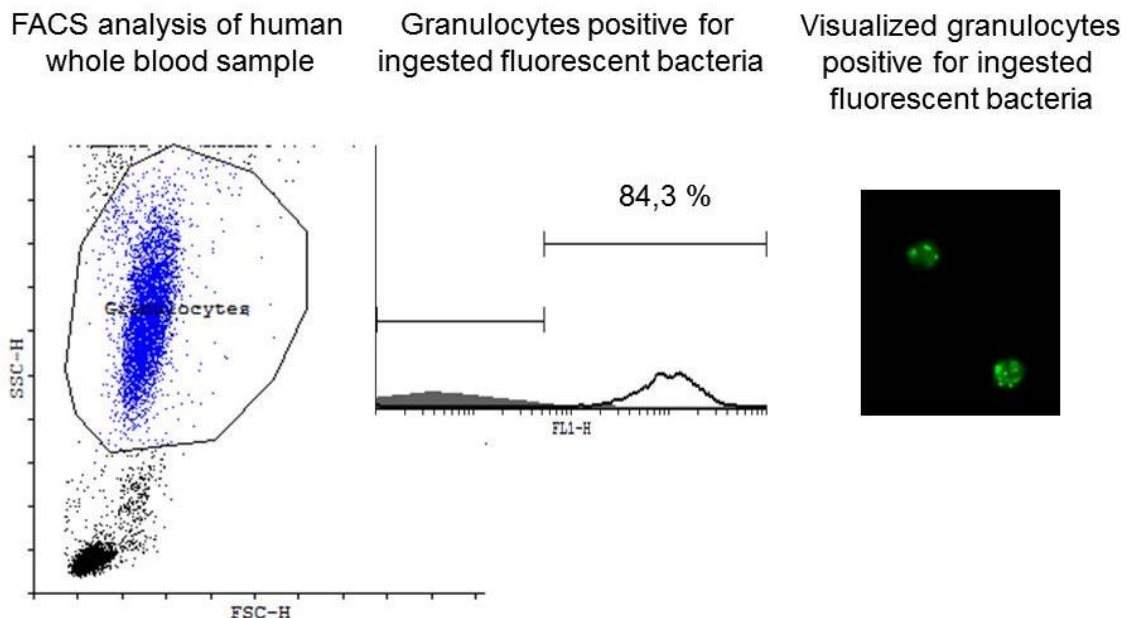


Fig. 34 Engulfment of *S. aureus* Newman by granulocytes from human whole blood samples.

Granulocytes were identified from human whole blood samples by their granularity and cell size. Bacteria were stained with CFSE to determined granulocytes positive for ingested staphylococci based on their fluorescence signal.

6.7.3. Investigation of hUK-66 IgG1- dependent opsono-phagocytosis of *S. aureus* by human neutrophils in whole blood

In the following study, the therapeutic impact of hUK-66 IgG1 was analysed in the process of opsono-phagocytosis. The process describes that a pathogen is marked for ingestion and destruction by a phagocyte. The antigen binding domain of the antibody binds the antigen IsaA, whereas the Fc portion of the antibody binds to an Fc receptor on the phagocyte. The ability of granulocytes from healthy donors and patients at high risk for staphylococcal infection was analysed to ingest *S. aureus* Newman in the presence and absence of hUK-66 IgG1 and determined by flow cytometry analysis.

In a preliminary experiment the uptake of bacteria by granulocytes derived from healthy donors respectively patients at high risk for staphylococcal infections was determined independent of antibody addition in order to determine the baseline for unassisted uptake of bacteria. Therefore, *S. aureus* strain Newman was stained with the fluorescence dye CFSE. CFSE crosses the cell wall of bacteria and binds covalently to residues inside the bacterial cell to avoid cross reaction with hUK-66 IgG1 binding on the bacteria cell surface. After incubation of human whole blood with CFSE stained bacteria for 20 min at 37°C, granulocytes positive for fluorescence signal were analysed by flow cytometry. Results are presented in figure 35 and show percentage of fluorescent positive cells (ingested fluorescent bacteria out of a total 10000 gated granulocytes). Granulocytes from healthy donors revealed a significantly higher percentage of granulocytes positive for ingested *S. aureus* Newman than granulocytes from dialysis, diabetes or patients with AOD. After 20 min of incubation with fluorescent *S. aureus*, 95% of granulocytes from healthy donors were positive for ingested, fluorescently labelled bacteria. Results of the patient groups demonstrate that 39% of granulocytes from dialysis patients had engulfed bacteria, 32% of granulocytes from diabetes patients were positive for staphylococci and 40% of granulocytes from patients with diagnosed AOD ingested *S. aureus* Newman. These results indicate that granulocytes from patient at high risk for a staphylococcal infection are affected in their ability to engulf *S. aureus* Newman compared to granulocytes from healthy donors.

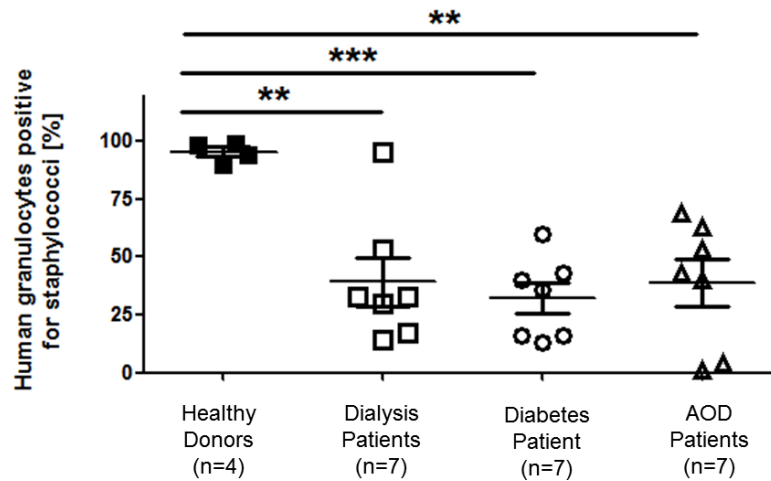


Fig. 35 Engulfment of *S. aureus* Newman by granulocytes from clinical relevant patient groups and healthy donors.

Heparinized human blood samples (n=4-7) from healthy donors, patients undergoing dialysis, diabetes- or AOD patients were infected with CFSE stained *S. aureus* Newman for 20 min at 37°C. Granulocytes ingested fluorescent bacteria were measured by flow cytometry. In the blood samples of healthy donors, 39% granulocytes are positive for *S. aureus* Newman uptake. In the problematic patients, fluorescent *S. aureus* Newman was detected by 39% of granulocytes from dialysis patients, 32% of granulocytes from diabetes patients and 40% of granulocytes from patients with AOD. Individual data points of one blood sample and mean values of each group are shown as percentage. ** P<0.01, t-test.

In the next step the impact of hUK-66 regarding phagocytosis especially for the impaired blood donors was evaluated. In this regard, human whole blood samples were incubated with fluorescent-conjugated bacteria in the presence of 0.075 or 0.9 mg/ml hUK-66 IgG1 or with Trastuzumab as isotype control for 20 min at 37°C. Figure 36 clearly shows that phagocytosis of *S. aureus* using blood from healthy donors results in very high percentages of ingested bacteria independent of additional antibody applied. The percentage of positive granulocytes is not increased in the presence of the IC (97%) or hUK-66 IgG1 (97%). While, the percentage of granulocytes positive for phagocytosed fluorescent bacteria from patients at high risk for staphylococcal infection was significantly reduced. Unexpectedly, the addition of anti-IsaA specific antibodies to patient's blood did not have any beneficial effect for phagocytosis of bacteria compared to untreated samples. In both patient groups, 39% of granulocytes were positive for ingested bacteria (Fig. 36B and D). However, samples from dialysis patients treated with hUK-66 IgG1 0.075 mg/ml demonstrate 37% and samples treated with 0.9 mg/ml reveal 45% positive granulocytes. Samples from AOD patients, treated with 0.075 mg/ml, reveal 36% of granulocytes positive for ingested bacteria and 44% of granulocytes were positive after treated with 0.9 mg/ml hUK-66 IgG1 (Fig. 36D).

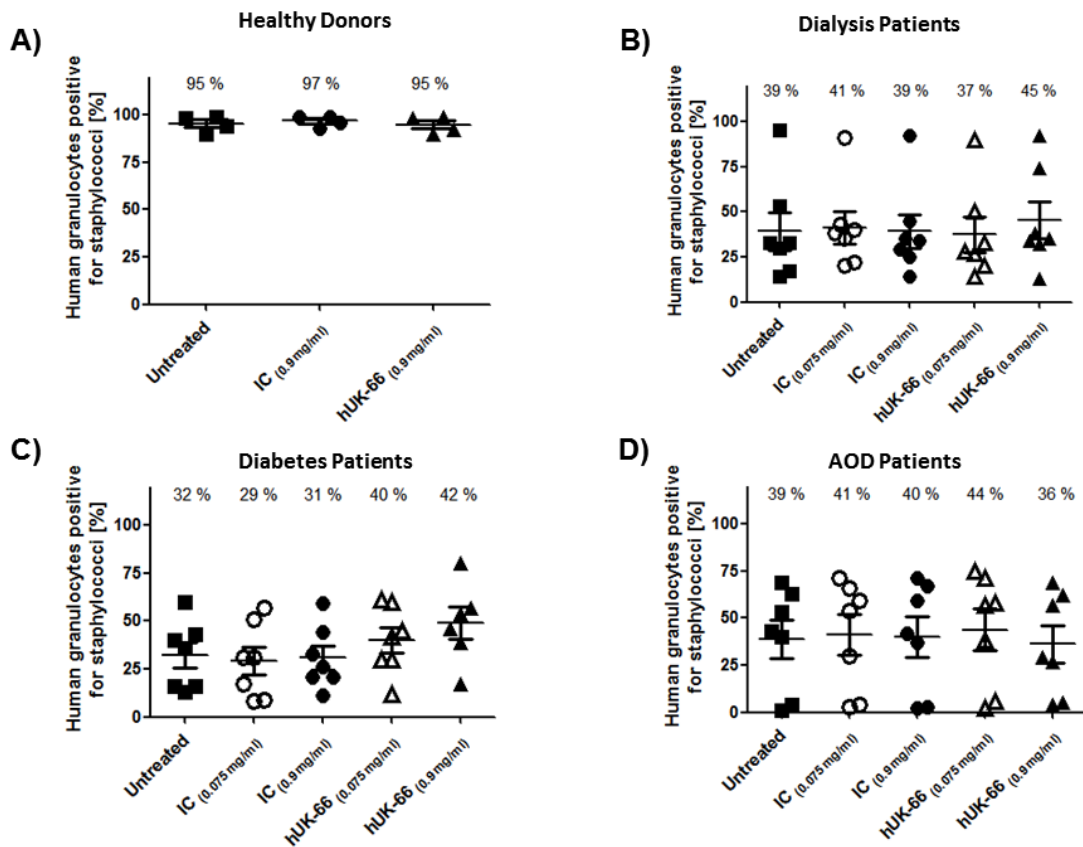


Fig. 36 Engulfment of *S. aureus* Newman by granulocytes from clinical relevant patient groups and healthy donors.

Heparinized human blood samples (n=4-7) from healthy donors, patients undergoing dialysis, diabetes and AOD were infected with CFSE stained *S. aureus* Newman for 20 min at 37°C. Granulocytes ingested fluorescent bacteria were measured by flow cytometry. (A) In the blood samples of healthy donors, 95% granulocytes are positive for *S. aureus* Newman uptake. The percentage of granulocytes with ingested bacteria was not improved in the presence of IC (97%) or hUK-66 IgG1 (95%). (B-D) In the problematic patients, fluorescent *S. aureus* Newman was detected in 39% of granulocytes from dialysis patients. The presence of IC using 0.075 mg/ml results in 39% and the higher concentration of 0.9 mg/ml results in 41% positive granulocytes. The treatment of hUK-66 IgG1 does not result in an increased percentage of granulocytes positive for fluorescent bacteria uptake. hUK-66 IgG1 added in a concentration of 0.075 mg/ml reveals 37% and the concentration of 0.9 mg/ml results in 45% positive granulocytes. In blood from diabetes patients, 32% of granulocytes are positive for ingested bacteria in the untreated group. However, an improved phagocytosis rate was detected in the presence of hUK-66 IgG1. A dose of 0.075 mg/ml results in 40% and the concentration of 0.9 mg/ml results in 42% positive granulocytes, but not in the presence of IC (lower concentration 29%, higher concentration 31%). 40% of granulocytes from patients with AOD were positive for fluorescent bacteria in the untreated group. The presence of IC with a concentration of 0.075 mg/ml and 0.9 mg/ml demonstrate 40% and 41% of positive granulocytes. The treatment group of 0.075 mg/ml hUK-66 IgG1 demonstrates 36% and with 0.9 mg/ml presents 44% positive granulocytes. Individual data points of one blood sample and mean values of each group are shown as percentage.

As for the other patients, blood samples derived from subject with diabetes, a very low overall phagocytosis rate of 32% was observed. Again neither addition of the control antibody nor either hUK-66 concentrations had a significant positive effect on the uptake of bacteria. 32% of granulocytes were positive for ingested fluorescent bacteria in the untreated samples. Treatment with IC has no effect on the phagocytosis rate since the lower concentration of 0.075 mg/ml results in 29% of granulocytes positive for fluorescent bacteria and the higher concentration of 0.9 mg/ml reveals 32% positive granulocytes compared to

the 32% positive granulocytes from the untreated samples. However, samples incubated with hUK-66 IgG1 reveal an increase of granulocytes positive for ingested bacteria treated with a concentration of 0.075 mg/ml (40%) and the higher dose of 0.9 mg/ml (42%) compared to untreated samples with 32% of positive granulocytes.

Overall, after 20 min of incubation with *S. aureus* Newman, granulocytes from healthy donors, dialysis patients and patients with diagnosed AOD reach the maximum of phagocytic activity and the treatment with hUK-66 IgG1 revealed no enhancement. In contrast, a 10% increase of phagocytosis rate was detected in granulocytes from diabetes patients treated with hUK-66 IgG1.

6.7.4. Investigation of hUK-66 IgG1 dependent respiratory burst induction in human neutrophils

Phagocytosis is an essential process of the host defence to battle bacterial infections. Ingested bacteria are killed by oxygen-dependent and oxygen-independent mechanisms. In the following experiment, the oxidative burst activity (oxygen-dependent mechanism) of neutrophils infected with bacteria was quantified by flow cytometry. In this regard, the products of the oxidative burst like superoxide anion, hydrogen peroxide and hypochlorous acid can be quantitatively monitored by the addition of the substrate DHR 123, a substrate which reacts with metabolites and radiates a fluorescent signal. To produce ROS in response to staphylococcal infection, granulocytes of healthy donors and of selected patient groups at high risk for staphylococcal infection were incubated 20 min with *S. aureus* Newman. As presented in figure 37, 82% of the gated granulocytes within the blood of healthy donors respond to the infection with the production of ROS. Results of the patient groups showed that 33% of granulocytes of dialysis patients produced oxidative burst in the presence of *S. aureus* Newman; 30% of granulocytes from patients with diabetes were positive for oxidative burst development and 40% of granulocytes from patients with AOD. Therefore, the data demonstrate that granulocytes of indicated patient groups show significantly reduced development of reactive oxygen species in the presence of *S. aureus* Newman compared to granulocytes from healthy subjects (Fig. 37).

Based on these results, hUK-66 IgG1's potency to restore the generation of oxygen species to level seen with granulocytes of healthy patients was analysed. For these studies, two concentrations of hUK-66 IgG1 were tested 0.075 mg/ml and 0.9 mg/ml. Trastuzumab was chosen as an IgG1 isotype control.

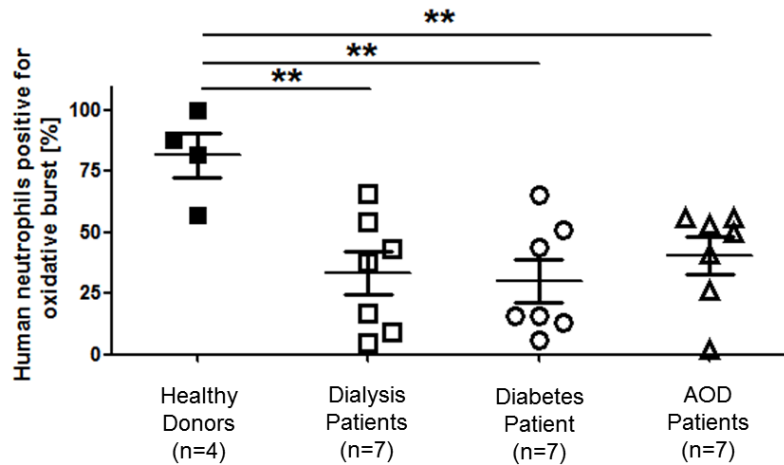


Fig. 37 Development of respiratory burst after *S. aureus* Newman infection in granulocytes from clinical relevant patient groups compared to healthy donors.

Heparinized human blood samples (n=4-7) from healthy donors, patients undergoing dialysis, diabetes and AOD were infected with *S. aureus* Newman for 20 min at 37°C. The generation of reactive oxygen species (ROS) by granulocytes were analysed by flow cytometry. In the blood samples of healthy donors, *S. aureus* Newman caused 82% ROS-positive granulocytes. In the problematic patients, a ROS development was detected in 33% of blood samples from dialysis patients, in 30% of blood samples from diabetes patients and in 40% of blood samples from patients with AOD. Individual data points of one blood sample and mean values of each group are shown as percentage. ** > P 0.01

Blood samples were infected with *S. aureus* Newman for 20 min at 37°C and the percentage of granulocytes that generated an oxidative burst in the treated and untreated samples was measured by flow cytometry.

82% of granulocytes from healthy donors are positive for oxidative burst after contact with *S. aureus* Newman. Samples treated with the isotype control antibody (IC) demonstrate that 81% of granulocytes were positive for respiratory burst and 85% granulocytes generated an oxidative burst in the presence of hUK-66 IgG1 (Fig. 38A). Results indicated that hUK-66 treatment did not enhance the development of oxidative burst in human granulocytes. However, a hUK-66 IgG1 specific increase in the generation of oxidative species in granulocytes from patient at high risk for staphylococcal infection was observed. At higher concentration of 0.9 mg/ml hUK-66 IgG1 54% of granulocytes were positive for oxidative burst in blood samples from dialysis patient, compared to samples treated with the isotype control (34%) and untreated samples (33%). Concomitantly, granulocytes of dialysis patients showed an evaluated signal of 30% in oxidative burst compared to untreated or 32% isotype control treated samples respectively (Fig. 38B). Furthermore, granulocytes from diabetes and AOD patients treated with hUK-66 IgG1 showed an increased respiratory burst with 46% and 55% positive cells. In comparison, samples of AOD patients treated with the isotype control, resulted in 32%, and 37% positive granulocytes, and untreated samples, resulted in 41% positive granulocytes, respectively (Fig. 38C,D).

Overall, application of hUK-66 IgG1 at a higher dosage (0.9 mg/ml) induced an elevated oxidative burst response (20%) of granulocytes derived of patients at high risk upon infection.

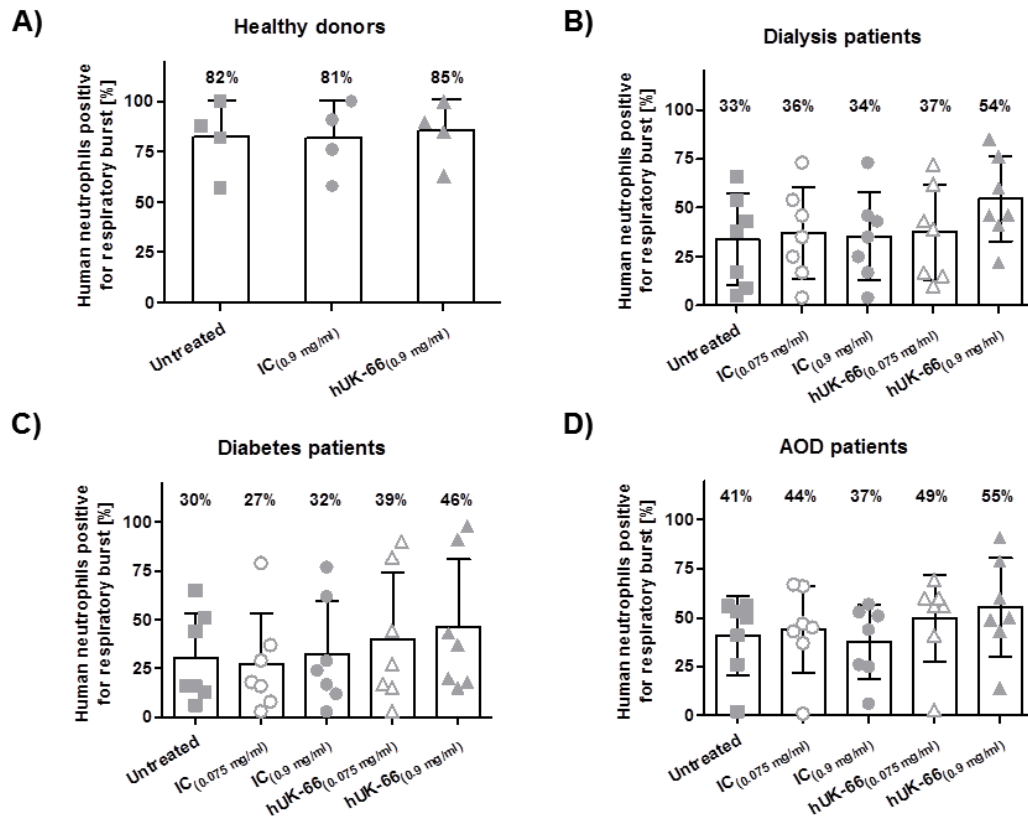


Fig. 38 Development of respiratory burst after *S. aureus* Newman infection in granulocytes from clinical relevant patient groups and healthy donors.

Heparinized human blood samples (n=4-7) from healthy donors, dialysis patients, diabetes patients and patients with AOD were infected with *S. aureus* Newman in the presence of two different concentrations of hUK-66 IgG1 for 20 min at 37°C. Trastuzumab served as matched IgG1 isotype control (IC). Neutrophils positive for the development of reactive oxygen species (ROS) were analysed by flow cytometry. (A) In blood of healthy donors, the presence of bacteria caused 82% ROS-positive neutrophils. The presence of hUK-66 IgG1 results in 85% neutrophils positive for ROS development. (B-D) In blood samples of patients at high risk, hUK-66 IgG1 results in an increase of 21%, 16% and 14% neutrophils positive for ROS development, respectively compared to the untreated samples. Individual data points were superimposed with bar. Mean values of each group are shown as percentage.

Phagocytosis by polymorph nuclear granulocytes is a multistep and multifactorial process and an essential arm of host defence against bacterial infections. The previous studies focused on the ingestion of *S. aureus* Newman and the development of oxidative burst by host granulocytes. In the following study it is clarified whether the application of the humanized antibody did not only stimulate the recognition and induction of oxygen species but also resulted in the killing of the bacteria.

6.7.5. Investigation of hUK-66 IgG1 dependent killing of *S. aureus* Newman by human whole blood

The phagocytosis and the development of reactive oxygen species are necessary for the killing of intracellular microorganisms. However, *S. aureus* has diverse strategies to avoid phagocytic killing. Therefore, the following studies focused on the antibody dependent killing

of *S. aureus* Newman by granulocytes from healthy donors and patients at high risk for staphylococcal infections based on the fact, that the selected patient groups are known for their granulocyte dysfunctions.

Antibody mediated killing of *S. aureus* Newman was investigated using whole blood samples using physiological conditions. The treatment with hUK-66 IgG1 at a concentration of 0.9 mg/ml resulted in a significant reduction of viable bacteria by 41% compared to the control sample (Fig. 39A). Samples treated with 0.9 mg/ml Gammunex[®] demonstrated a prominent decrease reduction by 16% of viable bacteria, while samples treated with IC revealed a reduction by 9% of viable bacteria. The lower molar concentration of hUK-66 IgG1 (0.075 mg/ml) had no significant effect in the reduction of viable bacteria (10%). When hUK-66 IgG1 (0.9 mg/ml) was added to blood samples from dialysis patients, diabetes patients and patients suffering from AOD, the number of viable bacteria was significantly reduced to cfu of samples with 0.075 mg/ml hUK-66 (33%), isotype control (31%) or untreated samples (27%), respectively (Fig. 39B-D). Furthermore, the lower concentration of hUK-66 IgG1 (0.075 mg/ml) was effective in samples from diabetes patients by demonstrating a reduction of viable bacteria by 14%. However, neither Trastuzumab nor Gammunex[®] demonstrated a significant effect when added to samples from the three selected patient groups.

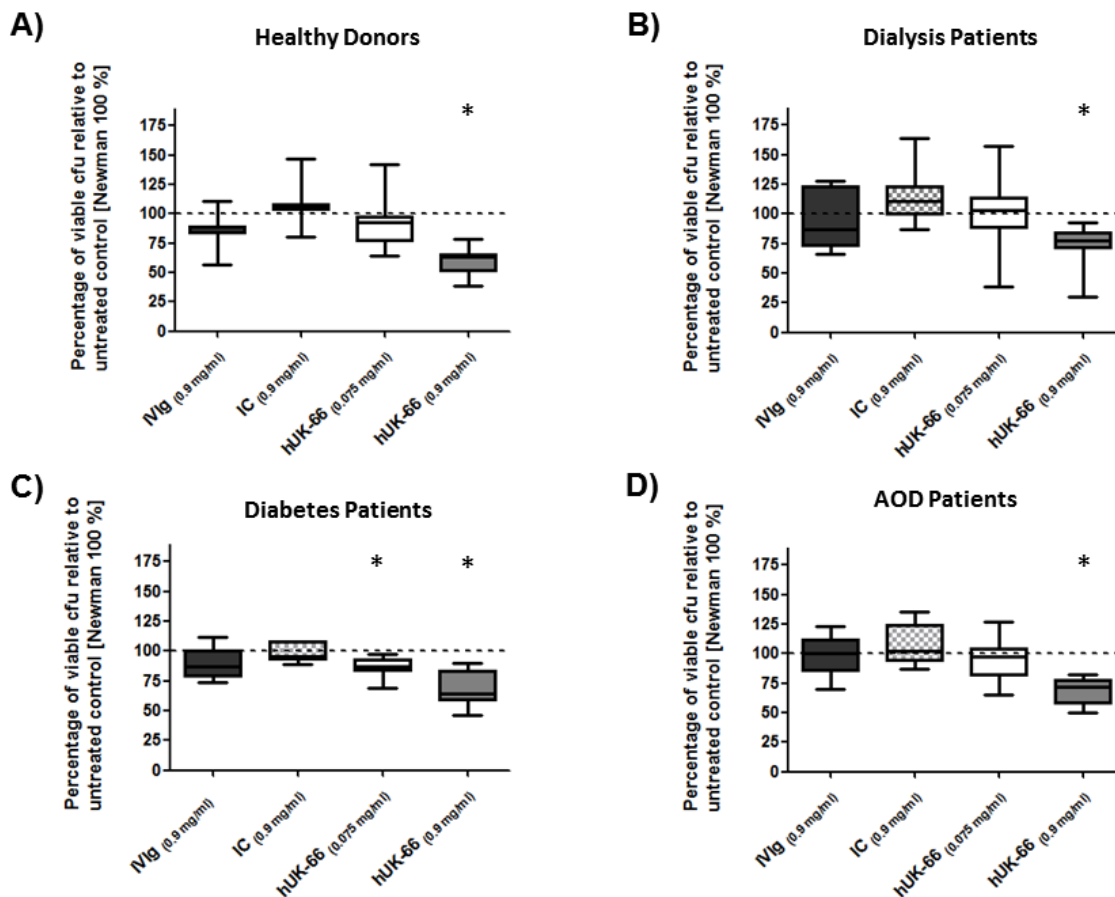


Fig. 39 hUK-66 IgG1 dependent killing of *S. aureus* Newman by granulocytes from healthy donors and patients at high risk.

Heparinized human blood samples ($n=7$) from healthy donors, dialysis patients, diabetes patients and patients with AOD were infected with *S. aureus* Newman in the presence of two different concentrations of hUK-66 IgG1 for 20 min at 37°C. Trastuzumab served as matched IgG1 isotype control (IC) and the intravenous human immunoglobulin preparation Gammunex® (IVIg) serves as a second positive control. Total viable bacteria were recovered after eukaryotic cell lysis and enumerated by plate counting. The values were plotted relative to the level of untreated samples (set 100%). The mean percentage of viable *S. aureus* recovered in the blood from (A) healthy donors, (B) dialysis patients, (C) diabetes patients and (D) patients with AOD was significantly reduced by the treatment of 0.9 mg/ml hUK-66 IgG1 compared to untreated samples. The values of reduction were 41%, 27%, 33% and 31%, respectively. Furthermore, 0.075 mg/ml hUK-66 IgG1 results in a reduction of viable bacteria by 14% in blood samples of diabetes patients. The treatment with IC and IVIg revealed no significant reduction of viable bacteria in all blood samples. Data are illustrated as box-and-whisker plot. The dash line in the graph demonstrates the 100% reference value of untreated samples. * $P < 0.05$, t-test.

In summary, addition of the hUK-66 IgG1 antibody has a beneficial effect on killing of bacteria. Importantly, granulocytes derived from immunocompetent as well as immunocompromised volunteers showed an increased killing of bacteria.

6.7.6. *In vitro* analysis of biological activity of hUK-66 IgG1 in purified human PMNs

In the previous *in vitro* studies, the killing assays were performed with human whole blood samples to analyse killing capacity of human granulocytes under physiological conditions.

These conditions, including plasma and complement, support natural behaviour of granulocytes. However, the results of these killing assays also include the capacity of the complement system to clear pathogens. To extend analysis for mode of action; the complement components well known for unspecific phagocytosis of opsinin marked bacteria were excluded by using purified PMNs. In this regard, PMNs were purified from human whole blood samples from healthy donors, infected with *S. aureus* Newman and incubated for 1 h at 37°C. After lysis of cells, viable bacteria were detected by plating and overnight incubation. All observed killing of bacteria by PMNs were mediated by applied antibodies. The hUK-66 IgG1 dependent killing was analysed by using different concentrations of hUK-66 in the range from 0.05 µg/ml to 500 µg/ml. To investigate, if the mode of action is dependent on functional FcγRs, the deglycosylated mutant of hUK-66 IgG1 N297A were also tested with the same concentrations. Rituximab served as matched IgG1 isotype control (IC) tested with the same concentrations. Results from figure 40 demonstrate a hUK-66 IgG1 dependent and complement independent killing of *S. aureus* Newman in a concentration dependent manner. Samples treated with 50 µg/ml hUK-66 IgG1 revealed a significant reduction of viable bacteria compared to the untreated samples and samples treated with IC and deglycosylated mutant hUK-66 IgG1 N297A. This effect was improved by a higher dose of 500 µg/ml. Treatment using 500 µg/ml hUK-66 IgG1 resulted in a more effective reduction of viable bacteria compared to the concentration of 50 µg/ml hUK-66 IgG1. The viable bacteria isolated from the samples treated with the deglycosylated mutant hUK-66 IgG1 N297A were comparable to the number of viable bacteria of the untreated samples. The isotype control Rituximab also reduced the number of viable bacteria when applied in a concentration of 500 µg/ml. Results from this study demonstrate that the killing of *S. aureus* Newman by hUK-66 IgG1 is concentration dependent. In addition, the application of the deglycosylated antibody mutant proofed that killing of staphylococci is dependent on the FcγRs. In fact using the *in vitro* killing assays we provided strong evidence that the hUK-66 antibody promotes not only uptake of bacteria but more important killing itself and therefore is a potential candidate for antibody based therapy.

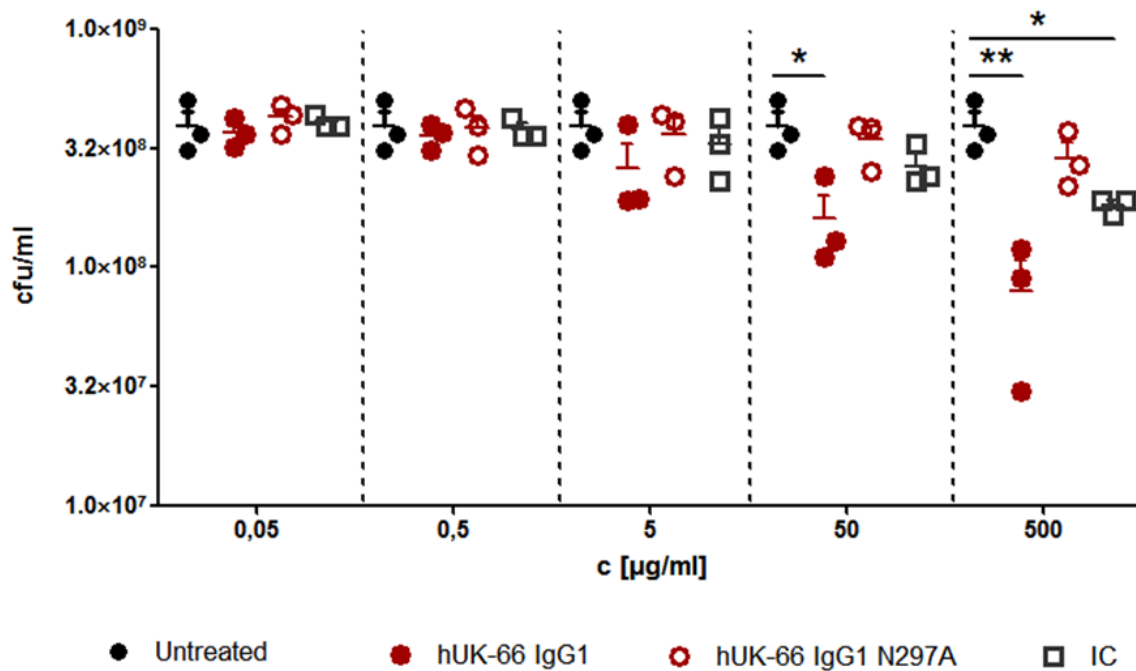


Fig. 40 hUK-66 IgG1 dependent killing of *S. aureus* Newman by purified human granulocytes from healthy donors.

PMNs were purified from human blood samples (n=3) from healthy donors and were infected with *S. aureus* Newman in the presence of different concentrations of hUK-66 IgG1, the deglycosylated hUK-66 IgG1 N297A and Rituximab for 1 h at 37°C. Rituximab served as matched IgG1 isotype control (IC). Total viable bacteria were recovered after eukaryotic cell lysis and enumerated by plate counting. The values were plotted as cfu/ml. The mean value of viable *S. aureus* recovered from PMNs from healthy donors was significantly reduced by the treatment of 50 and 500 µg/ml hUK-66 IgG1, respectively compared to untreated samples and samples treated with deglycosylated mutant hUK-66 IgG1 N297A. The treatment with IC revealed a significant reduction of viable bacteria in samples treated with 500 µg/ml. * $P < 0.05$, ** $P < 0.01$ t-test.

6.7.7. *In vitro* analysis of combined hUK-66 IgG1 and hUK-tox antibody in human whole blood samples

During the last decade, various active and passive immunization strategies have been assessed in clinical trials. Importantly, despite promising data, clinical trials in humans have uniformly failed yet [145]. These negative results prompted a discussion whether or not immunotherapeutic agents based on a unique target generally have limited efficacy to treat or prevent *S. aureus* diseases in humans. Therefore, multi-valent immunotherapy approaches against *S. aureus* are expected to have the best chance of clinical success when used in combinatorial therapy, potentially incorporating opsonic killing of bacteria and toxin neutralization.

One of the major virulence factors in the disease pathogenesis of *S. aureus* is the alpha-toxin. This toxin is secreted as a water-soluble monomer by the majority of clinical relevant *S. aureus* strains [146]. By its ability to forming pores, alpha-toxin injures the lung and other tissues and by this causing a myriad of diseases ranging from minor skin infections to life-threatening deep tissue infections and toxinses [147]. In various animal models,

immunization with antibodies directed against the staphylococcal alpha-toxin protects against *S. aureus* colonization or infection and results in a significant increase of survival in the treated animals compared to untreated animals. Based on the promising animal data, a hUK-tox IgG1 antibody was chosen to be tested in a combinatorial therapy with hUK-66 IgG1. The combination of two anti-staphylococcal antibodies which have two different modes of action: hUK-66 IgG1 mediates antibody-dependent killing of *S. aureus* and hUK-tox blocks an important pathogenic mechanism of *S. aureus* by neutralize alpha-toxin, is a promising approach for an anti-staphylococcal therapy. Therefore, the *in vitro* killing assays with human whole blood samples from healthy donors were performed by human cells infected with *S. aureus* Newman. The impact of the combinatorial therapy was analysed by testing two concentrations: a low dose, which consists of 0.075 mg/ml hUK-66 and 0.02 mg/ml hUK-tox and a high dose, which contains 0.9 mg/ml hUK-66 and 0.2 hUK-tox. Gammunex[®] served as negative control, based on the fact that no reduction of viable cfu was detected in previous studies and was added to investigate the effect on viable bacteria of hUK-tox antibodies. The virulence factor alpha-toxin is secreted by most clinical relevant *S. aureus* strains; therefore cell culture supernatant of *S. aureus* Newman wild type and an isogenic alpha-toxin mutant was prepared and used for the killing assays.

Results from these assays are presented in figure 41. The untreated control samples incubated with cell culture supernatant from wild type *S. aureus* Newman revealed a higher percentage of viable cfu compared to the samples incubated with cell culture supernatant from *S. aureus* Newman Δhla . Human blood samples incubated with the antibody combination in the lower concentration demonstrated no reduction of viable bacteria compared to the untreated control. However, samples incubated with 0.9 mg/ml hUK-66 IgG1 and 0.2 mg/ml IVIg showed a significant reduction of viable bacteria compared to the antibody combinations hUK-66/hUK-tox and IVIg/hUK-tox. The presence of alpha-toxin indicates an important benefit for the survival of *S. aureus* based on the fact that the percentage of viable bacteria incubated with cell culture of its isogenic alpha-toxin mutant is reduced compared to samples incubated with cell culture supernatant from wild type. This experiment demonstrates that the presence of alpha-toxin has an important effect on *S. aureus* pathogenesis. Overall, in this assay no combinatorial effect for the killing of pathogenic staphylococci was observed.

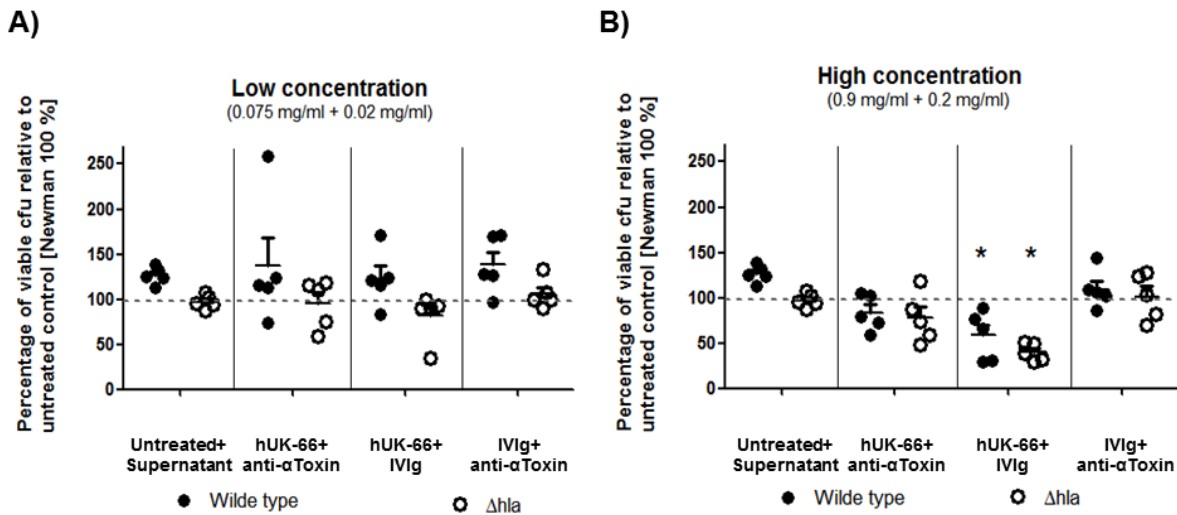


Fig. 41 Combinatorial therapy approach of hUK-66 IgG1 and hUK-tox IgG1 in *in vitro* killing assays with human whole blood samples.

Heparinized human blood samples ($n=5$) from healthy donors were infected with *S. aureus* Newman in the presence of two different concentrations and the combinations hUK-66/hUK-tox, hUK-66/IVIg and IVIg/hUK-tox 1 h at 37°C. Gammunex[®] served as control antibody (IVIg) to adjust antibody concentration. Total viable bacteria were recovered after eukaryotic cell lysis and enumerated by plate counting. The values were plotted as percentage of cfu relative to untreated control. The mean value of viable *S. aureus* recovered from samples treated with the higher dose of hUK-66/IVIg was significantly reduced compared to untreated samples and samples treated with other antibody combinations or lower dose. The dash line presented percentage of viable bacteria from control samples incubated without cell culture supernatant. * $P<0.05$, t-test.

6.8. *In vitro* mouse blood killing assays to investigate the therapeutic efficacy of murine and humanized UK-66 combined with hUK-tox IgG1

The humanized monoclonal antibody hUK-66 demonstrated reduced efficacy in the mouse pneumonia model compared to the murine counterpart mUK-66. To evaluate the impact of species background of the antibodies on phagocytosis and killing, killing assays with mouse whole blood was performed with both antibodies. The secreted alpha-toxin of *S. aureus* causes pore formation and induces proinflammatory signal molecules in mammalian cells. Therefore, cell culture supernatant of a 13 h grown culture of *S. aureus* Newman was used to analyse the efficacy of hUK-tox IgG1 antibody in an *in vitro* killing assay with mouse whole blood (Fig. 42).

The antibody mUK-66 revealed a high biological activity *in vitro*. The antibody combination of 0.075 mg/ml mUK-66 with 0.02 mg/ml IVIG resulted in an enhanced killing rate of 50% compared to the untreated samples. The higher dose of 0.9 mg/ml mUK-66 and 0.2 mg/ml IVIG revealed a bacterial survival of 34%. The exchange of IVIG with the hUK-tox at the same concentrations resulted in a viable cfu of 63% with the lower dose and 71% with the higher dose. The antibody combination of hUK-66 with IVIG revealed 75% of viable cfu in the lower concentration and 92% survival of bacteria in the higher one. The antibody

combination of hUK-66 and hUK-tox resulted in a survival rate of 71% (lower concentration) and 93% (higher concentration). The survival rate of bacteria in the presence of combined hUK-tox and IVIG demonstrated 93% survival at the lower concentration and 84% survival at the higher concentration. Overall, only the antibody combination including mUK-66 revealed effective killing of *S. aureus* Newman compared to the untreated control using mouse whole blood assays.

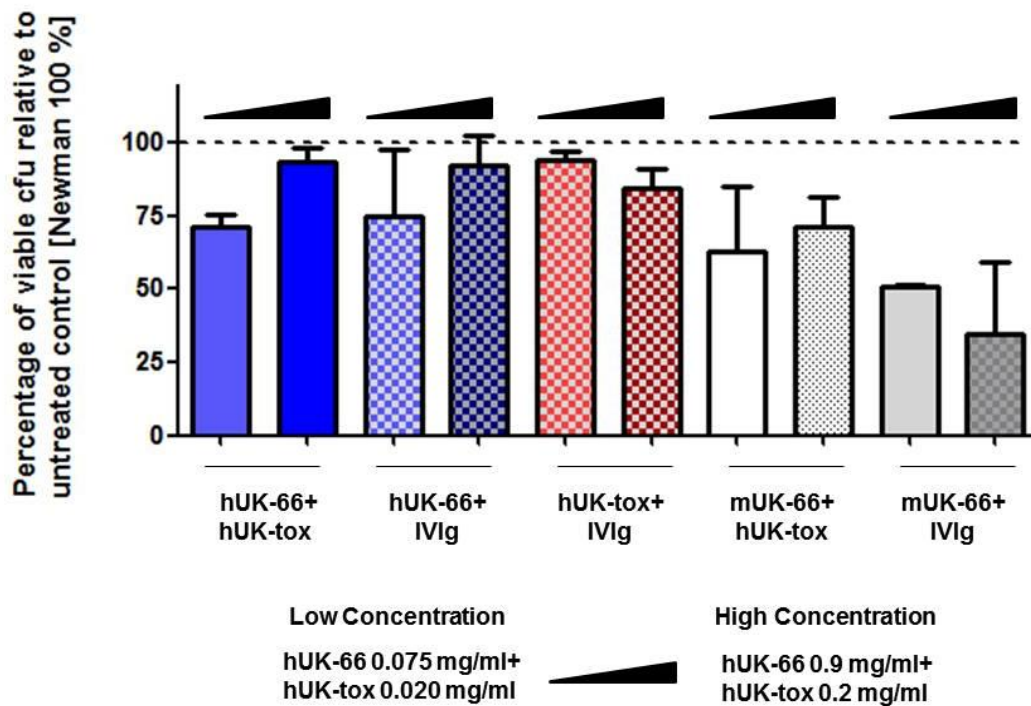


Fig. 42 Antibody dependent killing of *S. aureus* Newman by granulocytes from mouse whole blood samples.

Heparinized mouse blood samples (n=6) from healthy mice were infected with *S. aureus* Newman in the presence of the antibody combination hUK-66 with IVIG, mUK-66 with IVIG, hUK-66 with hUK-tox, mUK-66 with hUK-tox and hUK-tox with IVIG for 60 min at 37°C. The intravenous human immunoglobulin preparation Gammunex® (IVIg) serves as positive control. Total viable bacteria were recovered after eukaryotic cell lysis and enumerated by plate counting. The values were plotted relative to the level of untreated samples (set 100%). The mean percentage of viable *S. aureus* recovered from mouse blood from 0.075 mg/ml hUK-66 with 0.02 mg/ml hUK-tox was 73% and 93% from samples incubated with the higher concentration. The survival rate of samples incubated with hUK-66 and IVIG at lower concentration was 75% and at higher concentration 92%. The combination of hUK-tox and IVIG at lower concentration was 94% and at higher concentration 84%. The antibody combination of mUK-66 with hUK-tox at lower dose revealed a bacterial survival of 63% and the higher dose of 73%. mUK-66 combined with IVIG demonstrated 50% survival at the lower concentration and 34% survival at the higher concentration. The dash line in the graph demonstrates the 100% reference value of untreated samples.

6.8.1. Fc part of hUK-66 IgG1 and hUK-tox IgG1 is bound by FcγR1a of HEK293 cells

Results from the *in vitro* assays with human and mouse whole blood revealed that the biological activity of mUK-66 and hUK-66 is reduced, if there combined with hUK-tox.

Although, both antibodies are specific for different staphylococcal antigens, they are designed as IgG1 isotype. In the following experiments, the binding of hUK-66 IgG1, IgG2, IgG4 and hUK-tox IgG1 Fc parts by FcγR1a is investigated. The binding studies were performed using binding ELISA and flow cytometry analysis. Results from binding ELISA with cell culture supernatant of FcγR1a expressed by HEK293 cells demonstrate that hUK-66 IgG1 and hUK-tox IgG1 are bound by FcγR1a in a concentration dependent manner. Binding affinity of FcγR1a to Fc region of both antibodies is comparable (Fig. 43A). Flow cytometry experiments with HEK293 cells expressing FcγR1a on their cell surface reveal binding of hUK-66 IgGs (Fig. 43B) FcγR1a binding of hUK-66 IgGs is concentration dependent. The affinity of FcγR1a to hUK-66 IgGs was detected as: IgG1>IgG4>IgG2. All generated hUK-66 IgG1, IgG2 and IgG4 are bound by the major high affinity phagocyte receptor FcγR1a.

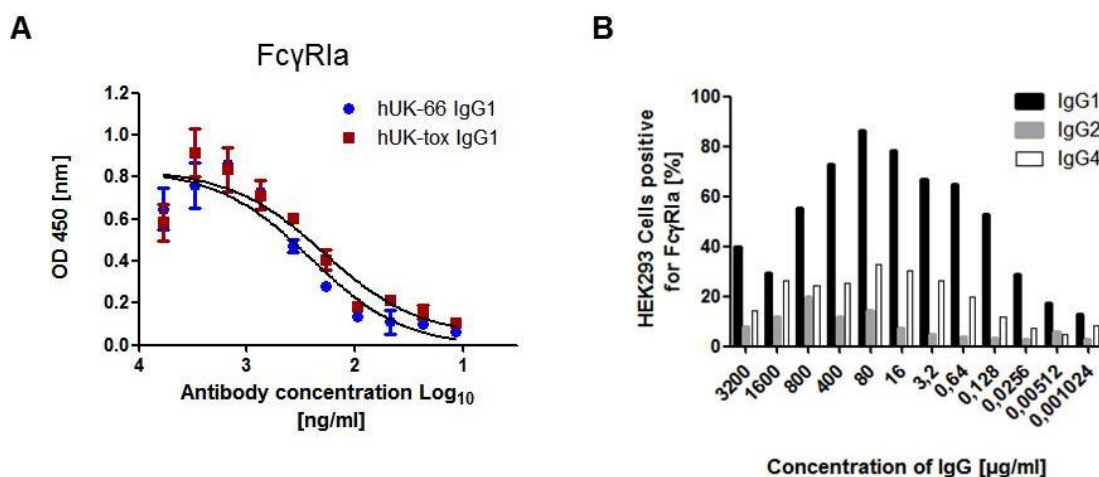


Fig. 43 Characterization of binding of different hUK-66 isotypes by FcγR1a.

(A) For binding ELISA studies humanized antibodies hUK-66 IgG1 and hUK-tox IgG1 were coated to the surface of ELISA plates and 100 μl/well cell culture supernatant from transiently expressed HEK293 cells was added. Binding of FcγR1a was detected by HRP conjugated anti-His antibody. (B) Binding of different hUK-66 isotypes by cell surface expressed FcγR1a was analysed with a FITC-conjugated anti-human IgG antibody using flow cytometry. The hUK-66 isotypes demonstrate concentration dependent binding to FcγR1a: IgG1>IgG4>IgG2 (Experiment performed by T. Schmitter).

In the following study, the binding by further relevant phagocytosis receptors such as FcγR1a (low responder) and FcγR1a (high responder) was analysed. Therefore, HEK293 cells were transfected to express recombinant FcγR1a on their cell surface. The expression was confirmed by PE-conjugated anti-CD64 antibody for FcγR1a and by PE-conjugated anti-CD32 antibody for FcγR1a expression. The bound hUK-66 IgG1 antibody was detected with anti-PE-conjugated anti-human Fab antibody. Results from this study are presented in figure 44A. These experiments clearly demonstrate that, the most important FcγRs which are necessary for phagocytosis of opsonized bacteria by professional phagocytes recognize hUK-66 IgG1 in a concentration dependent manner.

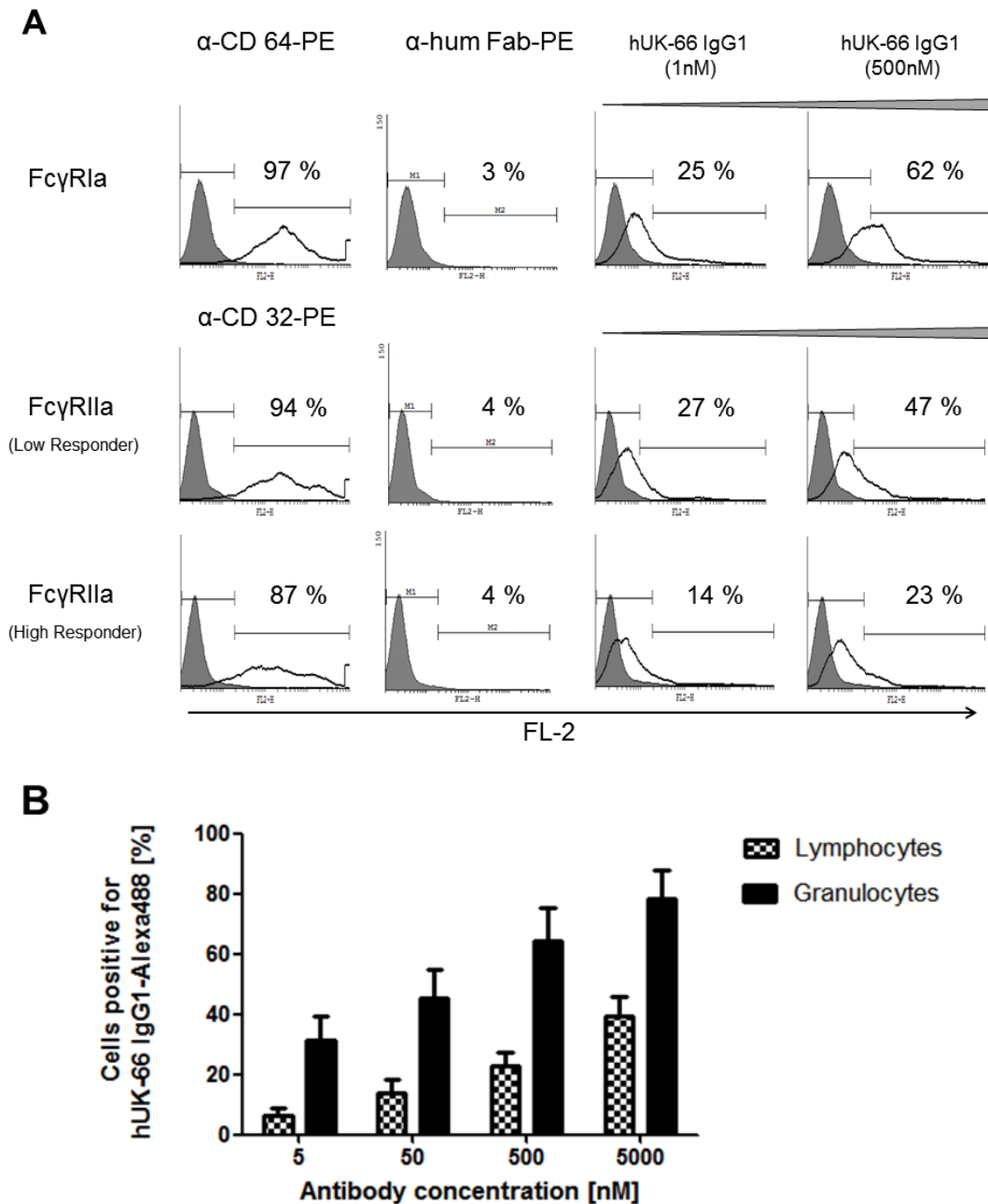


Fig. 44 Binding of hUK-66 IgG isotypes by recombinant and native Fc γ Rs.

(A) The binding of hUK-66 IgG1 by Fc γ R1a and Fc γ R1a was analysed with transfected HEK293 cells. The expression of the Fc γ Rs was confirmed by PE-conjugated anti-CD64 and anti-CD32 antibodies. The concentration dependent binding of hUK-66 IgG1 was detected via PE-conjugated anti-human Fab IgG1 antibody. Results from flow cytometry experiments demonstrate hUK-66 binding of most important Fc γ Rs. (B) hUK-66 IgG1 was conjugated with fluorescence dye Alexa488 to analyse the binding of native Fc γ Rs on granulocytes and lymphocytes in human whole blood. Data of the flow cytometry experiments reveal a concentration dependent binding of Alexa488-conjugated hUK-66 IgG1 by granulocytes and lymphocytes. SD and mean were determined from three independent experiments.

The binding of hUK-66 IgG1 by native Fc γ Rs was analysed using human whole blood. For these experiments, hUK-66 IgG1 was conjugated with Alexa488. Human PMNs positive for hUK-66 IgG1 binding, detected via fluorescence signals, are presented in figure 44B. The antibody hUK-66 IgG1 is bound by granulocytes and lymphocytes in a concentration dependent manner.

The results of the binding studies demonstrate that hUK-66 IgG1 binds efficiently its target IsaA and has the potential to mediate effector functions after its binding by FcγRs, as shown in this work, recombinantly expressed by HEK293 cells and on human PMNs.

6.9. Characterization of UK-66 IgG1's therapeutic potency using a mouse pneumonia model

Community-acquired, health-care associated and nosocomial pneumonia due to methicillin-resistant *S. aureus* are underestimated and spreading worldwide. Several resistant strains are epidemic in hospitals and cause estimated 1.5 million cases of pneumonia per year [148].

Therefore, a mouse model of intranasal *S. aureus* infection followed by pneumonia was established to analyse mouse and hUK-66's potency for prophylactic and therapeutic treatment. For the infection, *S. aureus* Newman stock samples from the exponential growth phase were prepared by U. Wallner and the infectious dose for the used stock was determined before antibodies were tested. To determine survival proportions, mice were monitored daily following intranasal infection and body weight was documented. Mice were counted as dead, if they met one of the following criteria: 1) Clear signs of morbundancy, like immobility or shaking, 2) Lost of body weight over 20% for two days. Mice that were sacrificed were counted as dead for the particular time point.

Figure 45 presents the results of *S. aureus* Newman titration experiments for infection dose finding. The intranasal inoculum of 2×10^8 cfu/20 μl reveals 25% survival of mice three days after infection and was chosen as infection dose. The lower dose of 1×10^8 cfu/20 μl demonstrate no signs of morbundancy or mortality and 3×10^8 cfu/20 μl results in a very aggressive course of infection within 24 h. Every charge of prepared *S. aureus* Newman stocks were tested before and all tested charges reveal a constant infection dose of 2×10^8 cfu/20 μl which results in 10-35% survival of Balb/c mice three days after intranasal infection.

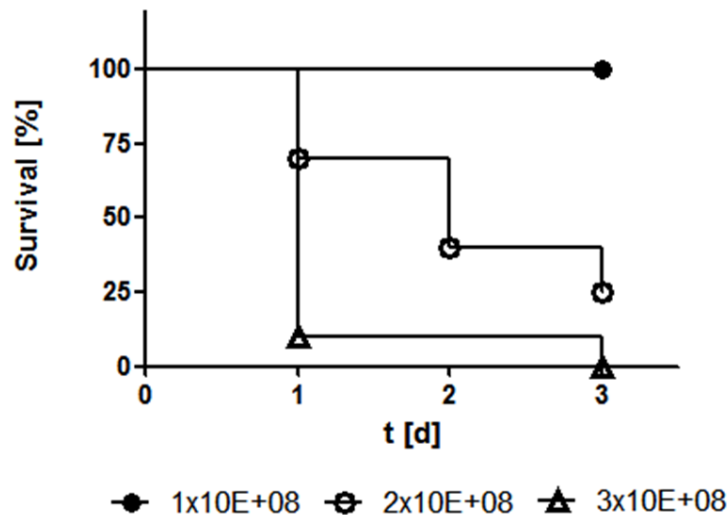


Fig. 45 Determination of *S. aureus* Newman survival proportion following intranasal application.

To determine survival proportions, mice were infected with 1×10^8 , 2×10^8 and 3×10^8 cfu/20 μ l intranasally and monitored daily. The dose of 2×10^8 cfu/20 μ l reveals a survival rate of 25% and was chosen as infection dose. The survival rate was determined in two independent experiments ($n=10$ per group). Survival curves were prepared using GraphPad Prism 5 and statistical significance was determined using Log Rank test, *** $P < 0.001$.

6.10. Prophylactic treatment of *S.aureus* induced pneumonia with mUK-66 IgG1

After determination of the infection dose, the prophylactic efficacy of mUK-66 IgG1 in a mouse pneumonia model was analysed. Studies of Lorenz *et al.*, demonstrated mUK-66 IgG1 therapeutic efficacy in a murine venous catheter-related infection model and in a murine sepsis survival model [149]. To evaluate, the therapeutic potential of mUK-66 IgG1 in other diseases caused by *S. aureus* the antibody was applied in a mouse pneumonia model. The antibody was given intranasally at 5 mg/kg and 0.5 mg/kg, respectively one hour before infection with *S. aureus* Newman and the survival rate was determined over a period of 72 h. The outcome of these experiments is presented in figure 46. Mice treated with mUK-66 revealed significant protection at both concentrations resulting in survival rates of 100% and 90%, respectively compared to the mock treated group at the end of the experiment. The MOPC mouse IgG1 antibody served as isotype control. Mice treated with 5 mg/kg MOPC showed a survival rate of 90% compared to the untreated mice, while mice treated with 0.5 mg/kg MOPC demonstrated 30% survival.

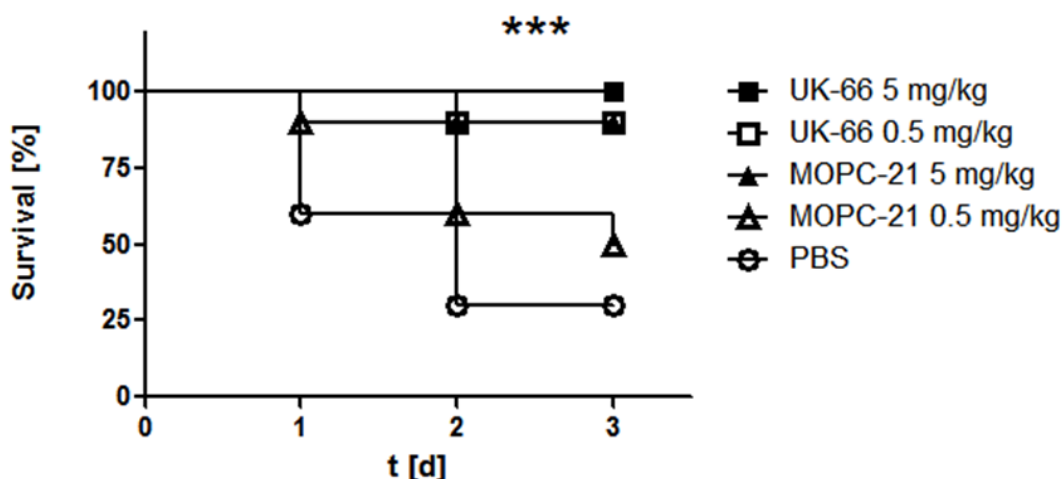


Fig. 46 Prophylactic treatment of mouse pneumonia with mUK-66 IgG1.

Mice (n=10) were treated intranasally with mUK-66 at indicated concentrations and infected one hour later via intranasal infection with 2×10^8 cfu/20 μ l *S. aureus* Newman. Body weight and survival were monitored over 72 h and survival curves were generated with Graph Pad Prism5 software. After three days of infection, 100% of mice treated with 5 mg/kg mUK-66 survived pneumonia. For the other groups survival rate were 90% after treatment with 0.5 mg/kg mUK-66, 90% after treatment with 5 mg/kg isotype control MOPC, 50% treated with 0.5 mg/kg MOPC, and 30% treated with PBS. Statistical significance was determined using Log Rank test, *** $P < 0.001$.

Intranasal application of mUK-66 IgG1 was performed to locate antibody direct at the side of infection. Results from this study exhibited the therapeutic efficacy of mUK-66 IgG1 in the mouse pneumonia model. However, the common clinical application of antibodies is the intravenous route of injection.

6.11. Therapy of pneumonia by prophylactic treatment with mUK-66 IgG1

In this study, the prophylactic efficiency of mUK-66 IgG1 in the mouse pneumonia model was investigated. Animals received an intravenous injection of either PBS (served as control) or mUK-66 IgG1 at different concentrations, injected into the lateral tail vein one hour prior intranasal infection with *S. aureus* Newman. Animals were monitored 72 h for signs of morbidity and body weight and clinical signs were documented. Mice were counted as dead, if they met one of the criteria described above.

Results from three independent survival experiments are demonstrated in figure 47. After three days of infection, the survival rate for the PBS control group was 23%. The group treated with 60 mg/kg mUK-66 resulted in 70% survival of mice and the group treated with 20 mg/kg mUK-66 revealed 60% survival rate. In treatment groups with 5 and 1 mg/kg mUK-66, respectively a survival of 27% and 20% of animals were observed at the end of the experiments. Direct comparison of the treatment groups to the PBS control group revealed significant protection by mUK-66 IgG1 applied prophylactically in a concentration of 20 and 60 mg/kg, respectively. In contrast, concentrations at or below 5 mg/kg showed no benefit.

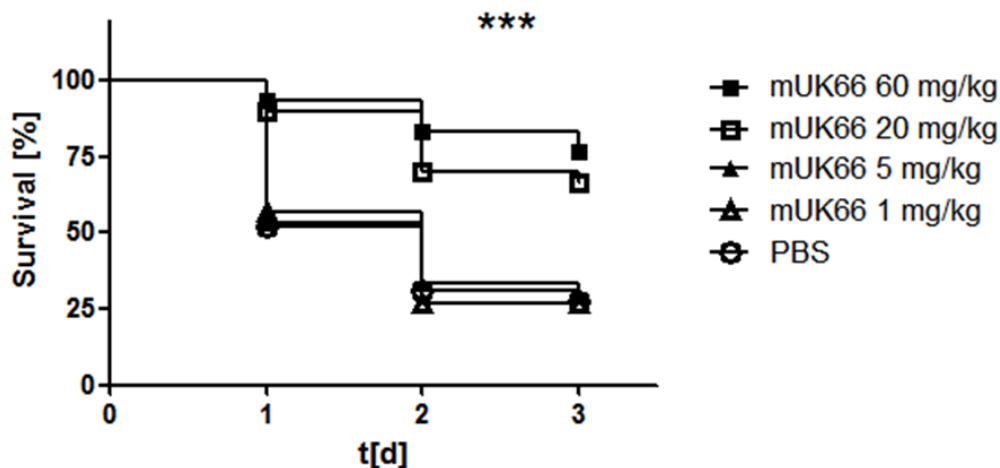


Fig. 47 Prophylactic treatment of mice with mUK-66 in *S. aureus* induced pneumonia.

Mice (n=30 per group) were injected intravenously with mUK-66 at indicated concentrations and infected one hour later via intranasal infection with 2×10^8 cfu/20 μ l *S. aureus*. Body weight and survival were monitored over 72 h and survival curves were generated with Graph Pad Prism5 software. After three days of infection, 70% of mice treated with 60 mg/kg mUK-66, 60% treated with 20 mg/kg mUK-66, 27% treated with 5mg/kg mUK-66, 20% treated with 1 mg/kg mUK-66 and 23% treated with PBS survived during the course of infection. The survival rate was determined in three independent experiments. Statistical significance was determined using Log Rank test, *** $P < 0.001$.

6.12. Treatment of *S. aureus* pneumonia with mUK-66 IgG1 in a therapeutic infection model

The data of the prophylactic treatment with mUK-66 IgG1 revealed significant protection resulting in an increased survival rate of the treated animals. To investigate the therapeutic efficiency of mUK-66, the effective dose of 60 mg/kg was applied intranasally 1 h after infection with *S. aureus* Newman. An isotype IgG1 matched mouse antibody served as control. The results, presented in figure 48 demonstrate that mUK-66 IgG1 has no significant therapeutic efficacy when applied 1 h after infection. Survival rates of mUK-66 IgG1-, isotype- and PBS-treated groups revealed 27%, 25% and 18% survival of mice, respectively.

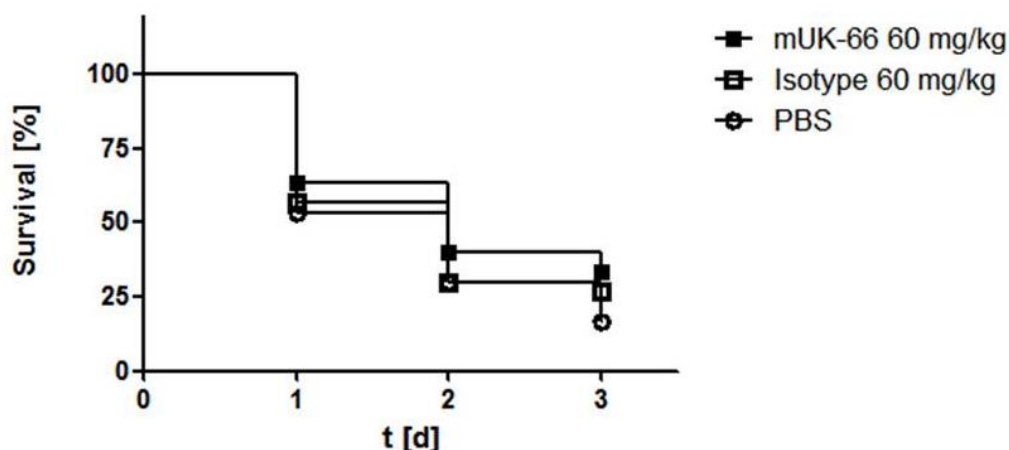


Fig. 48 Therapeutic efficacy of mUK-66 in *S. aureus* induced pneumonia.

Mice (n=30) were infected intranasally with 2×10^8 cfu/20 μ l *S. aureus* Newman and one hour after infection, mUK-66 IgG1 was injected intravenously at indicated concentrations. Body weight and survival were monitored over 72 h and survival curves were generated with Graph Pad Prism5 software. After three days of infection, 27% of mice treated with 60 mg/kg, 25% treated with isotype control and 18% treated with PBS survived the infection. The survival rate was determined in three independent experiments. Statistical significance was determined using Log Rank test, $P < 0.05$.

6.13. Prophylactic therapy of pneumonia with humanized antibody hUK-66 IgG1

Since the murine antibody mUK-66 was able to protect mice against lethal *S. aureus* pneumonia, treatment with the humanized IgG1 antibody hUK-66 was tested in the prophylactic pneumonia model. Mice were infected intranasally with 2×10^8 cfu/20 μ l *S. aureus* Newman. According to the localization of infection in the lung, hUK-66 IgG1 was applied intranasally to ensure maximal interaction of antibody and bacteria. The intranasal application was also chosen to reduce the dose of hUK-66 IgG1. In these experiments, two concentrations of hUK-66 IgG1 was analysed and Rituximab served as matched human isotype control. Results from these studies are presented in figure 49. The intranasal application of hUK-66 IgG1 revealed a significant protection of mice treated prophylactically with 0.5 and 5 mg/kg hUK-66 (93% and 80%) compared to mice treated with 0.5 and 5 mg/kg Rituximab (52% and 63%) or with PBS (52%).

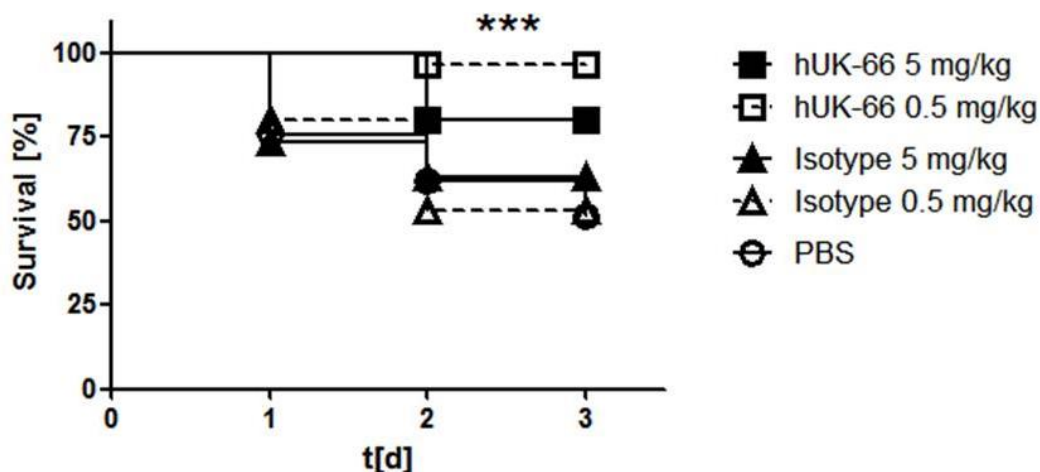


Fig. 49 Prophylactic treatment of mice with hUK-66 IgG1 in *S. aureus* induced pneumonia.

Mice (n=30) were injected intranasally with hUK-66 at indicated concentrations and infected one hour later via intranasal application with 2×10^8 cfu/20 μ l *S. aureus* Newman. Body weight and survival were monitored over 72 h and survival curves were generated with Graph Pad Prism5 software. After three days of infection, 93% of mice treated with 0.5 mg/kg hUK-66, 80% treated with 5 mg/kg hUK-66, 63% treated with 5 mg/kg Rituximab, 52% treated with 0.5 mg/kg Rituximab and 52% treated with PBS survived *S. aureus* induced pneumonia. The survival rate was determined in three independent experiments. Statistical significance was determined using Log Rank test, *** $P < 0.001$.

Overall, results from the prophylactic treatment of pneumonia demonstrate that both mouse and hUK-66 IgG1 achieve therapeutic efficacy after prophylactic application. In particular, the intranasal injection of UK-66 resulted in a significant increase of survival in the hUK-66-treated groups compared to mice treated with PBS.

In the past, various immunization strategies have been examined in clinical trials and animal models. Despite promising experimental data, clinical trials in humans have not been successful yet. However, recent studies provide evidence that humans with intact immune systems and protective antibodies have a lower risk for developing invasive infections [145]. Clinical isolates of *S. aureus* secreted the cytolytic alpha-toxin, which binds to a wide variety of eukaryotic cells, resulting in osmotic lysis of cells or regulatory dysbalance by disturbing the ion equilibrium. Humanized antibodies against alpha-toxin were therefore chosen as candidate for an antibody therapy in which the opsono-phagocytotic activity of hUK-66 IgG1 was combined with neutralization of harmful effector functions of *S. aureus* alpha-toxin by a hUK-tox IgG1.

6.14. Prophylactic therapy of pneumonia with hUK-tox IgG1

S. aureus alpha-toxin is an important virulence determinant and was confirmed as a valid target for immunoprophylaxis against staphylococcal disease [147]. The passive immunization of mice with hUK-tox antibodies provided promising efficacy in different mouse infection models, such as skin and soft-tissue infections and pneumonia [142] [150].

In the following mouse experiments, the effective dose of the generated hUK-tox IgG1 was examined in the established pneumonia mouse model. Figure 50 presents survival curves of mice experiments. Mice treated with 10 or 5 mg/kg hUK-tox IgG1 revealed significant protection compared to mice treated with 1, 0.1 mg/kg hUK-tox IgG1 or PBS, respectively.

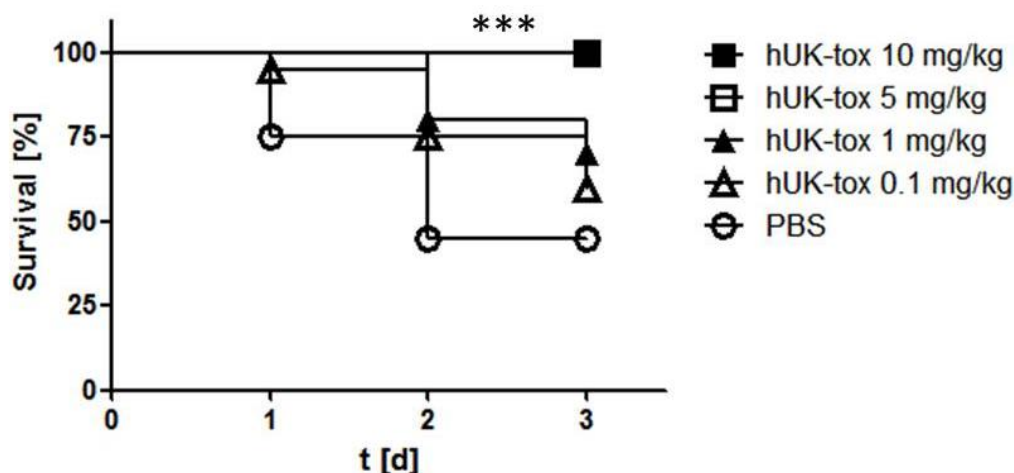


Fig. 50 Prophylactic treatment of mice with hUK-tox IgG1 in *S. aureus* induced pneumonia.

Mice (n=20) were injected intravenously with hUK-tox at indicated concentrations and infected one hour later via intranasal infection with 2×10^8 cfu/20 μ l *S. aureus* Newman. Body weight and survival were monitored over 72 h and survival curves were generated with Graph Pad Prism5 software. After three days of infection, 100% of mice treated with 10 and 5 mg/kg hUK-tox, 75% treated with 1 mg/kg hUK-tox, 60% treated with 0.1 mg/kg and 45% treated with PBS survived pneumonia. The survival rate was determined in two independent experiments. Statistical significance was determined using Log Rank test, *** $P < 0.001$.

Mice treated with 10 or 5 mg/kg hUK-tox IgG1 demonstrated 100% protection in this model. Moreover, the lower concentrations of 1 and 0.1 mg/kg hUK-tox IgG1 resulted in 75% and 60% survival of mice compared to 45% survival in the group treated with PBS.

The effective dose of hUK-tox IgG1 in the pneumonia model was determined as 5 mg/kg.

6.15. Treatment of *S. aureus*-induced pneumonia with hUK-tox IgG1

Next, efficacy of hUK-tox IgG1 in a therapeutical model where the antibodies are applied one hour post infection was investigated. The therapeutic efficacy of hUK-tox was examined in the mouse pneumonia model as alpha-toxin is one critical factor in tissue damage during pneumonia. Mice were infected with 2×10^8 cfu/20 μ l *S. aureus* Newman and treated with 10 mg/kg hUK-tox IgG1, 10 mg/kg IgG1 matched isotype control Rituximab or PBS. Results are presented in figure 51 and indicated that the group treated with hUK-tox IgG1 revealed a significant protection (50% survival) one hour after infection compared to mice treated with PBS (15% survival). Two days after infection, mice treated with hUK-tox IgG1 demonstrated

a significant protection (90% survival) compared to mice treated with the isotype control (60% survival). These findings indicate the therapeutic efficacy of hUK-tox IgG1.

In previous experiments, the prophylactic and therapeutic efficacy of UK-66 IgG1 and hUK-tox IgG1 was investigated. Both antibodies reveal a significant protection after prophylactic application in the mouse pneumonia model. However, therapeutic efficacy was only weak under the test conditions for the hUK-tox IgG1 and no protection was observed with hUK-66.

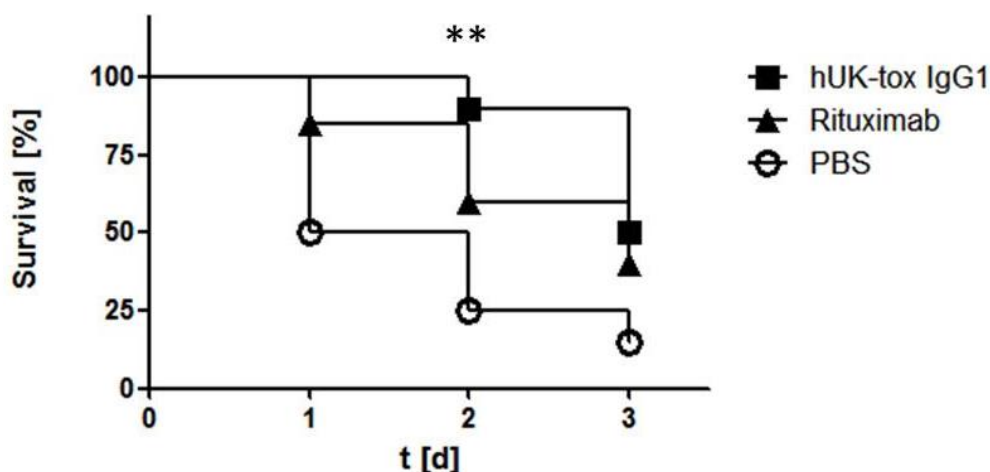


Fig. 51 Therapeutic treatment of mice with hUK-tox IgG1 in *S. aureus* induced pneumonia.

Mice ($n=20$) were infected with 2×10^8 cfu/20 μ l *S. aureus* Newman and hUK-tox IgG1 was injected intravenously at indicated concentrations one hour after infection. Body weight and survival were monitored over 72 h and survival curves were generated with Graph Pad Prism5 software. After three days of infection, 50% of mice treated with 10 mg/kg hUK-tox IgG1, 40% treated with isotype control and 15% treated with PBS survive. The survival rate was determined in two independent experiments. Statistical significance was determined using Log Rank test, $**P < 0.01$.

6.16. Therapeutic efficacy of combination of hUK-66 and hUK-tox IgG1 in a mouse pneumonia model

S. aureus is a complex microorganism and well-adapted to its human host. In considering such biological complexity, approaches based on single antigens have not been successful yet. Therefore, a combination of functional antibodies targeting different *S. aureus* antigens and addressing independent mode of action by mediating different effector functions seems a promising approach.

In the following studies, the efficacy of a combinatorial antibody-based therapy targeting two important staphylococcal antigens, IsaA and alpha-toxin, was investigated using the mouse pneumonia model. First, the benefit of the combined antibody therapy compared to the single antibodies was investigated using a prophylactic set up.

Mice treated with the combination of hUK-66 and hUK-tox IgG1 revealed a higher protection during pneumonia than mice treated with either hUK-66 IgG1 or hUK-tox IgG1 (Fig. 52). Mice

treated with the antibody combination showed a better survival rate (83% survival) than single treatment with either hUK-tox IgG1 (83% vs 73% survival) or hUK-66 IgG1 (83% vs 40% survival). Treatment with isotype control or PBS resulted in significant better survival rates (83% vs 30%) after 72 h.

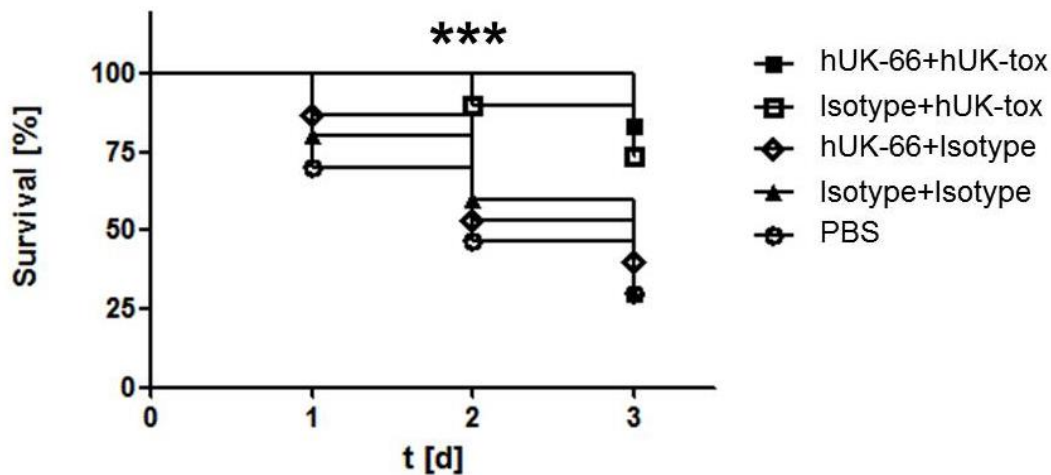


Fig. 52 Prophylactic treatment of mice with combined hUK-66 and hUK-tox IgG1 in *S. aureus* induced pneumonia.

Mice (n=30) were injected intravenously a combination of hUK-66 IgG1 and hUK-tox, a combination of hUK-66 with isotype control antibodies, hUK-tox IgG1 combined with isotype control, isotype control Rituximab alone or PBS at indicated concentrations. After antibody application, mice were intranasally infected with 2×10^8 cfu/20 μ l *S. aureus* Newman. Body weight and survival were monitored over 72 h and survival curves were generated with Graph Pad Prism5 software. After three days of infection, 83% of mice treated with combined hUK-66 and hUK-tox antibody survived pneumonia, 73% of mice treated with hUK-tox survived, 40% treated with hUK-66 IgG1, 30% treated with Rituximab and 30% treated with PBS survived, respectively. The survival rate was determined in three independent experiments. Statistical significance was determined using Log Rank test, *** $P < 0.001$.

6.17. Treatment of *S. aureus*-induced pneumonia with combination of hUK-66 and hUK-tox IgG1 in a mouse pneumonia model

Combination of hUK-66 and hUK-tox IgG1 demonstrated a markedly improved survival when applied one hour before infection in a mouse pneumonia model. Previous experiments revealed that hUK-66 single treatment did not increase survival of mice in a therapeutic model where the antibodies were intravenously applied one hour after infection. However, survival of mice was improved by application of hUK-tox IgG1 under the same test conditions. Thus, in the following study, the benefit of a combined therapy of hUK-66 IgG1 and hUK-tox IgG1 in a therapeutic treatment regimen was investigated. Mice were treated intravenously with combined hUK-66 (60 mg/kg) and hUK-tox (10 mg/kg), hUK-66 (60 mg/kg) and Rituximab (10 mg/kg), Rituximab (60 mg/kg) and hUK-tox (10 mg/kg), Rituximab (70 mg/kg) and PBS one hour after intranasal infection (Fig. 53).

At the beginning of infection during the first 24 h, therapeutic efficacy of hUK-66 combined with hUK-tox IgG1 was improved compared to the single treatments. However, three days after infection no significant benefit of the combination compared to the single therapy could be observed.

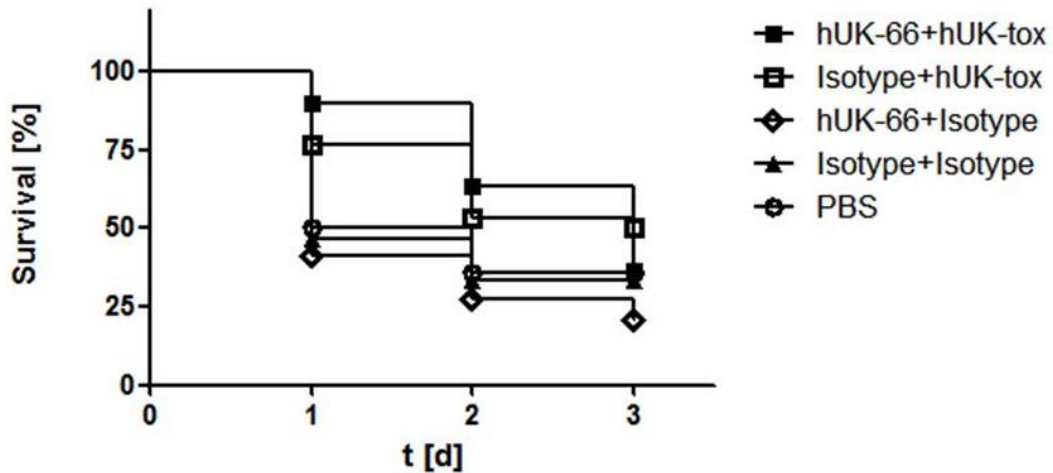


Fig. 53 Therapeutic treatment of mice with combined hUK-66 and hUK-tox IgG1 in *S. aureus*-induced pneumonia.

Mice (n=30) were intranasally infected with 2×10^8 cfu/20 μ l *S. aureus* Newman and injected intravenously with combined hUK-66 IgG1 and hUK-tox-toxin, hUK-66 IgG1, hUK-toxin IgG1, isotype control Rituximab or PBS at indicated concentrations one hour after infection. Body weight and survival were monitored over 72 h and survival curves were generated with Graph Pad Prism5 software. After three days of infection, 35% of mice treated with combined antibody therapy, 50% of mice treated with hUK-tox IgG1, 20% treated with hUK-66 IgG1, 35% treated with Rituximab and 35% treated with PBS survived. The survival rate was determined in three independent experiments. Statistical significance was determined using Log Rank test.

7. Discussion

S. aureus is responsible for the majority of skin and soft tissue infections, including impetigo, folliculitis and wounds [151] and can also cause invasive and life threatening infections, such as bacteremia, abscesses, pneumonia, osteomyelitis, meningitis, endocarditis and sepsis [152]. Furthermore, *S. aureus* is the predominant cause of a variety of nosocomial infections, including ventilator-associated pneumonia, intravenous catheter-associated infections, postsurgical wound infections, as well as invasive infections in neutropenic patients and in patients undergoing solid organ and hematopoietic stem cell transplants [22]. The treatment of these infections has been complicated by the emergence of methicillin-resistant *S. aureus* (MRSA) strains, which are becoming increasingly resistant to multiple antibiotics. Both hospital- and community-associated infections with *S. aureus* have increased in the past 20 years. History has shown that the introduction of a new antibiotic is frequently followed by the development of bacterial antibiotic resistance [23], [24]. The therapeutic options for these pathogens are extremely limited and the need of new treatment options in the presence of growing numbers of elderly patients and patients undergoing surgery or transplantation and a dramatic increases in population in neonatal intensive care units will produce an even greater number of immunocompromised individuals at risk of these infections [37], [38].

Antibodies are the fastest-growing category of therapeutic agents entering clinical studies and cover a wide spectrum of applications in the field of basic research, diagnostics, autoimmune response, inflammatory diseases, oncology and rheumatology. Using antibodies to treat infectious diseases is now being fuelled by the wide dissemination of antibiotic resistant microorganisms, the inefficacy of antimicrobial drugs in immunocompromised patients and the fact that antibody-based therapies provide immunity against pathogens immediately.

The main objective of this thesis was to generate and characterize a humanized anti-staphylococcal antibody including its antigen binding properties and biological activity against the immunodominant staphylococcal antigen IsaA. The results showed that hUK-66 not only bound specifically to its target antigen IsaA, hUK-66 also induced effective killing of bacteria in blood samples taken from healthy donors. Furthermore, even patients at high risk of *S. aureus* infections (patients with diabetes, patients on dialysis, and patients with AOD) benefit from hUK-66 treatment by showing reduction of viable bacteria *in vitro*. The reduction of viable bacteria is of paramount importance to avoid serious infection. Based on these results, the hUK-66 IgG1 is a promising candidate of an antibody-based therapy against antibiotic-resistant *S. aureus*.

7.1. Humanization and reshaping of murine UK-66 antibody

The murine UK-66 demonstrates specific and high affine binding to its target IsaA and reveals biological activity in different mouse models. In this study, the murine UK-66 was humanized for an anti-staphylococcal therapy in humans. Based on the mouse variable domain sequence, the antigen binding domain was humanized by grafting the CDRs onto human frameworks obtained from the closest human germ line V segments. Humanized antibodies have decisive advantages over rodent antibodies. In comparison to humanized antibodies, rodent antibodies have a short serum half-life and can only trigger some effector functions. Furthermore, mouse antibodies can elicit unwanted immune response, so called human anti-mouse antibodies (HAMA). This reaction reduces their clinical effectiveness, since the human immune system cleans rodent antibodies rapidly, the produced human antibodies block the therapeutic effect and hypersensitivity reaction can occur [64]. However, humanization of a mouse antibody can result in reduced affinity to its target. Analysis of the binding affinity of hUK-66 compared to mUK-66 demonstrated a 10-fold reduction in binding affinity (Fig. 19). Nevertheless, hUK-66 revealed a high affinity of 4,8 nM to IsaA. The binding affinity of humanized antibody can be reconstructed by identifying the frame work residues, which interacts with the antigen binding site. This process is called framework substitution. High binding affinities are critical for neutralization of toxins and for multiple interactions [153]. In case of hUK-66, the multiple interactions are the mediation of phagocytosis. Furthermore, humanization of a rodent antibody reduced its immunogenicity and can extend its serum half-life over 75 h [64]. Here, it has to be mentioned that the immunogenicity of an antibody is dependent on the immune state of the patient, the dose and application route of the antibody, the frequency of application, and the antibody's epitope. Cell-bound antigens demonstrated much higher immunogenicity than soluble antigens [154]. In general, patients treated with mAbs can develop a cytokine releasing syndrome (CRS). This side effect presents an excessive secretion of pro-inflammatory mediators [155]. Immune responses to murine components of antibodies have been described as a major cause of CRS. These reasons explain why the clinical development of mAbs is towards humanized antibodies.

Antibody therapeutics belongs to a well-established drug class and the development and clinical experience gained from the generation and optimization of one antibody is applicable to other antibodies [156]. From all antibodies with clinical application: 29% are chimeric antibodies and 25% are humanized antibodies [157]. In the 1980s, 80% of all mAbs were of mouse origin. This number dropped to 7% during the 2000. The humanization of antibodies acts in concert with the reshaping of antibodies for therapy in humans. Antibody engineering has two advantages over mouse antibodies: (1) The effector function can be selected and (2) the antigen binding domain can be optimized by minimizing the anti-globulin response [158],

[159]. The choice of the constant domain centers on whether specific effector functions are required and the need for a suitable *in vivo* half-life [160]. The hUK-66 antibody was designed as IgG1, IgG2 and IgG4 antibody based on the fact that different IgG subclasses mediate various effector functions. In the case of *S. aureus*, it is unknown which host defence is the most effective one against this pathogen. The isotype IgG3 has not been chosen for antibody development because of its shorter half-life, its susceptibility of the larger hinge region to proteolysis, its allotypic polymorphism and the production is very complex and expensive. Most of the humanized antibodies in the clinical application belong to the IgG1 subclass. The antibody hUK-66 IgG1 was designed as IgG1 by the properties of this immunoglobulin class to induce phagocytosis, complement activation and to mediate antibody-dependent cell-mediated cytotoxicity [161]. The host immune response against protein antigens is mainly an IgG1 response. Antibodies against carbohydrate antigens are usually IgG2 antibodies. This subclass activates the alternative pathway of the complement. For IgG4 antibodies neutralization properties and long-term t-cell stimulation have been described. All antibody isotypes have the same antigen binding domain. In this thesis, hUK-66 was constructed as IgG1, IgG2, and IgG4 isotype, respectively. It was expected that all hUK-66 isotypes reveal the same binding affinity to IsaA. Interestingly, hUK-66 IgG1 demonstrated the highest and IgG2 the lowest affinity (Fig. 22). Reasons for this result could be the binding affinity of the secondary antibody. Since all antibodies were tested with the same incubation protocol and the same concentration of antibody, the binding affinity of the secondary anti-IgG2 must be much lower than the affinity of the anti-IgG1 and anti-IgG4 antibodies to its corresponding Fc part. The Fc region is very important for the mediation of effector functions via FcγR binding. IgG1 activates the complement pathway via C1q binding and has a high affinity to FcγRI. This receptor, expressed on phagocytes, plays a key role for phagocytosis. The results from the FcγR binding assay indicate that hUK-66 IgG1 is bound by FcγRIa, FcγRIIa (low responder) and FcγRIIa (high responder). The outcome from this assay reflects the binding behaviour described in the literature: isotypes IgG2 and IgG4 demonstrated less affinities to the most important receptors for phagocytosis [160]. All in all the natural selection has generated four human IgG isotypes because each has a unique purpose in the ever-changing defence tactics against pathogens.

Antibodies developed for therapeutic applications possess several clinically relevant mechanisms of action. The reshaping of the Fc part allows to define the effector function of the antibody and to include further functions like complement-dependent cytotoxicity, antibody-dependent cellular cytotoxicity (ADCC) and antibody-dependent cellular phagocytosis [162]. The clinical potential can be readily be increased by improving existing properties through protein alteration or carbohydrate optimization. Today, different engineering technologies have been developed to modulate the binding affinity of the Fc region of therapeutic antibodies to enhance or suppress FcγR-dependent immune effector

functions. There are two strategies to improve antibody efficacy: (1) Modifying the structure of the Fc-attached oligosaccharides or (2) by engineering the Fc-polypeptide backbone. One of the key amino acids in the Fc backbone is the Asn297. Glycoengineering at this position has significant effects on the binding affinity to FcγRs and are more potent at mediating ADCC [163]. The use of glycoengineering confers two relevant properties: antibodies can be improved for effector functions, even in individuals harbouring low-affinity allotypes of FcγRs and the activity of antibody can be preserved even in the presence of high concentrations of nonspecific serum IgGs that compete with conventional therapeutic Abs for FcγRs and impair their activity [164]. Antibody glycosylation also has an impact on FcγR binding and antibody activity. Branching sugar residues such as N-acetylglucosamine or fucose have been implicated in affecting antibody activity *in vitro* and *in vivo* [165]

The effector function is only one point for therapeutic success of the antibody. Another aspect is the half-life of the antibody in serum for a maximum therapeutic effect. Remodelling of the amino acid backbone can prolong serum half-life by protecting the antibody from clearance. Another technique is the fusion of the antibody candidate with albumin. Studies by Igawa et al. revealed an extended half-life in serum until three weeks [166]. Antibody conjugates cannot only prolong serum half-life but fused with toxins, cytokines or antibiotics the utility of therapeutic antibodies can be extended [167].

7.2. IsaA – The right target for an antibody based therapy

The limitation of antibody therapeutics is the restriction of targets to those expressed on the bacterial cell surface. *S. aureus* expresses a wide diversity of cell surface proteins essential for growth and virulence of the pathogen. Immunotherapeutic strategies based on virulence-associated determinants such as adhesins or toxins show varying efficacy, which is dependent on disease type and the causative strain. IsaA was selected as target antigen for immunotherapy based on its expression *in vivo* during sepsis caused by MRSA. In the study by Lorenz et al, the antibody response in human sera from sepsis patients 1 day after the detection of MRSA was compared with those from the same patients during the course of infection 5-15 days after the detection of MRSA in blood culture. Results from this study revealed a significant higher titer of anti-staphylococcal antibodies in patients with diagnosed sepsis at later time points compared to early time points and also to healthy individuals and colonized persons. Notable, none of the patients with high anti-staphylococcal antibody titers died of a septic shock [116]. Especially, antibodies against the 29 kDa IsaA protein were developed in patients with diagnosed sepsis. Furthermore, a study by van der Kooi-Pol focused on the immune response of *S. aureus* colonized epidermolysis bullosa (EB) patients demonstrated that these patients revealed a high anti-IsaA antibody titer in sera. Interestingly, EB patients who developed anti-IsaA antibodies did not suffer from *S. aureus*

bacteraemia [168]. These facts suggest that anti-IsaA antibodies are protective against invasive *S. aureus*. Moreover, IsaA is presented on the bacterial surface of the major clinical and community-associated MRSA/MSSA lineages and is expressed during different growth phases. Results from the binding studies indicated that hUK-66 binds not only recombinant IsaA but also native IsaA of the most clinically relevant MRSA strains including CC5, CC8, CC22, CC45, CC239, USA300, and USA400 [169].

7.3. Generation of hUK-66 producing cell lines

Different research cell lines were generated to provide sufficient amounts of antibodies for initial biochemical and functional testing using the Lonza Biologics' Glutamine Synthetase (GS) gene expression system [170]. The binding and the *in vitro* studies were performed with hUK-66 antibodies produced *in house*. Therefore, UK-66 specific antibody fragments were generated. The scFv and scFv-Fc fragments are composed of the antigen binding domain of UK-66 and were expressed by HEK 293 cells. The amount of antibody necessary for *in vivo* experiments was produced by the companies Evitria and Catalent. A set of clones was generated for each construct: hUK-66 IgG1, IgG2, IgG4. During cell line generation, different methods were tested to increase the production rate and to select high producer clones. However, when comparing the specific productivity of individual cell lines, the production of specific antibodies was improved, but no high producer clone was detected. Interestingly, the MSX refinement is more efficient to select higher producer than the single cell dilution method with constant MSX concentration. Nevertheless, product titers of each construct three days after cultivation are in line with titers described in literature [171]. Problems in productivity are perhaps due to the large size of antibody molecules and the difficult assembling of separately expressed light and heavy chain via disulphide bonds [172]. Furthermore, low protein expression and poor survival might also be a result of trapped misfolded proteins that are not exported from the cell but rather subjected to mechanisms like the unfolded protein response. Cells that cannot cope with the high load of misfolded protein will undergo apoptosis [173], [174]. A correlation between viable cell density and productivity was not investigated. Interestingly, the applied feeding strategy revealed that cells cultivated in normal RPMI media demonstrated comparable productivity rate compared to cells cultivated in specialized CHO media. However, a specifically optimization addressing the requirements of the hUK-66 IgG constructs will likely enhance the productivity of full length antibodies. A great variety of feed media and strategies exist and special protocols for the development of defined processes for monoclonal antibody production are available [175].

Analysis of product quality and integrity of in-process samples by Western Blot and ELISA revealed distinct, protein specific staining for scFv, scFv-Fc and full hUK-66 antibodies

throughout the culture. Additional signals in Western Blot can be explained by protease activity [176]. Samples of the full length IgG with additional protein fractions of lower molecular weight were detectable at 25 kDa and 50 kDa. These signals resulted from incomplete protein assembly and protein misfolding. The heavy chains are not secreted unless assembled with the light chain, while the light chain can be secreted as monomers or dimers [177], [178]. Therefore, the expression of light chain is a limiting step in antibody folding and a low ratio of HC:LC has been reported to be favourable for optimal assembly and high expression yields [179]. The precise balance of HC:LC ratio is difficult to achieve and several approaches have been made. The construct used in this work is a double vector system, which included the genes of the heavy and light chain. The expression vector was designed in a bi-cistronic fashion in order to ensure for a favourable transcription efficiency of heavy and light chain due to the identical integration locus. An intron was inserted between the promoter and coding sequence since it has been shown that splicing is involved in efficient transport from the nucleus to the cytoplasm [180]. The gene for the antibody heavy chain was cloned 5' to that of the light chain using pEE12.4 because the transcript is twice as large as that of the light chain and is expected to be processed more slowly. The sufficient light chain ration was guaranteed by the availability of separate promoters for each gene. The plasmid DNA was transfected as supercoiled. The respective clone pools were compared in productivity and based on the first binding assays only marginal differences could be observed.

The purification of antibody via Fc specific Protein G resins clear the final preparation from fragments or light chain dimers. Protein G is highly specific for binding the Fc part of antibodies and purities of > 90% are reported after purification [181]. The proteins from all constructs were purified to satisfied purity applying the protein G method.

One of the major bottlenecks in the development of a stable transfected cell line was the requirement of a homogenous high-producing cell line. Therefore, the producer cell line had to be single cell derived. Different techniques exist for single cell cloning like limiting dilution and FACS sorting. In this work, the limiting dilution was performed to select high producer clones and to confirm uniformity in the antibody production process. In this approach, cells were seeded into a 96-well plate in different dilutions. The well with the highest distance to the well A1 will be further diluted into a new 96 well plate. During this work, the producer cell line for the different constructs consists of mini-pools. Based on the fact that the productivity of the single cell clones was limited. The generation of a high producer clone was not possible during cell line development.

The MSX refinement was used to select higher producer clones from the mini-pool cell clones. Along with this method, product titer could be increased from 0.36 µg/ml to 4.0 µg/ml of producer clones cultivated in 200 µM MSX. For the different time points the productivity

was different between the groups of 150-200-300 μM MSX. In the 150 and 200 μM MSX groups, a deficiency in production was restored to the next time point of measurement. This might be due to the high load of recombinant protein being expressed, which can lead to saturation of cellular folding machinery [182]. With optimized fed batch cultivation, cell lines can reach a specific productivity of up 1-5 g/l [183]. Nevertheless, the antibody production of the generated cell lines covered the need for the *in vitro* experiments.

7.4. Therapeutic efficacy of hUK-66 *in vitro*

As described in various studies the antibody response to IsaA plays an important role for the protection against invasive *S. aureus* infections [168], [184], [185]. *In vitro* studies were performed to investigate that hUK-66 binds to *S. aureus* and also trigger protective mechanisms during *S. aureus* infection. Studies by Lorenz et al demonstrated the therapeutic efficacy of mUK-66 IgG1 in two different mouse models: a central venous catheter-related infection and a sepsis survival model. In both models, mUK-66 IgG1 revealed protection against staphylococcal infection. Furthermore, Lorenz et al., 2011 demonstrated the activation of professional phagocytes by mUK-66 IgG1 and the antibody dependent production of microbial induced reactive oxygen metabolites. Based on these results, *in vitro* studies with human whole blood samples were performed to analyse the biological activity of hUK-66 IgG. Various experiments were performed to clarify the following questions: 1) Does the hUK-66 IgG antibody demonstrate any biological activity in blood samples of donors infected with *S. aureus*? 2) Which IgG subclass reveals the most effective effector function during a *S. aureus* infection? 3) Do even immunocompromised patients with high risk at *S. aureus* infection benefit from therapy with hUK-66?

First, the biological activity of hUK-66 antibody was analysed with whole blood samples from healthy donors. For this experiment, different isotypes of hUK-66 were included to investigate the most effective phagocytic function of the antibodies which could serve as an indicator of biological activity to combat a *S. aureus* infection. These experiments focused on the antibody-mediated bacteria elimination due to opsonophagocytic killing of *S. aureus*. Furthermore, besides healthy volunteers blood samples from patients at high risk including diabetic patients, patients undergoing dialysis and AOD patients were included to assess the specific IsaA-mediated killing of *S. aureus* in those patient populations.

7.4.1. *In vitro* characterization of hUK-66 and hUK-66 related subclasses

Antibodies against microbes neutralize these agents, opsonize them for phagocytosis, sensitize them for antibody-dependent cellular cytotoxicity, and activate the complement system. These various effector functions are mediated by different IgG subclasses. The IgG

class was chosen by its property to be bound by Fc receptors expressed on phagocytes and its role in promoting phagocytosis. Fc receptors for different Ig isotypes are expressed on different leukocyte populations. Of these Fc receptors, the most important for phagocytosis are receptors for IgG antibodies, called FcγRs. There are three types of FcγRs, which have different affinities for different IgG subclasses, and are expressed on different cell types. The high affinity FcγR is called FcγRI (CD64). It strongly binds human IgG1 and IgG3 and is expressed on macrophages, monocytes, neutrophils and eosinophils. FcγRs with low affinity to IgG are FcγRII (CD32) and FcγRIII (CD16). Both receptors are expressed on neutrophils. All IgG subclasses are bound by all FcγRs with different affinity [186]. To analyse which IgG subclass promotes phagocytosis most efficiently, hUK-66 was designed as IgG1, IgG2 and IgG4. These isotypes were tested for their biological efficacy against *S. aureus* using blood samples from healthy donors. The assays were performed in physiological conditions to simulate the closest natural infection situation. The biological efficacy of hUK-66 isotypes were compared to the untreated samples and samples treated with the isotype control. As described in literature, the isotype IgG1 is the most effective one to mediate antibody dependent phagocytosis in humans by binding to the FcγRI [165]. This fact was confirmed by the performed killing assays with blood samples of healthy volunteers. In these assays, the hUK-66 IgG1 revealed the most effective killing of *S. aureus*. Results from these studies also demonstrate the importance of antibody mediated phagocytosis, since the other isotypes failed to kill *S. aureus* efficiently. Interestingly, hUK-66 IgG4 revealed a reduction of viable *S. aureus* compared to samples treated with hUK-66 IgG2. Both isotypes have comparable binding affinities to the most important FcγRs. Therefore, the killing of *S. aureus* must be mediated by other mechanisms. The main function of IgG4 is to interfere with immune inflammation induced by complement-fixing antibodies. Furthermore, IgG4 is predominantly expressed under chronic antigen exposure why it may play an important role of antigen neutralization and to recruit the alternative complement pathway [187], [188]. For reliable results, two control antibodies were included into the experiments. As a matched IgG1 isotype control antibody, Trastuzumab was chosen. This antibody is used in clinic for the treatment of cancer by targeting the HER-2 receptor and revealed no cross reactivity to *S. aureus*. As another control Gammunex was chosen. Gammunex is purified and pooled IgG of normal human serum and is used in clinic for the treatment of patients with primary immunodeficiencies [189]. Actually, Gammunex should be served as positive control in the performed killing assays since the used IVIg preparation contained high titers of anti-staphylococcal antibodies and more important high titers of anti-IsaA antibodies (Fig. 32). However, results from killing assays revealed that Gammunex mediated no antibody-dependent killing of *S. aureus* in the designed experimental set up. Based on these results in the *in vitro* assays, it is suggested that Gammunex contained only a minor fraction of active antibodies. The terminal sialic-acid residues have recently been demonstrated to be centrally

involved in antibody activity. In normal human serum which is used for the production of purified IgG preparations such as IVIG, a minor proportion of the IgG molecules carry terminal sialic-acid residues that are attached to the N297-linked sugar moiety [164]. This residue is highly important for the FcγR interaction resulting in phagocytosis of pathogens [190]. Another reason could be that the dose of 0.9 mg/ml IVIg neither contains enough active anti-staphylococcal antibodies nor anti-IsaA antibodies to mediate effective antibody dependent killing. The high dose of ineffective antibodies can also block FcγRs so that the active antibodies cannot mediate their functions.

As complement forms one of the first barriers of innate immunity any pathogenic microorganism has to cross this important layer of immune defence in order to establish an infection. The individual complement reactions develop in a sequential manner, allowing regulation that modulates the intensity of the response and adjusts the effector functions for the specific immune response [191]. Complement was identified more than 100 years ago as a result of its 'complementary' bactericidal activity and its role in phagocytosis of cellular debris [192]. Complement activation in turn activates pro-inflammatory mediators, generates anaphylactic peptides, cytolytic compounds and antimicrobial compounds, recruits effector cells and induces effector responses [193]. Mononuclear phagocytes and neutrophils ingest microbes for intracellular killing with and without antibodies. Nevertheless this process is strongly promoted by specific surface coating of the microbes with antibodies. However, the efficacy of an IgG antibody in mediating effector functions is not only determined by its subclass. Several factors are important for the biological function of antibodies, including the expression of the target protein on the cell surface, the signalling pathways associated with the target protein and the availability of complement proteins acting in concert with and effector cells. By using whole blood samples, a reduction of viable cfu was observed in samples without additional antibodies. Therefore, these untreated samples were set as 100% to analyse the antibody dependent killing of *S. aureus*.

Data from killing assays, performed with blood samples from healthy donors and patients at high risk for *S. aureus* infection, demonstrate that hUK-66 enhances killing of *S. aureus*. In consideration with the data from the assays with purified PMNs and hUK-66 N479A mutant in concert with the data from the FcγR binding assays, the hUK-66 mode of action is closely related with phagocytosis. In all killing assays comparing different IgG subclasses of hUK-66, hUK-66 IgG1 revealed the highest efficacy of bacterial killing and was subsequently chosen as lead candidate for further characterization of its biological activity.

7.4.2. *In vitro* analysis of biological activity of hUK-66 IgG1 in blood samples of high risk patients

During the last decade, active and passive immunization strategies have been examined in clinical trials. Despite promising experimental data, clinical trials in human have not yielded positive results. However, the importance of immune clearance is emphasized by the fact that humans with intact immune system combat them successfully. Furthermore, recent studies underlined the role of protective antibodies. Persons with increased levels of protective anti-staphylococcal antibodies have a lower risk of death due to bacteremia and sepsis [194], [195]. Nevertheless, immunocompromised patients are mainly affected by *S. aureus* infections and therefore they are the target population, which have to benefit from immunotherapy. IsaA was selected as target for an antibody based therapy, since all analysed patients surviving staphylococcal sepsis produced significant levels of anti-IsaA antibodies. The rationale behind the development of an antibody based therapy is that most of the persons suffer from a *S. aureus* infection do not generate sufficient levels of functional antibodies against *S. aureus* or infected individuals lacking of the development of a rapid functional immune response. For the functional characterization of hUK-66 blood samples from vulnerable patient groups: patients with diabetes, end-stage renal disease and AOD were selected. The selected patient groups revealed increased susceptibility to staphylococcal infection due to an impairment of innate immunity [196], [197]. Neutrophils act as first-line-of-defence cells and the reduction of their functional activity contributes to the high susceptibility to and severity of infections. Clinical investigations in diabetic patients and experimental studies in diabetic rats and mice clearly demonstrated consistent defects of neutrophil chemotactic, phagocytic and microbicidal activities [198]. These alterations have been reported to occur during inflammation in diabetes mellitus include: impairment of neutrophil adhesion to the endothelium and migration to the site of inflammation, production of reactive oxygen species and reduced release of cytokines and prostaglandin by neutrophils, increased leukocyte apoptosis and reduction in lymph node retention capacity [199], [200], [201], [202], [203]. Most of diabetic patients have a worse prognosis once infection is established.

Patients treated with dialysis suffering from uremia, the classical state of immune hyporesponsiveness and chronic activation of the immune system. Infection rates are several times higher in dialysis populations than in age-matched segments of general population [204], [205]. Infectious causes have consistently ranked second to cardiovascular diseases in reported causes of death in dialysis populations. In the United States during the years 2002-2004, mortality rates in dialysis populations were 20 times higher than those in the general population and mortality was attributed to septicaemia in 10% [206]. Major bacterial infections, like septicaemia and pneumonia, are characterized by pronounced inflammatory

activation, with downstream effects that include oxidative stress, abnormal endothelial function, coagulation system disequilibrium, abnormal cardiac myocyte function and diminished cellular oxygen availability [207]. These criteria are a characteristic of patients with disorders of phagocytic cells, which result in a high frequency of infections [208].

Patients suffering from AOD are more susceptible to *S. aureus* infections. AOD is the obstruction of the arteries and affects over 27 million individuals in Europe and North America [209]. Critical for this kind of disease is the high level of oxidative stress markers in the blood stream, which directly and indirectly enhances inflammatory pathways [210]. Bloemenkamp et al., identified in a multicentre, population-based, case-control study, that the inflammatory response correlated with frequently infections in AOD patients [211]. Furthermore, AOD patients revealed a broad range of biomarkers in their blood samples. Especially, the C-reactive protein is associated with the inflammatory state of the immune system [212]. The imbalance of fibrinogen, intercellular adhesion molecules, homocysteine and the levels of lipoprotein results in a malnutrition of immune cells. Further factors, like lysozyme and defensins are antimicrobial substances and defects in these soluble mediators can compromise host defence.

Neutrophil oxidative burst is a critical antimicrobial mechanism, which involves the conversion of dimolecular oxygen into superoxide anion by the NADPH oxidase complex. The entire complex is required for the production of superoxide, O_2^- . Superoxide itself is a weakly microbicidal agent. Metabolism to H_2O_2 by superoxide dismutase results in a more microbicidal compound, and H_2O_2 can be converted to HOCl by myeloperoxidase. Both H_2O_2 and HOCl are strongly microbicidal. Additional biochemical reactions produce peroxynitrite anion and nitryl chloride, which contribute additional microbicidal activities [213]. Patients with deficiencies in NADPH oxidase demonstrated a significant reduction of reactive oxygen species and suffer from recurrent life-threatening infections of Gram-positive *S. aureus* [214]. Among the most common bacterial infections observed in patients with deficiencies in NADPH oxidase are those involving *S. aureus* [214]. Patients with deficiencies in NADPH oxidase suffer from chronic granulomatous disease (CGD). CGD is caused by mutations in any one of four genes that encode the subunits of phagocyte NADPH oxidase. Of the 410 CGD mutations identified, 95% cause the complete or partial loss of NADPH oxidase function. Moreover in patients, *S. aureus* account for 33-62% of all intensive care unit pneumonia and are associated with significant morbidity and mortality [215]. Based on the fact, that the critical effector pathway required for *S. aureus* clearance is neutrophil oxidative burst, the oxidative burst of selected patient groups at high risk for *S. aureus* infection was investigated in the presence of the therapeutic antibody hUK-66 IgG1 [216]. Diabetes patients reveal a higher baseline of reactive oxygen species in blood compared to healthy donors [217]. These studies also showed that, after stimulation of diabetic PMNs, the level of

respiratory burst was lower than that of PMNs from healthy donors [218]. These results were also represented in our phagoburst studies. The percentage of PMNs from diabetic patients was strongly reduced compared to the PMNs from healthy donors. The same phenomenon is observed in dialysis patients. The high frequency of bacterial infections in end stage renal disease patients suggests that PMN dysfunction may be involved in the immune deficiency in this population [219]. However, the chosen patient groups have frequent and repetitive exposure to potential infectious risk factors during their normal course of therapy. The factors related to PMN dysfunction are not completely understood and have ascribed to malnutrition, iron unbalance, uremic toxins and zinc deficiency as well as disruption of cutaneous protective barriers and the affinity of bacteria for foreign polymeric materials [220]. Based on these factors it is hypothesized that the complement cascade is activated. This activation results in a leukocyte activation and primarily activated leukocytes are less susceptible to natural stimuli like microorganisms [221]. Changes in PMN function may result from alterations at different levels: 1) receptor expression and activation, 2) signal transfer by secondary messengers and target proteins and 3) dysfunction of the metabolic pathways and result in insufficient chemotaxis, impaired ingestion, decrease production of free radical, reduced metabolic activity and a significant inefficiency of bacterial killing. Changes in receptor expression have been demonstrated for dialysis, diabetes and patients suffering from AOD. A decrease in receptor expression is described for formyl-methionine-leucine-phenylalanine and Fc receptors [222]. The dysfunction of metabolic pathways is essential factor of PMNs of patients at high risk for *S. aureus* infections. The enzyme NAD(P)H oxidase converts oxygen to superoxide free radicals. The energy necessary for this process is delivered by the hexose monophosphate that breaks down glucose into CO₂. Studies of Vanholder et al., revealed a profound disturbance of PMN glycolysis in response to challenge [223]. The inhibition is parallel for different stimuli: latex beads, *S. aureus*, f-MLP and PMA. The fact that all of these stimuli including the direct activator PMA show a depression of the activation mechanisms, suggest that a common distal metabolic pathway is disturbed.

The defect in opsonization may be more important in dialysis patients, where a depletion of opsonins has been evidenced [224]. However, the high level of toxins in blood affects all selected patient groups by an imbalance of the bicarbonate buffer system of the blood. Furthermore, the enhanced availability of cytokines may result in the exhaustion of the immune system. Schleiffenbaum et al., demonstrated that the preincubation of PMNs with TNF caused functional deactivation of respiratory burst, corresponding with a down-regulation of TNF receptors [225]. The sum of all these factors may explain why the engulfment and the respiratory burst of phagocytes from the selected patient groups are significantly reduced compared to those of the phagocytes from healthy volunteers. Interestingly, the engulfment as well as the development of respiratory burst of phagocytes between the selected patient groups is comparable and may be resulted from the interaction

of common factors, like electrolyte abnormality, metabolic acidosis, the vascular insufficiency, the increased level of chemokines and cytokines, and the under-supply of phagocytes with nutrients.

The results from the *in vitro* studies demonstrated that the hUK-66 IgG1 did not enhance the ingestion of *S. aureus* by phagocytes from healthy volunteers or patients. For the phagocytes from healthy volunteers, it was detected that without additional antibody, over 90% of phagocytes had ingested bacteria. This clearly demonstrates that opsonization with serum host factors, such as antibody and complement results in the maxima recognition and phagocytosis of invading microorganisms. Consequently, the engulfment of *S. aureus* could not be improved under these conditions by hUK-66 IgG1. To draw a conclusion, hUK-66 IgG1 is not able to induce phagocytosis of inactive or impaired phagocytes. Noteworthy, the reduced percentage of activated phagocytes from selected patient groups ingested *S. aureus* most effectively, since the presence of additional antibody cannot improve phagocytosis. Related to the results from the oxidative burst of phagocytes from healthy volunteers, hUK-66 IgG1 cannot increase the percentage of phagocytes which are positive for respiratory burst. A possible explanation is, that already over 80% of detected phagocytes are positive for oxygen species and that the other 20% of phagocytes are inactive or dead. However, blood samples from selected patient groups incubated with hUK-66 revealed a higher percentage of oxidative burst positive cells compared to untreated samples or samples treated with the isotype control. Based on these results, hUK-66 activates phagocytes to produce oxygen species following FcγRs binding. These receptors activate signal transduction pathways that prolong cell survival, facilitate phagocytosis, release of cytokines and chemokines, elicit degranulation and promote reactive oxygen species production [226]. These processes are promoted by hUK-66, while the engulfment of staphylococci is unaffected by hUK-66. These results act perfectly in concert with the data of Lu et al, [227].

The phagocytosis process can be distinguished in several phases: attachment of opsonized particles by specific receptors, pseudopod extensions and completion of the engulfment resulting in the formation of a phagosome (Fig. 54). The next steps involve mobilization and fusion of the phagosome with different granule types resulting in the release of granule content that is required for killing [228]. The *in vitro* results of the engulfment experiments revealed that the hUK-66 antibody did not enhance the engulfment of *S. aureus* but increased the killing of phagocytosed bacteria. Neutrophils are capable of engulfing as many as 50 bacteria whereby a substantial amount of surface area is internalized while maintaining cell size and shape [229]. Besides opsonins and their ligands also physical parameters have influence on this process like particle size and shape. The bacterial size can be increased by natural changes in cellular morphology or via antibody-mediated agglutination [230]. However, even if the phagocytosis process is normal of patients at high risk, a clear defect is

observed in killing of *S. aureus in vitro* [231]. Furthermore, for effective bacterial killing, a critical concentration of neutrophils is required in suspension.

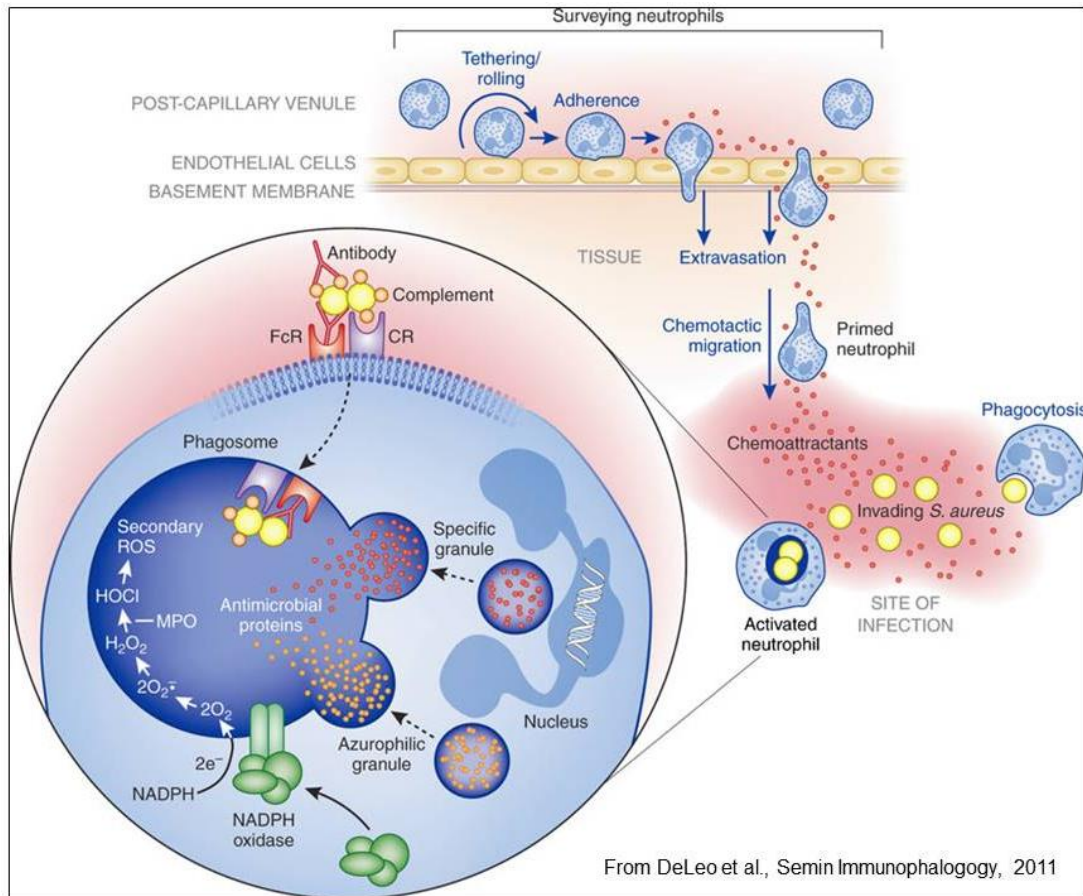


Fig. 54 Overview of neutrophil dependent killing of *S. aureus*.

Chemotactic molecules diffuse from the site of infection and into the bloodstream bind specific receptors on the neutrophil surface, arresting the rolling process and induce firm adherence to the endothelial wall. Once in the tissue, primed neutrophils chemotactically migrate to the site of infection where they recognize and engulf invading microorganisms. Within the phagosome of the activated neutrophil, microbes are destroyed by NADPH oxidase-derived reactive oxygen species and antimicrobial proteins released upon granule fusion with the phagosome (degranulation).

In vitro experimental killing demonstrates that a critical neutrophil concentration dictates the outcome. The individual maximum bearable bacterial concentration dependent on: neutrophil concentration, phagocytic activity and patient barrier integrity and can be varied by orders of magnitude between patients [232]. The effector function of hUK-66 IgG1 is mediated by FcγR binding and results in an enhancement of bacterial killing. This hUK-66 IgG1 dependent mechanism has a beneficial effect with granulocytes derived from immunocompetent persons as well as immunocompromised patients. This finding is further confirmed by *in vitro* killing assays performed with purified PMNs and hUK-66 IgG1 Fc mutant, which cannot be bound by FcγRs due to N297A mutation. Interestingly, the PMN samples incubated with the isotype control Rituximab demonstrated more effective killing than PMNs incubated with the hUK-66 IgG1 N297A Fc mutant. A possible explanation for this observation can be, that the isotype control contains intact glycosylated Fc parts, which can activate PMNs. The isotype control revealed killing only at high concentration of 500

µg/ml. The high antibody density may result in the development of immune complexes, which are more effective for PMN activation than Fc mutant opsonized bacteria complexes. The deglycosylated mutant cannot be bound by FcγRs, so that the killing stimulus consists only in the presence of bacteria. The presence of intact Fc parts by the isotype control is an extra stimulus, which may explain the moderate bacteria reduction.

The complete mode of action of hUK-66 IgG1 cannot be fully explained by *in vitro* results. However, there is a link between the increased oxidative burst reaction and the enhanced killing capacity of phagocytes from patients as well as from healthy volunteers. Therefore, hUK-66 IgG1 may act as a priming agent, serving to enhance phagocyte responses to *S. aureus*. Priming was first described in the early 1980s and is defined as the ability of a primary agonist to enhance the production of superoxide in response to a stimulus [233]. The priming process occurs on almost all levels of phagocyte functions: cytokine secretion, leukotriene synthesis, degranulation and microbicidal activities [226]. It is thought that priming prepares phagocytes for maximal response to invading microorganisms and thereby promoting efficient clearance. This assessment is borne out by the fact that the more responsive state of the neutrophil is attributable to assembly of the NADPH oxidase, reorganization of the plasma membrane, redistribution of signalling molecules into lipid rafts, modulation of intracellular signalling, mobilization of secretory vesicles, enrichment of specific surface receptors, cytokine secretion and transcriptional regulation of several gene families [228]. Results from *in vitro* studies clearly demonstrated that hUK-66 IgG1 mediates killing of *S. aureus* by binding FcγRs. Usually, *S. aureus* is recognized directly by its pathogen-associated molecular patterns (PAMPS) via pattern recognition receptors (PRRs). The engagement of two separate receptors activates signal transduction pathways may explain the increase oxidative burst and the enhancement of killing capacity [226] (Fig. 55).

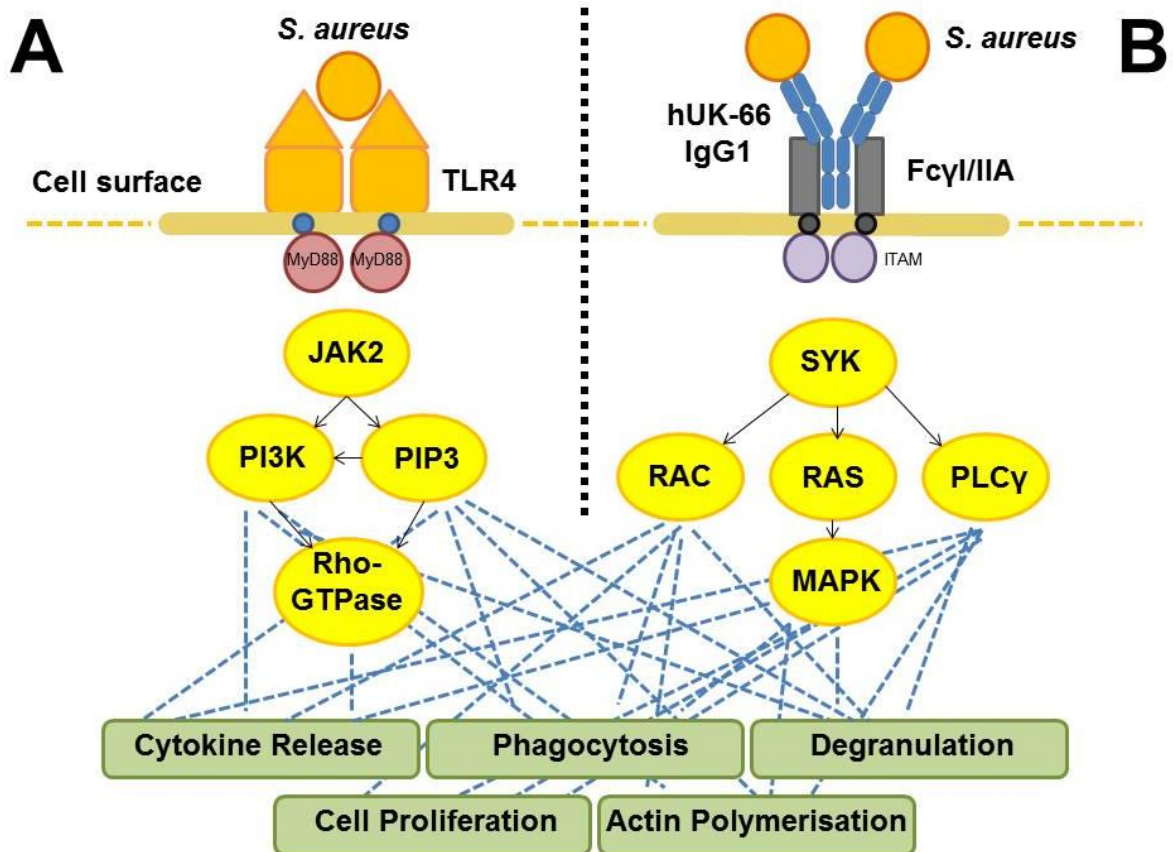


Fig. 55 Work hypothesis of hUK-66 IgG1 function.

A priming effect of phagocytes is mediated by a second stimulus. Besides the activation of phagocytes via PAMPs and PRRs, the binding of hUK-66 IgG1 by FcγRs mediate further signal pathways, which results in enhancement of phagocytosis. A) Signal pathways activate via PAMPs and PRRs binding. B) Signal cascade stimulates via hUK-66 IgG1 and FcγRs interaction. TLR4 Toll-loke receptor 4

The hUK-66 IgG1 opsonizes bacteria by binding of IsaA on the bacterial cell surface and mediates opsono-phagocytosis and killing. The hUK-tox antibody neutralizes the secreted alpha-toxin. This toxin is secreted as a water-soluble monomer by the majority of clinical relevant *S. aureus* strains [146, 147]. By its ability to forming pores, alpha-toxin injures the lung and other tissues and by this is involved in many diseases caused by *S. aureus* ranging from minor skin infections to life-threatening deep tissue infections and toxinoses [147]. In various animal models, immunization with antibodies directed against the staphylococcal alpha-toxin protects against *S. aureus* colonization or infection and results in a significant increase of survival in the treated animals compared to untreated animals (J. Wardenburg, 2008). Based on the promising animal data, a humanized anti-alpha-toxin IgG1 antibody was chosen to be tested in a combinatorial therapy with hUK-66 IgG1. The results from these assays revealed that the combination of hUK-66 IgG1 and hUK-tox IgG1 increases the efficacy of antibody-mediated immunotherapy (Fig. 26). Analysis focused on the FcγRs binding of hUK-66 IgG1 and hUK-tox revealed that both antibodies are bound by high affinity receptor FcγRIa and FcγRII, the most important FcγRs which mediates phagocytosis. For intensive investigation, an improved experimental set up has to be designed to analyse combinatorial effects of two antibodies with different effector mechanism *in vitro*.

7.5. Therapeutic efficacy of hUK-66 *in vivo*

A recent increase in staphylococcal infections caused by MRSA, combined with frequent, prolonged ventilator support of an aging, often chronically ill population, has resulted in a large increase in cases of MRSA pneumonia in the health care setting [234]. Additionally, caMRSA pneumonia has become more prevalent. Historically, this type of pneumonia affects younger patients, follows infection with influenza virus, and is often severe, requiring hospitalization and causing the death of a significant proportion. Both haMRSA and caMRSA are important causes of pneumonia and present diagnostic and therapeutic challenges [235]. Indeed, MRSA now accounts for 20-40% of all hospital-acquired pneumonia and ventilator-associated pneumonia [236]. To date, not only methicillin-resistant *S. aureus* are highly prevalent, but also resistances to treatment with fluorquinolones, macrolides, clindamycin, gentamicin, rifampicin, trimethoprim/ sulphonamide and mupirocin are reported (European Antimicrobial Resistance Surveillance System annual report 2008 and 2009.). Following the use of vancomycin as an antibiotic of last resort, intermediate and highly vancomycin-resistant *S. aureus* strains are observed. Confronted with this situation, a model of *S. aureus* Newman-induced pneumonia in adult Balb/c mice was established to investigate the therapeutic potential of mUK-66, hUK-66 and hUK-tox in prophylactic and therapeutic treatment. This infection model was chosen since it closely mimics the clinical and pathological features of pneumonia in humans. Both, human and mouse, develop an inducible bronchus-associated lymphoid tissue (iBALT) in case of infection, which initiate a local immune response and maintain memory cells in the lung [237]. Furthermore, with regard to the pneumonia model, mouse and human develop a similar immune response. The first line of defence against microorganisms in human is neutrophils. After infection, neutrophils dominate the infected site early while macrophages dominate infected sites at later stages. For the pneumonia model in mouse, Chen et al., demonstrate an equal immune response by comparing the cell number found in bronchoalveolar lavage fluid, after 1 and 3 days of infection. After 1 day of infection, the percentage of PMNs was dominated in MRSA-infected mice and after 3 days of infection the percentage of neutrophils decreased, while the percentage of macrophages increased. Macrophages dominated in the PBS group [238].

The *S. aureus* mediated pneumonia was induced by intranasal application of bacteria by dropping bacterial suspension onto the nose of appropriate anesthetized mouse. This way of bacterial inoculation ensures that approximately two-third of the inoculum could be recovered from the lungs which are in good accordance to results presented by other scientific groups using this mouse model [239]. *S. aureus* is not a natural colonizer of mice [240]. Therefore, mice had to be infected with a high bacteria inoculum to induce pneumonia related clinical symptoms. This high bacterial burden results in a progressive and rapid course of disease, reflecting in a mortality rate of approximately 50% at 24 h, and an additional 20% of the

animals succumbed to infection within 48 h following inoculation. Therefore, the effectiveness period of the therapeutic antibody to mediate protection is extremely limited. After establishment of the infection dose, first *in vivo* experiments were performed with mUK-66 to validate the mouse model. The intranasal application of antibody was chosen to locate the antibody direct at the side of infection. As it was shown in previous experiments using different mouse models, mUK-66 mediates 100% protection at an effective dose of 5 mg/kg in a prophylactic setting by intranasal application. Based on these results the pneumonia model was chosen to evaluate the therapeutic efficacy of hUK-66 and further hUK-tox. Noteworthy, the common clinical application of antibodies is the intravenous route of infection. The intravenous application includes security, efficacy and rapid delivery of medication. Medication dose can easily be monitored and is especially useful if long term therapy is proposed. Furthermore, the intravenous application is less painful than the administration of medicine subcutaneously or intramuscularly. However, intravenous application is more costly than oral or injectable administration by the higher concentration of medication necessary to be injected into the circulatory system to reach the effective dose at the side of infection. Furthermore, the rapid changes in the circulatory system result in a limit time of therapy, usually no more than 72 hours [241]. This situation explains why the effective dose of hUK-66 is dependent on the application route and increases from 5 mg/kg administered intranasally to 60 mg/kg intravenously.

Multiple *S. aureus* virulence factors contribute to the pathogenesis of pneumonia and staphylococcal IsaA is not regarded as a classical virulence factor compared to alpha-toxin. The alpha-toxin of *S. aureus* plays a critical role in the induction of pneumonia by causing damage to alveolar epithelia and erythrocytes [242]. After binding to receptor sites on cell surfaces, alpha-toxin forms heptameric assembly and funnel-shape pore that perforates host cell membranes [243], [244]. The effects of alpha-toxin are both concentration and cell-type dependent and include cell lysis, release of proinflammatory mediators and cytokines, and induction of apoptosis [243]. Therefore, alpha-toxin impaired the function of the lung's air-blood barrier. Studies by Bramley et al. revealed that *S. aureus* mutants lacking *hla* have reduced virulence in invasive disease models and larger numbers of staphylococci are required to kill mice [245]. These studies were persuaded by Wardenburg et al. and demonstrated that *S. aureus hla* mutant are less virulent than the wild type. Animals infected with *hla* mutant strain appeared to be moderately ill within 24 h and only a small number of these animals succumbed to the infection [239], [246]. These studies revealed also the virulent power of alpha-toxin. The hUK-tox mode of action is the neutralization of the alpha-toxin to inhibit the pathogenic effect on host cells. To the current knowledge, IsaA does not interact with the host and is not a virulence factor per definition. The fact that IsaA is associated with bacterial cell surface allowed the design of antibodies which mediate bacterial killing by phagocytosis. The hUK-tox antibody mediates direct effector function

compared to hUK-66 which has an indirect mode of action. The different modes of action of both antibodies are clearly demonstrated in the *in vivo* results. Related to the dose of efficacy, hUK-tox mediates 100% protection in a prophylactic set up at a concentration of 5 mg/kg compared to hUK-66 which mediates 70% protection at a concentration of 60 mg/kg. The importance of effective concentration at the site of infection is conducted by the fact that 0.5 mg/kg of hUK-66 mediates 100% protection by intranasal application compared to 60 mg/kg of hUK-66 mediated 70% protection by intravenous application.

Further aspects have to be considered by evaluating the therapeutic efficacy of mUK-66, hUK-66 IgG1 and hUK-tox. hUK-tox neutralizes alpha-toxin via binding and thereby the pore-forming process is inhibited. No further effector cells have to be activated and no receptor interaction is necessary.

All in all, the mouse pneumonia model is useful to demonstrate therapeutic efficacy of antibodies which act directly on *S. aureus* virulence factors but needs further improvements to be a useful model to analyse therapeutic efficacy of antibodies with indirect mode of action like hUK-66. Furthermore, the high bacterial burden necessary to induce pneumonia by *S. aureus* in mice provides a very small effectiveness period for the antibody in a prophylactic setting. All results of *in vivo* experiments clearly demonstrate that both antibodies hUK-66 and hUK-tox have therapeutic efficacy to inhibit *S. aureus* induced pneumonia using as a prophylactic treatment. To demonstrate the therapeutic efficacy of an antibody, a less aggressive model would be more useful, especially infection models with a slow course of disease and a small number of bacteria to induce the disease, like the models of sepsis and endocarditis. It is important to note that the susceptibility of mice to staphylococcal infection is significantly less than that of humans [137]. Due to the high bacterial load necessary to induce the disease in mouse, there are high demands for the antibody to mediate protection and in general the disease conditions are different to the human situation. The large inoculum required to cause pneumonia in these animals demonstrates the remarkable ability of the murine immune system to eliminate *S. aureus* from the lung. Hopefully, the enlargement of knowledge about this model system of immunocompetent mice may enhance our understanding of pulmonary immunity against *S. aureus*. One attempt to circumvent the limitations of the model is to analyse anti-staphylococcal antibodies in rabbits, which are naturally prone to *S. aureus* infections. For example *S. aureus* is able to colonize rabbits [247]. Moreover, both rabbit and human neutrophils for are susceptible for *S. aureus* virulence factor PVL, which is not the case for mice [248]. The development of an effective anti-staphylococcal therapy will require the development of animal models that are more closely approximate to human infections. *S. aureus* is not a natural colonizer of mice. Therefore many of the virulence factors elaborated by *S. aureus* to evade the human immune system may prove more difficult to study in mice, with PVL being a prime example

[240]. The challenge of translating findings in mice to humans was further illustrated by a publication by Soek *et al.* The study demonstrated that inflammatory responses are fairly consistent in humans, but not in mice [249]. Furthermore, the balance of lymphocytes and neutrophils in adult animals is quite different: human blood is neutrophil rich (50-70%) whereas mouse blood has a strong preponderance of lymphocytes (75-90%) [250]. One of the first lines of defence is antimicrobial peptides, called defensins. They are important in mucosal defence in the gut and in epithelial defence. Neutrophils are a rich source of defensins in humans, but defensins are not expressed by neutrophils in mice [251]. There is strong evidence by a study of Ober *et al.*, that the human and mouse FcRn have the same function by regulating the serum half-lives of IgG. Thus, humanized antibodies may be cleared more rapidly in mice than in human [252]. Noteworthy, there are well-known differences in expression of Ig isotypes between mice and humans. Mice express four subclasses of IgG: IgG1, IgG2a, IgG2b and IgG3. In humans there are also four subclasses of IgG: IgG1, IgG2, IgG3 and IgG4. While different subclasses have different abilities to bind FcR or complement and IgG1 antibody mediates different effector functions in mice than in humans [253]. For the development of an effective anti-staphylococcal therapy, it is most important to learn more about the natural immunity to *S. aureus* infections of immunocompetent hosts. The mechanisms of natural immunity are poorly understood. *S. aureus* disposes over broad range of virulence factors and strategies to evade human immune response and to colonize human. However, colonizers must not necessarily develop *S. aureus* induced clinical symptoms.

8. Outlook

Antibody molecules demonstrate unique and complex characteristics. How complex the development of an antibody based therapy against *S. aureus* is, demonstrate the fact that each patient develops a unique *S. aureus* specific immune response, after infection. The most critical step is the number of days to reach protective antibody levels. Therefore, it is quite challenging to develop an antibody therapy based on a single staphylococcal component. The cause of failure of previous staphylococcal immunotherapies is complex and suffers from inadequate target selection. A pathogen, which is armed with a broad range of virulence factors, is able to remain pathogenicity even when antigens are neutralized or blocked.

In this work, the potential of hUK-66 was investigated as a candidate for a single anti-staphylococcal immunotherapy and in combination with the alpha-toxin neutralizing antibody hUK-tox. In summary, hUK-66 was shown to bind specifically to IsaA without cross-reactivity with other staphylococcal surface proteins. Binding of hUK-66 to FcγRI and FcγRIIIa expressed by neutrophils as well as the induction of a respiratory burst were also demonstrated. Furthermore, hUK-66 was shown to induce bacterial killing in whole blood *in vitro* and was consequently also active in pneumonia models in mice. These experiments were exclusively performed with the *S. aureus* strain Newman. However, *S. aureus* strains are diverse and very versatile in their antigenic repertoire, therefore it is important to investigate the prophylactic effectiveness of hUK-66 and hUK-tox with further clinical relevant *S. aureus* strains. In this context, the specific mode of action of hUK-66 and hUK-tox during pulmonary infection of mice has to be defined with clinical important *S. aureus* strains and their isogenic mutants. Furthermore, it has to be investigated whether hUK-66 and hUK-tox protection against pneumonia is also protective against other forms of *S. aureus* infection like bacteremia, sepsis or osteomyelitis.

The pharmacology of hUK-66 and hUK-tox has been characterized in terms of target affinity and selectivity, *in vitro* functionality as well as an *in vivo* efficacy. These data clearly demonstrate that the antibody molecules hUK-66 and hUK-tox possess several prerequisites for a successful immunotherapy against *S. aureus*. However safety and pharmacokinetics of both antibodies are not investigated yet as well as the safety, toxicity and bioavailability by analysis of tissue cross-reactivity in animal tissues of the combination of hUK-66 and hUK-tox. The main aim of the future non-clinical development will be to demonstrate the safety of a dose leading to a multiple of the human target exposure in animals. Local tolerance will be evaluated by histopathological examinations of the injection sites and toxicokinetics in animals will give information on potential pharmacokinetic interactions of the two antibodies.

To expand our knowledge of interaction with hUK-66 and hUK-tox with the immune system further studies have to be performed to investigate the influences of cytokine development in human immune cells as well as the effect on b- and t-cell stimulation. All data will be used to identify a safe starting dose for a planned First-in-Man study.

The independent observation by van der Kooi Pol et al., and Lorenz et al., that human anti-IsaA antibody are critical for successful protection during *S. aureus* infection demonstrates the potential of hUK-66 as a candidate for immunotherapy. Furthermore, the therapeutic combination of hUK-66 and hUK-tox includes two different effector mechanisms and allows to combat *S. aureus* from two sides at once. The combination of two efficient anti-staphylococcal antibodies reveals a new therapeutic strategy for untreatable *S. aureus* so far.

9. References

- [1] K. B. Crossley, K. K. Jefferson, L. Gordon und G. Fowler, *Staphylococci in Human Disease*, Wiley Online Library, 2009.
- [2] Ogston, „On Abscesses". *Classics in Infectious Diseases*," *Rev Infect Dis*, pp. 122-128, January-February 1884.
- [3] W. C. Noble, H. A. Valkenburg und C. H. L. Wolters, „Carriage of *Staphylococcus aureus* in random samples of a normal population," *J. Hyg.*, pp. 567-573, June 1967.
- [4] M. Casewell und R. L. Hill, „The carrier state: methicillin-resistant *Staphylococcus aureus*," *J Antimicrob Chemother.*, Juli 1986.
- [5] J. Kluytmans, A. van Belkum und H. Verbrugh, „Nasal carriage of *Staphylococcus aureus*: epidemiology, underlying mechanisms, and associated risks," *Clinical Microbiology Reviews*, pp. 505-520, July 1997.
- [6] A. M. Cole, S. Tahk, A. Oren, D. Yoshioka, Y. H. Kim, A. Park und T. Ganz, „Determinants of *Staphylococcus aureus* nasal carriage," *Clin Diagn Lab Immunol.*, pp. 1064-1069, November 2001.
- [7] R. P. Wenzel und T. M. Per, „The significance of nasal carriage of *Staphylococcus aureus* and the incidence of postoperative wound infection," *Journal of Hospital Infection*, pp. 13-24, April 1995.
- [8] C. von Eiff, K. Becker, K. Machka, H. Stammer und G. Peters, „Nasal carriage as a source of *Staphylococcus aureus* bacteremia. Study Group," *N Eng J Med*, pp. 11-16, January 2001.
- [9] H. F. Wertheim, M. C. Vos, A. Ott, A. van Belkum, A. Voss, J. A. Kluytmans, P. H. van Keulen, C. M. Vandenbroucke-Grauls, M. H. Meester und H. A. Verbrugh, „Risk and outcome of nosocomial *Staphylococcus aureus* bacteremia in nasal carriers versus non-carriers," *Lancet*, pp. 703-705, August 2004.
- [10] C. U. Tuazon, A. Perez, T. Kishaba und J. N. Sheagren, „*Staphylococcus aureus* among insulin-injecting diabetic patients. An increased carrier rate," *JAMA*, March 1975.
- [11] C. U. Tuazon und J. N. Sheagren, „Increased Rate of Carriage of *Staphylococcus aureus* among Narcotic Addicts," *Journal of Infectious Diseases*, pp. 725-727, 1975.
- [12] V. L. Yu, A. Goetz, M. Wagener, P. B. Smith, J. D. Rihs, J. Hanchett und J. J. Zuravleff, „*Staphylococcus aureus* Nasal Carriage and Infection in Patients on Hemodialysis," *The New England Journal of Medicine*, pp. 91-96, July 1986.
- [13] H. J. Weinstein, „The Relation between the Nasal-*Staphylococcal*-Carrier State and the Incidence of Postoperative Complications," *The New England Journal of Medicine*, pp. 1303-1308, June 1959.
- [14] T. Weinke, R. Schiller, F. J. Fehrenbach und H. D. Pohle, „Association between *Staphylococcus aureus* nasopharyngeal colonization and septicemia in patients infected with the human immunodeficiency virus," *European Journal of Clinical Microbiology and Infectious Diseases*, November 1992.

- [15] K. S. Tan, K. O. Lee, K. C. Low, A. M. Gamage, Y. Liu, C. Y. G. Tan, H. Q. V. Koh, S. Alonso und Y. H. Gan, „Glutathione deficiency in type 2 diabetes impairs cytokine response and control of intracellular bacteria,“ *The Journal of clinical investigation*, pp. 2289-2300, June 2012.
- [16] G. C. K. W. Koh, S. J. Peacock, T. van der Poll und W. J. Wiersinga, „The impact of diabetes on the pathogenesis of sepsis,“ *Eur J Clin Microbiol Infect Dis*, pp. 379-388, April 2012.
- [17] A. Tranaeus und Q. Yao, „Immune dysfunction in dialysis patients-prevention and treatment strategies,“ *Peritoneal Dialysis International*, pp. 161-166, November 2007.
- [18] A. Lecube, G. Pachon, J. Petriz, C. Hernandez und R. Simo, „Phagocytic activity is impaired in type 2 diabetes mellitus and increases after metabolic improvement,“ *Plos one*, pp. 1-6, August 2011.
- [19] L. F. McCaig, C. L. McDonald†, S. Mandal† und D. B. Jernigan†, „Staphylococcus aureus-associated Skin and Soft Tissue Infections in Ambulatory Care,“ *Emerg. Infect. Dis.*, pp. 1715-1723, November 2006.
- [20] G. J. Moran, A. Krishnadasan, R. J. Gorwitz, G. E. Fosheim, L. K. McDougal, R. B. Carey und D. A. Talan, „Methicillin-Resistant S. aureus Infections among Patients in the Emergency Department,“ *The new england journal of medicine*, pp. 666-674, August 2006.
- [21] F. D. Lowy, „Staphylococcus aureus infections,“ *The New England Journal of Medicine*, pp. 520-532, August 1998.
- [22] Daum, Brad, Spellberg und Robert, „Development of a vaccine against Staphylococcus,“ *Semin Immunopathol*, pp. 335-348, November 2012.
- [23] F. R. DeLeo, M. Otto, B. N. Kreiswirth und H. F. Chambers, „Community-associated methicillin-resistant Staphylococcus aureus,“ *The Lancet*, pp. 1557-1568, May 2010.
- [24] F. R. DeLeo und H. F. Chambers, „Reemergence of antibiotic-resistant Staphylococcus aureus in the genomics era,“ *The Journal of Clinical Investigation*, pp. 2464-2474, September 2009.
- [25] T. J. Foster und M. Höök, „Surface protein adhesins of Staphylococcus aureus,“ *Trends in Microbiology*, pp. 484-488, December 1998.
- [26] T. Chavakis, K. Wiechmann, K. T. Preissner und M. Herrmann, „Staphylococcus aureus interactions with the endothelium: The role of bacterial “Secretable Expanded Repertoire Adhesive Molecules” (SERAM),“ *Thromb Haemost*, pp. 278-285, June 2005.
- [27] B. Sinha, P. F. François, O. Nüsse, M. Foti, O. M. Hartford, P. Vaudaux, T. J. Foster, D. P. Lew, M. Herrmann und K. H. Krause, „Fibronectin-binding protein acts as Staphylococcus aureus invasin via fibronectin bridging to integrin alpha5beta1.,“ *Cell Microbiol.*, pp. 101-117, September 1999.
- [28] R. Wang, K. R. Braughton, D. Kretschmer, T.-H. L. Bach, S. Y. Queck, M. Li, A. D. Kennedy, D. W. Dorward, S. J. Klebanoff, A. Peschel, F. R. DeLeo und M. Otto, „Identification of novel cytolytic peptides as key virulence determinants for community-associated MRSA,“ *Nature Medicine*, pp. 1510-1514, November 2007.
- [29] T. J. Foster, „Immune evasion by staphylococci,“ *Nature*, pp. 946-958, December 2005.

- [30] I. Jongerius, J. Köhl, M. K. Pandey, M. Ruyken, K. P. v. Kessel, J. A. v. Strijp und S. H. Rooijackers, „Staphylococcal complement evasion by various convertase-blocking molecules,“ *The Journal of Experimental Medicine*, pp. 2461-2471, September 2007.
- [31] H. Grundmann, M. Aires-de-Sousa, J. Boyce und E. Tiemersma, „Emergence and resurgence of methicillin-resistant *Staphylococcus aureus* as a public-health threat,“ *Lancet*, pp. 874-885, September 2006.
- [32] G. C. Schito, „The importance of the development of antibiotic resistance in *Staphylococcus aureus*,“ *Clin Microbiol Infect*, pp. 3-8, December 2006.
- [33] G. R. Nimmo, G. W. Coombs, J. C. Pearson, F. G. O'Brien, K. J. Christiansen, J. D. Turnidge, I. B. Gosbell, P. Collignon und M.-L. McLaws, „Methicillin-resistant *Staphylococcus aureus* in the Australian community: an evolving epidemic,“ *Med J Aust*, pp. 384-388, 2006.
- [34] G. J. Moran, A. Krishnadasan, R. J. Gorwitz, G. E. Fosheim, L. K. McDougal, R. B. Carey und D. A. Talan, „Methicillin-resistant *S. aureus* infections among patients in the emergency department,“ *N Engl J Med.*, pp. 666-674, August 2006.
- [35] S. F. Graves, S. D. Kobayashi und F. R. DeLeo, „Community-associated methicillin-resistant *Staphylococcus aureus* immune evasion and virulence,“ *J Mol Med*, pp. 109-114, February 2010.
- [36] G. Sakoulas und R. C. Moellering, „Increasing Antibiotic Resistance among Methicillin-Resistant *Staphylococcus aureus* Strains,“ *Clin Infect Dis*, pp. 360-367, 2008.
- [37] G. H. Talbot, J. Bradley, E. J. J. E. D. Gilbert, M. Scheld und J. G. Bartlett, „Bad bugs need drugs: an update on the development pipeline from the Antimicrobial Availability Task Force of the Infectious Diseases Society of America,“ *Clin Infect Dis.*, pp. 657-668, April 2006.
- [38] B. Spellberg, J. H. Powers, E. P. Brass, L. G. Miller und J. E. Edwards Jr., „Trends in antimicrobial drug development: implications for the future,“ *Clin Infect Dis.*, pp. 1279-1286, May 2004.
- [39] C. Saylor, E. Dadachova und A. Casadevall, „Monoclonal antibody-based therapies for microbial diseases,“ *Vaccine*, December 2010.
- [40] E. Bishop, S. Melvani, B. P. Howden, P. G. Charles und M. L. Grayson, „Good clinical outcomes but high rates of adverse reactions during linezolid therapy for serious infections: a proposed protocol for monitoring therapy in complex patients,“ *Antimicrob Agents Chemother.*, pp. 1599-1602, April 2006.
- [41] H. W. Boucher und G. Sakoulas, „Perspectives on Daptomycin resistance, with emphasis on resistance in *Staphylococcus aureus*,“ *Clin Infect Dis.*, pp. 601-608, September 2007.
- [42] S. Tsiodras, H. S. Gold, G. Sakoulas, G. M. Eliopoulos, C. Wennersten, L. Venkataraman, R. C. Moellering und M. J. Ferraro, „Linezolid resistance in a clinical isolate of *Staphylococcus aureus*,“ *Lancet*, pp. 207-208, July 2001.
- [43] R. M. Carlton, „Phage therapy: past history and future prospects,“ *Arch Immunol Ther Exp*, pp. 267-274, 1999.

- [44] S. J. Dancer, „The effect of antibiotics on methicillin-resistant *Staphylococcus aureus*,“ *J. Antimicrob. Chemother.*, pp. 246-253, December 2007.
- [45] C. von Eiff, J. F. Kokai-Kun, K. Becker und G. Peters, „In vitro activity of recombinant lysostaphin against *Staphylococcus aureus* isolates from anterior nares and blood.,“ *Antimicrob Agents Chemother.*, pp. 3613-3615, November 2003.
- [46] U. Storz, *Intellectual Property Issues*, Springer, 2012.
- [47] J. M. Patti, „A humanized monoclonal antibody targeting *Staphylococcus aureus*,“ *Vaccine*, pp. 39-43, September 2004.
- [48] H. W. Boucher, G. H. Talbot, J. S. Bradley, J. E. Edwards Jr., D. Gilbert, L. B. Rice, M. Scheld, B. Spellberg und J. Bartlett, „Bad Bugs, No Drugs: No ESKAPE! An Update from the Infectious Diseases Society of America,“ *Clinical Infectious diseases*, pp. 1-12, January 2009.
- [49] J. M. Reichert, „Monoclonal Antibodies as Innovative Therapeutics,“ *Current Pharmaceutical Biotechnology*, pp. 423-430, December 2008.
- [50] J. M. Reichert, C. J. Rosenzweig, L. B. Faden und M. C. Dewitz, „Monoclonal antibody successes in the clinic,“ *Nature Biotechnology*, pp. 1073-1078, September 2005.
- [51] E. A. Behring und S. Kitasato, Ueber das Zustandekommen der Diphtherie-Immunität und der Tetanus-Immunität bei Tieren, Berlin: Deutch.Med.Woch., 1890.
- [52] A. Casadevall und M. D. Scharff, „Serum Therapy Revisited: Animal Models of Infection and Development of Passive Antibody Therapy,“ *Antimicrobial Agents and Chemotherapy*, pp. 1695-1702, August 1994.
- [53] A. Casadevall und M. D. Scharff, „Return to the past: the case for antibody-based therapies in infectious diseases,“ *Clin Infect Dis.*, pp. 150-161, July 1995.
- [54] A. Casadevall, E. Dadachova und L. Pirofski, „Passive antibody therapy for infectious diseases,“ *Nature reviews Microbiology*, pp. 695-703, September 2004.
- [55] H. Wu, D. S. Pfarr, G. A. Losonsky und P. A. Kiener, „Immunoprophylaxis of RSV infection: advancing from RSV-IGIV to palivizumab and motavizumab.,“ *Curr Top Microbiol Immunol.*, pp. 103-123, 2008.
- [56] G. Köhler und C. Milstein, „Continuous cultures of fused cells secreting antibody of predefined specificity,“ *Nature*, pp. 495-497, August 1975.
- [57] A. L. Nelson, E. Dhimolea und J. M. Reichert, „Development trends for human monoclonal antibody therapeutics,“ *Nature reviews drug discovery*, pp. 767-774, October 2010.
- [58] L. Olsson und H. Kaplan, „Human-human hybridomas producing monoclonal antibodies of predefined antigenic specificity,“ *Proc. Natl. Acad. Sci. USA*, pp. 5429-5431, September 1980.
- [59] L. Olsson, R. B. Andreasen, A. Ost, B. Christensen und P. Biberfeld, „Antbody producing human human hybridomas,“ *J. Exp. MED*, pp. 537-550, February 1984.

- [60] D. Kozbor und J. C. Roder, „Requirements for the establishment of high-titered human monoclonal antibodies against tetanus toxoid using the Epstein-Barr virus technique.“ *J Immunol.*, pp. 1275-1280, October 1981.
- [61] A. S. Kang, D. R. Burton und R. A. Lerner, „Combinatorial immunoglobulin libraries in phage,“ *Methods Companion Methods Enzymology*, pp. 111-118, 1991.
- [62] L. L. Green, M. C. Hardy, C. E. Maynard-Currie, H. Tsuda, D. M. Louie, M. J. Mendez, H. Abderrahim, M. Noguchi, D. H. Smith, Y. Zeng, N. E. David, H. Sasai, D. Garza, D. G. Brenner, J. F. Hales, R. P. McGuinness, D. J. Capon, S. Klapholz und A. Jakob, „Antigen-specific human monoclonal antibodies from mice engineered with human Ig heavy and light chain YACs,“ *Nature Genetics*, pp. 13-21, 1994.
- [63] T. D. Brock, *Milestones in Microbiology*, Englewood Cliffs: ASM Press, 1961.
- [64] G. Winter und W. J. Harris, „Antibody-based therapy: Humanized antibodies,“ *TIPS*, pp. 139-143, May 1993.
- [65] C. M. Velicer, S. R. Heckbert, J. W. Lampe, J. D. Potter, C. A. Robinson und S. H. Taplin, „Antibiotic use in relation to the risk of breast cancer,“ *JAMA*, pp. 827-835, February 2004.
- [66] K. Wickens, N. Pearce, J. Crane und R. Beasley, „Antibiotic use in early childhood and the development of asthma,“ *Clinical and Experimental Allergy*, pp. 766-771, October 1999.
- [67] J. Pachi, P. Svoboda, F. Jacobs, K. Vandewoude, B. van der Hoven, P. Spronk, G. Masterson, M. Malbrain, M. Aoun, J. Garbino, J. Takala, L. Drogha, J. Burnie und R. Matthews, „A Randomized, Blinded, Multicenter Trial of Lipid-Associated Amphotericin B Alone versus in Combination with an Antibody-Based Inhibitor of Heat Shock Protein 90 in Patients with Invasive Candidiasis,“ *Clinical Infectious Diseases*, pp. 1404-1413, January 2006.
- [68] M. Akiyama, K. Oishi, M. Tao, K. Matsumoto und M. Pollack, „Antibacterial properties of *Pseudomonas aeruginosa* immunotype 1 lipopolysaccharide-specific monoclonal antibody (MAb) in a murine thigh infection model: combined effects of MAb and ceftazidime,“ *Microbiol Immunol*, pp. 629-635, 2000.
- [69] M. Prabakaran, N. Prabhu, F. He, Q. Hongliang, H. Ho, J. Qiang, T. Meng, M. Goutama und J. Kwang, „Combination Therapy Using Chimeric Monoclonal Antibodies Protects Mice from Lethal H5N1 Infection and Prevents Formation of Escape Mutants,“ *Plos One*, May 2009.
- [70] J. Meulen, E. van den Brink, L. L. M. Poon, W. E. Marissen, C. S. W. Leung, F. Cox, C. Y. Cheung, A. Q. Bakker, J. A. Bogaards, E. van Deventer, W. Preiser, H. W. Doerr, V. T. Chow und J. Goudsmit, „Human Monoclonal Antibody Combination against SARS Coronavirus: Synergy and Coverage of Escape Mutants,“ *Plos Medicine*, July 2006.
- [71] C. Pedraz, X. Carbonell-Estrany, J. Figueras-Aloy und J. Quero, „Effect of palivizumab prophylaxis in decreasing respiratory syncytial virus hospitalizations in premature infants,“ *Pediatric Infectious Disease Journal*, pp. 823-827, September 2003.

- [72] B. Oesterreich, B. Lorenz, T. Schmitter, R. Kontermann, M. Zenn, B. Zimmermann, M. Haake, U. Lorenz und K. Ohlsen, „Characterization of the biological anti-staphylococcal functionality of hUK-66 IgG1, a humanized monoclonal antibody as substantial component for an immunotherapeutic approach.“ *Hum Vaccin Immunother.*, February 2014.
- [73] R. Waibel, R. Alberto, J. Willuda, R. Finnern, R. Schibli, A. Stichelberger, A. Egli, U. Abram, J. P. Mach, A. Plückthun und P. A. Schubiger, „Stable one-step technetium-99m labeling of His-tagged recombinant proteins with a novel Tc(I)-carbonyl complex.“ *Nat Biotechnol.*, pp. 897-901, September 1999.
- [74] A. Kortt, O. Dolezal, B. E. Power und P. J. Hudson, „Dimeric and trimeric antibodies: high avidity scFvs for cancer targeting.“ *Biomolecular Engineering*, pp. 95-108, October 2001.
- [75] C. A. Janeway Jr, P. Travers, M. Walport und weitere, *Immunobiology: The Immune System in Health and Disease.*, New York: Garland Science, 2001.
- [76] Murphy, *Immunobiology*, New York: Garland Science, 2012.
- [77] E. Metchnikoff, *Immunity in Infective Disease*, New York: Johnson Reprint Corp., 1968.
- [78] K. M. Rigby und F. R. DeLeo, „Neutrophils in innate host defense against *Staphylococcus aureus* infections.“ *Semin Immunopathol*, pp. 237-259, October 2011.
- [79] L. V. Dekker, *Protein Kinase C Isotype Function in Neutrophils*, Eureka, 2003.
- [80] S. H. Zigmond, „Chemotaxis by polymorphonuclear leukocytes.“ *J. Cell Biology*, pp. 269-287, May 1978.
- [81] E. Caron und A. Hall, „Identification of two distinct mechanisms of phagocytosis controlled by different Rho GTPases.“ *Science*, pp. 1717-1721, 1998.
- [82] P. Bruhns, „Properties of mouse and human IgG receptors and their contribution to disease models.“ *Blood*, pp. 5640-5649, 2012.
- [83] J. G. Hirsch, „Cinemicrophotographic observations on granule lysis in polymorphnuclear leucocytes during phagocytosis.“ *J Exp Med*, pp. 827-834, 1962.
- [84] R. I. Lehrer, J. Hanifin und M. J. Cline, „Defective bactericidal activity in myeloperoxidase-deficient human neutrophils.“ *Nature*, pp. 78-79, July 1969.
- [85] B. M. Babior, R. S. Kipnes und J. T. Curnutte, „The production by leukocytes of superoxide, a potential bactericidal agent.“ *Journal of clinical investigation*, pp. 741-744, March 1973.
- [86] J. T. Curnutte und B. M. Babior, „The effect of bacteria and serum on superoxide production by granulocytes.“ *Journal of clinical investigation*, pp. 1662-1672, June 1974.
- [87] M. B. Hampton, J. Kettle und C. C. Winterbourn, „Inside the neutrophil phagosome: oxidants, myeloperoxidase, and bacterial killing.“ *Blood*, pp. 3007-3017, November 1998.
- [88] A. W. Segal und A. Abo, „The biochemical basis of the NADPH oxidase of phagocytes.“ *TIBS*, pp. 43-47, February 1993.

- [89] B. M. Babior, R. S. Kipnes und J. T. Curnutte, „Biological defense mechanisms: The production by leukocytes of superoxide, a potential bactericidal agent,“ *J Clin Invest*, p. 741, 1973.
- [90] S. J. Chanock, J. E. Benna, R. M. Smith und B. M. Babior, „The respiratory burst oxidase,“ *Journal of Biological Chemistry*, pp. 24519-24522, October 1994.
- [91] J. A. Winkelstein, M. C. Marino, R. B. Johnston Jr., J. Boyle, J. Curnutte, J. I. Gallin, H. L. Malech, S. M. Holland, H. Ochs, P. Quie, R. H. Buckley, C. B. Foster, S. J. Chanock und H. Dickler, „Chronic granulomatous disease. Report on a national registry of 368 patients,“ *Medicine*, pp. 155-169, May 2000.
- [92] N. V. Serbina, T. P. Salazar-Mather, C. A. Biron, W. A. Kuziel und E. G. Pamer, „TNF/*i*NOS-producing dendritic cells mediate innate immune defense against bacterial infection,“ *Immunity*, pp. 59-70, 2003.
- [93] Q. S. Gao, M. Sun, S. Tyutyulkova, D. Webster, A. Rees, A. Tramontano, R. J. Massey und S. Paul, „Molecular cloning of a proteolytic antibody light chain,“ *J Biol Chem*, pp. 32389-93, December 1994.
- [94] H. S. Thompson, M. L. Davies, M. J. Watts, A. E. Mann, F. P. Holding, T. O'Neill, J. T. Beech, S. J. Thompson, G. D. Leesman und J. T. Ulrich, „Enhanced immunogenicity of a recombinant genital warts vaccine adjuvanted with monophosphoryl lipid A,“ *Vaccine*, pp. 1993-1999, December 1998.
- [95] R. Schier, A. McCall, G. P. Adams, K. W. Marshall, H. Merritt, M. Yim, R. S. Crawford, L. M. Weiner, C. Marks und J. D. Marks, „Isolation of picomolar affinity anti-c-erbB-2 single-chain Fv by molecular evolution of the complementarity determining regions in the center of the antibody binding site,“ *J Mol Biol*, pp. 551-567, November 1996.
- [96] M. Ohlin und C. A. Borrebaeck, „Low affinity, antibody binding of an Escherichia coli-derived component,“ *FEMS Immunol Med Microbiol.*, pp. 161-168, February 1996.
- [97] P. Martineau und J. M. Betton, „In vitro folding and thermodynamic stability of an antibody fragment selected in vivo for high expression levels in Escherichia coli cytoplasm,“ *J Mol Biol*, pp. 921-929, October 1999.
- [98] D. Filpula, „Antibody engineering and modification technologies,“ *Biomolecular Engineering*, pp. 201-215, March 2007.
- [99] A. Skerra und A. Plückthun, „Assembly of a Functional Immunoglobulin Fv Fragment in Escherichia coli,“ *Science*, pp. 1038-1042, March 1988.
- [100] J. Huston, D. Levinson, M. Mudgett-Hunter, M. Tai, J. Novotny, M. N. Margolies, R. J. Ridge, R. E. Brucoleri, E. Haber, R. Crea und H. Oppermann, „Protein engineering of antibody binding sites: Recovery of specific activity in an anti-digoxin single-chain Fv analogue produced in Escherichia coli,“ *Proc. Natl. Acad. Sci.*, pp. 5879-5883, August 1988.
- [101] L. G. Presta, „Evolving an anti-toxin antibody,“ *Nature Biotechnology*, pp. 63-64, January 2007.
- [102] S. H. Pincus, H. Fang, R. A. Wilkinson, T. K. Marcotte, J. E. Robinson und W. C. Olson, „In Vivo Efficacy of Anti-Glycoprotein 41, But Not Anti-Glycoprotein 120, Immunotoxins in a Mouse Model of HIV Infection,“ *Journal of Immunology*, pp. 2236-2241, December 2002.

- [103] G. A. Leget und M. S. Czuczman, „Use of rituximab, the new FDA-approved antibody,“ *Curr Opin Oncol.*, pp. 548-551, November 1998.
- [104] M. M. Goldenberg, „Trastuzumab, a recombinant DNA-derived humanized monoclonal antibody, a novel agent for the treatment of metastatic breast cancer.,“ *Clin. Ther.*, pp. 309-318, February 1999.
- [105] K. A. Chester und R. E. Hawkins, „Clinical issues in antibody design,“ *Trends Biotechnology*, pp. 294-300, August 1995.
- [106] G. L. Boulianne, N. Hozumi und M. J. Shulman, „Production of functional chimaeric mouse/human antibody,“ *Nature*, pp. 643-646, December 1984.
- [107] S. L. Morrison, M. J. Johnson, L. A. Herzenberg und V. T. Oi, „Chimeric human antibody molecules: mouse antigen-binding domains with human constant region domains.,“ *Proc Natl Acad Sci U S A*, pp. 6851-6855, November 1984.
- [108] D. M. Knight, C. Wagner, R. Jordan, M. F. McAleer, R. DeRita, D. N. Fass, B. S. Coller, H. F. Weisman und J. Ghrayeb, „The immunogenicity of the 7E3 murine monoclonal Fab antibody fragment variable region is dramatically reduced in humans by substitution of human for murine constant regions.,“ *Mol Immunol.*, pp. 1271-1281, November 1995.
- [109] J. R. Adair, „Engineering antibodies for therapy,“ *Immunol. Rev.*, pp. 5-40, December 1992.
- [110] L. Riechmann, M. Clark, H. Waldmann und G. Winter, „Reshaping human antibodies for therapy,“ *Nature*, pp. 323-327, March 1988.
- [111] P. T. Jones, P. H. Dear, J. Foote, M. S. Neuberger und G. Winter, „Replacing the complementarity-determining regions in a human antibody with those from a mouse,“ *Nature*, pp. 522-525, May 1986.
- [112] J. Maynard und G. Georgiou, „Antibody engineering,“ *Annu. Rev. Biomed. Eng. 2000. 02:339–76*, pp. 339-376, 2000.
- [113] M. Brüggemann und M. J. Taussig, „Production of human antibody repertoires in transgenic mice,“ *Curr Opin Biotechnol.*, pp. 455-458, August 1997.
- [114] D. J. Schofield, A. R. Pope, V. Clementel, J. Buckell, S. D. Chapple, K. F. Clarke, J. S. Conquer, A. M. Crofts, S. R. Crowther, M. R. Dyson, G. Flack, G. J. Griffin, Y. Hooks, W. J. Howat, A. Kolb-Kokocinski, S. Kunze, C. D. Martin, G. L. Maslen, J. N. Mitchell, M. O'Sullivan, R. L. Perera und W. Roake, „Application of phage display to high throughput antibody generation and characterization,“ *Genome Biology*, August 2007.
- [115] H. X. Liao, M. C. Levesque, A. Nagel, A. Dixon, R. Zhang, E. Walter, R. Parks, J. Whitesides, D. J. Marshall, K. K. Hwang, Y. Yang, X. Chen, F. Gao, S. Munshaw, T. B. Kepler, T. Denny, M. A. Moody und B. F. Haynes, „High-throughput isolation of immunoglobulin genes from single human B cells and expression as monoclonal antibodies.,“ *J. Virol. Methods*, pp. 171-179, June 2009.
- [116] U. Lorenz, K. Ohlsen, H. Karch, M. Hecker, A. Thiede und J. Hacker, „Human antibody response durin sepsis against targets expressed by methicillin resistant *Staphylococcus aureus*,“ *FEMS*, Nr. 29, pp. 145-153, 2000.

- [117] O. Schneewind, P. Model und V. A. Fischetti, „Sorting of protein A to the staphylococcal cell wall,“ *Cell*, pp. 267-281, July 1992.
- [118] N. Sakata, S. Terakubo und T. Mukai, „Subcellular location of the soluble lytic transglycosylase homologue in *Staphylococcus aureus*,“ *Current Microbiology*, pp. 47-51, 2004.
- [119] A. R. MUSHEGIAN*†, K. J. FULLNER*, E. V. KOONIN† und E. W. NESTER*†, „A family of lysozyme-like virulence factors in bacterial pathogens of plants and animals,“ *Proc. Natl. Acad. Sci. USA*, pp. 7321-7326, March 1996.
- [120] A.-M. W. H. Thunnissen*, A. J. Dijkstra†, K. H. Kalk*, H. J. Rozeboom*, H. Engel*†, W. Keck† und B. B. W. Dijkstra*†, „Doughnut-shaped structure of a bacterial muramidase revealed by X-ray crystallography,“ *LETTERS TO NATURE*, pp. 750-753, February 1994.
- [121] M. R. Stapleton, M. J. Horsburgh, E. J. Hayhurst, L. Wright, I.-M. Jonsson, A. Tarkowski, J. F. Kokai-Kun, J. J. Mond und S. J. Foster, „Characterization of IsaA and SceD, Two Putative Lytic Transglycosylases of *Staphylococcus aureus*,“ *JOURNAL OF BACTERIOLOGY*, pp. 7316-7325, 2007.
- [122] D. E. Payne, N. R. Martin, K. R. Parzych, A. H. Rickard, A. Underwood und B. R. Boles, „Tannic Acid Inhibits *Staphylococcus aureus* Surface Colonization in an IsaA-Dependent Manner,“ *Infection and Immunity*, pp. 496-504, December 2012.
- [123] N. Sakata und T. Mukai, „Production profile of the soluble lytic transglycosylase homologue in *Staphylococcus aureus* during bacterial proliferation,“ *FEMS Immunology & Medical Microbiology*, pp. 288-295, January 2007.
- [124] S. Fuchs, J. Pane-Farre, C. Kohler, M. Hecker und S. Engelmann, *JOURNAL OF BACTERIOLOGY*, pp. 4275-4289, June 2007.
- [125] S. Dubrac und T. Msadek, „Identification of Genes Controlled by the Essential YycG/YycF Two-Component System of *Staphylococcus aureus*,“ *JOURNAL OF BACTERIOLOGY*, pp. 1175-1181, February 2004.
- [126] P. M. DUNMAN, E. MURPHY, S. HANEY, D. PALACIOS, G. TUCKER-KELLOGG†, S. WU, E. L. BROWN, R. J. ZAGURSKY, D. SHLAES und S. J. PROJAN, „Transcription Profiling-Based Identification of *Staphylococcus aureus* Genes Regulated by the *agr* and/or *sarA* Loci,“ *JOURNAL OF BACTERIOLOGY*, pp. 7341-7353, December 2001.
- [127] N. T. Blackburn und A. J. Clarke, „Assay for lytic transglycosylases: a family of peptidoglycan lyases,“ *Analytical Biochemistry*, pp. 388-393, April 2000.
- [128] E. Scheurwater, C. W. Reid und A. J. Clarke*, „Lytic transglycosylases: Bacterial space-making autolysins,“ *The International Journal of Biochemistry & Cell Biology*, pp. 586-591, March 2007.
- [129] N. T. Blackburn, „Identification of Four Families of Peptidoglycan Lytic Transglycosylases,“ *Journal of Molecular Evolution*, pp. 78-84, January 2001.
- [130] J.-V. Höltje, D. Mirelman, N. Sharon und U. Schwarz, „Novel Type of Murein Transglycosylase in *Escherichia coli*,“ *JOURNAL OF BACTERIOLOGY*, pp. 1067-1076, December 1975.

- [131] C. Heidrich, A. Ursinus, J. Berger, H. Schwarz und J.-V. Höltje, „Effects of Multiple Deletions of Murein Hydrolases on Viability, Septum Cleavage, and Sensitivity to Large Toxic Molecules in *Escherichia coli*,“ *Journal of Bacteriology*, pp. 6093-6099, November 2002.
- [132] J.-V. Höltje, „Growth of the Stress-Bearing and Shape-Maintaining Murein Sacculus of *Escherichia coli*,“ *Microbiology and Molecular Biology reviews*, pp. 181-203, March 1998.
- [133] G. Koraimann, „Lytic transglycosylases in macromolecular transport systems of Gram-negative bacteria,“ *Cellular and Molecular Life Sciences CMLS*, pp. 2371-2388, November 2003.
- [134] K. A. Cloud-Hansen, Peterson, S. Brook, E. V. Stabb, W. E. Goldman, M. J. McFall-Ngai und J. Handelsman, „Breaching the great wall: peptidoglycan and microbial interactions,“ *Nature Reviews Microbiology*, pp. 710-716, September 2006.
- [135] A. W. Bernheimer und L. L. Schwartz, „Isolation and Composition of staphylococcal alpha toxin,“ *J. gen. Microbiol*, pp. 455-468, June 1963.
- [136] S. Bhakdi und J. Trantum-Jensen, „Alpha-toxin of *Staphylococcus aureus*,“ *Microbiology and Molecular Biology Reviews*, pp. 733-751, December 1991.
- [137] D. Parker und A. Prince, „Immunopathogenesis of *Staphylococcus aureus* pulmonary infection,“ *Seminars in Immunopathology*, pp. 281-297, March 2012.
- [138] L. Song, M. R. Hobaugh, C. Shustak, S. Cheley, H. Bayley und J. E. Gouaux, „Structure of staphylococcal alpha-hemolysin, a heptameric transmembrane pore,“ *Science*, pp. 1859-1866, December 1996.
- [139] I. Inoshima, N. Inoshima, G. A. Wilke, M. E. Powers, K. M. Frank, Y. Wang und J. Bubeck Wardenburg, „A *Staphylococcus aureus* pore-forming toxin subverts the activity of ADAM10 to cause lethal infection in mice,“ *Nature medicine*, pp. 1310-1314, October 2011.
- [140] A. D. Kennedy, J. Bubeck Wardenburg, D. J. Gardner, D. Long, A. R. Whitney, K. R. Braughton, O. Schneewind und F. R. DeLeo, „Targeting of Alpha-Hemolysin by Active or Passive Immunization Decreases Severity of USA300 Skin Infection in a Mouse Model,“ *Journal of Infectious diseases*, pp. 1050-1058, October 2010.
- [141] B. E. Ragle und J. Bubeck Wardenburg, „Anti-Alpha-Hemolysin Monoclonal Antibodies Mediate Protection against *Staphylococcus aureus* Pneumonia,“ *Infection and immunity*, pp. 2712-2718, July 2009.
- [142] C. Tkaczyka, L. Hua, R. Varkey, Y. Shi, L. Dettinger, R. Woods, A. Barnes, R. MacGill, S. Wilson, P. Chowdhury, C. Stover und B. Sellman, „Identification of anti-alpha Toxin monoclonal antibodies that reduce the severity of *Staphylococcus aureus* dermonecrosis and exhibit a correlation between affinity and potency,“ *Clinical and Vaccine Immunology*, pp. 377-385, March 2012.
- [143] D. Foletti, P. Strop, L. Shaughnessy, A. Hasa-Moreno, M. G. Casas, M. Russell, C. Bee, S. Wu, A. Pham, Z. Zeng, J. Pons, A. Rajpal und D. Shelton, „Mechanism of action and in vivo efficacy of a human-derived antibody against *Staphylococcus aureus* α -hemolysin,“ *Journal of Molecular Biology*, pp. 1641-1654, 2013.

- [144] S. Wang, „Advances in the production of human monoclonal antibodies,“ *Antibody Technology Journal*, Bd. 1, Nr. 4, 2011.
- [145] K. U. Jansen, D. Q. Girgenti, I. L. Scully und A. S. Anderson, „Vaccine review: "Staphylococcus aureus vaccines: problems and prospects".,“ *Vaccine*, pp. 2723-2730, June 2013.
- [146] G. S. Gray und M. Kehoe, „Primary Sequence of the a-Toxin Gene from Staphylococcus aureus,“ *Infection and Immunity*, pp. 615-618, November 1984.
- [147] B. J. Berube und J. Bubeck Wardenburg, „Staphylococcus aureus α -Toxin: Nearly a Century of Intrigue,“ *Toxins*, pp. 1140-1166, June 2013.
- [148] A. W. Karchmer und A. S. Bayer, „Methicillin-Resistant Staphylococcus aureus: An Evolving Clinical Challenge,“ *Clin Infect Dis.*, 2008.
- [149] U. Lorenz, B. Lorenz, T. Schmitter, K. Streker, C. Erck, J. Wehland, J. Nickel, B. Zimmermann und K. Ohlsen, „Functional Antibodies Targeting IsaA of Staphylococcus aureus Augment Host Immune Response and Open New Perspectives for Antibacterial Therapy,“ *Antimicrobial Agents and Chemotherapy*, pp. 165-173, January 2011.
- [150] L. Hua, J. J. Hilliard, Y. Shi, C. Tkaczyk, L. I. Cheng, X. Yu, V. Datta, S. Ren, H. Feng, R. Zinsou, A. Keller, T. O'Day, Q. Du, L. Cheng, M. Damschroder, G. Robbie, J. Suzich, C. K. Stover und B. R. Sellman, „Assessment of an anti-alpha-toxin monoclonal antibody for prevention and treatment of Staphylococcus aureus-induced pneumonia.,“ *Antimicrob Agents Chemother.*, 2014.
- [151] R. S. Daum, „Skin and soft-tissue infections caused by methicillin-resistant Staphylococcus aureus,“ *The New England Journal of Medicine*, 2007.
- [152] R. J. Gordon und F. D. Lowy, „Pathogenesis of methicillin-resistant Staphylococcus aureus infection,“ *Clin. Infect. Dis.*, 2008.
- [153] M. L. S. V. Hetherington, „Correlation between Antibody Affinity and Serum Bactericidal Activity in Infants,“ *Journal of Infectious Diseases*, pp. 753-756, 1992.
- [154] T. T. Hansel, H. Kropshofer, T. Singer, J. A. Mitchell und A. J. T. George, „The safety and side effects of monoclonal antibodies,“ *Nature reviews drug discovery*, pp. 325-335, April 2010.
- [155] F. R. Brennan, L. D. Morton, S. Spindeldreher, A. Kiessling, R. Allenspach und A. Hey, „Safety and immunotoxicity assessemnet of immunomodulatory monoclonal antibodies,“ *MAbs*, pp. 233-255, 2010.
- [156] P. J. Carter, „Potent antibody therapeutics by design,“ *Nature reviews Immunology*, pp. 343-357, May 2006.
- [157] J. M. Reichert, C. J. Rosensweig, L. B. Faden und M. C. Dewitz, „Monoclonal antibody successes in the clinic,“ *Nat Biotechnol.*, pp. 1073-1078, September 2005.
- [158] M. S. Neuberger, G. T. Williams, E. B. Mitchell, S. S. Jouhal, J. G. Flanagan und T. H. Rabbitts, „A hapten-specific chimaeric IgE antibody with human physiological effector function,“ *Nature*, pp. 268-270, March 1985.
- [159] L. Riechmann, M. Clark, H. Waldmann und G. Winter, „Reshaping human antibodies for therapy,“ *Nature*, pp. 323-327, March 1988.

- [160] J. G. Salfeld, „Isotype selection in antibody engineering,“ *Nature reviews Biotechnology*, pp. 1369-1372, December 2007.
- [161] M. Brüggemann, G. T. Williams, C. I. Bindon, M. R. Clark, M. R. Walker, R. Jefferis, H. Waldmann und M. S. Neuberger, „Comparison of the effector functions of human immunoglobulins using a matched set of chimeric antibodies,“ *J Exp Med*, pp. 1351-1361, November 1987.
- [162] S. Herter, M. C. Birk, C. Klein, C. Gerdes, P. Umana und M. Bacac, „Glycoengineering of therapeutic antibodies enhances monocytes/macrophage-mediated phagocytosis and cytotoxicity,“ *Journal of immunology*, pp. 2252-, December 2013.
- [163] K. Mori, S. Iida, N. Yamane-Ohnuki, Y. Kanda, R. Kuni-Kamochi, R. Nakano, H. Imai-Nishiya, A. Okazaki, T. Shinkawa, A. Natsume, R. Niwa, K. Shitara und M. Satoh, „Non-fucosylated therapeutic antibodies: the next generation of therapeutic antibodies,“ *Cytotechnology*, pp. 109-114, December 2007.
- [164] J. N. Arnold, M. R. Wormald, R. B. Sim, P. M. Rudd und R. A. Dwek, „The Impact of Glycosylation on the Biological Function and Structure of Human Immunoglobulins,“ *Annual Review of Immunology*, pp. 21-50, April 2007.
- [165] F. Nimmerjahn und J. F. Ravetch, „Divergent Immunoglobulin G Subclass Activity Through Selective Fc Receptor Binding,“ *Science*, pp. 1510-1512, December 2005.
- [166] F. Mimoto, H. Katada, S. Kadono, T. Igawa, T. Kuramochi, M. Muraoka, Y. Wada, K. Haraya, T. Miyazaki und K. Hattori, „Engineered antibody Fc variant with selectively enhanced FcγRIIb binding over both FcγRIIaR131 and FcγRIIaH131,“ *Protein Eng Des Sel.*, pp. 589-598, October 2013.
- [167] L. G. Presta, „Engineering antibodies for therapy,“ *Current pharmaceutical biotechnology*, pp. 237-256, September 2002.
- [168] M. M. van der Kooi-Pol, „High anti-staphylococcal antibody titers in patients with epidermolysis bullosa relate to long-term colonization with alternating types of *Staphylococcus aureus*,“ *Journal of investigative dermatology*, pp. 847-850, September 2012.
- [169] R. Kock, K. Becker, B. Cookson, J. E. van Gemert-Pijnen, S. Harbarth, J. Kluytmans, M. Mielke, G. Peters, R. L. Skov und M. J. Struelens, „Methicillin-resistant *Staphylococcus aureus* (MRSA): burden of disease and control challenges in Europe.,“ *European communicable disease bulletin*, 2010.
- [170] R. B. Bebbington, „Expression of antibody genes in nonlymphoid mammalian cells,“ *Methods: Companion methods Enzymol.*, pp. 136-145, 1991.
- [171] D. Müller, A. Karle, B. Meissburger, I. Höfig und R. Stork, „Improved pharmacokinetics of recombinant bispecific antibody molecules by fusion to human serum albumin,“ *J Bio Chem*, pp. 12650-12660, April 2007.
- [172] A. Skerra, „The Functional Expression of Antibody Fv Fragments in *E. coli*: improved vectors and a generally applicable purification technique,“ *Nature Biotechnology*, pp. 273-278, 1991.
- [173] C. Hetz, „The unfolded protein response: controlling cell fate decisions under ER stress and beyond,“ *Nat Rev Mol Cell Biol*, pp. 897-903, January 2012.

- [174] N. S. Kim, „Overexpression of bcl-2 inhibits sodium butyrate-induced apoptosis in Chinese hamster ovary cells resulting in enhanced humanized antibody production,“ *Biotechn. Bioeng.*, pp. 184-193, 2008.
- [175] N. Kochanowski, M. L. Siriez und G. Roosens, „Medium and feed optimization for fed-batch production of a monoclonal antibody in CHO cells,“ *BMC Proc.*, November 2011.
- [176] J. Vives, S. Juanola, J. Cairó und F. Gòdia, „Metabolic engineering of apoptosis in cultured animal cells: implications for the biotechnology industry,“ *Metab. Eng.*, pp. 124-132, April 2003.
- [177] P. Burrows und M. LeJeune, „Evidence that murine pre-B cells synthesise murine heavy chains but no light chains,“ *Nature*, pp. 838-840, August 1979.
- [178] S. L. Morrison, „Heavy chain-producing variants of a mouse myeloma cell line,“ *J Immunol.*, pp. 655-659, 1975.
- [179] S. Schlatter, S. H. Stansfield, D. M. Dinnis, A. J. Racher und J. R. Birch, „On the optimal ratio of heavy to light chain genes for efficient recombinant antibody production by CHO cells,“ *Biotechnol. Prog.*, pp. 122-133, 2005.
- [180] H. Le Hir und M. M. Nott, „How introns influence and enhance eukaryotic gene expression,“ *Trends Biochem Sci.*, pp. 215-220, April 2003.
- [181] R. L. Fahrner, B. G. Knudsen, H. L. Basey, C. D. Galan, W. Feuerhelm und M. Vanderlaan, „Industrial purification of pharmaceutical antibodies: development, operation and validation of chromatography processes,“ *Biotechnol Genet Eng Rev*, pp. 301-327, 2001.
- [182] A. Chakrabarti, V. Aaron und W. Chen, „A review of the mammalian unfolded protein response,“ *Biotechnol. Bioeng.*, pp. 5234-5241, 2011.
- [183] M. Butler, „Recent advances in technology supporting biopharmaceutical production from mammalian cells,“ *Appl Microbiol Biotechnol*, pp. 885-894, November 2012.
- [184] H. Etz, D. B. Minh, T. Henics, A. Dryla, B. Winkler, C. Triska, A. P. Boyd, J. Söllner, W. Schmidt, U. v. Ahsen, M. Buschle, S. R. Gill, J. Kolonay, H. Khalak und C. M. Fraser, „Identification of in vivo expressed vaccine candidate antigens from *Staphylococcus aureus*,“ *PNAS*, pp. 6573-6578, May 2002.
- [185] P. M. den Reijer, N. Lemmens-den Toom, S. Kant, S. V. Snijders, H. Boelens, M. Tavakol, N. J. Verkaik, A. v. Belkum, H. A. Verbrugh und W. J. B. v. Wamel, „Characterization of the humoral immune response during *Staphylococcus aureus* bacteremia and global gene expression by *Staphylococcus aureus* in human blood,“ *Plos One*, January 2013.
- [186] P. Bruhns, B. Iannascoli, P. England, D. A. Mancardi, N. Fernandez, S. Jorieux und M. Daëron, „Specificity and affinity of human Fcγ receptors and their polymorphic variants for human IgG subclasses,“ *Blood*, pp. 3716-3725, April 2009.
- [187] J. K. Frazer und J. D. Capra, *Immunoglobulins: Structure and Function*, Philadelphia: Fundamental Immunology, 1999.
- [188] J. S. R.C. Aalberse, „IgG4 breaking the rules,“ *Immunology*, pp. 9-19, January 2002.

- [189] H. P. Hartung, L. Mouthon, R. Ahmed, S. Jordon, K. B. Laupland und S. Jolles, „Clinical applications of intravenous immunoglobulins (IVIg)-beyond immunodeficiencies and neurology,“ *Clin Exp Immunol. Dec*, pp. 23-33, December 2009.
- [190] F. Nimmerjahn und J. V. Ravetch, „The antiinflammatory activity of IgG: the intravenous IgG paradox,“ *JEM*, 2007.
- [191] C. A. Ogden und K. B. Elkon, „Role of complement and other innate immune mechanisms in the removal of apoptotic cells.,“ *Curr Dir Autoimmun*, pp. 120-142, 2006.
- [192] P. F. Zipfel und C. Skerka, „Complement regulators and inhibitory proteins,“ *Nature review Immunology*, pp. 729-740, October 2009.
- [193] M. C. Carroll, „The complement system in regulation of adaptive immunity,“ *Nat Immunol.*, pp. 981-986, October 2004.
- [194] R. P. Adhikari, A. O. Ajao, M. J. Aman, H. Karauzum, J. Sarwar, A. D. Lydecker, J. K. Johnson, C. Nguyen, W. H. Chen und M. C. Roghmann, „Lower antibody levels to Staphylococcus aureus exotoxins are associated with sepsis in hospitalized adults with invasive S. aureus infections.,“ *J. infect. Dis.*, pp. 915-923, September 2012.
- [195] M. M. van der Kooi-Pol, C. P. de Vogel, G. N. Westerhout-Pluister, Y. K. Veenstra-Kyuchukova, J. C. Duipmans, C. Glasner, G. Buist, G. S. Elsinga, H. Westra und H. P. Bonarius, „High anti-staphylococcal antibody titers in patients with epidermolysis bullosa relate to long-term colonization with alternating types of Staphylococcus aureus,“ *Journal of investigative dermatology*, pp. 847-850, September 2012.
- [196] A. K. Daoud, M. A. Tayyar, I. M. Fouda und N. A. Harfeil, „Effects of diabetes mellitus vs. in vitro hyperglycemia on select immune cell functions,“ *J Immunotoxicol.*, pp. 36-41, March 2009.
- [197] J. M. Mylotte und A. Tayara, „Staphylococcus aureus Bacteremia: Predictors of 30-Day Mortality in a Large cohort,“ *Journal of clinical investigation*, pp. 1170-1174, April 2000.
- [198] T. C. Alba-Loureiro, C. D. Munhoz, J. O. Martins, G. A. Cerchiaro, C. Scavone, R. Curi und P. Sannomiya, „Neutrophil function and metabolism in individuals with diabetes mellitus,“ *Brazilian Journal of Medical and Biological Research*, pp. 1037-1044, Mai 2007.
- [199] A. Mowat und J. Baum, „Chemotaxis of polymorphonuclear leukocytes from patients with diabetes mellitus,“ *N Eng J Med*, pp. 621-627, 1971.
- [200] S. Yende, T. van der Poll, M. J. Lee, D. T. Huang, A. B. Newman, L. Kong, J. A. Kellum, T. B. Harris, D. Bauer, S. Satterfield und D. C. Angus, „The influence of pre-existing diabetes mellitus on the host immune response and outcome of pneumonia: analysis of two multicentre cohort studies,“ *Thorax*, pp. 870-877, June 2010.
- [201] J. S. Tan, J. L. Anderson, C. Watanakunakorn und J. P. Phair, „Neutrophil dysfunction in diabetes mellitus,“ *J Lab Clin Med*, pp. 26-33, 1975.
- [202] J. D. Bagdade, K. L. Nielson und R. J. Bulger, „Reversible abnormalities in phagocytic function in poorly controlled diabetic patients,“ *Am J Med Sci*, pp. 1031-1035, 1989.

- [203] J. Jakelic, S. Kokic, I. Hozo, J. Maras und D. Fabijanic, „Nonspecific immunity in diabetes: hyperglycemia decreases phagocytic activity of leukocytes in diabetic patients.“ *Med Arh*, pp. 9-12, 1995.
- [204] R. N. Foley, „Infectious complications in chronic dialysis patients,“ *Peritoneal Dialysis International*, pp. 167-171, November 2008.
- [205] R. N. Foley, C. Wang und A. J. Collins, „Cardiovascular risk factor profiles and kidney function stage in the U.S. general population: the NHANES III study.“ *Mayo Clin Proc*, pp. 1270-1277, 2005.
- [206] United States Renal Data System (USRDS), „Atlas of end-stage renal disease in the United States,“ 2006.
- [207] R. S. Hotchkiss und I. E. Karl, „The pathophysiology and treatment of sepsis,“ *N Engl J Med*, pp. 138-150, 2003.
- [208] T. Andrews und K. E. Sullivan, „Infections in patients with inherited defects in phagocytic function,“ *Clinical microbiology reviews*, pp. 597-621, October 2003.
- [209] G. Brevetti, G. Giugliano, L. Brevetti und W. R. Hiatt, „Inflammation in PAD,“ *Circulation*, pp. 1862-1875, 2010.
- [210] F. G. Fowkes, E. Housley, R. A. Riemersma, C. C. Macintyre, E. H. Cawood, R. J. Prescott und C. V. Ruckley, „Smoking, lipids, glucose intolerance and blood pressure as risk factors for peripheral atherosclerosis compared with ischemic heart disease in the Edinburgh Artery Study,“ *Am J Epidemiol*, pp. 44-49, 1992.
- [211] D. G. Bloemenkamp, W. P. Mali, B. C. Tanis, F. R. Rosendaal, M. A. van den Bosch, J. M. Kemmeren, A. Algra, J. M. Ossewaarde, F. L. Visseren, A. M. van Loon und Y. van der Graaf, „Chlamydia pneumoniae, Helicobacter pylori and cytomegalovirus infections and the risk of peripheral arterial disease in young women,“ *Atherosclerosis*, pp. 149-156, 2002.
- [212] A. D. Pradhan, S. Shrivastava, N. R. Cook, N. Rifai, M. A. Creager und P. M. Ridker, „Symptomatic peripheral arterial disease in women: nontraditional biomarkers of elevated risk,“ *Circulation*, pp. 823-831, Februar 2008.
- [213] N. D. Burg und M. H. Pillinger, „The neutrophil: function and regulation in innate and humoral immunity,“ *Clin Immunol.*, pp. 7-17, April 2001.
- [214] T. Assari, „Chronic Granulomatous Disease; fundamental stages in our understanding of CGD,“ *Med Immunology*, September 2006.
- [215] National Nosocomial Infections Surveillance System (NNIS), „National Nosocomial Infections Surveillance System Report, Data Summary from January 1990 - May 1999,“ *American Journal of Infection Control*, pp. 520-532, June 1999.
- [216] D. B. Graham, C. M. Robertson, J. Bautista, F. Mascarenhas, M. J. Diacovo, V. Montgrain, S. K. Lam, V. Cremasco, W. M. Dunne, R. Faccio, C. Coopersmith und W. Swat, „Neutrophil-mediated oxidative burst and host defense are controlled by a Vav-PLCgamma2 signaling axis in mice,“ *J. of Clinical Investigation*, pp. 3445-3452, November 2007.

- [217] M. Delamaire, D. Maugendre, M. Moreno, M. C. Le Goff, H. Allannic und B. Genetet, „Impaired leucocyte functions in diabetic patients,“ *Diabet. Med.*, pp. 29-34, January 1997.
- [218] W. Marhoffer, M. Stein, E. Maeser und K. Federlin, „Impairment of polymorphnuclear leukocyte function and metabolic control of diabetes,“ *Diabetes Care*, pp. 256-260, February 1992.
- [219] M. J. Sarnak und B. L. Jaber, „Mortality caused by sepsis in patients with end-stage renal disease compared with the general population,“ *Kidney International*, pp. 1758-1764, April 2000.
- [220] C. Sardenberg, P. Suassuna, M. C. Andreoli, R. Watanabe, M. A. Dalboni, S. R. Manfredi, O. P. dos Santos, E. G. Kallas, S. A. Draibe und M. Cendoroglo, „Effects of uraemia and dialysis modality on polymorphonuclear cell apoptosis and function,“ *Nephrol Dial Transplant*, pp. 160-165, January 2006.
- [221] R. A. Ward, B. Schmidt, M. Blumenstein und H. Gurland, „Evaluation of phagocytic cell function in an ex vivo model of hemodialysis,“ *Kidney Int*, pp. 776-782, 1990.
- [222] M. S. Cohen, D. M. Elliott, T. Chapöinski, M. M. Pike und J. E. Niedel, „A defect in the oxidative metabolism of human polymorphonuclear leukocytes that remain in circulation early in hemodialysis,“ *Blood*, pp. 1283-1289, December 1982.
- [223] R. Vanholder, S. Ringoir, A. Dhondt und R. Hakim, „Phagocytosis in uremic and hemodialysis patients: a prospective and cross sectional study,“ *Kidney Int.*, pp. 320-327, February 1991.
- [224] D. L. Gordon, J. L. Rice und V. M. Avery, „Surface phagocytosis and host defence in the peritoneal cavity during continuous ambulatory peritoneal dialysis,“ *Eur J Clin Microbiol Infect Dis.*, pp. 191-197, arch 1990.
- [225] B. Schleiffenbaum und J. Fehr, „The tumor necrosis factor receptor and human neutrophil function. Deactivation and cross-deactivation of tumor necrosis factor-induced neutrophil responses by receptor down-regulation,“ *J Clin Invest.*, pp. 184-195, July 1990.
- [226] S. D. Kobayashi, J. M. Voyich, C. Burlak und F. R. DeLeo, „Neutrophils in the innate immune response,“ *Arch Immunol Ther Exp*, pp. 505-517, 2005.
- [227] T. Lu, A. Porter, A. Kennedy, S. Kobayashi und F. DeLeo, „Phagocytosis and Killing of Staphylococcus aureus by human neutrophils,“ *Journal of Innate Immunity*, April 2014.
- [228] R. S. Flannagan, V. Jaumouille und S. Grinstein, „The cell biology of phagocytosis,“ *Annu Rev Pathol.*, pp. 61-98, September 2012.
- [229] K. P. M. van Kessel, J. Bestebroer und J. A. G. van Strijp, „Neutrophil-mediated phagocytosis of Staphylococcus aureus,“ *Front Immunol.*, September 2014.
- [230] P. Pacheco, D. White und T. Sulchek, „Effects of microparticle size and Fc density on macrophage phagocytosis,“ *Plos one*, April 2013.
- [231] C. D. Ellson, K. Davidson, G. J. Ferguson, R. O'Connor, L. R. Stephens und P. T. Hawkins, „Neutrophils from p40phox^{-/-} mice exhibit severe defects in NADPH oxidase regulation and oxidant-dependent bacterial killing,“ *J Exp Med.*, 1927-1937 August 2006.

- [232] R. Malka, B. Wolach, R. Gavrieli, E. Shochat und V. Rom-Kedar, „Evidence for bistable bacteria-neutrophil interaction and its clinical implications,“ *J clin. Invest.*, pp. 3002-3011, August 2012.
- [233] L. C. McPhail, C. C. Clayton und R. Snyderman, „The NADPH oxidase of human polymorphonuclear leukocytes. Evidence for regulation by multiple signals.,“ *J Biol Chem*, pp. 5768-5775, 1984.
- [234] A. Bjarnasonabc, H. Asgeirssonc, O. Baldurssonc, K. G. Kristinssonad und M. Gottfredssonac, „Mortality in healthcare-associated pneumonia in a low resistance setting: a prospective observational study.,“ *Infection Diseases*, pp. 130-136, March 2013.
- [235] E. Rubenstein, M. H. Kollef und D. Nathwani, „Pneumonia Caused by Methicillin-Resistant Staphylococcus aureus,“ *CID*, pp. 378-385, 2008.
- [236] M. H. Kollef, A. Shorr, Y. P. Tabak, V. Gupta, L. Z. Liu und R. S. Johannes, „Epidemiology and outcomes of health-care-associated pneumonia: results from a large US database of culture-positive pneumonia.,“ *CHEST*, pp. 3854-3862, March 2006.
- [237] T. Randall, „Bronchus-associated lymphoid tissue (BALT) structure and function,“ *Adv. Immunol.*, pp. 187-241, 2010.
- [238] J. Chen, G. Feng, Q. Guo, J. Bubeck Wardenburg, S. Lin, I. Inoshima, R. Deaton, J. X. J. Yuan, J. G. N. Garcia, R. F. Machado, M. Otto und R. G. Wunderink, „Transcriptional Events during the Recovery from MRSA Lung Infection: A Mouse Pneumonia Model,“ *Plos one*, August 2013.
- [239] J. Bubeck Wardenburg, R. J. Patel und O. Schneewind, „Surface proteins and exotoxins are required for the pathogenesis of Staphylococcus aureus pneumonia,“ *Infection and Immunity*, pp. 1040-1044, Februar 2007.
- [240] G. Y. Liu, „Molecular Pathogenesis of Staphylococcus aureus Infection,“ *Pediatric research*, pp. 71-77, January 2009.
- [241] K. N. Prasad, W. C. Cole, B. Kumar und K. Che Prasad, „Scientific rationale for using high-dose multiple micronutrients as an adjunct to standard and experimental cancer therapies.,“ *J Am Coll Nutr.*, pp. 473-475, October 2001.
- [242] M. C. McElroy, H. R. Harty, G. E. Hosford, G. M. Boylan, J.-F. Pittet und T. J. Foster, „Alpha-Toxin Damages the Air-Blood Barrier of the Lung in a Rat Model of Staphylococcus aureus-Induced Pneumonia,“ *Infect Immun*, pp. 5541-5544, October 1999.
- [243] J. T.-J. S. Bhakdi, „Alpha-toxin of Staphylococcus aureus.,“ *Microbiol. Rev.*, pp. 733-751, December 1991.
- [244] I. Inoshima, N. Inoshima, G. A. Wilke, M. E. Powers, K. M. Frank, Y. Wang und J. Bubeck Wardenburg, „A Staphylococcus aureus pore-forming toxin subverts the activity of ADAM10 to cause lethal infection in mice.,“ *Nature Medicine*, pp. 1310-1314, September 2011.
- [245] A. J. Bramley, A. H. Patel, M. O'Reilly, R. Foster und T. J. Foster, „Roles of alpha-toxin and beta-toxin in virulence of Staphylococcus aureus for the mouse mammary gland.,“ *Infect Immun*, pp. 2489-2494, August 1989.

- [246] J. Bubeck Wardenburg und O. Schneewind, „Vaccine protection against *Staphylococcus aureus* pneumonia.“ *Journal of Experimental Medicine*, pp. 287-294, February 2008.
- [247] D. Viana, L. Selva, P. Segura, J. R. Penadés und J. M. Corpa, „Genotypic characterization of *Staphylococcus aureus* strains isolated from rabbit lesions.“ *Veterinary microbiology*, pp. 288-298, 2007.
- [248] B. Löffler, M. Hussain, M. Grundmeier, M. Brück, D. Holzinger, G. Varga, J. Roth, B. C. Kahl, R. A. Proctor und G. Peters, „*Staphylococcus aureus* panton-valentine leukocidin is a very potent cytotoxic factor for human neutrophils.“ *PLoS pathogens*, 2010.
- [249] J. Seok, H. S. Warren, A. G. Cuenca, M. N. Mindrinos, H. V. Baker, W. Xu, D. R. Richards, G. P. McDonald-Smith, H. Gao, L. Hennessy, C. C. Finnerty, C. M. López, S. Honari, E. E. Moore, J. P. Minei, J. Cuschieri, P. E. Bankey, J. L. Johnson, J. Sperr, A. B. Nathens, T. R. Billiar, M. A. West, M. G. Jeschke, M. B. Klein, R. L. Gamelli, N. S. Gibran, B. H. Brownstein, C. Miller-Graziano, S. E. Calvano, P. H. Mason, P. J. Cobb, L. G. Rahme, S. F. Lowry, R. V. Maier, L. L. Moldawer, D. N. Herndon, R. W. Davis, W. Xiao und R. G. Tompkins, „Genomic responses in mouse models poorly mimic human inflammatory diseases.“ *Proc Natl Acad Sci U S A*, pp. 3507-3512, February 2013.
- [250] D. C. Doeing, J. L. Borowicz und E. T. Crockett, „Gender dimorphism in differential peripheral blood leukocyte counts in mice using cardiac, tail, foot, and saphenous vein puncture methods.“ *BMC Clin Pathol.*, September 2003.
- [251] A. Risso, „Leukocyte antimicrobial peptides: multifunctional effector molecules of innate immunity.“ *J Leukoc. Biol.*, pp. 785-792, December 2000.
- [252] R. J. Ober, C. G. Radu, V. Ghetie und E. S. Ward, „Differences in promiscuity for antibody-FcRn interactions across species: implications for therapeutic antibodies.“ *International immunology*, pp. 1551-1559, 2001.
- [253] J. Mestas und C. C. W. Hughes, „Of mice and not men: Differences between mouse and human immunology.“ *Journal of immunology*, pp. 2731-2738, 2004.

10. List of figures

Fig. 1 Coloured and non-coloured electron microscope image of <i>S. aureus</i>	13
Fig. 2 Percentage of MRSA isolates worldwide.....	14
Fig. 3 Emergence of antibiotic-resistant <i>S. aureus</i>	16
Fig. 4 Development of an antibody based therapy: historical overview.....	17
Fig. 5 Schematic structure of an IgG antibody molecule.....	19
Fig. 6 Antibodies mediate a large panel of direct and indirect functions.	20
Fig. 7 The mechanism of Phagocytosis.....	21
Fig. 8 Antibody engineering for designing antibodies and their functional fragments.....	23
Fig. 9 Humanization of murine antibody by CDR grafting.....	24
Fig. 10 Hypothetical structure of IsaA.....	26
Fig. 11 Function of lytic transglycosylase (LT).....	27
Fig. 12 Pore formation by alpha-toxin (AT).....	28
Fig. 13 Cloning strategy for UK-66 scFv fragemnts.....	42
Fig. 14 Pipette scheme to perform a single cell dilution.....	44
Fig. 15 Sequence of antigen binding domain UK-66	56
Fig. 16 Purification of mouse and humanized scFv UK-66 fragments: (A) SDS-Page and (B) Western Blot analysis.....	57
Fig. 17 Purification of rIsaA using expression strain <i>E. coli</i> M15Rep4 (A) SDS-Page and (B) Western Blot analysis.....	58
Fig. 18 Comparative Western Blot studies of mouse and humanized scFv fragments.....	59
Fig. 19 Comparative binding studies of mouse and humanized scFv fragments: (A, C) binding ELISA, (B, D) competitive ELISA.	60
Fig. 20 Humanized UK-66 scFv-Fc fragment detects IsaA expressed on the bacterial cell surface using indirect immunofluorescence (A) and ELISA studies with viable bacteria (B).	61
Fig. 21 Mouse and humanized UK-66 scFv-Fc fragments bind specifically IsaA on the bacterial surface determined by FACS analysis.	62
Fig. 22 Comparative binding studies of mouse and humanized scFv fragments: (A) Binding ELISA, (B) Competitive ELISA.	64
Fig. 23 Affinity of mouse and humanized UK-66 IgG1 analysed by SPR.....	65
Fig. 24 Binding of hUK-66 IgG1 to IsaA expressed on different <i>S. aureus</i> strains.	66
Fig. 25 hUK-66 IgG1 binds specifically native expressed IsaA of different <i>S. aureus</i> strains.	67
Fig. 26 Expression of hUK-66 IgG1 by CHO-K1 (A) and scFv-Fc UK-66 by HEK293 (B).	68
Fig. 27 Production rate of hUK-66 IgG1, IgG2 and IgG4 expression of randomly selected stable CHO-K1 clones.....	69
Fig. 28 Productivity of clone hUK-66 IgG1 (28) after MSX refinement.....	69
Fig. 29 Productivity of hUK-66 IgG1 after three passages of single cell dilution of clone 28. 70	
Fig. 30 Adaption of CHO-K1 hUK-66 IgG1 producer to FCS free medium.	71
Fig. 31 Productivity of clone 28-200 μ M MSX in a bioreactor system.....	71

Fig. 32 Impact of hUK-66 IgG isotypes on antibody dependent killing of <i>S. aureus</i> Newman.	73
Fig. 33 Analysis of cell population in human whole blood samples by flow cytometry.	74
Fig. 34 Engulfment of <i>S. aureus</i> Newman by granulocytes from human whole blood samples.	74
Fig. 35 Engulfment of <i>S. aureus</i> Newman by granulocytes from clinical relevant patient groups and healthy donors.....	76
Fig. 36 Engulfment of <i>S. aureus</i> Newman by granulocytes from clinical relevant patient groups and healthy donors.....	77
Fig. 37 Development of respiratory burst after <i>S. aureus</i> Newman infection in granulocytes from clinical relevant patient groups compared to healthy donors.	79
Fig. 38 Development of respiratory burst after <i>S. aureus</i> Newman infection in granulocytes from clinical relevant patient groups and healthy donors.....	80
Fig. 39 hUK-66 IgG1 dependent killing of <i>S. aureus</i> Newman by granulocytes from healthy donors and patients at high risk.....	82
Fig. 40 hUK-66 IgG1 dependent killing of <i>S. aureus</i> Newman by purified human granulocytes from healthy donors.	84
Fig. 41 Combinatorial therapy approach of hUK-66 IgG1 and hUK-tox IgG1 in <i>in vitro</i> killing assays with human whole blood samples.....	86
Fig. 42 Antibody dependent killing of <i>S. aureus</i> Newman by granulocytes from mouse whole blood samples.....	87
Fig. 43 Characterization of binding of different hUK-66 isotypes by FcγR1a.	88
Fig. 44 Binding of hUK-66 IgG isotypes by recombinant and native FcγRs.	89
Fig. 45 Determination of <i>S. aureus</i> Newman survival proportion following intranasal application.....	91
Fig. 46 Prophylactic treatment of mouse pneumonia with mUK-66 IgG1.....	92
Fig. 47 Prophylactic treatment of mice with mUK-66 in <i>S. aureus</i> induced pneumonia.	93
Fig. 48 Therapeutic efficacy of mUK-66 in <i>S. aureus</i> induced pneumonia.....	94
Fig. 49 Prophylactic treatment of mice with hUK-66 IgG1 in <i>S. aureus</i> induced pneumonia.	95
Fig. 50 Prophylactic treatment of mice with hUK-tox IgG1 in <i>S. aureus</i> induced pneumonia.....	96
Fig. 51 Therapeutic treatment of mice with hUK-tox IgG1 in <i>S. aureus</i> induced pneumonia.....	97
Fig. 52 Prophylactic treatment of mice with combined hUK-66 and hUK-tox IgG1 in <i>S. aureus</i> induced pneumonia.....	98
Fig. 53 Therapeutic treatment of mice with combined hUK-66 and hUK-tox IgG1 in <i>S. aureus</i> - induced pneumonia.....	99
Fig. 54 Overview of neutrophil dependent killing of <i>S. aureus</i>	113
Fig. 55 Work hypothesis of hUK-66 IgG1 function.....	115

11. List of tables

Table 4.1 Equipment.....	30
Table 4.2 Consumables	31
Table 4.3 Chemicals	31
Table 4.4 Buffer and Solutions.....	32
Table 4.5 Enzymes, Kits and Reagents	33
Table 4.6 Media and Supplements.....	34
Table 4.7 Antibodies	34
Table 4.8 Plasmids	35
Table 4.9 Bacterial strains.....	35
Table 5.1 Preparation scheme for PCR.....	40
Table 5.2 PCR Program for amplification of UK-66 heavy and light chain	40
Table 5.3 PCR program for amplification of antigen binding domain scFv UK-66.....	40
Table 5.4 Cell lines description	45
Table 5.5 cell lines and stable transfected cell lines	46
Table 5.6 Preparation of SDS-PAGE (separation gels)	49
Table 5.7 Preparation of SDS-PAGE (sample gels)	49

12. List of abbreviations

abbreviation	explanation
ADCC	antibody dependent cellular cytotoxicity
Amp	ampicillin
AOD	arterial occlusive disease
AT	alpha-toxin
CA-MRSA	community associated MRSA
CDC	complement dependent cytotoxicity
CDR	complementarity determining regions
CFU	colony forming units
CH	constant domain of heavy chain
CHO	Chinese hamster ovary cells
DMSO	dimethylsulfoxid
E.coli	Escherichia coli
FCS	Fetal Calf Serum
Fc γ R	Fc gamma receptor
FITC	fluorescein isothiocyanate
FR	framework
GS	glutamine synthetase
HAMA	human anti-mouse antibodies
HA-MRSA	hospital associated MRSA
HEK293	human embryonal kidney
HRP	horseradish peroxidase
hUK-66	human anti-IsaA antibody
hUK-tox	human anti-alpha-toxin antibody
IgG	immunoglobulin G
IMAC	immobilized metal ion affinity chromatography
IPTG	isopropyl- β -D-thiogalactopyranosid
IsaA	immunodominant staphylococcal antigen A
IVIg	intravenous immunoglobulin
Kan	Kanamycin
K _D	dissociation constant
LB	lysogeny broth
LT	lytic transglycosylase
mAb	monoclonal antibody
MRSA	methicillin resistant Staphylococcus aureus
MSX	methione sulfoximine
mUK-66	mouse anti-IsaA antibody
NSO	murine myeloma cells

PBS	phosphate-buffered saline
PBS-T	phosphate-buffered saline with Tween
PCR	Polymerase chain reaction
PG	peptidoglykane
PMN	polymorphonuclear leukocytes
PRSA	Penicillin resistant Staphylococcus aureus
rlsaA	rekombinant IsaA
ROS	reactive oxygen species
RT	room temperature
S.aureus	Staphylococcus aureus
scFv	single chain Fv fragment
SLT	soluble lytic transglycosylase
spa	staphylococcal protein A
SPR	surface plasmon resonance
ST	Sequence type
TBS	tris-buffered saline
TBST	tris-buffered saline with Tween
TMB	3,3',5,5'-Tetramethylbenzidine
VH	variable region of heavy chain
VL	variable region of light chain
Zeo®	Zeocin

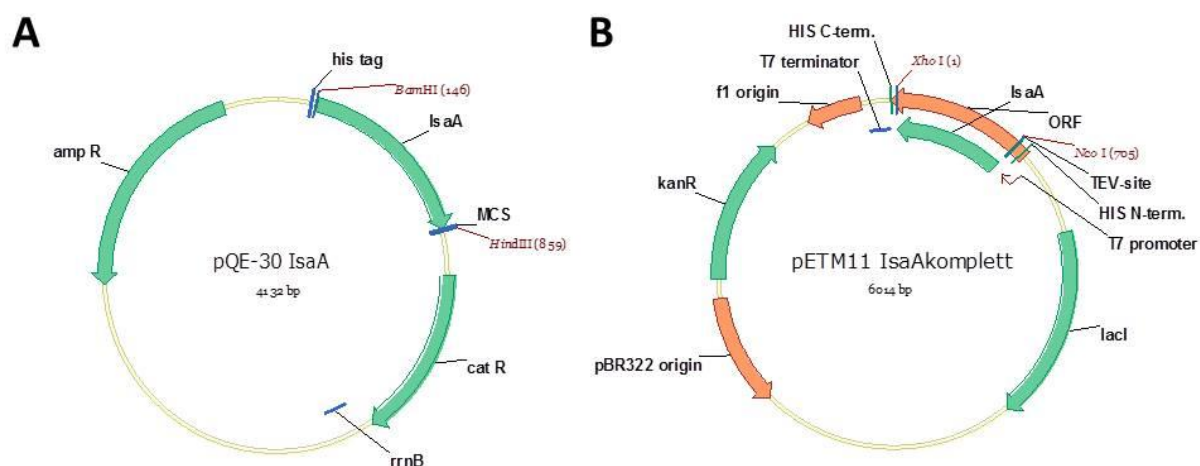
13. Appendix

13.1. IsaA

13.1.1. IsaA-Nucleotide sequence

Start-Atg aaa aag aca att atg gca tca tca tta gca gtg gca tta ggt gta aca ggt tac gca gca ggt aca gga cat caa gca cac gct gct gaa gta aac gtt gat caa gca cac tta gtt gac tta gcg cat aat cac caa gat caa tta aat gca gct cca atc aaa gat ggt gca tat gac atc cac ttt gta aaa gat ggt ttc caa tat aac ttt act tca aat ggt act aca tgg tca tgg agc tat gaa gca gct aat ggt caa act gct ggt ttc tca aac gtt gca ggt gca gac tac act act tca tac aac caa ggt tca gat gta caa tca gta agc tac aat gca caa tca agt aac tca aac gtt gaa gct gtt tca gct cca act tac cat aac tac agc act tca act act tca agt tca gtg aga tta agc aat ggt aat act gca ggt gct act ggt tca tca gca gct caa atc atg gct caa cgt act ggt gtt tca gct tct aca tgg gct gca atc atc gct cgt gaa tca aat ggt caa gta aat gct tac aac cca tca ggt gct tca ggt tta ttc caa act atg cca ggt tgg ggt ccg aca aac act gtt gac caa caa atc aac gca gct gtt aaa gca tac aaa gca caa ggt tta ggt gct tgg gga ttc **taa-Stop** (702bp)

13.1.2. IsaA-Vector maps



IsaA expression vector systems:

IsaA was expressed in two vector systems: pQE-30 and pETM11 to generate IsaA with a C- and N-terminal His-Tag for purification. Both systems are suitable for *E. coli* and IsaA from both systems are functional.

13.2. Antigen binding domains

13.2.1. Antigen binding domain scFv mUK-66

The amino acid sequence of the variable antigen binding of the heavy chain is coloured in yellow and the light chain is highlighted in blue. The heavy and light chain are connected by a peptide sequence (sequence is underlined).

AAQPAMADVKLVESGGGLVKLGGSLKLSACSASGFTFSNYYMSWVRQTPEKRLELVADINGN
GGSTYYPDTVKGRFTISRDNANTLYLQMSSLKSEDTALYYCVRRGGYYALDYWGQGTTVT
VSSGGGGSGGGGSGGGGDVVMTQTPLSLPVSLGDQASISCRSSQSLVHINGNTYLHWYLO
KPGQSPKLLIYRVSNRFSGVPDRFSGSGSGTDFTLKISRVEAEDLGVYFCSQSTHV
PWTFGGGTKLELKR

13.2.2. Antigen binding domain scFv hUK-66(1)

The amino acid sequence of the variable antigen binding of the heavy chain is coloured in yellow and the light chain is highlighted in blue. The heavy and light chain are connected by a peptide sequence (sequence is underlined).

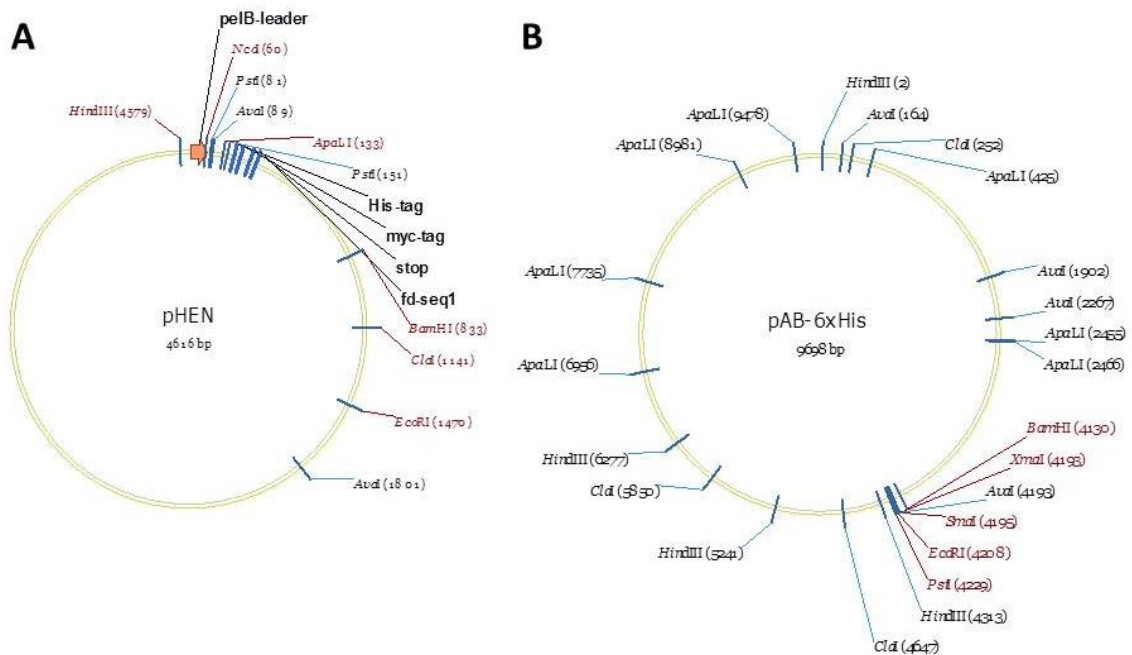
EVQLLES GGGLVQP GGSLRLSCAASGFTFSNYYMSWVRQAPGKGLEWVSDINGNGGSTY
YPDTVKGRFTISRDNANTLYLQMNSLRAEDTAVYYCVRRGGYYALDYWGQGTTVTVS
SGGGGSGGGGSGGGGEIVLTQSPGTLSPGERATLSCRSSQSLVHINGNTYLHWYQQKP
GQAPRLLIYRVSNRFSGIPDRFSGSGSGTDFTLTISRLEPEDFAVYYCSQSTHVPWT
FGGGTKLELKR

13.2.3. Antigen binding domain scFv hUK-66(2)

The amino acid sequence of the variable antigen binding of the heavy chain is coloured in yellow and the light chain is highlighted in blue. The heavy and light chain are connected by a peptide sequence (sequence is underlined).

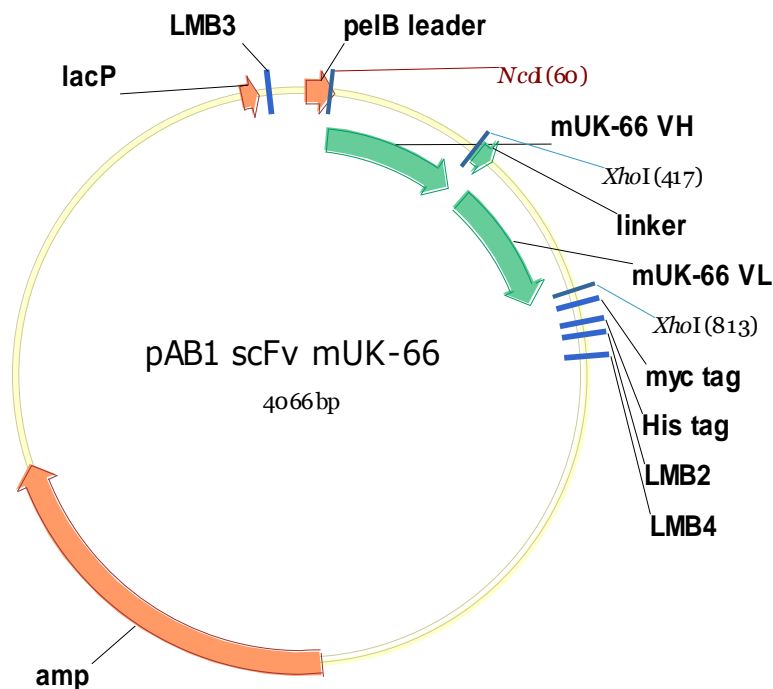
EVQLLES GGGLVQP GGSLRLSCAASGFTFSNYYMSWVRQAPGKGLEWVSDINGNGGSTY
YPDTVKGRFTISRDNANTLYLQMNSLRAEDTAVYYCVRRGGYYALDYWGQGTTVTVS
SGGGGSGGGGSGGGGDVVMTQTPLSLSVTPGQPASISCRSSGSLVHINGNTYLHWYLQKP
GQSPQLLIYRVSNRFSGVPDRFSGSGSGTDFTLKISRVEAEDVGVYYCSQSTHVPWTFGG
GTKLELKR

13.2.4. Vectors used for cloning antigenbinding domains scFv



Antigen binding domain expression vector systems:

The antigen binding domain of heavy and light chain was combined with a (SG4)₃ linker. Therefore the nucleotide sequence of heavy and light chain was cloned into the vector pHEN2. The complete scFv sequence, includes the sequence of the antigen binding domain of heavy and light chain as well as the linker, was then cloned into the expression vector pAB.



Antigen binding domain expression vector with scFv mUK-66:

The murine antigen binding domain UK-66 was cloned into the expression vector pAB as scFv fragment and two purification tags: His-Tag and Myc-Tag.

14. Curriculum vitae

Name: Babett Oesterreich
Date and Place of Birth: 14.07.1985, Greifswald
Address: Falkenplatz 1A
23456 Lübeck, Germany
Mobile phone: (+49) 176 72466680
E-mail: babett.oesterreich@gmx.de

14.1. Professional Experience and Education

June 2014 - present: **Development Specialist for Parasitology:**
EUROIMMUN AG Medical Laboratory Diagnostics,
Lübeck

**October 2010 -
June 2014:** **PhD-thesis (Go Bio-Project):**
Preclinical development of an antibody based therapy against
multi-resistant *Staphylococcus aureus*. Institute for Molecular
Infection Biology, PD Dr. Knut Ohlsen, University of Wuerzburg

**November 2009 -
October 2010:** **Diploma-thesis:**
Molecular biological analysis for the development of antibody
based therapy against *Staphylococcus aureus*. Institute for
Molecular Infection Biology, PD Dr. Knut Ohlsen, University of
Wuerzburg

**October 2005 -
October 2010:** **Studies of Biology (2007-2010):**
Major study: Julius-Maximillian University of Wuerzburg
Major subject: Microbiology
Minor subjects: Neurobiology, Genetics

Semester abroad at University of Leeds (Jan. - May 2009):
Laboratory Research Project: Microbiological and genic
analysis of borrelidin resistance and fitness in *S. aureus*
SH1000. Prof. Ian Chopra, Antimicrobial Research Centre,
University Leeds

Practical Training (Nov.-Dec. 2008):
Institute for Medical Microbiology, University of Dresden
Serotyping of *Legionella pneumophila*, Fluorescence analysis of
intracellular microorganisms

Intermediate Diploma (2005-2007):
Studies of Biology at the Ernst-Moritz-Arndt University of
Greifswald

Practical Training (September 2006):

Institute for Medical Microbiology, University of Greifswald
Cultivation and Identification of microorganisms

Practical Training (July-Oct. 2005):

Nursing: Neurosurgery, Ophthalmology
University hospital Greifswald, Nursing home Kursana Domizil
Greifswald

August 1996 – July 2005 Alexander von Humboldt Gymnasium Greifswald, Degree: Abitur

14.2. Qualification

Training course: Animal welfare and laboratory animal science, University of Wuerzburg
Cellular and Molecular Immunology, University of Wuerzburg
Cell based assays for screening, European Screening Port, Hamburg

Workshop: Project management, GMP/GLP, Rules of Good Scientific Practise,
Patent Law, Poster Design and Poster Presentation

First-aider

14.3. Publication

B. Oesterreich, B. Lorenz, T. Schmitter, R. Kontermann, M. Zenn, B. Zimmermann, M. Haake, U. Lorenz, and K. Ohlsen. Characterization of the biological anti-staphylococcal functionality of hUK-66 IgG1, a humanized monoclonal antibody as substantial component for an immunotherapeutic approach. Journal of Human Vaccines and Immunotherapeutics. Volume 10 (4): 926-937.

14.4. Conference Contribution

Oesterreich, B., Lorenz, L., Kontermann, R., Erck, C., and Ohlsen, K. (2011). Humanization of the murine anti-IsaA antibody - a potential target for an antibody-based therapy against multi-resistant *Staphylococcus aureus*. Poster (Award) DGHM, Essen

Oesterreich, B., Lorenz, L., Kontermann, R., Erck, C., and Ohlsen, K. (2011). Development of a humanized antibodies - The defense against multi-resistant *Staphylococcus aureus*. Poster Bio Bang, Würzburg

Oesterreich, B., Lorenz, L., Kontermann, R., Erck, C., and Ohlsen, K. (2011). Identification of immunodominant antigens for a protective immunotherapy against *Staphylococcus aureus*. Poster FEMS, Würzburg

Oesterreich, B., Lorenz, L., Kontermann, R., Erck, C., and Ohlsen, K. (2012). Humanized antibodies - a therapeutic tool against multi-resistant *S. aureus*. Poster Pathophysiology of Staphylococci in the Post-Genomic Era, Banz

Oesterreich, B., Lorenz, L., Kontermann, R., Erck, C., and Ohlsen, K. (2012). From target to the antibody-based therapy against MRSA. Poster EPOS, Würzburg

Oesterreich, B., Lorenz, L., Kontermann, R., Erck, C., and Ohlsen, K. (2012). Immunodominant staphylococcal antigen A- a promising target for an antibody-based therapy. Poster DGHM, Hannover

Oesterreich, B., Lorenz, L., Kontermann, R., Erck, C., and Ohlsen, K. (2012). The road from target to therapy - the development of an antibody-based therapy. Presentation VAAM, Tübingen

Oesterreich, B., Lorenz, L., Kontermann, R., Erck, C., and Ohlsen, K. (2012). The key for a protective immunotherapy against *Staphylococcus aureus*. Poster Mol Micro, Würzburg

Oesterreich, B., Lorenz, L., Kontermann, R., Erck, C., and Ohlsen, K. (2013). Antibody engineering opens the gate for a new treatment option against MRSA. Poster VAAM, Bremen

Oesterreich, B., Lorenz, L., Kontermann, R., Erck, C., and Ohlsen, K. (2013). From target to therapy - Expression and characterization of an anti-staphylococcal antibody. Poster DGHM, Rostock

Oesterreich, B., Lorenz, L., Kontermann, R., Erck, C., and Ohlsen, K. (2014). From target to therapy - Humanized antibody UK-66 induces killing of *S. aureus* in samples of healthy blood donors. Poster Mol Micro, Würzburg

Oesterreich, B., Lorenz, L., Kontermann, R., Erck, C., and Ohlsen, K. (2014). From target to therapy - Humanized antibody UK-66 induces killing of *S. aureus* in blood samples of high risk patients. Poster Mol Micro, Würzburg